EVALUATION OF LIQUEFACTION POTENTIAL OF SOIL USING GENETIC PROGRAMMING

PRADYUT KUMAR MUDULI

EVALUATION OF LIQUEFACTION POTENTIAL OF SOIL USING GENETIC PROGRAMMING

A thesis submitted to
National Institute of Technology, Rourkela
for the award of the degree
of
Doctor of Philosophy
in
CIVIL ENGINEERING
by

PRADYUT KUMAR MUDULI

Department of Civil Engineering
National Institute of Technology Rourkela -769008
Odisha, India
August 2013

Dedicated to

My Parents & Wife

CERTIFICATE

This is to certify that the thesis entitled ***"Evaluation of Liquefaction Potential of Soil Using Genetic Programming"*** *being submitted by Mr.Pradyut Kumar Muduli for the award of the degree of Doctor of Philosophy (Civil Engineering) of NIT Rourkela, is a record of bonafide research work carried out by him under my supervision and guidance. Mr. Pradyut Kumar Muduli has worked for more than three years on the above problem in the Department of Civil Engineering, National Institute of Technology Rourkela and this has reached the standard for fulfilling the requirements and the regulation relating to the degree. The contents of this thesis, in full or part, have not been submitted to any other university or institution for the award of any degree or diploma.*

Dr. Sarat Kumar Das

Place: Rourkela Associate Professor

Date:

ACKNOWLEDGEMENTS

At the outset, I would like to thank the Almighty for granting me His kindness, love and strength to accomplish this thesis.

It gives me immense pleasure to express my gratitude to Prof. S. K. Das, my supervisor, for his constant supervision, encouragement, and guidance during the entire period of my research programme at NIT, Rourkela. I am also highly grateful to him for sharing his invaluable expertise and research insight with me. Above all, thanks for being such an attentive mentor and having your door open as a friend.

I wish to express my sincere thanks to the Doctoral Scrutiny Committee members, Prof. N. Roy, Prof. S. P. Singh, Prof. M.R. Barik and Prof. D. P. Tripathy, for their suggestions and interest in my research work.

I gratefully acknowledge the Department of Employment and Technical Education & Training, Government of Odisha for sponsoring me to carry out the research work at NIT Rourkela. I would like to mention special word of thanks to Mr. V.V. Yadav, IAS, the Ex. Director, Technical Education and Training, Odisha without his kind support I would not have been allowed study leave.

My colleagues at NIT, Rourkela have been a tremendous asset, providing both support and critique when it was needed. Thanks are due to Mr. P. K. Mohanty, Mr. S K Nayak, Mr. D. Jena, Mr. R. N. Behera, and Mr. P. Subramanium, research scholars of Civil Engineering Department, with whom I shared the moments of hardship and happiness. Their moral support and encouragements at times rejuvenated my energy for research

Last, but not least, I would also like to acknowledge the support and love from my two daughters, sisters and brother in laws of my family. I am sincerely grateful to my parents for their immeasurable support and encouragement in the need of the hour. Finally, I would like to extend my heartfelt gratitude to my wife, whose strong encouragement, dedication and understanding was with me throughout this journey.

ABSTRACT

Out of the various seismic hazards, soil liquefaction is a major cause of both loss of life and damage to infrastructures and lifeline systems. Soil liquefaction phenomena have been noticed in many historical earthquakes after first large scale observations of damage caused by liquefaction in the 1964 Niigata, Japan and 1964 Alaska, USA, earthquakes. Due to difficulty in obtaining high quality undisturbed samples and cost involved therein, in-situ tests, standard penetration test (SPT) and cone penetration test (CPT), are being preferred by geotechnical engineers for liquefaction potential evaluation with limited use of other in-situ tests like shear wave velocity tests and Baker penetration tests. The liquefaction evaluation in the deterministic framework is preferred by the geotechnical engineering professionals because of its simple mathematical approach with minimum requirement of data, time and effort. However, for important life line structures, there is a need of probabilistic and reliability methods for taking risk based design decisions. In recent years, soft computing techniques such as artificial neural network (ANN), support vector machine (SVM) and relevance vector machine (RVM) have been successfully implemented for evaluation liquefaction potential with better accuracy compared to available statistical methods. In the recent past, evolutionary soft computing technique genetic programming (GP) based on Darwinian theory of natural selection is being used as an alternate soft computing technique.

The objective of the present research is to develop deterministic, probabilistic and reliability-based models to evaluate the liquefaction potential of soil using multi-gene genetic programming (MGGP) based on post liquefaction SPT and CPT database.

Here, the liquefaction potential is evaluated and expressed in terms of liquefaction field performance indicator, referred as a liquefaction index (*LI*) and factor of safety against the occurrence of liquefaction (F_s). Further, the developed LI_p models have been used to develop both SPT and CPT-based *CRR* models. These developed *CRR* models in conjunction with the widely used $CSR_{7.5}$ model, form the proposed MGGP-based deterministic methods. The efficiency of both the developed SPT and CPT-based

deterministic models has been compared with that of available statistical and ANN-based models on the basis of independent database. Two examples have been solved to show the use of developed deterministic methods to find out the extent of ground improvement works needs to be done in terms of $N_{1,60}$ and q_{c1N} using the adopted factor of safety.

The probabilistic evaluation of liquefaction potential has been performed where liquefaction potential is expressed in terms of probability of liquefaction (P_L) and the degree of conservatism associated with developed deterministic models are quantified in terms of P_L. Using Bayesian theory of conditional probability the F_s is related with the P_L through the developed mapping functions. The developed SPT and CPT-based probabilistic models have been compared in terms of the rate of successful prediction within different limits of P_L**,** with that of the available statistical and ANN-based probabilistic models. Two examples, one from SPT and the other from CPT-based data, have been illustrated to show the use of developed probabilistic methods to take risk-based design decision for a site susceptible to liquefaction.

Further reliability analysis following first order reliability method (FORM) has been carried out using high quality SPT and CPT database, which considers both model and parameter uncertainties. The uncertainties of input parameters were obtained from the database. But, a rigorous reliability analysis associated with the Bayesian mapping function approach was followed to estimate model uncertainty of the limit state, which has been represented by a lognormal random variable, and is characterized in terms of its two statistics, namely, the mean and the coefficient of variation. Four examples, two from SPT data (one liquefied and the other non-liquefied case) and the other two from CPT data (one liquefied and the other non-liquefied case), have been illustrated to show the procedure of reliability-based liquefaction potential evaluation in terms of notional probability of liquefaction (P_L) considering the corresponding "true" model uncertainty as obtained for SPT and CPT-based limit state models in the analysis.

The development of compact and comprehensive model equation using deterministic methods based on both SPT and CPT data will enable geotechnical professional to use it

with confidence and ease. The presentation of probabilistic methods in conjunction with deterministic factor of safety *(F_s)* value gives the measure of probability of liquefaction corresponding to particular *Fs*. The present works also illustrate the effect of model and parameter uncertainties while discussing the reliability analysis. Design charts have been presented and discussed with examples using both SPT and CPT data.

Table of Contents

LIST OF TABLES

LIST OF FIGURES

List of Abbreviations and Symbols

Abbreviations

AAE	average absolute error
CDF	cumulative distribution function
COV	coefficient of variation
CRR	cyclic resistance ratio
CSR	Cyclic stress ratio
$CSR_{7.5}$	Cyclic stress ratio adjusted to a benchmark earthquake of moment magnitude of 7.5
FORM	first order reliability method
FOSM	first order second moment method
GP	genetic programming
LI	liquefaction index
MAE	maximum absolute error
MGGP	multi-gene genetic programming
MSF	the magnitude scaling factor
PDF	probability density function
RMSE	root mean square error

Symbols

A	material attenuation factor
C_B	correction for borehole diameter
C_E	correction for hammer energy efficiency
C_N	factor to normalize N_m to a common reference effective overburden stress
C_R	correction for "short" rod length
C_S	correction for non-standardized sampler configuration
D_{50}	mean grain size
E	Nash-Sutcliff coefficient of efficiency
E_f	Error function
ER	percentage of the theoretical free-fall energy (i.e., estimated rod energy ratio expressed in percentage);
f	MGGP functions defined by the user
F	liquefaction index function
FC	fines content in percentage
F_s	factor of safety against occurrence of liquefaction
g	acceleration due to gravity and
G_{max}	maximum number of genes
I_c	soil type index
k	shape parameter
K_α	static shear stress correction factor
K_σ	overburden correction factor
L	Liquefied cases
LI	liquefaction index
M	earthquake magnitude on Richter scale
MSF	magnitude scaling factor
M_w	earthquake magnitude on moment magnitude scale
N	number of data points

NL	Non-liquefied cases
n	number of terms of target expression
N_1	overburden stress corrected SPT value
$N_{1,60}$	corrected SPT blow count (i.e., corresponds to the N_m value after correction for overburden, energy, equipment and procedural effects in SPT method)
$N_{1,60,cs}$	clean sand equivalence of the corrected SPT blow count
N_{60}	N_m value corresponds to an equivalent 60% hammer efficiency
N_m	measured SPT blow count
P_L	probability of liquefaction
R	correlation coefficient
R^2	coefficient of determination
R_f	friction ratio
S_i	sensitivity
Z	performance function
γ_{cyc}	cyclic shear strain
γ_t	threshold shear strain
Δu	increase in pore water pressure
σ_v'	effective vertical stress at the depth under consideration
r	distance of the site from the center of energy release
z	depth of soil layer under consideration
τ_{av}	average equivalent uniform shear stress
σ_v	total vertical stress at the depth under consideration
a_{max}	peak horizontal ground surface acceleration
r_d	stress reduction factor
$(\tau_{max})_d$	maximum shear stress on soil element considering it as deformable body
$(\tau_{max})_r$	maximum shear stress on soil element considering it as rigid body
q_c	cone tip resistance
q_{c1N}	normalized cone tip resistance

f_s	sleeve friction
d_w	depth of ground water table
d_{max}	maximum tree depth
c_0	bias
λ	scale parameter
μ_z	mean of performance function
σ_z	standard deviation of performance function
β	reliability index
p_f	probability of failure
$\boldsymbol{\Phi}(\cdot)$	CDF of standard normal variable
ξ_i	standard deviation of the equivalent normal variable
λ_i	mean of the equivalent normal variable;
μ_{zi}	mean of the random variable, z_i
δ_{zi}	coefficient of variation of z_i
c_{mf}	model factor
μ_{cmf}	mean of c_{mf}
β_1	reliability index without considering model uncertainty
β_2	reliability index considering model uncertainty

Chapter 1
INTRODUCTION

1.1 GENERAL

Natural hazards like earthquake, tsunami, flood, cyclone and landslides pose severe threat to human life and its environment. There is a huge social and economic consequence immediately after the occurrence of a natural disaster. The adverse effects of disasters are much more in developing countries where the population is very large and the socioeconomic factors force the people to live in vulnerable areas. It is estimated, on average natural disaster claim 1000 lives and cause damage exceeding one billion US$ each week. Due to natural hazards in the last century around 30% of total casualties and 60% of the total property loss caused by the various major natural hazards around the world is due to earthquake only (www.em-dat.net/ngdc.noaa.gov). The natural hazards are no more considered as the curse of God, but can be mitigated with suitable identification, evaluation and analysis of the same.

The advent of high speed digital computers, development of new computational algorithms and their application to new areas cutting across various disciplines in science and engineering went hand in hand. In recent years such efforts have increased phenomenally. In the following section an effort has been made briefly to trace the need for evaluation of seismic hazard and use of soft computing techniques for liquefaction susceptibility analysis to decide upon the course of studies to be taken up in the present thesis.

1.2 RECENT TRENDS OF NATURAL HAZARDS

A study was made to observe the recent trends in natural hazards to identify the need of the present research. Case histories of different major natural disasters, occurred during 1911-2010 around the world as well as in India, are collected from international and national disaster databases such as en.wikipedia.org, em-dat.net, ngdc.noaa.gov, nidm.net, sarc-

sdmc.nic.in etc. The conflicting data have been verified considering the authenticity of the database. The major natural hazards include earthquake, Tsunami, flood, Cyclone and landslide. The number of occurrences of the aforesaid natural disasters as reported, the casualties and the property loss caused due to these disasters during the last one century (1911-2010) are studied thoroughly and presented as follows.

The number of occurrences of the major natural disasters in the last century is increasing continuously over the years, whereas there is a decrease in the total numbers of people died (Fig. 1.1). This shows the better preparedness, implementation of early warning systems and other preventive measures adopted gradually by the world community has got a positive impact on prevention of loss of life. However, the property damage caused by the major natural disasters has been increased during the same period of time (Fig. 1.1). This clearly indicates that the existing disaster mitigation measures are not adequate to protect the infrastructures completely from catastrophic nature of the hazards.

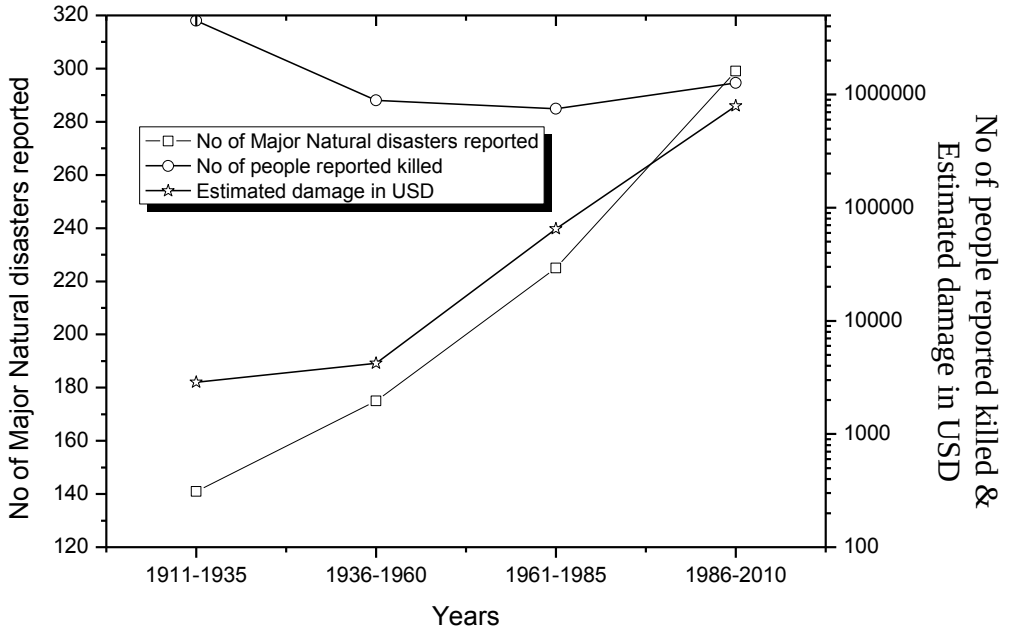

Fig.1.1 Major natural disasters in the world, during 1911-2010, reported causality and property loss in USD.

Figs. 1.2a and 1.2b show the variation of human death and property losses, respectively due to different major natural hazards during the last century. It can be seen that the causality is the maximum due to flood but the property loss is maximized due to earthquake. However, when the data are presented in terms of quarter century for human death (Fig. 1.3) and property loss (Fig. 1.4), it was observed that in last 50 years the effect of the flood has been reduced in terms of human death and property loss. However, the human death and property damage due to earthquake has steadily increased over the same period. This may be due to the fact that the prediction models for flood forecasting have become effective in combination with warning system and society has become less prone to this disaster. In case of earthquake due to increase in urbanization and lack of an adequate mitigation system, its destructive effect has been increased.

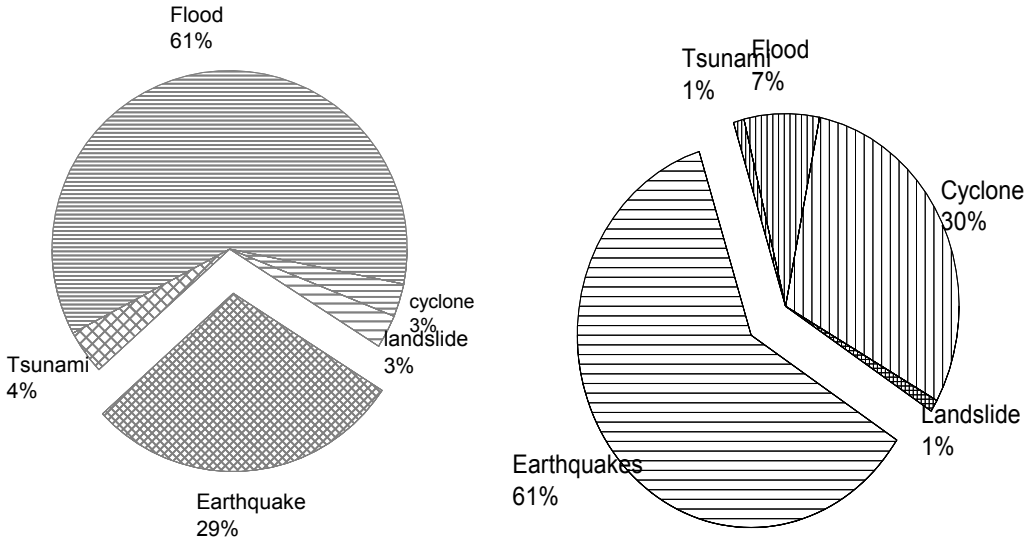

(a) (b)

Fig. 1.2 Distribution of (a) human death and (b) property loss due to different Major natural Disasters in world (1911-2010)

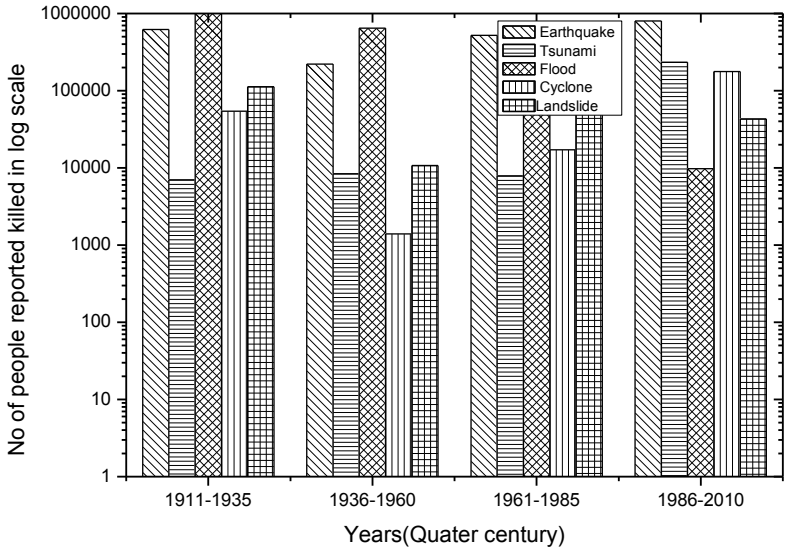

Fig. 1.3 Number of people reported killed by major natural hazards in World during

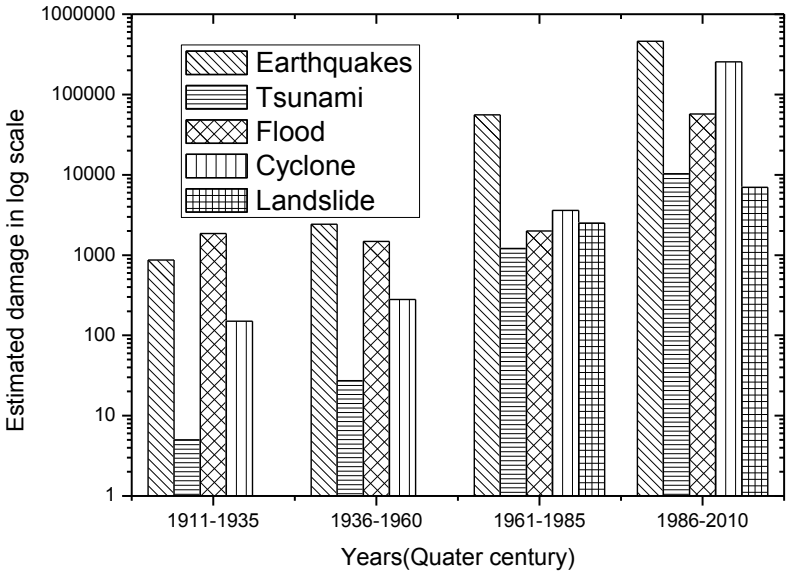

Fig. 1.4 Estimated Damage (Million US$) caused by reported major Natural Disasters in World during 1911-2010, presented in terms of quarter century

1.3 SOIL LIQUEFACTION

Seismic hazards can be categorized as ground shaking, structural hazards, liquefaction, landslides, retaining structure failures, lifeline hazards, tsunamis. Out of the above, seismically induced liquefaction of soil is a major cause of both loss of life and damage to infrastructures and lifeline systems. The soil liquefaction phenomenon was known in early stage of development of soil mechanics by Terzhagi and Peck (1948) to explain the phenomenon of sudden loss of strength in loose sand deposit. It was recognized as the main cause of slope failure in saturated sandy deposit. Though, soil liquefaction phenomena have been recognized since long, it was more comprehensively brought to the attention of engineers, seismologists and scientific community of the world by several devastating earthquakes around the world; Niigata and Alaska (1964), Loma Prieta (1989), Kobe (1995),Kocaeli (1999) and Chi-Chi (1999) earthquakes (Baziar and Jafarian 2007). Since then, a numerous investigations on field and laboratory revealed that soil liquefaction may be better described as a disastrous failure phenomenon in which saturated soil loses strength due to increase in pore water pressure and reduction in effective stress under rapid loading and the failed soil acquires a degree of mobility sufficient to permit movement from meters to kilometers. Soil liquefaction can cause ground failure in the way of sand boils, major landslides, surface settlement, lateral spreading, lateral movement of bridge supports, settling and tilting of buildings, failure of waterfront structure and severe damage to the lifeline systems etc.

Soil liquefaction can be classified into two groups as flow liquefaction and cyclic liquefaction. The flow liquefaction can occur when the shear stress required for static equilibrium of a soil is greater than the shear strength of soil in its liquefied state. The cyclic liquefaction occurs even if static shear stress is less than the shear strength of liquefied soil. Here, the deformations produced are driven by both cyclic and static shear stress. Generally the deformations develop incrementally during earthquake shaking. It can produce large permanent deformations during earthquake shaking. The cyclic liquefaction occurs under a much broader range of soil and site conditions than flow liquefaction. But, its effect can range from insignificant to highly damaging.

The liquefaction hazard evaluation involves liquefaction susceptibility analysis, liquefaction potential evaluation, assessment of effect of liquefaction (i.e., the extent of ground failure caused by liquefaction) and study of response of various foundations in liquefied soil. These are the major concern of geotechnical engineers. In the present study, the focus is on liquefaction potential evaluation, which determines the likelihood of liquefaction triggering in a particular soil in a given earthquake. Evaluation of the liquefaction potential of a soil subjected to a given seismic loading is an important first step towards mitigating liquefaction-induced damage. Though, different approaches like cyclic strain-based, energy-based and cyclic stress-based approaches are in use, the stress based approach is the most widely used methods for evaluation of liquefaction potential of soil (Krammer, 1996). Thus, the focus of present study is on the evaluation of liquefaction potential on the basis of the cyclic stress-based approach.

There are two types of cyclic stress based-approach available for assessing liquefaction potential. One is by means of laboratory testing (e.g., cyclic tri-axial test and cyclic simple shear test) of undisturbed samples, and the other involves the use of empirical relationships that relate observed field behavior with in-situ tests such as standard penetration test (SPT), cone penetration test (CPT), shear wave velocity measurement (V_s) and the Becker penetration test (BPT).

The methods like finite element, finite difference, statistically-derived empirical methods based on back-analyses of field earthquake case histories are used for liquefaction analysis. Finite element and finite difference analyses are the most complex and accurate of the above methods. However, liquefied sediments are highly variable over short distances, developing a sufficiently accurate site model for a detailed numerical model requires extensive site characterization effort. Desired constitutive modeling of liquefiable soil is very difficult, even with considerable laboratory testing. Hence, in-situ tests along with the post liquefaction case histories-calibrated empirical relationships have been used widely around the world. The cyclic stress-based simplified methods based on in-situ test such as SPT, CPT, V_s measurements and BPT are commonly preferred by the geotechnical engineer to evaluate the liquefaction potential of soils throughout most part of world.

The stress-based simplified procedure is pioneered by Seed and Idriss (1971). The SPT-based simplified method, developed by Seed and Idriss (1971), has been modified and improved through several revisions (Seed and Idriss 1982; Seed et al. 1983; Seed et al. 1985; Youd et al. 2001) and remains the most widely used methods around the world. Robertson and Campanella (1985) first developed a CPT based method for evaluation of liquefaction potential, which is a conversion from the SPT based method using empirical correlation of SPT-CPT and follows the same stress-based approach of Seed and Idriss (1971). Thereafter, various CPT-based methods of soil liquefaction potential evaluation using statistical and regression analysis techniques have been developed (Seed and de Alba 1986; Olsen 1988; Shibata and Teparaksa 1988; Mitchell and Tseng 1990; Stark and Olson 1995; Suzuki et al. 1995; Olsen 1997; Robertson and Wride 1998; Youd et al. 2001). Several V_S-based simplified methods have been developed (Dobry et al. 1981; Stokoe et al. 1988; Tokimatsu and Uchida 1990; Robertson et al. 1992; Kayen et al. 1992; Lodge 1994; Andrus and Stokoe 2000; Juang et al. 2000a; Juang et al. 2001; Andrus et al. 2003) and are in use. But, very few BPT-based simplified methods (Harder and Seed 1986 and Youd et al. 2001) have been developed and primarily for gravelly soil.

For a given soil resistance index, such as the corrected SPT blow count, the boundary curve yields liquefaction resistance of a soil, which is usually expressed as the cyclic resistance ratio (*CRR*). Under a given seismic loading, which is usually expressed as the cyclic stress ratio (*CSR*) the liquefaction potential of a soil is evaluated in terms of a factor of safety (F_s), which is defined as the ratio of *CRR* to *CSR*. The approach of expressing liquefaction potential of soil in terms of F_s is referred to as a deterministic method and is very much preferred by geotechnical professionals due its simplicity for use.

However, due to parameter and model uncertainties, Fs>1 does not always indicate non-liquefaction and also does not necessarily guarantee zero chance of soil being liquefied. Similarly Fs≤1 may not always correspond to liquefaction and may not guarantee 100% chance of being liquefied (Juang et al. 2000b). The boundary surface that separates liquefaction and non-liquefaction cases in the deterministic methods is considered as a performance function or "limit state function" and is generally biased towards the

conservative side by encompassing most of the liquified cases. But, the degree of conservatism is not quantified (Juang et al. 2000b). Thus, attempts have been made by several researchers (Haldar and Tang 1979; Lioet al. 1988; Youd and Nobble 1997b; Toprak et al. 1999) to assess liquefaction potential in terms of probability of liquefaction (P_L) using statistical or probabilistic approaches.

The above in-situ test-based models are all data-driven as they are based on statistical analyses of the databases of post liquefaction case histories. The calculation of P_L using these empirical models requires only the mean values of the input variables, whereas the uncertainty in the parameters and the model are excluded from the analysis. Thus, resulting P_L might be subjected to error if the effect of parameter and model uncertainty is significant. These difficulties can be overcome by adopting reliability based probabilistic analysis of liquefaction, which considers both model and parameter uncertainties. In the framework of reliability analysis, the boundary curve separating liquefaction and non-liquefaction is a limit state. To conduct a thorough reliability analysis, knowledge of the uncertainties that are associated with both the input parameters and the limit state model is required. However, most of the existing simplified methods have not been fully examined for its model uncertainty, though the simplified methods tend to be conservative to some extent.

Soft computing techniques such as; artificial neural network (ANN) (Goh, 1994; Juang et al., 2000; Hanna et al., 2007; Samui and Sitharam, 2011), support vector machine (SVM) (Pal, 2006; Goh and Goh, 2007; Samui and Sitharam, 2011) and relevance vector machine (RVM) (Samui, 2007) have been used to develop liquefaction prediction models based on an in-situ test database, which are found to be more efficient compared to statistical methods. However, the ANN has poor generalization, attributed to attainment of local minima during training and needs iterative learning steps to obtain better learning performances. The SVM has better generalization compared to ANN, but the parameters ‘C’ and insensitive loss function (ε) needs to be fine tuned by the user. Moreover, these techniques will not produce a comprehensive relationship between the inputs and output and are also called as ‘black box’ system.

In the recent past, genetic programming (GP) based on Darwinian theory of natural selection is being used as an alternate soft computing technique. The GP is defined as the next generation soft computing technique and also called as a 'grey box' model (Giustolisi et al., 2007) in which the mathematical structure of the model can be derived, allowing further information of the system behaviour. The GP models have been applied to some difficult geotechnical engineering problems (Yang et al., 2004; Javadi et al., 2006; Rezania and Javadi, 2007; Alavi et al., 2011; Gandomi and Alavi, 2012b; Muduli et al., 2013) with success. However, its use in liquefaction susceptibility assessment is very limited (Alavi and Gandomi, 2012; Gandomi and Alavi, 2012b; Gandomi and Alavi, 2013). The main advantage of GP and its variant multi-gene genetic programming (MGGP) over traditional statistical methods and other soft computing techniques is its ability to develop a compact and explicit prediction equation in terms of different model variables.

1.4 MOTIVATION FOR THE RESEARCH

From the above discussions, it can be seen that different approaches and methodologies have been used to develop predictive models for evaluation of liquefaction potential over the years by various researchers. But any improvement to the existing methods for assessing liquefaction potential is considered as a contribution to the field of geotechnical engineering in mitigating the liquefaction hazards. In recent years, artificial intelligence techniques such as ANN, SVM and RVM have been successfully implemented for evaluation liquefaction potential. Though, GP has been implemented to solve some complex geotechnical problems its use in liquefaction potential evaluation is very limited. Muduli et al. (2013) observed that the efficacy of GP-based predictive model for uplift capacity of suction caisson outperformed the other soft computing technique-based (ANN, SVM, RVM) prediction models in terms of different statistical performance criteria. Now a days, the performance-based design concepts in earthquake engineering have been receiving wide acceptance. One of the vital features of performance-based design in the perspective of geotechnical earthquake engineering is an assessment of liquefaction potential in terms of the probability of liquefaction. Precise estimation of the probability of liquefaction requires information of both parameter and model uncertainties. The issue of model uncertainty has been addressed

in the research presented in this dissertation through rigorous genetic programming based-reliability analyses, which is considered to be significant.

1.5. OBJECTIVES AND SCOPE OF THE RESEARCH

The objective of the present research is to develop deterministic, probabilistic and reliability-based models to evaluate the liquefaction potential of soil using multi-gene genetic programming based on reliable post liquefaction SPT and CPT database.

The scopes of the research are as follows:

i. To develop deterministic models implementing MGGP on the basis of available post liquefaction SPT and CPT data base
ii. To develop SPT and CPT-based probabilistic models using Bayesian mapping function approach to relate F_s to P_L
iii. To explore the use of first order reliability method (FORM) for assessing liquefaction potential of soil in terms of P_L on the basis of available SPT and CPT database
iv. To estimate model uncertainties of the developed MGGP-based models for liquefaction potential evaluation using rigorous reliability analysis
v. To validate developed models by comparing the efficacy of the proposed models with available models on the basis of independent database

1.6 ORGANIZATION OF THESIS

This thesis consists of seven chapters and the chapters have been organized in following order.

After a brief introduction, the recent trend in natural hazards, the motivation, the scope and objective of the research work are presented in Chapter 1, that sets the stage for the entire thesis.

A detailed literature review pertaining to liquefaction susceptibility analysis has been presented in Chapter 2. The various approaches of liquefaction triggering analysis, in-situ test-based methods used for liquefaction susceptibility evaluation, methods of analysis and analysis tools used are discussed in this chapter.

Chapter 3 pertains to a detailed description of the methodology (analysis tool), genetic programming (GP), used for development of different models for evaluation of liquefaction potential. The description and implementation of the GP in general and its variant, multi-gene genetic programming (MGGP), is described citing examples.

In Chapter 4, on the basis of post liquefaction SPT and CPT database separate deterministic models are developed using the MGGP method. The efficiencies of developed models are compared with the existing ANN and SVM models. The developed models are also compared with other methods using independent database. While describing GP as an alternate predictive tool, aspects like the GP parameters, different statistical measures to compare different methods are also discussed.

The probabilistic evaluation of liquefaction susceptibility evaluation is discussed in Chapter 5. This chapter covers implementation of Bayesian mapping function for probabilistic evaluation of liquefaction potential by using the developed SPT and CPT-based deterministic models of Chapter 4. In this chapter efficiency of the developed models are compared with the available SPT and CPT-based probabilistic models using independent database.

Chapter 6 presents the use of the first order reliability method (FORM) for evaluating the probability of liquefaction in detail, and uncertainties of the developed SPT and CPT-based limit state models are estimated through rigorous reliability analysis. The robustness of the Bayesian mapping approach is also demonstrated in this chapter. In the absence of existing model for comparison, development of 'best' model using cross validation method is also discussed in this chapter.

In Chapter 7, generalized conclusions made from various studies in this thesis, are presented and the scope of the future work is indicated. The general layout and method of liquefaction potential evaluation of soil using different in-situ test data and different methods are shown in a flow diagram (Fig. 1.5) for ready reference.

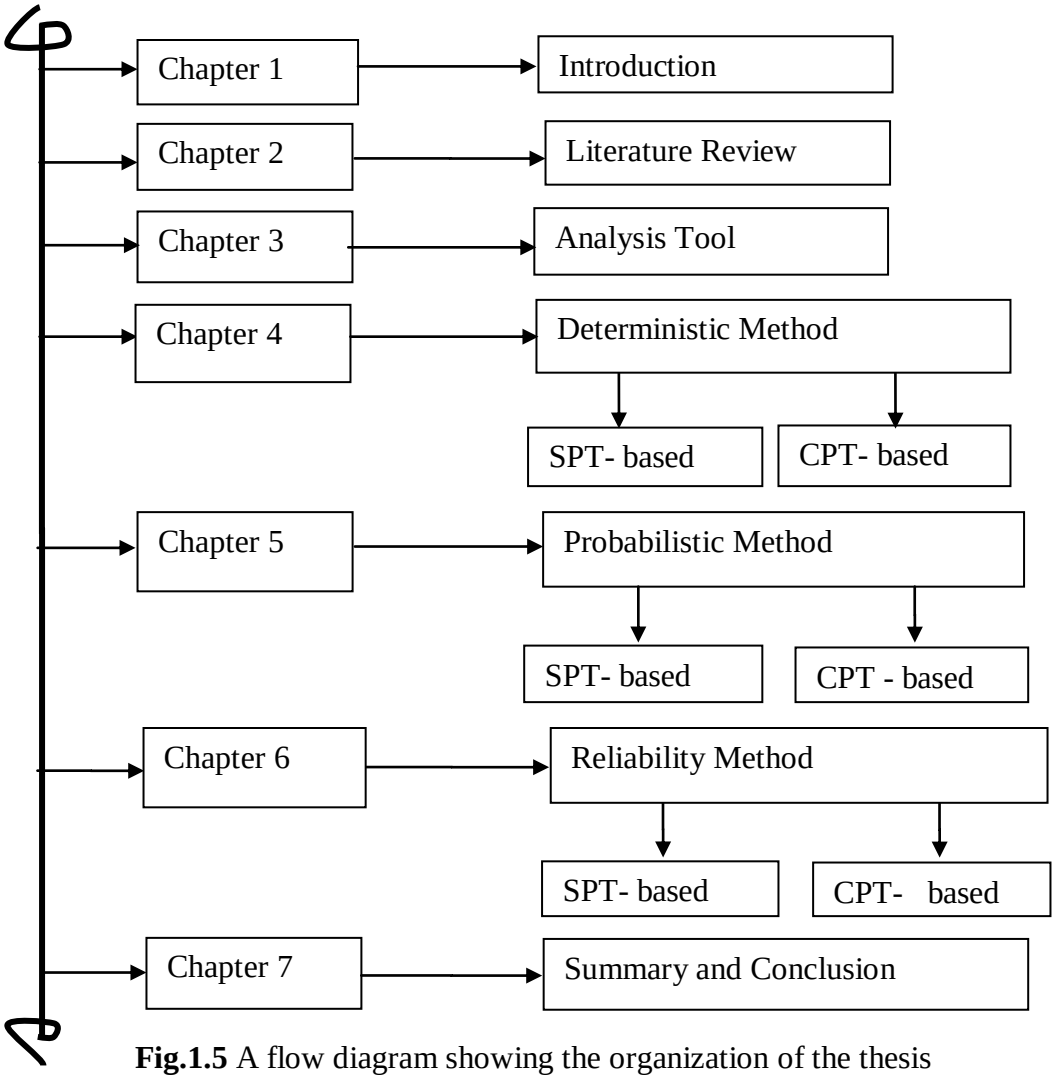

Fig.1.5 A flow diagram showing the organization of the thesis

Chapter 2
LITERATURE REVIEW

2.1 INTRODUCTION

The liquefaction hazard evaluation involves liquefaction susceptibility analysis, liquefaction potential evaluation, assessment of effect of liquefaction (i.e. the extent of ground failure caused by liquefaction) and study of response of various foundations in liquefied soil. These are the major concerns of geotechnical engineers. But, in the present study, the focus is on liquefaction potential evaluation, which determines the likelihood of liquefaction triggering in a particular soil in a given earthquake. This Chapter presents a review of the various liquefaction potential evaluation methods. All these available research works are presented in four different parts. Part I focuses on different approaches of liquefaction potential evaluation and Part II discusses about widely used stress-based approach in particular with emphasis on the in-situ test based methods. The available methods of analysis within the framework of stress-based approach such as deterministic method, probabilistic method and reliability method, which are in use for assessment of liquefaction potential are discussed in Part III. The various analysis tools used in model development for assessing liquefaction potential are described in the last part.

2.2 LIQUEFACTION POTENTIAL EVALUATION

Once a particular soil is found to be susceptible to liquefaction on the basis of various susceptibility criteria as mentioned in Kramer (1996) the next step in the liquefaction hazard evaluation process is the evaluation of liquefaction potential, which is the main topic of the present study. The major factors controlling the liquefaction potential of a saturated cohesion-less soil in level ground is the intensity and duration of earthquake shaking and the density and effective confining pressure of the soil. Several approaches are used for evaluating liquefaction potential, including (i) the energy-based approach, (ii) the cyclic

stress-based approach and the (iii) the cyclic strain-based approach. Each of the above three methods are described briefly in the following subsections.

2.2.1 Energy-based approach

The energy-based approach is theoretically very much appropriate for liquefaction potential evaluation, as the dissipated energy reflects both cyclic stress and strain amplitudes.When a dry soil is cyclically loaded it causes densification at the expense of energy as energy is required to rearrange the individual soil particles. For a saturated soil densification causes an increase in pore water pressure under un-drained condition as the amount of energy required to rearrange soil grains decreases due to decrease in contact forces. Using this principle Davis and Berrill (1982) developed energy based formulation, in which the dissipated seismic energy at a site is considered responsible for the progressive development of pore water pressure, and also presented an expression as a criterion for liquefaction. Berrill and Davis (1985) revised their earlier formulation and developed an expression for the pore pressure increase by taking into account a non-linear relationship between the pore pressure increase and dissipated energy, effect of natural attenuation and reassessing the magnitude-total radiated energy relationship:

$$\frac{\Delta u}{\sigma_v^{'}} = \frac{120A^{0.5}10^{0.75M}}{rN_1^{1.5}\sigma_0^{'\,0.75}} \tag{2.1}$$

where Δu = increase in pore water pressure, $\sigma_v^{'}$ = effective vertical stress at depth of interest, N_1 = corrected standard penetration value of the site soil layer under investigation, A = material attenuation factor, M= earthquake magnitude on the Richter scale, r = distance of the site from the centre of energy release. Law et al. (1990) used the above energy principles and developed a criterion for liquefaction occurrence in sands as given below.

$$\frac{10^{1.5M}}{2.28\times10^{-10}N_1^{11.5}r^{4.3}} \geq 1.0 \tag{2.2}$$

Several other investigators have established relationships between the pore pressure development and the dissipated energy during ground shaking (Figueroaet al. 1994; Ostadan et al. 1996). The liquefaction triggering can be formulated by comparing the calculated unit energy from the time series record of a design earthquake with the resistance to liquefaction in terms of energy based on in-situ soil properties (Lianget al. 1995; Dief 2000). The energy-based methods, however, is less commonly used due to non-availability of quality data for calibration of these methods.

2.2.2 Cyclic strain-based approach

The cyclic strain-based approach to evaluate of liquefaction potential is based on experimental evidence that shows densification of dry sands is effectively controlled by cyclic strain rather than cyclic stress and there exist a threshold volumetric strain below, which densification does not occur. Since there are tendencies of sand to density when dry, this is directly related to its tendency to develop excess pore pressure when saturated. This shows that pore pressure generation is more fundamentally related to cyclic strains than cyclic stress. In this approach earthquake induced loading is expressed in terms cyclic strains. The time history of the cyclic shear strain can be estimated from the ground response analysis. As it is difficult to predict cyclic strain accurately, Dorby et al.(1982) developed a simplified method for estimating uniform cyclic strain (γ_{cyc}) from the amplitude of the uniform cyclic stress as originally proposed by Seed and Idriss (1971). Once γ_{cyc} is calculated it is compared with threshold shear strain (γ_t). If $\gamma_{cyc} < \gamma_t$, no pore water pressure will be generated and thus liquefaction cannot be initiated. If $\gamma_{cyc} > \gamma_t$, the occurrence of liquefaction is possible. Liquefaction potential can be evaluated in this approach by comparing the earthquake induced cyclic loading in terms of the amplitude of a series of an equivalent number of uniform strain cycles with liquefaction resistance, which is expressed in terms of the cyclic strain amplitude required to initiate liquefaction in the same number of cycles. Liquefaction can be triggered at depths where loading exceeds the liquefaction resistance. Dorby et al.(1984) developed a torsional tri-axial test for measurement of liquefaction resistance by imposing cyclic strains under un-drained conditions on a cylindrical tri-axial specimen by strain controlled cyclic torsion. The developed cyclic shear strain induces excess pore pressure in the specimen. Unlike cyclic stress approach cyclic

strain approach is not commonly used as cyclic strain amplitudes can to be predicted as accurately as cyclic stress amplitude and the cyclic strain-controlled testing equipment is less readily available than the cyclic stress-controlled testing equipment (Kramer and Elgamal, 2001). Thus, the focus of this chapter is on the evaluation of liquefaction potential using the cyclic stress-based methods.

2.2.3 Cyclic stress-based approach

In this approach the earthquake induced loading is expressed in terms of cyclic shear stress, which is compared with the liquefaction resistance of soil expressed also in terms of cyclic shear stress. The location at which the loading exceeds the resistance of the soil liquefaction is expected to occur. The earthquake loading can be estimated in two ways: (i) by a detailed ground response analysis (ii) by the simplified method as originally proposed by Seed and Idriss (1971) and its subsequent modifications. The simplified methods are widely used than the first method. The uniform cyclic shear stress amplitude due to earthquake loading for level (or gently sloping) ground can be evaluated as per the simplified model developed by Seed and Idriss (1971), which is presented below.

$$\tau_{av} = 0.65 \frac{a_{\max}}{g} \sigma_v r_d \tag{2.3}$$

where τ_{av} = the average equivalent uniform shear stress; σ_v = total vertical stress at the depth under consideration; a_{max} = the peak horizontal ground surface acceleration, g = acceleration due to gravity and r_d = the value of a stress reduction factor at the depth of interest that accounts for the flexibility of soil column (e.g., r_d= 1 corresponds to the rigid body behavior) as illustrated in Fig. 2.1. and r_d can be presented as: $r_d = \frac{(\tau_{\max})_d}{(\tau_{\max})_r}$. The $(\tau_{\max})_d$ is the maximum shear stress on soil element considering it as deformable body whereas $(\tau_{\max})_r$ is the maximum shear stress on soil element considering it as a rigid body. The factor 0.65 is used to convert the peak cyclic shear stress ratio to a cyclic stress ratio that is representative of the most significant cycles over the full duration of loading.

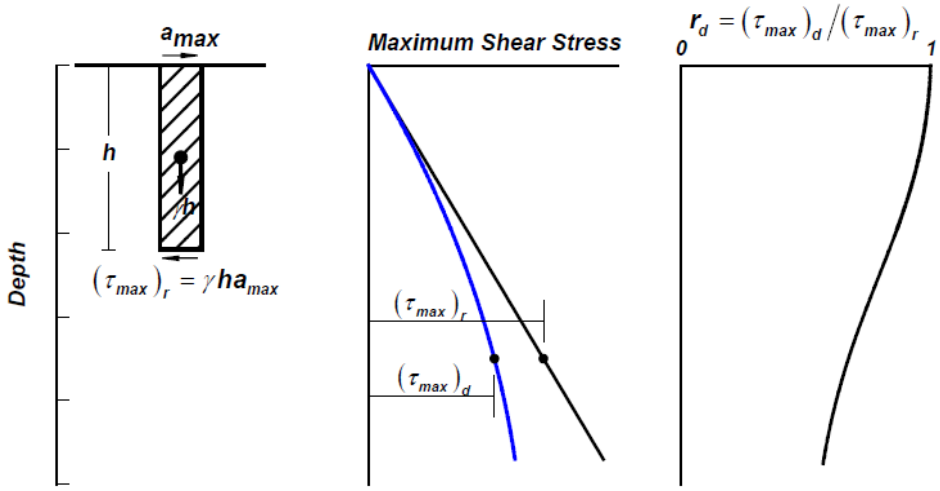

Fig. 2.1 Schematic for determining maximum shear stress, τ_{max}, and the stress reduction coefficient, r_d (Seed and Idriss 1971).

The liquefaction resistance of an element of soil depends on how close the initial state of soil is to the state corresponding to "failure" and also the nature of loading required to move the soil element from the initial state to failure state. Cyclic stress based approach is widely used and two types of methods under this approach are available for assessing liquefaction potential. One is by means of laboratory testing of undisturbed samples, and the other is based on empirical relationships that relate the field behavior with the in-situ tests.

2.2.3.1 Laboratory test-based methods:

Liquefaction resistance can be determined generally by two types of laboratory testing of undisturbed samples: (i) cyclic tri-axial test and (ii) cyclic simple shear test. In these tests liquefaction failures is defined as the point at which initial liquefaction is reached or at which some limiting cyclic strain amplitude is reached. Laboratory tests show that number of loading cycles required to produce liquefaction failure decreases with increase of shear stress amplitude and with the decrease of density of soil. Cyclic strength is normalized by initial effective overburden pressure to produce cyclic stress ratio (*CSR*). For cyclic simple shear test *CSR* is taken as the ratio of cyclic shear stress to the initial vertical effective stress i.e. $(CSR)_{ss} = \tau_{cyc}/\sigma'_v$. For cyclic tri-axial test it is taken as the ratio of maximum cyclic shear stress to the initial effective confining pressure and can be given as $(CSR)_{tx} = \sigma_{dc}/2\sigma_{3c}'$

whereσ_{dc} is cyclic deviator stress and $\sigma_{3c}^{'}$ is the effective confining pressure. The *CSR* of the above two tests are not equivalent as they impose quite different loading. The *CSR* values of both tests are related as $(CSR)_{ss}=c_r\,(CSR)_{tx}$, where c_r is a correction factor.

Seed and Lee (1966) defined initial liquefaction as the point at which the increase in pore pressure is equal to the initial effective confining pressure from their study of liquefaction of saturated sands during cyclic loading. Seed and Idriss (1967) developed an empirical procedure to evaluate the liquefaction potential of soil deposits by combining the development of pore water pressure obtained from laboratory results with the shear stress time history determined from the seismic response calculations. Seed et al. (1975) developed a model to determine the number of uniform stress cycles, N_{eq} (at an amplitude of 65% of the peak cyclic shear stress i.e, $\tau_{avg}=0.65\tau_{max}$) that would produce an increase in pore pressure equivalent to that of irregular time history by applying weighting procedure to a set of shear stress time histories from the recorded strong ground motions. Ishihara and Koseki (1989) showed that when the plasticity indices were below 10 the fines have little effect on liquefaction resistance. Chern and Chang (1995) developed a mathematical model for the evaluation of liquefaction characters of soil subjected to earthquake induced cyclic loading based on cyclic triaxial test results. Using the developed model and commonly used physical properties of soil the cyclic shear strength, number of cycles required to cause liquefaction and generation of excess pore water pressure can be evaluated without resorting to the complex laboratory cyclic shear test. Bray and Sancio (2006) confirmed through cyclic testing of a wide range of soils, which were found to liquefy in Adapazari during the 1999 Kocaeli earthquake, that these fine-grained soils are susceptible to liquefaction. Gratchev et al. (2006) examined the validity of the plasticity index (*PI*) as a criterion for estimating the liquefaction potential of clayey soils under cyclic loading. They found that an increase in *PI* decreased the soil potential to liquefy, and soil with *PI*>15 seemed to be non-liquefiable, a finding that is in agreement with the results of other researchers.

Though, evaluation of liquefaction potential based on laboratory test yields good results many engineers prefer to adopt the field performance correlation-based approach because of great difficulty and cost involved in obtaining undisturbed samples from cohesion-less soil

deposits. Here in this study focus is on in-situ test-based available methods for liquefaction potential evaluation.

2.2.3.2 In-situ Test based methods:

Soil liquefaction potential can be determined by using in-situ tests such as: (i) standard penetration test (SPT) (ii) cone penetration test (CPT) (iii) shear wave velocity (V_s) measurement (iv)Becker penetration test (BPT).

Due to difficulties in obtaining high quality undisturbed samples and subsequent high quality laboratory testing of granular soils, use of in-situ tests along with case histories-calibrated empirical relationships are generally resorted by the geotechnical engineers for the assessment of liquefaction potential of soils. The simplified procedure pioneered by Seed and Idris (1971) mostly depend on a boundary curve, which presents a limit state and separates liquefaction cases from the non-liquefaction cases basing on field observations of soil in earthquakes at the sites where in situ data are available. The boundary is usually drawn conservatively such that all cases in which liquefaction has been observed lie above it. In this approach the *CSR* is usually used as earthquake loading parameters and the cyclic resistance ratio (*CRR*) is represented by in-situ test parameters that reflect the density and pore pressure generation properties of soil. Out of the various in-situ methods as mentioned above SPT and CPT-based methods are widely used for liquefaction susceptibility analysis of soil.

SPT-based method

It is the most widely used methods among the available in-situ test methods as discussed above for evaluation of resistance of soil against the occurrence of liquefaction. Whitman (1971) first proposed to use liquefaction case histories to characterize liquefaction resistance in terms of measured in situ test parameters. Seed and Idriss (1971) did a pioneer work in developing a simplified empirical model, using laboratory tests and post liquefaction field observations in earthquakes, which presents a limit state function separating liquefied cases from the non-liquefied cases on the basis of SPT data. Seed et al. (1983) extended their

previous work in developing a modified model in which used *CSR* ($\tau_{av}/\sigma_v^{'}$) instead of peak ground acceleration (a_{max}) as a measure of seismic action and overburden pressure corrected SPT value (N_1) instead of relative density (D_r) as the site parameter representing its resistance to liquefaction. However, it has been addressed by many researchers that the SPT has been conventionally conducted by using different kinds of hammers in different parts of the world, with different energy delivery systems, which also have varying degrees of efficiency. Moreover, the borehole diameters and the sampling techniques also differ significantly, which in turn cause a large variability in the measured values depending on the combinations of actual test procedures and equipment used.

Seed et al. (1985) expressed the measured penetration resistance (N_m) in terms of $N_{1,60}$ where the driving energy in the drill rod is considered to be 60% of the free fall energy and correction for overburden effect is applied. Liquefaction resistance curves for sands with different fines contents are proposed, which is considered to be more reliable than the previous curves expressed in terms of mean grain size. Cyclic stress ratio, *CSR*, as proposed by Seed and Idriss (1971) and its subsequent modifications in Seed et. al.(1983), Seed et al.(1985), Youd et al. (2001), is defined as the average cyclic shear stress, τ_{av}, developed on the horizontal surface of soil layers due to vertically propagating shear waves normalized by the initial vertical effective stress, σ'_v, to incorporate the increase in shear strength due to increase in effective stress and is presented as follows:

$$CSR = \frac{\tau_{av}}{\sigma_v^{'}} = 0.65 \frac{a_{\max} \sigma_v}{g \sigma_v^{'}} r_d \tag{2.4}$$

where $\sigma_v^{'}$ = effective vertical stress at the depth under consideration. The value of *CSR* is corrected to an earthquake magnitude of 7.5, using the magnitude correction proposed by Seed et al. (1985). Seed et al.(1985) proposed a standard blow count N_{60}as given below:

$$N_{60} = N_m (ER/60\%) \tag{2.5}$$

where *ER*= percentage of the theoretical free-fall energy (i.e., estimated rod energy ratio expressed in percentage); and N_m= measured SPT blow count corresponding to the *ER*. The

value of $N_{60}$is corrected to an effective stress of 100 kPa. Thus, the overburden stress and energy corrected SPT value, $N_{1,60}$ is obtained by using the following relation:

$$N_{1,60} = C_N \times N_{60} \tag{2.6}$$

where C_N is the effective stress correction factor and is calculated from the following relation:

$$C_N = \frac{2.2}{\left(1.2 + \sigma'_v / P_a\right)} \tag{2.7}$$

where, Pa = 1atm of pressure in the same units used for σ'_v. Fig. 2.2 is a graph of calculating *CSR* and corresponding $N_{1,\,60}$ data from sites where liquefaction was or was not observed following past earthquakes with magnitudes of approximately 7.5. Liquefaction and non-liquefaction data were separated by Cyclic Resistance Ratio (*CRR*) curves. Curves were developed for granular soils with the fines content of 5% or less, 15%, and 35%. Fig. 2.2 is only applicable for magnitude of 7.5 earthquakes.

Juang et al. (2000) proposed an artificial neural network (ANN) -based *CRR* model based on SPT dataset and used Bayesian mapping function approach to relate factor of safety against the occurrence of liquefaction, F_s with probability of occurrence of liquefaction, P_L. Youd et al. (2001) published a summary paper of 1996 and 1998, NCEER workshop in which the updates and augmentations to the original "simplified procedure" of Seed and Idriss (1971); Seed et al.1983; and Seed et al (1985) for evaluation of liquefaction potential, are recommended using SPT-based methods and is still followed as the current state of the art on the subject of liquefaction potential evaluation. Cetin (2000) and Cetin et al. (2004) proposed new correlations for assessment of liquefaction triggering in soil.

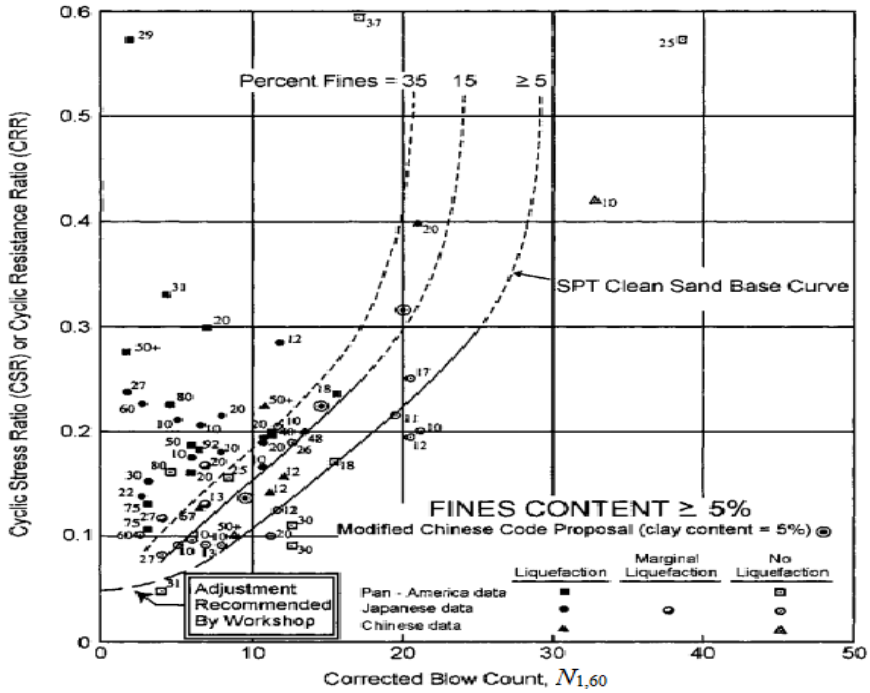

Fig. 2.2 SPT –based limit state boundary curves for Magnitude 7.5 earthquakes with data from liquefaction case histories (Modified from Youd et al. 2001)

These correlations are developed on the basis of an expanded and reassessed post liquefaction SPT database after making screening of field data case histories on a quality/uncertainty basis, incorporating improved knowledge and understanding of factors affecting interpretation of SPT data, using improved understanding of factors affecting site specific earthquake ground motion, implementing improved methods for assessment of in situ *CSR* and using higher order probabilistic tools, Bayesian updating technique. The resulting correlations reduce the uncertainty associated with the liquefaction potential evaluation with respect to the existing models and also resolve controversial issues like magnitude-correlated duration weighting factors, adjustment of fines content and corrections for overburden stress in the context of assessment of *CSR*. Idriss and Boulanger (2004) and Idriss and Boulanger (2006) re-examined the existing semi-empirical procedures for evaluating the liquefaction potential of saturated cohesion-less soils during earthquakes and recommended revised correlations for use in practice. In this paper the authors discussed about the parameters, which contribute to the *CSR* formulation like stress reduction factor, earthquake magnitude scaling factor, overburden correction factor, and also the overburden

normalization factor for penetration resistances and presented the modified relations for these parameters.

CPT-based method

Although, the above SPT-based method remains an important tool for evaluating liquefaction resistance, it has some drawbacks, primarily due to the variable nature of the SPT (Robertson and Campanella, 1985; Skempton, 1986), nowadays the cone penetration test (CPT) is becoming more acceptable as it is consistent, repeatable and able to identify a continuous soil profile. Thus, CPT is being used as a valuable tool for assessing various soil properties, including liquefaction potential of soil. A typical CPT involves pushing a 35.7mm diameter conical penetrometer into the ground at a standard rate of 2cm/sec, while electronic transducers record (generally at 2cm or 5cm intervals) the force on the conical tip, the drag force on a short sleeve section behind the tip, pore water pressure behind the tip (or sometimes at other locations). The tip force is divided by the cross sectional area of the penetrometer to determine the tip resistance, q_c and the sleeve drag force divided by the sleeve surface area to determine the sleeve friction, f_s. The main advantages of the CPT are that it provides a continuous record of penetration resistance and is less vulnerable to operator error than the SPT. The main disadvantages of the CPT are the difficulty in penetrating layers that have gravels or very high penetration resistance and need to perform companion borings or soundings to obtain actual soil samples.

Zhou (1980) first published liquefaction correlation directly based on case history CPT database of the 1978 Tangshan earthquake. He presented the critical value of cone penetration resistance separating liquefiable from non-liquefiable conditions to a depth of 15m. Seed and Idriss (1981) as well as Douglas et al. (1981) proposed the use of correlations between the SPT and CPT to convert the available SPT-based charts for use with the CPT data. Robertson and Campanella (1985) developed a CPT- based method for evaluation of liquefaction potential, which is a conversion from SPT-based method using empirical correlation of SPT-CPT data and follows the same stress-based approach of Seed and Idriss (1971). This method has been revised and updated by many researchers (Seed and de-Alba 1986; Shibata and Teparaksa 1988; Stark and Olson, 1995; Suzuki et al. 1995; Olsen 1997,

Robertson and Wride 1998). Most of the CPT based simplified methods are presented in a chart that defines the limit state function (i.e., a boundary curve) separating the liquefied and non-liquefied cases in a plot of the cyclic resistance ratio (*CRR*) versus corrected CPT tip resistance (*QC*). These methods also need the knowledge of mean particle size (D_{50}) and fines content (*FC*) which cannot be obtained from CPT measurements alone. For determining D_{50} and *FC* additional boreholes are required for collecting samples. Ishihara (1993) suggested that in case of liquefaction resistance evaluated by using CPT value for silty sands (>5% fines), the effects of fines could be estimated by adding some tip resistance increments to the measured tip resistance to obtain an equivalent clean sand tip resistance. For evaluating liquefaction potential only from CPT measurements, Olsen (1997) developed a *CRR* model using the parameters: q_c, σ'_v and friction ratio (R_f). Robertson and Wride (1998) proposed a separate method using soil behaviour type index, I_c, which was recommended for use by the 1998, National Center for Earthquake Engineering Research (NCEER) workshop and is also presented in the summary paper of Youd et al. (2001).Fig. 2.3is used to determine the *CRR* for clean sands [i.e., fines content (*FC*) ≤5%] from CPT data. This chart (i.e., Fig. 2.3) is valid for the magnitude 7.5 earthquake only.

As per Juang et al. (1999a), Robertson and Wride method and Olsen method are found to be quite comparable. Juang et al. (2003) also developed an ANN-based simplified method using soil type index (I_c) for evaluation of *CRR* of soil using post liquefaction CPT database and also used Bayesian mapping function approach to relate F_s with P_L. Moss (2003) and Moss et al. (2005) presented a CPT-based probabilistic model for evaluation of liquefaction potential using reliability approach and a Bayesian updating technique. Juang et al. (2006) used first order reliability method (FORM) for probabilistic assessment of soil liquefaction potential.

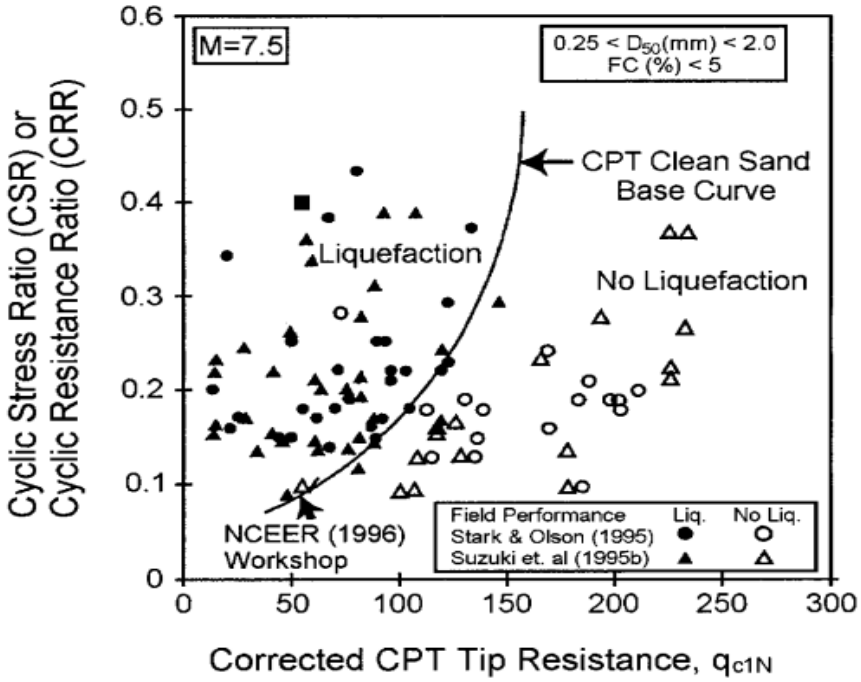

Fig.2.3 Curve recommended for calculation for *CRR* from CPT data (Reproduced from Robertson and Wride 1998).

Shear wave velocity (V_s)-based methods

The use of shear wave velocity (V_s) as a in-situ test index of liquefaction resistance of soil is very well accepted because both V_s and *CRR* are similar, but not proportional, influenced by void ratio, effective confining stresses, stress history, and geologic age. The followings are the main advantages of using V_s for evaluation of liquefaction potential: (i) V_s measurements are possible in soils that are difficult to penetrate with SPT and CPT or difficult to extract undisturbed samples, such as sandy and gravelly soils, and at sites where borings or soundings may not be permitted; (ii) V_s is a basic mechanical property of soil materials, directly related to small-strain shear modulus; and (iii) the small-strain shear modulus is a parameter required in analytical procedures for estimating dynamic soil response and soil-structure interaction analyses. But, the following disadvantages are also there when V_s is used for liquefaction resistance evaluations: (i) seismic wave velocity measurements are made at small strains, whereas pore-water pressure build up and the liquefaction triggering are medium- to high-strain phenomena; (ii) seismic testing does not provide samples for

classification of soils and identification of non-liquefiable soft clay-rich soils; and (iii) thin, low V_s strata may not be detected if the measurement interval is too large. Therefore, it is preferred to drill sufficient boreholes and conduct in-situ tests (SPT or CPT) to detect and demarcate thin liquefiable strata, non-liquefiable clay-rich soils, and silty soils above the ground water table that might become liquefiable should the water table rise. Few V_S-based simplified methods (Dobry et al. 1981; Stokoe et al. 1988; Tokimatsu and Uchida 1990; Robertson et al. 1992; Kayen et al. 1992; Lodge 1994; Andrus and Stokoe 1997; Andrus and Stokoe 2000; Juang et al. 2000a; Juang et al. 2001; Andrus et al. 2003) have been developed and are in use. But as Vs method is of recent origin and has not been verified with the historical post liquefaction database, Vs – based method is not that popular like SPT and CPT–based method.

BPT-based methods

Liquefaction resistance of non-gravelly soils has been assessed mostly through SPT and CPT, with rare V_s measurements. Several investigators have employed large-diameter penetrometers to overcome these difficulties; the Becker penetration test (BPT) in particular has become one of the more effective and widely used larger tools. The BPT was developed in Canada in the late 1950s and consists of a168-mm diameter, 3-m-long double-walled casing driven into the ground with a double-acting diesel-driven pile hammer. The hammer impacts are applied at the top of the casing and the penetration is continuous. The Becker penetration resistance is defined as the number of blows required to drive the casing through an increment of 300 mm. The BPT has not been standardized, and several different types of equipment and procedures have been used. There is currently very few liquefaction sites from which BPT data have been obtained. Thus the BPT cannot be directly correlated with field behaviour, but rather through estimating equivalent SPT N_m-values from BPT data and then applying evaluation procedures based on the SPT. This indirect method introduces substantial additional uncertainty into the calculate *CRR*. But, very few BPT-based simplified methods (Harder and Seed 1986 and Youd et al. 2001) have been developed primarily as it is only suitable for gravelly soil.

2.3 METHODS OF ANALYSIS

The basic analysis criterion in liquefaction potential evaluation is to compare the resistance (*CRR*) of soil with the loading (*CSR*) effects. These liquefaction triggering analyses are carried out using the following three methods based on the importance of the project.

Deterministic method

Probabilistic method

Reliability-based probabilistic method

A brief description and literature pertaining to above methods are presented separately.

2.3.1 Deterministic method

In deterministic approach, the F_s, which is defined as the ratio of *CRR* to *CSR*, is calculated on the basis of prediction of single values of load (*CSR*) and resistance (*CRR*) as shown in the Fig. 2.4 without considering the uncertainty associated in prediction of loading and resistance. It is assumed that there is 100% probability of occurrence of calculated *CRR* and *CSR*. In deterministic approach, F_s>1 corresponds to non-liquefaction and $F_s \leq 1$ corresponds to liquefaction. Here in this approach, only single F_s based on past experience is used to account for all the uncertainties associated with the load and resistance parameters. Though, this method of analysis does not provide adequate information about the behaviour of variables causing liquefaction, is still very much preferred by the geotechnical professionals due to its simple mathematical approach with minimum requirement of data, time and effort.

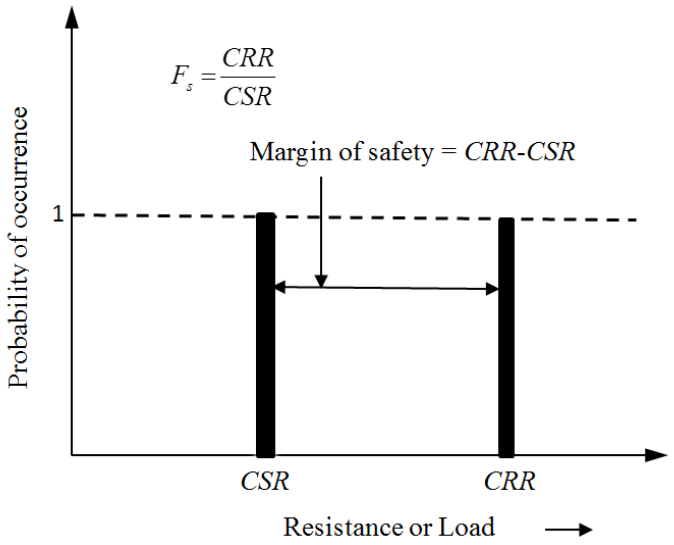

Fig. 2.4 Shows deterministic approach in liquefaction potential evaluation (modified from Becker 1996).

The most commonly used deterministic method to assess the liquefaction potential of a site is the "simplified procedure" originally developed by Seed and Idriss (1971) as discussed in earlier sections. This method has been modified and improved on several occasions for its use in different in-situ tests (Seed et al. 1983; Seed et al. 1985; Robertson and Campanella 1985; Shibata and Teparaksa 1988; Olsen 1997; Robertson and Wride 1998). National Center for Earthquake Engineering Research (NCEER) workshop, 1998, published the reviews of in-situ test-based deterministic methods for evaluation of liquefaction potential of soil (Youd et al., 2001). Factor of safety (F_s) against the occurrence of liquefaction for any earthquake is given by the following relation (Youd et al. 2001):

$$F_s = \left(CRR_{7.5,\sigma=1,\alpha=0} K_\sigma K_\alpha / CSR\right) MSF \tag{2.8}$$

where *CSR*= calculated cyclic stress ratio by using the Eq. (2.4); K_σ is the overburden correction factor and K_α is static shear stress correction factor; $CRR_{7.5}$ is determined from Fig. 2.2; MSF is the magnitude scaling factor used to adjust the *CRR* value to magnitude smaller or larger than 7.5 and it is calculated by using different formulae (Seed and Idriss, 1982; Ambraseys, 1988; Arango, 1996; Andrus and Stokoe, 1997; Youd and Noble,

1997a).The further design decisions for mitigation of liquefaction hazards are taken on the basis of evaluated F_s of a site.

2.3.2 Probabilistic method

Because of the parameter and model uncertainties, in liquefaction potential evaluation, F_s>1 does not always correspond to non-liquefaction that it cannot guarantee a zero chance of occurrence of liquefaction and similarly, $F_s \leq 1$ does not always correspond to liquefaction. This can be explained considering the variability of *CRR* and *CSR* as shown in the Fig. 2.5. If F_s is evaluated considering the mean values of *CRR* and *CSR* then, F_s is greater than1.0. But, as per the distributions of *CSR* and *CRR* shown in the Fig. 2.5,there is some probability that the *CRR* will be less than *CSR* as indicated by the shaded region of the figure, which will yield F_s< 1, proving the previous prediction wrong and a non-liquefied case may turn out to be a liquefied case. Thus, in recent years a lot of work has been done to assess the liquefaction potential in terms of probability of liquefaction (P_L).

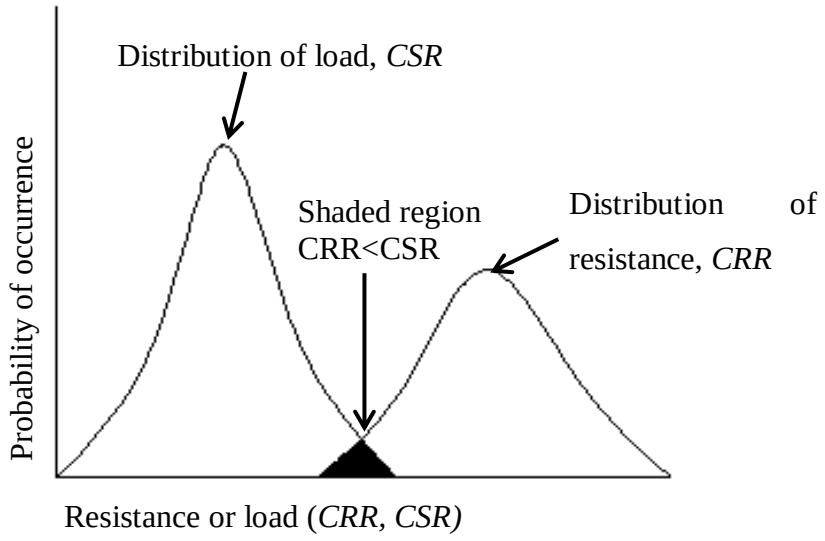

Fig. 2.5 Shows the possible distribution of *CRR* and *CSR* in liquefaction potential evaluation.

Haldar and Tang (1979) carried out second moment statistical analyses of the SPT-based limit state introduced by Seed and Idriss (1971) to estimate the P_L. Fardis and Veneziano (1981) used Bayesian regression technique to develop a model for evaluation of liquefaction

potential of sands using the results of 192 published cyclic simple shear tests taking into account the uncertainties caused by the effect of sample preparation, effect of system compliance, and stress non-uniformities. The developed model is only applicable to uniform and medium clean sands. Fardis and Veneziano (1982) presented a probabilistic method of liquefaction analysis of horizontally layered sand deposits subject to vertically propagating S waves. The method was able to predict well, the probability of liquefaction on the basis of post liquefaction case history of SPT data. Liao et al. (1988) developed logistic regression-based models using post liquefaction field performance database to quantify the probability of liquefaction as a function of parameters such as distance to earthquake, peak horizontal acceleration at the ground surface, normalized *CSR*, depth of ground water table, total vertical stress, effective vertical stress, corrected field SPT *N*-value, fines content, clay content, gravel content, and grain size at 50% passing. Hwang and Lee (1991) used a liquefaction potential probability matrix and a fragility curve based on the moment magnitude to determine probability of no, minor, moderate, and major liquefaction. They considered the uncertainties in both site parameters and seismic parameters to determine various earthquake-site models. The Fourier Acceleration amplitude spectrum (non-linear site response analysis) was used to determine ground motions for each case. A factor of safety based on SPT *N*-values is calculated to evaluate a probability of liquefaction index, which measures the severity of liquefaction. The shear stresses calculated by this method are close to those obtained by using simplified stress-based method pioneered by Seed and Idriss (1971). Youd and Nobble (1997b) and Toprak et al. (1999) used logistic regression analyses of post liquefaction field performance data to develop empirical equations for assessing P_L. Juang et al. (2000b) proposed a Bayesian mapping function based on SPT dataset to relate F_s with P_L. Juang et al. (2002a) found that the Bayesian mapping function approach is better than logistic regression approach for the site specific probability of liquefaction evaluation. The equation for determining liquefaction probability established through logistic regression has nothing to do with any deterministic methods whereas Bayesian mapping function preserves the characteristics of a particular deterministic method under consideration and provides an easy transition from F_s-based design to P_L-based design, thus it is the preferred approach. Juang et al.(2002b) compared three CPT- based

simplified methods, the Robertson method, the Olsen method, and the Juang method on the basis of developed Bayesian mapping functions for the corresponding deterministic methods within probabilistic framework using the case histories obtained from the 1999, Chi-Chi, Taiwan earthquake. They showed that the Juang method is more accurate than the other two methods in predicting the liquefaction potential of soils. Juang et al. (2003) developed a simplified CPT-based method using the Bayesian mapping function approach to relate F_s with P_L.

2.3.3 Reliability-based Probabilistic method

The probabilistic models as discussed above are all data-driven as they are based on statistical analyses of the databases of post liquefaction case histories. Calculation of P_L using these empirical models requires only the mean values of the input variables, whereas the uncertainty in the parameters and the model are excluded from the analysis. Resulting P_L might be subjected to error if the effect of the parameter and model uncertainty is significant. These difficulties can be overcome by adopting reliability based probabilistic analysis of liquefaction, which considers both model and parameter uncertainties.

Juang et al. (1999b) used advanced first order second moment (AFOSM) method to find out the reliability index (β) for liquefied and non-liquefied cases of the database, and developed a relationship between β and P_L using a Bayesian mapping function based on post liquefaction CPT database. They used ellipsoid method (Low and Tang 1997) to carry out the minimization analysis in reliability index calculation. For the reliability analysis authors assumed the coefficient of variation (COV) of the soil and seismic parameters. But, model uncertainty was not considered. Juang et al. (2000d) used AFOSM method with Monte Carlo simulation technique to find out minimum β for liquefied and non-liquefied cases, and also proposed a P_L-F_s relationship based on a Bayesian mapping function approach without considering model uncertainty. Cetin (2000) and Cetin et al. (2004) developed SPT-based probabilistic models for evaluation of liquefaction potential using first order reliability method (FORM) and a Bayesian updating technique. Similarly, Moss (2003) and Moss et al. (2005) presented a CPT-based probabilistic model for evaluation of liquefaction potential

using a mean value first-order second moment (MVFOSM) reliability approach and a Bayesian updating technique. Hwang and Yang (2004) developed a model using MVFOSM reliability analysis to calculate the relation among the probability of liquefaction, the factor of safety and the reliability index. Juang et al. (2006) used first order reliability method (FORM) along with the Bayesian mapping function approach for probabilistic assessment of soil liquefaction potential and carried out extensive sensitivity analyses to characterize uncertainties associated with their developed *CRR* model.

2.4 ANALYSIS TOOLS USED FOR LIQUEFACTION POTENTIAL EVALUATION

As discussed in the previous section, due to difficulty in developing analytical models for liquefaction susceptibility analysis of soil, because of complex constitutive model for liquefied soil, various empirical methods have been developed based on post-liquefaction database of laboratory and in-situ tests. Later, soft computing techniques are found to have better efficiency in developing the empirical models compared to traditional regression techniques. A brief literature on the above techniques and its applications are presented below.

2.4.1 Regression technique

The statistical regression techniques have been used to develop different soil liquefaction evaluation. Seed and Idriss (1971), Seed et al. (1984), Seed et al. (1985), Robertson and Campanella (1985),Shibata and Teparaksa (1988), Olsen (1997), Robertson and Wride (1998), Juang et al. (2000a), and Juang et al. (2003) used statistical regression techniques for development of their empirical models for evaluation of liquefaction potential using laboratory and in-situ test data.

2.4.2 Soft computing techniques

The soft computing techniques such as artificial neural network (ANN), support vector machines (SVM), relevance vector machine (RVM) etc. have been used recently for

liquefaction susceptibility analysis with success and found to have better performance compared to the statistical method. A brief description on application of the above soft computing techniques to the liquefaction evaluation is presented below.

2.4.2.1 Artificial neural network (ANN)

The ANN is a problem solving algorithm modelled on the structure of the human brain. Neural network technology mimics the brain's own problem solving process. The neurons are described as processing elements or nodes in mathematical model of the ANN. A network with an input vector of elements $x_l (l = 1, \ldots, N_i)$ is transmitted through a connection that is multiplied by weight w_{jl} to give the hidden unit $z_j (j = 1, \ldots, N_h)$

$$z_j = \sum_{l=1}^{N_i} w_{jl} x_l + b_{j0} \tag{2.9}$$

Where N_h is the number of hidden units and N_i is the number of input units. The hidden units consist of the weighted input and a bias (b_{j0}). A bias is simply a weight with constant input of 1 that serves as a constant added to the weight. These inputs are passed through a layer of transfer function/activation function f which produces:

$$r_j = f\left[\sum_{l=1}^{N_i} w_{jl} x_l + b_{j0}\right] \tag{2.10}$$

The activation functions are designed to accommodate the nonlinearity in the input-output relationships. Some common activation functions used in ANN are: (a) stepped (b) linear (c) logistic sigmoid and (d) hyperbolic tangent sigmoid (Das 2013). The outputs from hidden units pass another layer of filters, and are fed into another activation function F to produce output y ($k = 1, \ldots, N_o$):

$$y_k = F(v_k) = F\left[\sum_{j=1}^{N_h} w_{kj}\ f\left[\sum_{l=1}^{N_I} w_{jl} x_l + b_{j0}\right] + b_{k0}\right] \tag{2.11}$$

This way it continues depending upon the number of hidden layers and finally the output layer. This multilayer (hidden layer and output layer) with the nonlinear transfer function gives rise to a highly nonlinear function with a number of unknown parameters in terms of weights. Fig. 2.6 shows the typical architecture of a three layer ANN.

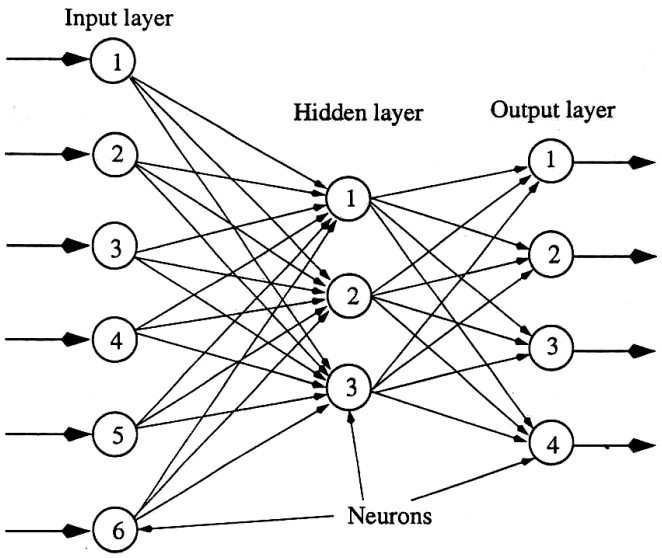

Fig.2.6 Typical architecture of a neural network (Reproduced from Das 2013).

Studies dealing with various engineering applications indicate that the ANN models are not significantly different from a number of statistical models. However, there has been little interaction between the neural network and statistical communities. In general, the problems dealt by ANNs are more complex, and as such, the dimensionality of the models tends to be much higher. The 'learning' or 'training' process in ANN in general, is a nonlinear optimization of an error function. The process is about optimizing the connection weight. This is equivalent to the parameter estimation phase in conventional statistical models. Steepest descent algorithm, which is known as gradient descent algorithm is mostly used in geotechnical engineering. The Levenberg-Marquardt (LM) algorithm is the other optimization used in the implementation of ANN in Geotechnical engineering.

As the characteristic of traditional nonlinear programming based optimization method are the initial point dependent, the results obtained using back propagation algorithm are sensitive to initial conditions (weight vector) (Shahin et al. 2002). The use of global optimization algorithms like genetic algorithm (GA) are also in use in geotechnical engineering (Goh 2002). Goh (2002) used GA to find out the optimum spread of probabilistic network for liquefaction analysis.

Goh (1994) first investigated the feasibility of use of ANN to model the relationship between soil and seismic parameters, and the liquefaction potential. He used a simple back propagation neural-network algorithm. The "best" model consists of eight input variables: corrected SPT value ($N_{1,60}$), fines content(FC), the mean grain size (D_{50}), equivalent dynamic shear stress (τ_{av}/σ'_v), σ_v, σ'_v, M_w, and a_{max}. From the parametric studies, the most important input parameters have been identified as $N_{1,60}$ and FC. The results obtained by the neural network model were compared with that of the statistical method of Seed et al. (1985). The liquefaction classification accuracy of the neural network model was found out to be 95% compared to 84% of Seed et al. (1985). Goh (1996) developed five neural network models to assess liquefaction potential using a post liquefaction CPT database. The sites were from sand and sandy silt deposits in Japan, China, United States and Romania representing the earthquakes that occurred during the period 1964-1983.The "best" model consists of five input variables: measured cone tip resistance q_c, σ'_v, D_{50}, M_w, and a_{max}. The efficiency of the developed model in terms of rate of successful prediction has been compared with that of the existing statistical method of Shibata and Teparaksa (1988), and found that the rate of successful prediction by both the models are equally good (i.e., 97%). From the parametric studies, the most important input parameter has been identified as q_c. Najjar and Ali (1998) used ANN to characterize the soil liquefaction resistance using post liquefaction CPT data obtained from various earthquake sites around the world. They presented a liquefaction potential assessment chart, which can be used by geotechnical professionals for liquefaction potential evaluation. Juang et al. (1999a) developed two ANN-based models to approximate the two existing CPT-based statistical methods: the Robertson method and the Olsen method using the same database. Based on the developed ANN models the rate of successful prediction of both liquefied and non-liquefied cases by Robertson method (89%) was found to be better than that of Olsen method (77%). Juang and Chen (2000a) used Levenberg-Marquardt neural network (LMNN) to a large database of shear wave velocity measurements to establish a limit state boundary that separates the zone of liquefaction from the zone of non-liquefaction. Juang et al. (2000c) developed an ANN-based *CRR* model using 225 cases of post liquefaction CPT data. The developed CPT-based limit state function forms the basis for the development of a reliability-based method for

assessing cyclic liquefaction potential. Goh (2002) used probabilistic neural network (PNN) to develop two separate models for evaluating seismic liquefaction potential based on CPT data and shear wave velocity data, respectively. It was observed that the overall rate of successful prediction of both liquefied and non-liquefied cases were 100% for CPT data and 98% for shear velocity measurement data. Rahman and Wang (2002) developed fuzzy artificial neural network models for assessment of liquefaction potential of a site using SPT-based post liquefaction case histories. The results from the developed models were compared with actual field observations and misclassified cases were identified. The models are found to have good predictive ability and can be used by the geotechnical professionals for preliminary evaluation of liquefaction potential of a site for which the input parameters are not well defined. Juang et al.(2003) used a large CPT-based database to develop an artificial neural network (LMNN) model for predicting the occurrence and non-occurrence of liquefaction in terms of a liquefaction field performance indicator (*LI*) based on derived soil (q_{c1N}, I_c, σ'_v) and seismic parameters ($CSR_{7.5}$). Further, using this ANN-based model a simplified *CRR* model was developed. The developed *CRR* model in conjunction with the existing $CSR_{7.5}$ model forms the deterministic method for evaluation of liquefaction potential where factor of safety is used for taking design decisions. Su and Tak (2006) developed a back propagation ANN model to predict the *CRR* of sands using the data obtained from un-drained cyclic triaxial and cyclic simple shear tests. It was found that the predicted *CRR* values are mostly sensitive to the variations in relative density thus confirming the ability of the developed model to identify the dominant dependence of liquefaction susceptibility on soil density already known from field and laboratory-based experimental observations. Baziar and Jafarian (2007) developed an artificial neural network (ANN)-based model to establish a correlation between soil parameters and the strain energy required to trigger liquefaction in sands and silty sands using a relatively large database of the results of cyclic triaxial, torsional shear and simple shear test. Hanna et al. (2007) developed a general regression neural network (GRNN) model based on 620 cases of post liquefaction SPT data from earthquakes of Turkey and Taiwan, 1999 using 12 soil and seismic input parameters: depth of soil layer (z), $N_{1,60}$, *FC*, depth of ground water table (d_w), σ_v, σ'_v, threshold acceleration (a_t), *CSR*,shear wave velocity (V_s) , internal friction angle of

soil (ϕ'), M_w, and a_{max}. From sensitivity analysis it was observed that $N_{1,60}$ was the most important parameter and V_s is the least significant parameter. Lee and Hsiung (2009) developed an MLP neural network model based on reliable SPT-based case history data to classify the cases of liquefaction and non liquefaction. Excellent performance and good generalization were achieved with overall 96.6% success rate. Using this model sensitivity analyses was made and a_{max} was found out to be the most significant parameter. Juang et al. (2006) developed an ANN-based reliability model using a post liquefaction CPT database. The model uncertainty of the developed limit state model was estimated. Samui and Sitharam (2011) developed a SPT-based ANN model for classification of liquefaction and non-liquefaction cases using post liquefaction database of 1999, Chi Chi Taiwan earthquake. The performance of the developed ANN model in terms of rate of successful prediction of liquefied cases and non-liquefied cases based on an independent database was found out to be 70.58%.

2.4.2.2 Support vector machine (SVM)

Support vector machine (SVM) is an emerging machine learning technology where prediction error and model complexity are simultaneously minimized. Unlike ANN modeling, which is based on biological inspired algorithm, the SVM is based on statistical learning theory. The support vector machine is becoming more popular due to its high generalization ability (Vapnik 1998). However, application of SVM to liquefaction triggering analysis is very much limited (Pal 2006; Goh and Goh 2007; Samui and Sitharam 2011), but it is found to have better generalization capability compared to ANN modeling.

Support Vector Machine (SVM) has originated from the concept of statistical learning theory pioneered by Boser et al. (1992). For liquefaction analysis the SVM is used as a regression technique by introducing a ε-insensitive loss function. In this section, a brief introduction on SVM for regression problem is presented. More details can be found in literature (Boser et al. 1992; Cortes and Vapnik 1995). Considering a set of training data $\{(x_1, y_1),....,(x_l, y_l)\}, x \in R^n, y \in r$. Where x is the input, y is the output, R^N is the N-dimensional vector space and r is the one-dimensional vector space.

The ε-insensitive loss function can be described in the following way

$$L_\varepsilon(y) = 0 \text{ for } |f(x) - y| < \varepsilon \text{ otherwise } L_\varepsilon(y) = |f(x) - y| - \varepsilon \quad (2.12)$$

This defines an ε tube so that if the predicted value is within the tube the loss is zero, while if the predicted point is outside the tube, the loss is equal to the absolute value of the deviation minus ε. The main aim in SVM is to find a function $f(x)$ that gives a deviation of ε from the actual output and at the same time is as flat as possible.

The final equation of SVM can be written as (Vapnik, 1998; Cristianini and Shwae-Taylor 2000; Smola and Scholkopf 2004).

$$f(x) = \sum_{i=1}^{nsv} \left(\alpha_i - \alpha_i^*\right) K\left(x_i . x_j\right) + b \quad (2.13)$$

where α_i, α_i^* are the Lagrangian Multipliers, *nsv* is the number of support vectors and $K(x_i.x_j)$ is kernel function. Some common kernels have been used such as polynomial (homogeneous), polynomial (nonhomogeneous), radial basis function, Gaussian function, sigmoid etc. for non-linear cases.

Pal (2006) developed SVM-based classification models using post liquefaction case histories based on reliable SPT and CPT database and observed that prediction accuracy was 96% and 97% respectively. Goh and Goh (2007) developed SVM model using CPT database and found that the overall liquefaction classification accuracy was 98%. Samui and Sitharam (2011) developed SPT-based SVM model for classification of liquefaction and no-liquefaction using post liquefaction database of 1999, Chi Chi Taiwan and found that the classification accuracy based on an independent dataset was 77.5%, which is better than that of their developed ANN model (70.58%).

2.4.2.3 Relevance vector machine (RVM)

The relevance vector machine (RVM) is a revised SVM tool. It is introduced by Tipping (2001) and is a sparse linear model, which is based on Bayesian formulation of linear model. Samui (2007) developed RVM model using reliable CPT-based liquefaction case history dataset for liquefaction potential assessment and revealed that overall performance was good in prediction, more accurate than ANN model. Das and Samui (2008) examined the potential of RVM-based classification approach to assess the liquefaction potential from the reliable CPT data by developing two models. The liquefaction prediction accuracy for Model-I and Model- II was 100% and 97.14%, respectively.

2.4.2.4 Genetic programming (GP)

In the recent past, genetic programming (GP) based on Darwinian theory of natural selection is being used as an alternate soft computing technique. The GP is defined as the next generation soft computing technique. According to the classification of modeling techniques based on colours (Giustolisi et al. 2007), whose meaning is related to the three levels of prior information required, white-, black-, and grey-box models are in use, each of which can be explained as follows. Black-box models (e.g., ANN, SVM etc.) are data-driven or regressive systems in which the functional form of relationships between model variables is unknown and needs to be estimated. Black-box models depend on data to map the relationships between model inputs and corresponding outputs rather than to find a feasible structure of the model input-output relationships. But, grey-box models are conceptual systems in which the mathematical structure of the model can be derived, allowing further information of the system behavior to be resolved. White-box models are systems that are based on first principles (e.g., physical laws) where model variables and parameters are known and have physical meaning by which the underlying physical relationships of the system can be explained. GP and its variant multi-gene GP (MGGP) can be classified as grey box techniques. Fig. 2.7 is a pictorial representation of the above classification, where higher the physical knowledge used during the model development, the better the physical interpretation of the phenomenon that the model allows the user.

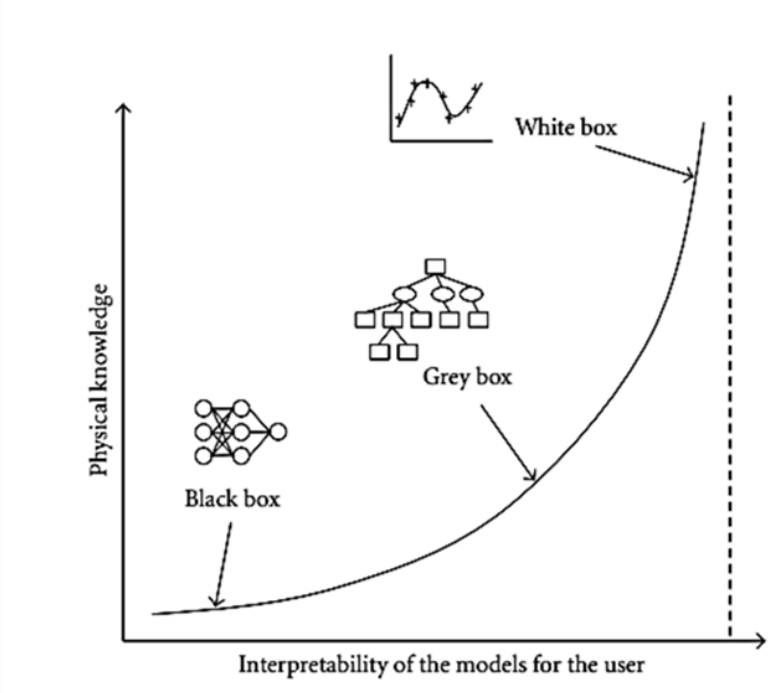

Fig. 2.7 Graphical classifications of soft computing modelling techniques (modified from Giustolisi et al. (2007)

The models developed using GP and its variants have been applied to some difficult geotechnical engineering problems (Yang et al., 2004; Javadi et al. 2006; Rezania and Javadi 2007; Alavi et al. 2011; Gandomi and Alavi 2012b) with success. The main advantage of GP and its variant multi-gene genetic programming (MGGP) over traditional statistical methods and other soft computing techniques is its ability to develop a compact and explicit prediction equation in terms of different model variables. However, its use in liquefaction susceptibility assessment is very limited (Gandomi and Alavi, 2012b). Gandomi and Alavi (2012b) developed a liquefaction classification model using post liquefaction CPT database. The overall classification accuracy of their model is 91.6%, which is considered to be very good. But, the performance of the developed model has not been compared with that of the existing models based on other soft computing techniques. The developed model has not also been tested with independent dataset other than testing data.

2.5 CONCLUSION

The following conclusions are drawn from the above literature study.

i. Though conceptually the energy-based approach is more appropriate for liquefaction potential evaluation, it is less commonly used than the cyclic stress-based approach due to non-availability of quality data for calibration of the developed models.

ii. The cyclic strain-based approach is less commonly used than the cyclic stress-based approach as the cyclic strain amplitudes cannot be predicted as accurately as cyclic stress amplitudes, and due to unavailability of equipment for cyclic strain-controlled testing.

iii. Though, evaluation of liquefaction potential based on laboratory test yields good results many geotechnical engineers prefer to adopt the field performance correlation-based approach because of great difficulty and cost involved in obtaining high quality undisturbed samples from cohesionless soil deposits.

iv. Out of the various in-situ methods SPT and CPT-based methods are widely used for liquefaction susceptibility analysis of soil due to availability of sufficient post liquefaction database of these methods.

v. Though, deterministic method of liquefaction potential is preferred by the geotechnical professionals but, probabilistic evaluation is very much required in actual practice, which helps in taking risk-based design decisions.

vi. For making an unbiased evaluation of liquefaction potential, the uncertainty of the limit state boundary surface is to be determined for which rigorous reliability analyses are required.

vii. Though, various soft computing techniques such as ANN, SVM, and RVM are in use and performing well in predicting the liquefaction susceptibility of soil the ANN has poor generalization. The SVM has better generalization compared to ANN, but the parameters ‘C’ and insensitive loss function (ε) needs to be fine tuned by the user. Moreover, these techniques will not

produce a comprehensive relationship between the inputs and output and are also called as ‘black box’ system.

Chapter 3

GENETIC PROGRAMMING AS AN ANALYSIS TOOL

3.1 INTRODUCTION

In the present study, multi-gene genetic programming (MGGP), the variant of GP is used to develop different prediction models for evaluation of liquefaction potential of soil within the framework of deterministic, probabilistic and reliability-based approach. As discussed in previous chapter, GP and its variant, MGGP have been used in limited geotechnical engineering problems and are not very common to geotechnical engineering professionals, hence, a detailed description is presented as follows.

3.2 GENETIC PROGRAMMING

Genetic Programming is a pattern recognition technique where the model is developed on the basis of adaptive learning over a number of cases of provided data, developed by Koza (1992). It mimics biological evolution of living organisms and makes use of the principles of genetic algorithms (GA). In traditional regression analysis the user has to specify the structure of the model, whereas in GP, both structure and the parameters of the mathematical model are evolved automatically. It provides a solution in the form of a tree structure or in the form of a compact equation using the given dataset. A brief description about GP is presented here for the completeness, but the details can be found in Koza (1992).

GP model is composed of nodes, which resembles a tree structure and thus, it is also known as GP tree. Nodes are the elements either from a functional set or terminal set. A functional set may include arithmetic operators (+, ×, ÷, or -), mathematical functions (sin (.), cos (.), tanh (.) or ln(.)), Boolean operators (AND, OR, NOT, etc.), logical expressions (IF, or THEN) or any other suitable functions defined by the user. The terminal set includes variables (like x_1, x_2, x_3, etc.) or constants (like 3, 5, 6, 9, etc.) or both. The functions and

terminals are randomly chosen to form a GP tree with a root node and the branches extending from each function nodes to end in terminal nodes as shown in Fig.3.1.The GP tree as shown in Fig. 3.1 presents a mathematical expression: tan ($6.5x_2/x_1$). Here the variables: x_1, x_2, and constant: 6.5 constitute the terminal nodes and the arithmetic operators: ×, / and the mathematical function: tan, constitute the functional nodes. The starting functional node (tan) from which the branching of other nodes begins with the GP tree is called the root node.

Initially a set of GP trees, as per user defined population size, is randomly generated using various functions and terminals assigned by the user. The fitness criterion is calculated by the objective function and it determines the quality of each individual in the population competing with the rest. At each generation a new population is created by selecting individuals as per the merit of their fitness from the initial population and then, implementing various evolutionary mechanisms like reproduction, crossover and mutation to the functions and terminals of the selected GP trees. The new population then replaces the existing population. This process is iterated until the termination criterion, which can be either a threshold fitness value or maximum number of generations, is satisfied. The best GP model, based on its fitness value that appeared in any generation, is selected as the result of genetic programming. A brief description of various evolutionary mechanisms in GP is presented below.

3.2.1 Initial Population

In the first step of genetic programming a number of GP trees are generated by randomly selecting user defined functions and terminals. These GP trees form the initial population.

3.2.2 Reproduction

In the second stage of the GP, a proportion of the initial population is selected and copied to the next generation and this procedure is called reproduction. The reproduction mechanism does not produce any new population. The generated GP trees of initial population are evaluated based on the fitness function and less than average populations are replaced by copies of the above average population thereby keeping the population size constant. So the

GP tree with high fitness enter the mating pool and the remaining ones die off. There are different operators of reproduction like: (1) Tournament selection, (2) Roulette wheel selection (3) Ranking selection. The number of the population taking part in the selection procedure is guided by a probability constant P_s.

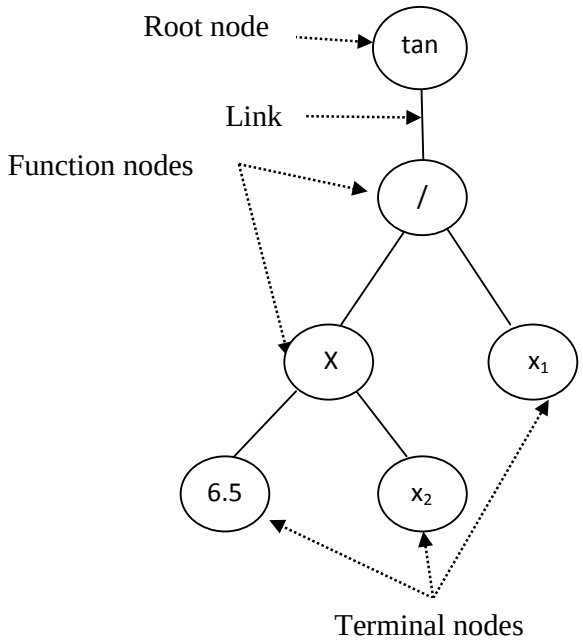

Fig.3.1 Typical GP tree representing a mathematical expression: tan $(6.5x_2/x_1)$.

3.2.2.1 Tournament selection

In this selection procedure, tournaments are played between a specific numbers of GP trees. The tournament size represents the number of GP trees taking part in the tournament. The winner survives and gets more number of copies and the looser does not go to the next generation.

3.2.2.2 Roulette Wheel Selection

Parents are selected according to their fitness. The better the GP trees are, the more chances they have, to be selected. This procedure is explained taking example of a Roulette wheel where all the GP trees in the population are placed. The size of the section in the Roulette wheel is proportional to the value of the fitness function of every GP tree - the bigger the value is, the larger the section is as shown in Fig. 2.2. A marble is thrown in the roulette wheel and the GP tree where it stops is selected. Clearly, the GP tree with bigger fitness value will be selected more times.

This process can be described by the following steps.

Step 1. Calculate the sum of all GP tree fitness in population; sum =*S*.

Step 2.Generate random number ***r*** from the interval (0, *S*)

Step 3.Go through the population and sum the fitness from 0 to sum S_i. When the sum S_i is greater then ***r***, stop and return the i^{th} GP tree.

Step 4. Repeat step 2 and 3

Of course, the step 1 is performed only once for each population.

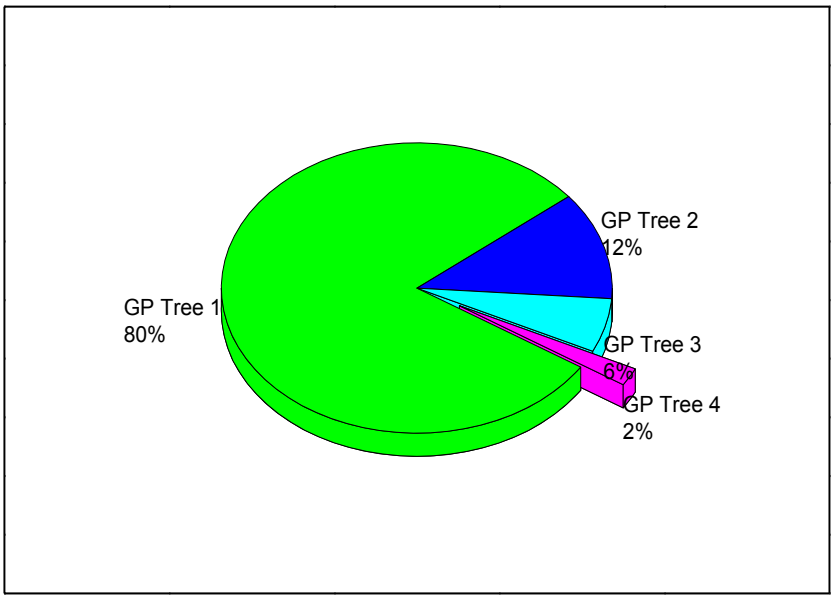

Fig.3.2 Roulette wheel showing the area of fitness of different GP trees

3.2.2.3 Ranking selection

The Roulette wheel selection will have problems when there are big differences between the fitness values. For example, if the best GP tree fitness is 90% of the sum of all fitness then the other GP trees will have very few chances to be selected. Ranking selection ranks the population first depending upon their respective fitness, and then every GP trees is assigned revised fitness value determined by this ranking. The worst will have the fitness 1, the second worst 2 etc. and the best will have fitness *N* (number of GP trees in population). Fig. 3.3 shows an example of the ranking selection procedure in which the initial fitness of the GP trees are 80, 12, 6 and 2 respectively. So the ranks assigned to the GP trees are 4, 3, 2 and 1 respectively. So the average ranking value is 2.5 and the revised fitness of the GP trees are obtained by dividing the ranks by the average ranking value (2.5) as 1.6, 1.2, 0.8 and 0.4 corresponding to 80, 12, 6 and 2, respectively. The final GP tree as per ranking selection is shown in Fig. 3.3. Now all the GP trees have a chance to be selected. However this method can lead to slower convergence, because the best GP tree does not differ so much from other ones.

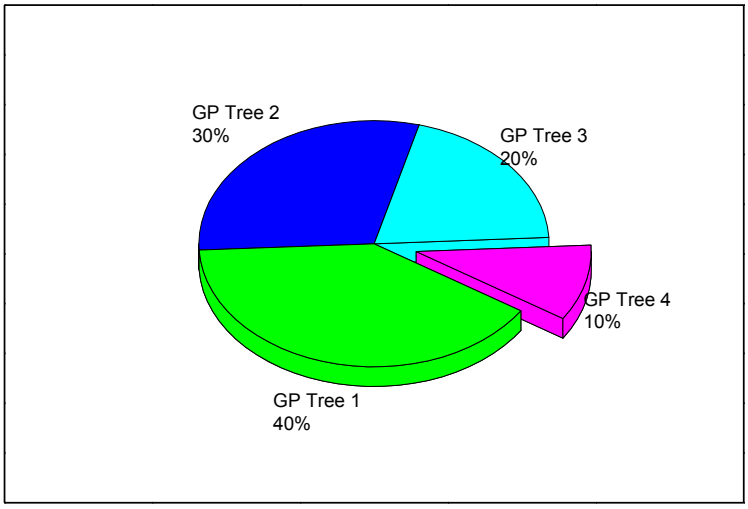

Fig.3.3 The area of fitness of different GP trees as per ranking selection

3.2.3 Crossover

In crossover operation, two GP trees (Parent1 and Parent2) are selected randomly from the population in the mating pool (Koza 1992). One node from each tree is selected randomly, the sub-trees under the selected nodes are swapped and two offspring (Offspring1 and Offspring 2) are generated. An example of crossover operation is shown in Fig. 3.4.

3.2.4 Mutation

In mutation operation a GP tree is first selected randomly from the population in the mating pool and any node of the tree is replaced by any other node from the same function or terminal set. A function node can replace only a function node and the same principle is applicable for the terminal nodes. An example of mutation operation is shown in Fig. 3.5 in which the functional node, "/" of the GP tree representing a mathematical expression: $\tan(x_1/x_2)$ is replaced by another functional node, "×" and thus, a new GP tree representing a mathematical expression: $\tan(x_1 \times x_2)$ is produced.

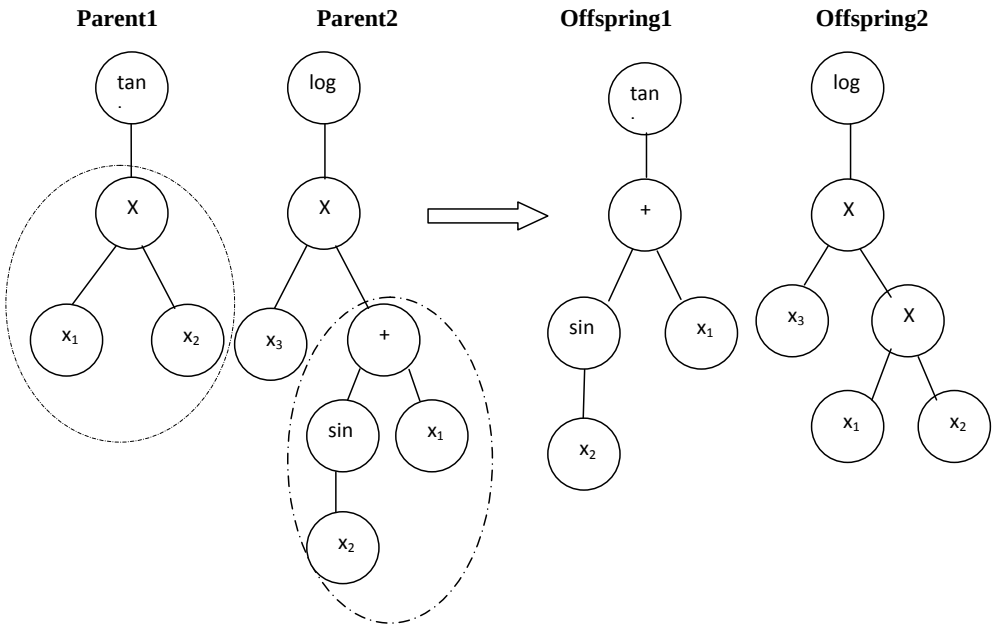

Fig. 3.4 A typical crossover operation in GP

Fig. 3.6 shows a typical flow diagram of MGGP procedure in which N_{gen} is the number of generation, P_s, P_c, and P_m are the probability of reproduction, crossover and mutation respectively.

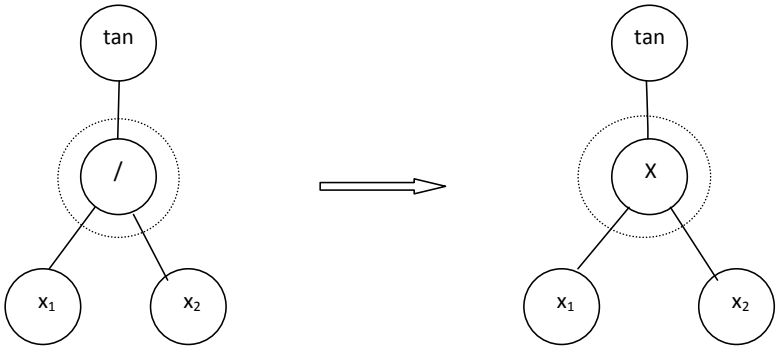

Fig. 3.5 A typical mutation operation in GP

3.3 MULTI-GENE GENETIC PROGRAMMING

MGGP is a variant of GP and is designed to develop an empirical mathematical model, which is a weighted linear combination of a number of GP trees. It is also referred to as symbolic regression. Each tree represents lower order non-linear transformations of input variables and is called a 'gene'. "Multi-gene" refers to the linear combination of these genes. Fig. 3.6 shows a typical flow diagram of MGGP procedure in which N_{gen} is the number of generation, $P_{s,}$ P_{c}, and P_{m} are the probability of reproduction, crossover and mutation, respectively.

Fig. 3.7 shows an example of MGGP model where the output is represented as a linear combination of two genes (Gene-1 and Gene- 2) that are developed using four input variables (x_1, x_2, x_3, x_4).Each gene is a nonlinear model as it contains nonlinear terms (sin(.) /log(.)). The linear coefficients (weights) of Gene-1 and Gene-2 (c_1 and c_2) and the bias (c_0) of the model are obtained from the training data using statistical regression analysis (ordinary least square method).

In MGGP procedure, initial population is generated by creating individuals that contain randomly evolved genes from the user defined functions and variables. In addition to the

standard GP evolution mechanisms as discussed earlier there are some special MGGP crossover mechanisms (Searson et al. 2010), which allow the exchange of genes between individuals and brief descriptions of them are presented as follows.

3.3.1 Two point high-level crossover

Two point high level crossover operation allows swapping of genes between two parent individuals in the mating pool and can be explained through an example, where the first parent individual is having four genes [G_1, G_2, G_3, G_4] and the second contains three genes [G_5, G_6, G_7] with G_{max} as 5. Two crossover points are selected randomly for each parent and genes enclosed by crossover points are denoted by {...}.

[G_1, {G_2, G_3, G_4}], [G_5, G_6,{G_7}]

The genes enclosed by the crossover points are swapped and thus, two offspring individuals are created as shown below.

[G_1, {G_7}], [G_5, G_6, {G_2, G_3, G_4}]

If swapping of genes results in an individual containing more genes than G_{max} then genes are randomly selected and removed until the individual contains G_{max} genes.

3.3.2 Low-level crossover

Standard GP sub-tree crossover is referred to as low level crossover. In this operation, first a gene is randomly selected from each of the parent individuals (any two) in the mating pool and then swapping of sub-trees under arbitrarily selected nodes of each gene is performed. The resulting trees replace the parent trees in the otherwise unchanged parent individuals, which go on to produce offspring individuals for the next generation without any deletion of genes.

Similarly, MGGP also provides six methods of mutation for genes (Gandomi and Alavi 2012a): (i) sub-tree mutation, (ii) mutation of constants using additive Gaussian perturbation, (iii) substitution of a randomly selected input node with another randomly

selected input node, (iv) substitute a randomly selected constant with another randomly generated constant (v) setting of randomly selected constant to zero, (vi) setting a randomly selected constant one.

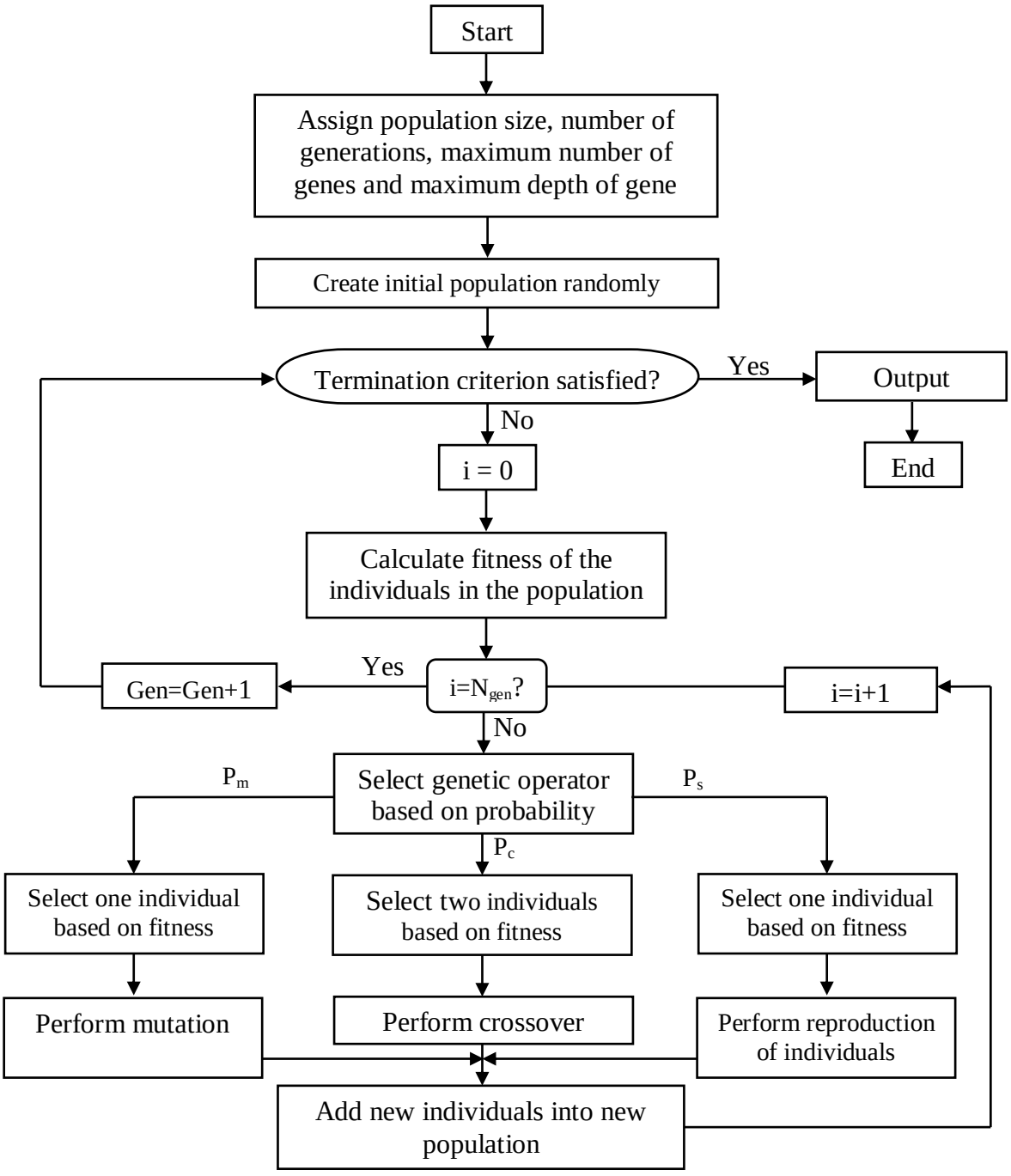

Fig. 3.6 A typical flow diagram for a multi-gene genetic programming procedure

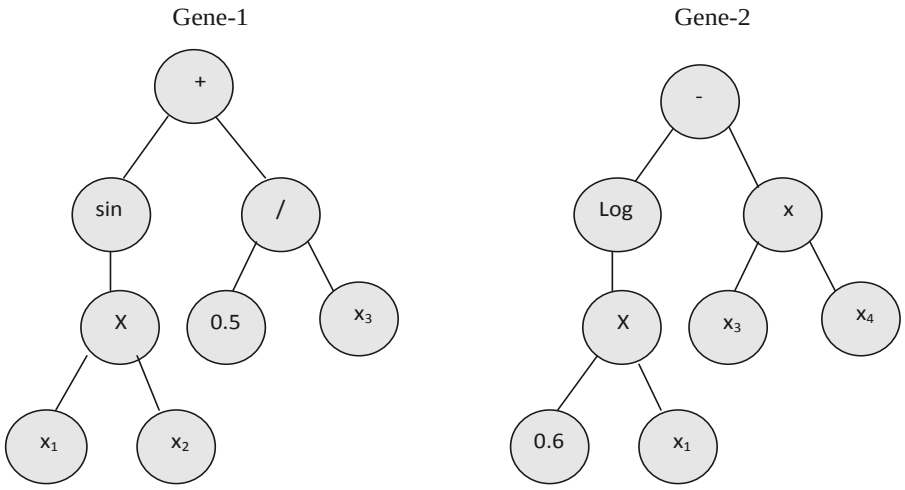

$$y = c_0 + c_1\left(sin\left(x_1 x_2\right) + \frac{0.5}{x_3} \right) + c_2\left(Log\left(0.6x_1\right) - x_3 x_4\right)$$

Fig. 3.7 An example of typical multi-gene GP model.

The probabilities of the each of the re-combinative processes (evolutionary mechanisms) can be set by the users for achieving the best MGGP model. These processes are grouped into categories referred to as events. Therefore, the probability of crossover, mutation and the direct reproduction event are to be specified by the user in such a way that the sum of these probabilities is 1.0. The probabilities of the event subtypes can also be specified by the user. For example, once the probability of crossover event is selected, it is possible to define the probabilities of a two point high-level crossover and low-level crossover keeping in mind that the sum of these event subtype probabilities must be equal to one.

Various controlling parameters such as function set, population size, number of generations, maximum number of genes allowed in an individual (G_{max}), maximum tree depth (d_{max}), tournament size, probabilities of crossover event, high level crossover, low level crossover, mutation events, sub-tree mutation, replacing input terminal with another random terminal, Gaussian perturbation of randomly selected constant, reproduction, and ephemeral random constants are involved in MGGP predictive algorithm. The generalization capability of the model to be developed by MGGP is affected by selection of these controlling parameters.

These parameters are selected based on some previously suggested values (Searson et al. 2010) and after following a trial and error approach for the problem under consideration. The function set (arithmetic operators, mathematical functions etc.) is selected by the user on the basis of physical knowledge of the system to be analysed. The number of programs or individuals in the population is fixed by the population size. The number of generation is the number of times the algorithm is used before the run terminates. The proper population size and number of generations often depend on the complexity of the problems. A fairly large number of population and generations are tested to find the best model. The increase in G_{max} and d_{max} value increases the fitness value of training data whereas the fitness value of testing data decreases, which is due to the over-fitting to the training data. The generalisation capability of the developed model decreases. Thus, in the MGGP-model development it is important to make a tradeoff between accuracy and complexity in terms G_{max} and d_{max}. There are optimum values of G_{max} and d_{max}, which produce a relatively compact model (Searson et al. 2010). The success of MGGP algorithm usually increases by using optimal values above of controlling parameters.

In the MGGP procedure a number of potential models are evolved at random and each model is trained and tested using the training and testing data respectively. The fitness of each model is determined by minimizing the root mean square error (*RMSE*) between the predicted and actual value of the output variable (*LI)* as the objective function (*f*),

$$RMSE = f = \sqrt{\frac{\sum_{i=1}^{n}\left(LI - LI_p\right)^2}{n}} \tag{3.1}$$

where n = number of cases in the fitness group. If the errors calculated by using Eq. (4.5) for all the models in the existing population do not satisfy the termination criteria, the evolution of a new generation of the population continues till the best model is developed as discussed earlier.

The general form of the MGGP based model of the present study can be presented as:

$$LI_p = \sum_{i=1}^{n} F\left[X, f(X), c_i\right] + c_0 \tag{3.2}$$

where LI_p = predicted value of liquefaction field performance indicator (LI), F = the function created by the MGGP referred herein as liquefaction index function, X = vector of input; c_i is a constant, f are the functions defined by the user, n is the number of terms of target expression and c_0= bias. The MGGP as per Searson et al. (2010) is used and the present models are developed and implemented using Matlab (Math Work Inc. 2005).

As discussed in previous chapter, though GP has been used in some limited application in geotechnical engineering, there are only two applications of MGGP in geotechnical engineering (Gandomi and Alavi 2012a, 2012b). In this study an initial attempt was made to compare the efficiency of the MGGP with ANN, SVM (Muduli et al. 2013). The efficacy of MGGP-based predictive model for uplift capacity of suction caisson outperformed the other soft computing technique-based (ANN, SVM, RVM) prediction models in terms of different statistical performance criteria.

3.4 CONCLUSIONS

The MGGP, a variant of GP is a biologically inspired algorithm with different operators like, reproduction, crossover and mutation. Unlike ANN and SVM, it has the advantage of obtaining a comprehensive expression for the output from the inputs for further analysis. A trade off is to be made between the complexity and accuracy of the method. There is a very limited application of MGGP in Geotechnical engineering. Based on preliminary study on application of MGGP to uplift capacity of suction pile, it has been observed that the performance of MGGP model is better than ANN, SVM and RVM models. Hence, in this thesis an attempt has been made in the following chapters to develop models for evaluation of liquefaction potential within the frame work of deterministic, probabilistic and reliability-based methods using MGGP.

Chapter 4
DETERMINISTIC MODELS FOR EVALUATION OF LIQUEFACTION POTENTIAL

4.1 INTRODUCTION

Though, different approaches like cyclic stress-based, cyclic strain-based, and energy-based approach are in use, the stress-based approach is the most widely used method for evaluation of liquefaction potential of soil (Krammer 1996). The SPT is the most widely used in situ test-based soil exploration method for liquefaction potential evaluation but, it has some drawbacks, primarily due to the variable nature of the SPT used around the world. Now a days cone penetration test (CPT) is also becoming more acceptable as it is consistent, repeatable and able to identify continuous soil profile.

Soft computing techniques such as artificial neural network (ANN), support vector machine (SVM), and relevance vector machine (RVM) have been used to develop liquefaction prediction models based on in-situ test database, which are found to be more efficient compared to statistical methods. The advantages and disadvantages of the above techniques have already been discussed in Chapter-I.

In the present study, an attempt has been made using MGGP to present a deterministic model based on post liquefaction SPT database (Hwang and Yang 2001). A limit state function that separates liquefied cases from the non-liquefied cases and also represents cyclic resistance ratio (*CRR*) of soil is developed by using MGGP. The developed *CRR* model in conjunction with widely used $CSR_{7.5}$ (Juang et al. 2000) is used to evaluate liquefaction potential in terms of F_s. Using an independent SPT dataset, a comparative study among the present MGGP model, available ANN and statistical models is also made in terms of rate of successful prediction of liquefaction and non-liquefaction cases based on F_s.

Similarly, an attempt has also been made to predict the liquefaction potential of soil in terms of liquefaction field performance indicator referred as liquefaction index (*LI*) (Juang et al. 2003) on the basis of a large database consisting of post liquefaction CPT measurements and field manifestations using MGGP. Two different MGGP models (Model-I and Model-II) are developed for predicting occurrence and non-occurrence of liquefaction taking different combination of input parameters. The parameters of Model-I are kept same as that of ANN model (Juang et al. 2003) to compare the efficacy of both the models in terms of rate of successful prediction of liquefaction and non- liquefaction. These parameters are further used for development of cyclic resistance ratio (*CRR*) model using MGGP similar to the most widely used statistical model of Robertson and Wride (1998) and ANN-based *CRR* model of Juang et al. (2003). In Model-II, the primary soil and seismic parameters of the CPT database are used to present a simple model that can easily be used by the practicing engineers. Goh and Goh (2007) have used the same parameters of the above database (Juang et al. 2003) for prediction of liquefaction susceptibility using SVM. Hence, liquefaction classification accuracies of the developed Model -II are compared with that of the SVM model of Goh and Goh (2007). Performances of the proposed MGGP based models (Model-I and Model-II) in terms of rates of successful prediction of liquefaction and non-liquefaction as per predicted *LI* values are also verified using an independent CPT database (Juang et al. 2006).The developed MGGP-based *CRR* model in conjunction with widely used $CSR_{7.5}$ (Juang et al. 2000) is used to evaluate liquefaction potential in terms of F_s. Similarly as mentioned above, using an independent CPT dataset (Juang et al. 2006), a comparative study among the present MGGP model, available ANN and statistical models is also made in terms of rate of successful prediction of liquefaction and non-liquefaction cases based on F_s.

4.2 DEVELOPMENT OF SPT-BASED DETERMINISTIC MODEL

The general form of MGGP-based model for LI_p based on SPT database can be presented here as:

$$LI_p = \sum_{i=1}^{n} F\left[X, f(X), c_i\right] + c_0 \tag{4.1}$$

where, LI_p= predicted value of liquefaction index (*LI*), F = the function created by the MGGP process referred herein as liquefaction index function, X = vector of input variables = $\{N_{1,60}, CSR_{7.5}\}$ where, $N_{1,60}$ = corrected blow count. Here in the present study, the general formulation of *CSR* as presented by Seed and Idriss (1971) and by Youd et al. (2001) is adopted with minor modification, i.e., *CSR* is adjusted to the benchmark earthquake (moment magnitude, M_w, of 7.5) by using the parameter, magnitude scaling factor (MSF).

$$CSR_{7.5} = 0.65\left(\frac{\sigma_v}{\sigma_v'}\right)\left(\frac{a_{max}}{g}\right)(r_d)\Big/MSF \tag{4.2}$$

where a_{max}= peak horizontal ground surface acceleration, g = acceleration due to gravity, r_d = shear stress reduction factor which is determined as per Youd et al. (2001):

$$r_d = 1.0 - 0.00765\,z, \text{for } z \le 9.15\text{m}$$

$$= 1.174 - 0.0267z, \quad \text{for } 9.15 \le z \le 23\text{m} \tag{4.3}$$

where *z* is depth under consideration.

The adopted MSF equation is presented below according to Youd et al. (2001).

$$MSF = \left(\frac{M_w}{7.5}\right)^{-2.56} \tag{4.4}$$

c_i is a constant, f is MGGP function defined by the user, n is the number of terms of model equation and c_0 is the bias. It is pertinent to mention here that Juang et al. (2000) also followed the above *CSR* formulation for development of their ANN-based *CRR* model. The MGGP as per Searson et al. (2010) is used and the present model is developed and implemented using Matlab (MathWorks Inc. 2005).

4.2.1 Database and preprocessing

In the present study, SPT-based dataset of post liquefaction case histories of Chi Chi, Taiwan, earthquake, 1999 is used (Hwang and Yang 2001). It contains information about soil and seismic parameters: measured SPT blow count (N_m), corrected blow count ($N_{1,60}$), fines content (FC),clay size content (CC), mean grain size (D_{50}), peak horizontal ground surface acceleration (a_{max}) and $CSR_{7.5}$, which are obtained from the SPT measurements at different sites of Taiwan along with field performance observations (LI). The soil in these cases ranges from sand to silty sand to sandy and clayey silt. The depths at which SPT measurements are reported in the database range from 1.3m -20.3m. The N_m values range from 01 to 50 and the $N_{1,60}$ values range from 0.93 to 49.29. The FC and CC values are in the range of 4-65% and 0-23% respectively. The $a_{\max}$ and $CSR_{7.5}$values are in the range of [0.055, 1g] and [0.041, 0.822] respectively. The moment magnitude, M_w of the 1999, Chi Chi, Taiwan, earthquake was 7.6. The database consists of total 288 cases, 164 out of them are liquefied cases and other 124 are non-liquefied cases. Out of the above data 202 cases are randomly selected for training and remaining 86 data are used for testing the developed model. Samui and Sitharam (2011) also used the above databases with the above number of training and testing data while developing ANN and SVM-based liquefaction classification models. Here, in the MGGP approach normalization or scaling of the data is not required which is an advantage over ANN and SVM approach.

4.2.2 Results and discussion

In this section, the result of deterministic model based on post liquefaction SPT database is presented. A limit state function that separates liquefied cases from the non-liquefied cases and also represents cyclic resistance ratio (CRR) of soil is also developed by using MGGP. The developed CRR model in conjunction with widely used $CSR_{7.5}$ (Juang et al. 2000) is used to evaluate liquefaction potential in terms of F_s and the results are presented in following sequence.

4.2.2.1 MGGP Model for Liquefaction Index

The MGGP-based model for liquefaction index is developed taking *LI* = 1 for liquefaction and *LI* = 0 for non-liquefaction field manifestations. In the MGGP procedure a number of potential models are evolved at random and each model is trained and tested using the training and testing cases respectively. The fitness of each model is determined by minimizing the *RMSE* between the predicted and actual value of the output variable (*LI)* as the objective function or the error function (E_f),

$$RMSE = E_f = \sqrt{\frac{\sum_{i=1}^{n}\left(LI - LI_p\right)^2}{n}} \tag{4.5}$$

where n = number of cases in the fitness group. If the errors calculated by using Eq. (4.5) for all the models in the existing population do not satisfy the termination criteria, the evolution of a new generation of the population continues till the best model is developed as discussed earlier in Chapter-III.

The selection of controlling parameters (as mentioned in Chapter-III) affects the efficacy of the model generated by the MGGP. Thus, optimum values of the parameters are selected for the development of LI_p model based on some previously suggested values (Searson 2009; Searson et al. 2010) and after following a trial and error approach and are presented in Table 4.1.

Using the optimum values of controlling parameters as given in the Table 4.1 different LI_p models were developed running the MGGP code several times. These models are analyzed with respect to physical interpretation of LI_p as well as their rate of successful prediction capability and the "best" LI_p model was selected. The developed model is presented below as Eq. (4.6).

$$LI_p = 2.824\tanh\left(8.2CSR_{7.5}\right) - 5.152\tanh\left(\frac{CSR_{7.5}}{N_{1,60}}\right) + 1.5\times10^{-5}\left(\frac{N_{1,60}}{CSR_{7.5}}\right)^2 - \frac{0.089N_{1,60}}{\exp\left(CSR_{7.5}\right)} - 0.964 \quad (4.6)$$

Table 4.1 Controlling parameter settings for MGGP-based LI_p model development.

Parameters	Ranges	Resolution	Selected optimum values
Population size	1000-4000	200	3000
Number of generations	100-300	50	150
Maximum number of genes (G_{max})	2-4	1	3
Maximum tree depth (d_{max})	2-5	1	4
Tournament size	2-8	1	7
Reproduction probability	0.01-0.07	0.02	0.05
Crossover probability	0.75-0.9	0.05	0.85
Mutation probability	0.05-0.15	0.05	0.1
High level cross over probability	0.1-0.4	0.1	0.2
Low level cross over probability	0.5-0.9	0.1	0.8
Sub-tree mutation	0.6-0.9	0.05	0.85
Substituting input terminal with another random terminal	0.05-0.2	0.05	0.05
Gaussian perturbation of randomly selected constant	0.05-0.2	0.05	0.1
Ephemeral random constant	[-10 10]	-	-

The developed LI_p model has been characterized by the Figs. 4.1, 4.2, 4.3. Fig. 4.1 shows the variation of the best fitness (log values) and mean fitness with with number of generations. It can be seen from this figure, the fitness values decrease with increasing the number of generations and its decrements. The best fitness was found at the 143rd generation (fitness =0.2466).The statistical significance of each of the four genes of the developed model is shown in Fig. 4.2. As shown in the Fig. 4.2a the weight (coefficient) of the the gene-2 is higher than the other genes and bias. The degree of significance of each gene using *p* values is also shown in Fig. 4.2b. It can be noted that the contribution of all the genes towards prediction of *LI*(i.e., LI_p) is very high except the Gene-2, as their corresponding *p* values are

very low, whereas the Gene-2 contribution is the least. Fig. 4.3 presents the population of evolved models in terms of their complexity (number of nodes) and fitness value.The developed models that perform relatively well with respect to the "best" model and are much less complex (having less number of nodes) than the "best" model in the population can be identified in this figure as green circles. The "best" model in the population is highlighted with a red circle.

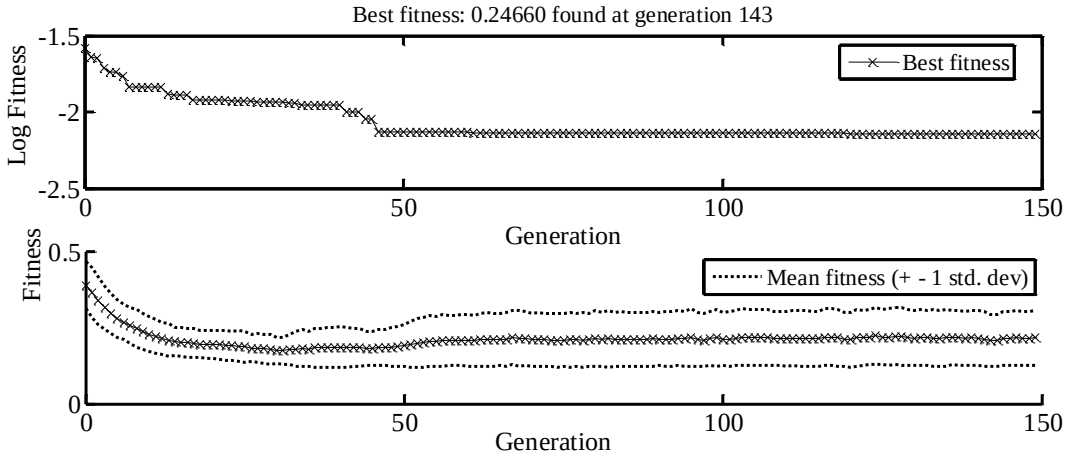

Fig. 4.1 Variation of the best and mean fitness with the number of generation.

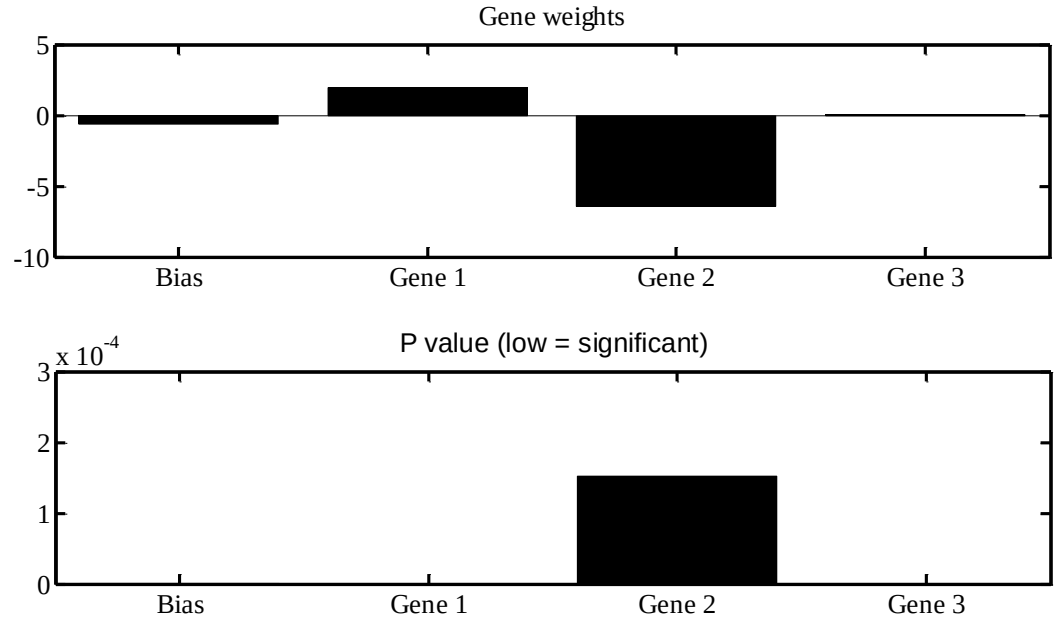

Fig.4.2 Statistical properties of the evolved MGGP-based LI_p model (on training data)

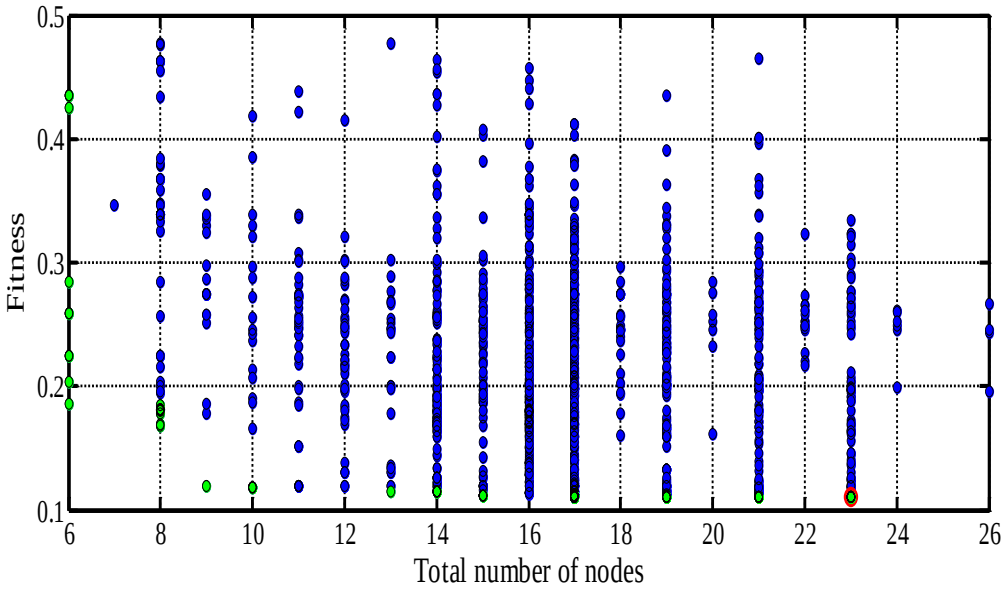

Fig 4.3 Population of evolved models in terms of their complexity and fitness.

Table 4.2 Comparison of results of developed MGGP based LI_p model with ANN and SVM models of Samui and Sitharam (2011)

Model	Input variables	Performance in terms of successful prediction (%)					
		MGGP	ANN	SVM	MGGP	ANN	SVM
		Training data			Testing data		
LI	$N_{1,60}$, $CSR_{7.5}$	94.55	94.55	96.04	94.19	88.37	94.19

A prediction in terms of LI_p is said to be successful if it agrees with field manifestation (LI) of the database. As per Table 4.2, the successful prediction rates of liquefied and non-liquefied cases are comparable, 94.55% for training and 94.19% for testing data, showing good generalization of the developed model. The overall success rate of the trained model in predicting liquefaction and non-liquefaction cases is 94.44%.Thus, it is evident from the results that the proposed MGGP based LI_p model is able to establish the complex relationship between the liquefaction index and its main contributing factors in terms of a model equation with a very high accuracy. In comparison, the classification accuracy of the ANN model was 94.55% and 88.37% for training and testing data respectively for the above

database as presented by Samui and Sitharam (2011). Similarly, the liquefaction classification accuracies for SVM model (Samui and Sitharam 2011) for training and testing dataset are 96.04% and 94.19% respectively. The efficiency of different models should be compared in terms of testing data than that with training data (Das and Basudhar 2008). Thus, it is found that MGGP-based prediction model (Eq.4.6) is better than the ANN-base model and at par with SVM-based model on the basis of rate of successful prediction of liquefaction and non-liquefaction cases. This LI_p model is further used to develop the proposed *CRR* model.

4.2.2.2 Generation of artificial points on the limit state curve

As discussed earlier artificial data points on the boundary curve are generated using the Eq. (4.6) to approximate a function, referred as limit state function that will separate liquefied cases from the non–liquefied ones, following a simple and robust search technique developed by Juang et al. (2000). The technique is explained conceptually with the help of Fig.4.4. Let a liquefied case, '*L*' (target output *LI*=1) of the database as shown in the Fig.4.4 can be brought to the boundary or limit state curve [i.e. when the case becomes just non-liquefied as per the evaluation by the Eq. (4.6)] if $CSR_{7.5}$ is allowed to decrease (path *P*) or $N_{1,60}$ is allowed to increase (path *Q*). Further, for a non-liquefied case, '*NL*' (target output *LI* = 0) of the database, the search for a point on the boundary curve involves an increase in $CSR_{7.5}$ (path *T*) or a decrease in $N_{1,60}$ (path *S*) and the desired point is obtained when the case just becomes liquefied as adjudged by Eq. (4.6). Fig.4.5 shows the detailed flowchart of this search technique for path '*P*' and '*T*'. A two dimensional ($N_{1,60}$, $CSR_{7.5}$) data point on the unknown boundary curve is obtained from each successful search.In this study, the limit state is defined as the 'limiting' $CSR_{7.5}$, which a soil can resist without occurrence of liquefaction and beyond which the soil will liquefy. Thus, for a particular soil at it's in- situ conditions, this limit state specifies its *CRR* value. A total of 115 two dimensional artificial data points (*CRR*, $N_{1,60}$), which are located on the boundary curve are generated using the developed model (Eq. 4.6) and the technique explained in Figs. 4.4 and 4.5. These data points are used to approximate the limit state function in the form of $CRR=f(N_{1,60})$ as per MGGP and is presented below.

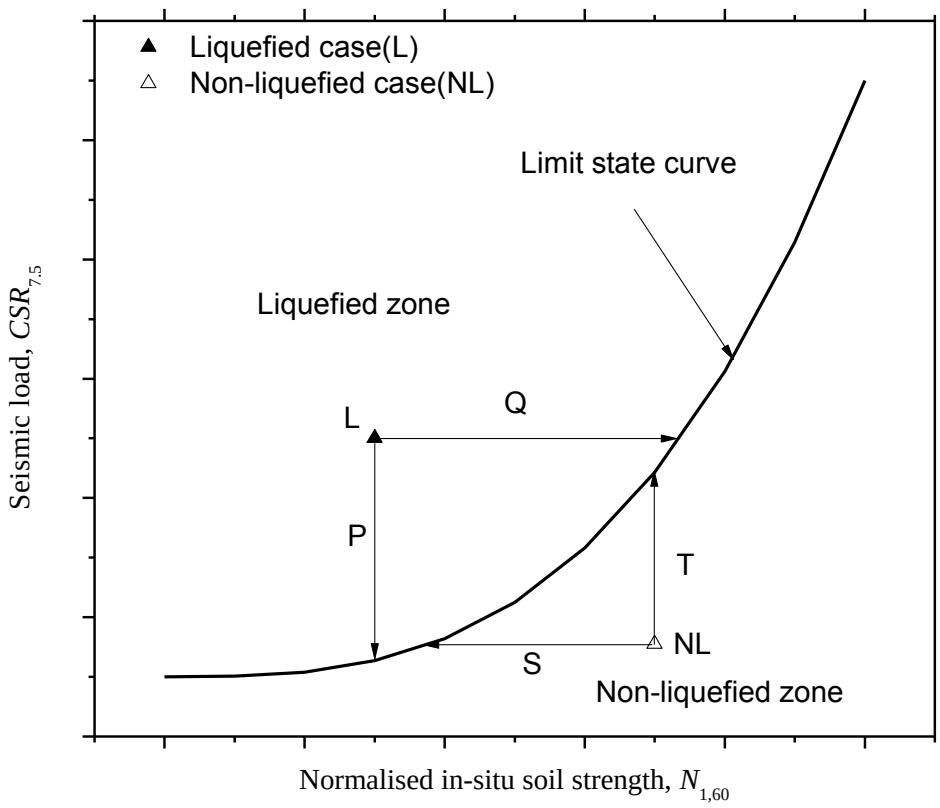

Fig. 4.4 Conceptual model for search technique for artificial data points on limit state curve (Modified from Juang et al. 2000)

4.2.2.3 MGGP Model for CRR

The multi-gene GP is also used for development of *CRR* model using 115 artificially generated data points, out of which 81 data points are selected randomly for training and rest 34 numbers for testing the developed model. The optimum values of the controlling parameters are obtained as explained above using the range of values given in Table 4.1.Several *CRR* models were obtained with the optimum values of controlling parameters by running the MGGP program several times. Then, the developed models were analyzed with respect to physical interpretation of *CRR* of soil and after careful consideration of various alternatives the following expression (Eq. 4.7) was found to be most suitable prediction model for *CRR*.

$$CRR = 0.008N_{1,60} - 0.613\cos\left(0.043N_{1,60}\right) + 0.077\cos\left(0.194N_{1,60}\right) + \frac{0.043}{N_{1,60}} + 0.609 \qquad (4.7)$$

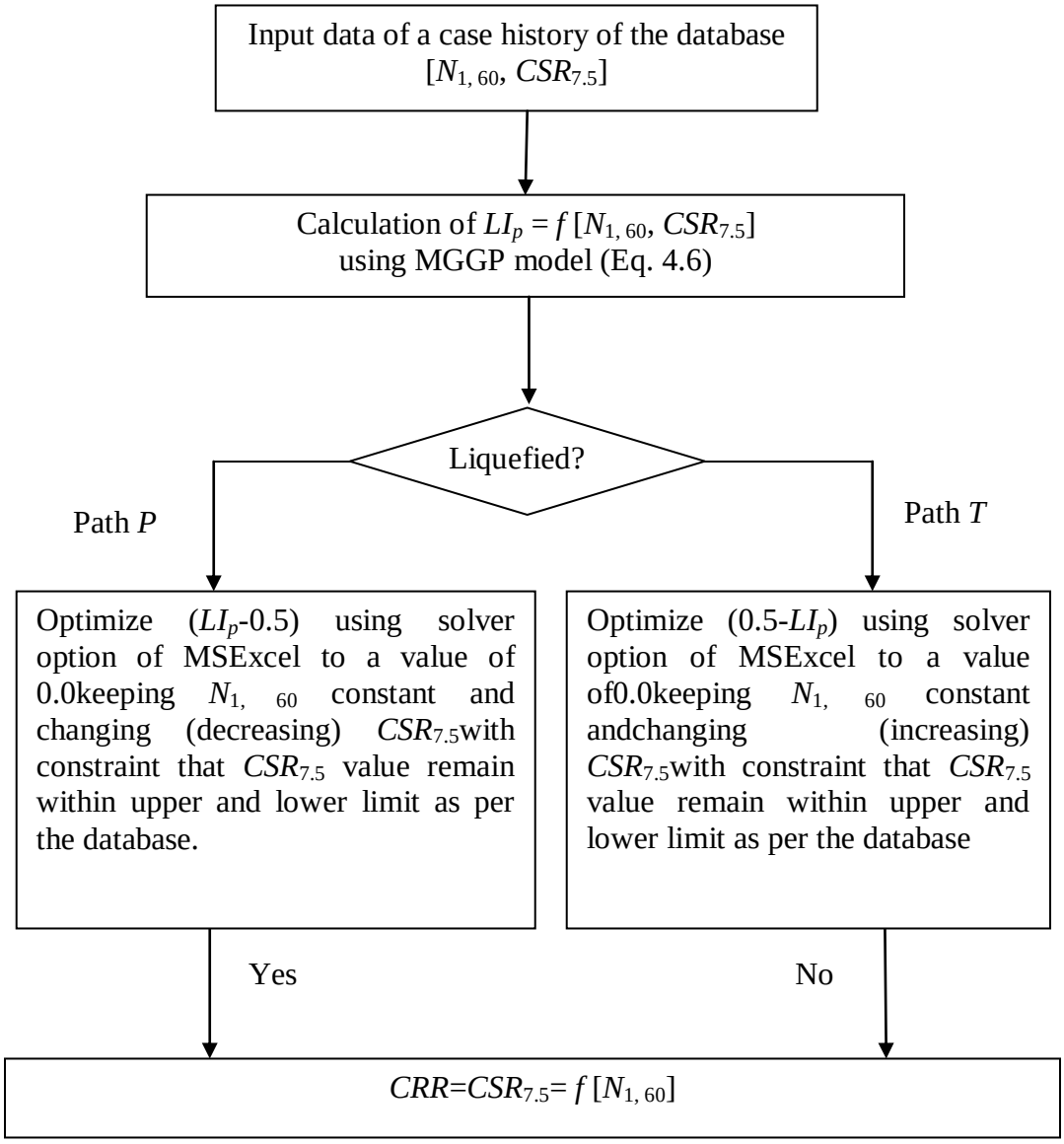

Fig.4.5 Search algorithm for data point on limit state curve

Table 4.3. Statistical performances of developed MGGP based *CRR* model

Data	*R*	R^2	*E*	*AAE*	*MAE*	*RMSE*
Training (81)	1.000	1.000	0.999	0.010	0.019	0.011
Testing (34)	0.999	0.999	0.999	0.011	0.019	0.013

The statistical performances of the developed *CRR* model can be evaluated in terms of the correlation coefficient (*R*), coefficient of determination (R^2) (Rezania and Javadi 2007), Nash-Sutcliff coefficient of efficiency (*E*) (Das and Basudhar 2008), *RMSE*, average absolute error (*AAE*) and maximum absolute error (*MAE*). These coefficients are defined as:

$$R = \frac{\sum_{i=1}^{n}\left(X_t - \overline{X_t}\right)\left(X_P - \overline{X_P}\right)}{\sqrt{\sum_{i=1}^{n}\left(X_t - \overline{X_t}\right)^2 \sum_{i=1}^{n}\left(X_P - \overline{X_P}\right)^2}} \tag{4.8}$$

$$R^2 = \frac{\sum_{i=1}^{n}\left(X_t\right)^2 - \sum_{i=1}^{n}\left(X_t - X_p\right)^2}{\sum_{i=1}^{n}\left(X_t\right)^2} \tag{4.9}$$

$$E = \frac{\sum_{i=1}^{n}\left(X_t - \overline{X_t}\right)^2 - \sum_{i=1}^{n}\left(X_t - X_p\right)^2}{\sum_{i=1}^{n}\left(X_t - \overline{X_t}\right)^2} \tag{4.10}$$

$$AAE = \frac{1}{n}\sum_{i=1}^{n}\left|X_t - X_p\right| \tag{4.11}$$

$$MAE = \max\left|X_t - X_p\right| \tag{4.12}$$

$$RMSE = \sqrt{\frac{\sum_{i=1}^{n}\left(X_t - X_p\right)^2}{n}} \tag{4.13}$$

where n is the number of case histories and X_t and X_p are the measured (i.e., target) and predicted values (of *CRR* in this case), respectively.

Thus, statistical performances: *R*, R^2, *E*, *RMSE*, *AAE* and *MAE* of the developed *CRR* model as presented in Table 4.3 for training and testing data are comparable showing good generalization capability of the *CRR* model. The performance of the above MGGP-based *CRR* model as shown in Fig. 4.6 clearly indicates that Eq. (4.7) is a very good

approximation of the limit state function. The liquefied and non-liquefied cases of the present data base are shown in Fig.4.7 along with the developed MGGP based limit state curve separating them.

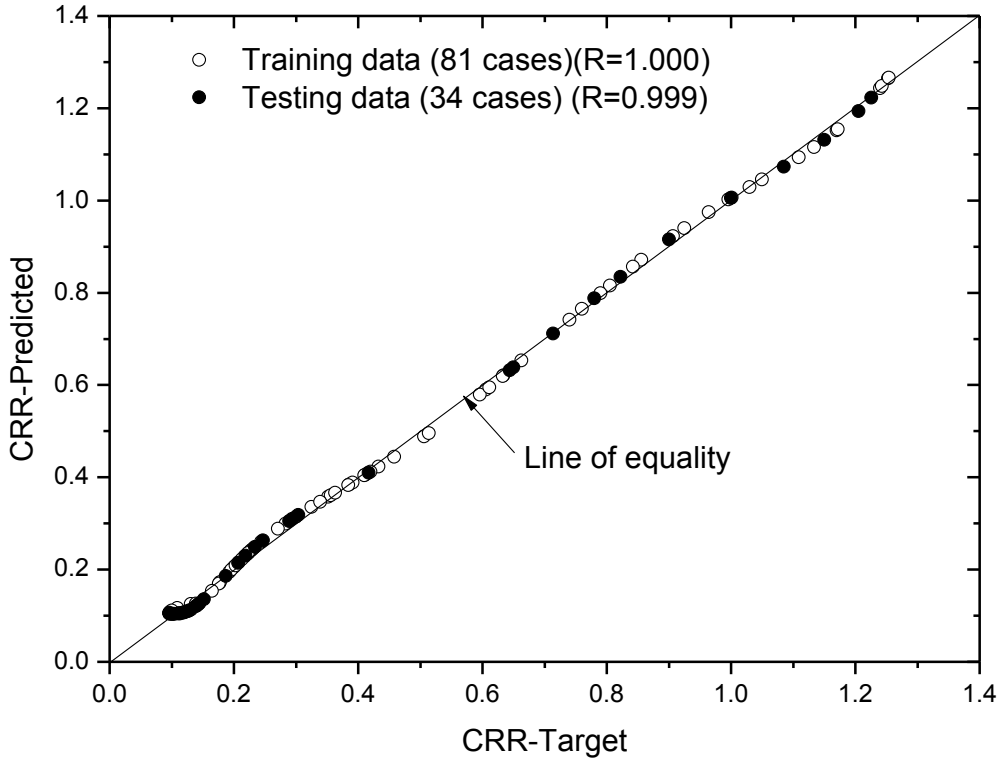

Fig. 4.6 Performance of proposed MGGP based *CRR* model

Factor of safety against occurrence of liquefaction (F_s) can be presented by Eq. (4.14)

$$F_s = CRR/CSR_{7.5} \tag{4.14}$$

The performance of the proposed *CRR* model is also evaluated by calculating the F_s for each case of the present database as discussed earlier. In present study, $F_s \leq 1$ refers to occurrence of liquefaction and F_s>1 refers to non-liquefaction. A prediction (liquefaction or non-liquefaction) is considered to be successful if it agrees with the field manifestation as recorded in the database. The success rate in predicting liquefied cases is 99.39% and that for non-liquefied case is 85.48% and the overall success rate is found to be 93.40%. The low rate of success for non-liquefied case may be due to following. In 1999, Chi-Chi

earthquake, at some locations, surface manifestations of liquefaction (sand boiling, settlement etc.) was not detected, though occurrence of liquefaction at some depth below ground level was observed. This was due to existence of thin capping layers above the liquefied layer. Therefore, at these locations occurrence of liquefaction at some depth below ground level cannot be excluded due to lack of liquefaction surface observations (Ku et al. 2004). Due to lack of surface manifestations as explained above the actual liquefied cases might have been considered as non-liquefied cases in the database.

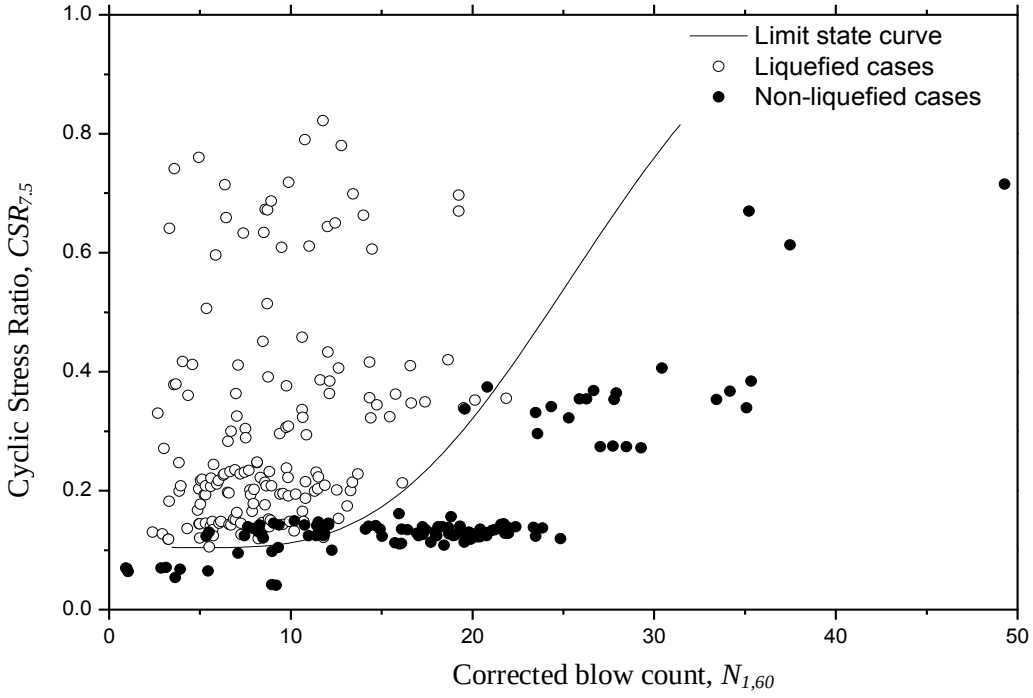

Fig.4.7 The developed MGGP based limit state curve separates liquefied cases from non-liquefied cases of the database of Hwang et al. (2001).

The *CRR* model (Eq. 4.7) in conjunction with the model for $CSR_{7.5}$ (Eq.4.2) forms proposed MGGP-based deterministic method, which can be used for evaluation of liquefaction potential in terms of F_s. Generally a higher factor of safety (1.1-1.5) may be recommended for design purpose to account for the possible uncertainties associated with the model and model parameters, as there is no scope of uncertainty analysis in deterministic approach. Selection of proper factor of safety depends on both technical and non-technical factors like

importance and economics of the project under consideration. The present MGGP method can also be used to assess the soil strength in terms of *CRR* or $N_{1,\,60}$ at a design level of seismic loading with a given F_s. This is explained by considering the example as presented by Juang et al. (2000). Let a sandy soil layer is having following properties: depth, z = 5.8m, vertical effective stress of soil at the depth studied, σ'_v=84kPa, vertical total stress of soil at that depth, σ_v= 111 kPa, fines content, FC=2%. The structure to be built at the site is to be designed for an earthquake of moment magnitude, M_w =7 and peak horizontal ground surface acceleration, a_{max}= 0.2g. In this case the $CSR_{7.5}$ is found out to be 0.14 as per equation presented by Eq.(4.2). If the F_s considered for the said project is 1.14, then minimum required *CRR* value as per the proposed deterministic method is 0.16. For a ground improvement project, the required $N_{1,\,60}$value corresponding to the obtained *CRR* value of 0.16 is found out to be 14.63 as per the Eq. (4.7). Thus, after ground improvement the $N_{1,\,60}$value should reach a value greater than 14.63.

4.2.2.4 Comparison with existing methods using independent database

It is always required to compare the efficacy of a newly developed method with that of the existing methods. In the present study the developed MGGP-based method is compared with the statistical and ANN-based methods as per Juang et al. (2000) in terms of rate of successful prediction of liquefied and non-liquefied cases. It is pertinent to mention here that the statistical method, which is presented in Juang et al. (2000), is an updated version of Seed et al. (1985) method (Youd and Idriss 1997). An independent post liquefaction SPT-based database (Idriss and Boulanger 2010) consisting of total 230 cases, out of which 115 cases having surface evidence of liquefaction, 112 cases of non-liquefaction and 3 marginal cases provides a good basis for comparison of efficacy of the above methods.

The F_s of the total 227 cases of the database (neglecting 3 marginal cases) are calculated using ANN-based method (Juang et al. 2000), statistical method (Juang et al.2000) and the proposed MGGP-based method following Eq. (4.7) and Eq. (4.2). The assessed F_s is used to judge the correctness of a prediction on the basis of field manifestations as explained earlier. As per the comparison presented in Table 4.4 the rate of successful prediction by the proposed MGGP-based method (87%) is better than that of the ANN-based method (82%)

and comparable with that of statistical method (89%) for liquefied cases. In case of non-liquefied cases the prediction accuracy of the present MGGP-based method (88%) is better than statistical method (78%) and close to ANN-based method (90%). The over all successful prediction rate of the present MGGP method (87%) is better than ANN (86%) and statistical (84%) methods. Though, all the three methods are comparable it can be observed that ANN-based method predicts non-liquefied (90%) cases better than liquefied (82%) cases and the statistical method predicts liquefied (89%) cases better than non-liquefied (78%) cases but, the prediction accuracy of the present MGGP method is equally good for both liquefied (87%) and non-liquefied (88%) cases. Thus, it can be noted that the present MGGP method is equally efficient in predicting liquefied and non-liquefied cases compared to ANN and statistical methods.

Table 4.4 Comparison of results of proposed MGGP-based model with Statistical and ANN-based models using an independent database of Idriss and Boulanger (2010).

Criterion (F_s)	Statistical method (Juang et al. 2000)		ANN based method (Juang et al. 2000)		MGGP based method (Present study)	
	No. of successful prediction	Rate (%)	No. of successful prediction	Rate (%)	No. of successful prediction	Rate (%)
Liquefied cases(115)	102	89	94	82	99	87
Non-liquefied cases(112)	87	78	100	90	98	88
Total cases(227)	189	84	194	86	197	87

It is pertinent to mention here that the proposed MGGP-based *CRR* model is a function of $N_{1,\ 60}$whereas the *CRR* models of ANN and statistical methods (Juang et al. 2000) are function of clean sand equivalence of the overburden stress corrected SPT blow count, $N_{1,60,cs.}$, the parameter which takes care of the effect of fines content on the resistance of soil. The ANN and the statistical methods are applicable for $N_{1,60,cs}$<35 and $N_{1,60,cs}$<30 respectively, otherwise the soil is considered to be too clay rich to liquefy (Juang et al. 2000). It is found that in the present database 27 cases are having $N_{1,60,cs}$ value more than or

equal to 35 and for 31 cases $N_{1,60,cs}$>= 30. For all these cases F_s is considered to be greater than 1 for the comparative study presented in Table 4.4. Even though, the proposed MGGP based *CRR* model does not incorporate fines content (*FC*) parameter, it predicts well all the 31 cases of database having $N_{1,60,cs}$>= 30 as non-liquefied cases. This shows the compactness as well as the effectiveness of the developed MGGP-based *CRR* model compared to the available ANN and statistical methods.

4.3. DEVELOPMENT OF CPT-BASED DETERMINISTIC MODEL

The general form of MGGP-based LI_p model on the basis of CPT database can be presented as:

$$LI_p = \sum_{i=1}^{n} F\left[X, f(X), c_i\right] + c_0 \tag{4.15}$$

where LI_p = predicted value of *LI*, *F*= the function created by the MGGP referred herein as liquefaction index function.

For Model-I: *X* = vector of input variables = $\{q_{c1N}, I_c, \sigma_v', CSR_{7.5}\}$, q_{c1N} = normalized cone tip resistance and is defined as per Juang et al. (2003):

$$q_{c1N} = \frac{q_c/100}{\left(\sigma_v'/100\right)^{0.5}} \tag{4.16}$$

where σ_v'= vertical effective stress of soil at the depth studied in kPa, q_c= measured cone tip resistance in kPa, I_c = soil type index and is defined as per Juang etal. (2003):

$$I_c = \left[\left(3.47 - log_{10} q_{c1N}\right)^2 + \left(log_{10} F + 1.22\right)^2\right]^{0.5} \tag{4.17}$$

where *F*=normalized friction ratio and defined as:

$$F = \left[f_s / \left(q_c - \sigma_v\right)\right] \times 100\% \tag{4.18}$$

where f_s = sleeve friction in kPa, σ_v = vertical total stress of soil at the depth studied in kPa, $CSR_{7.5}$ is the cyclic stress ratio adjusted to the benchmark earthquake of moment magnitude (M_w) of 7.5 as presented by Eq. (4.2).

Similarly, for Model-II, X== {qc, R_f, σ_v, σ_v', a_{max}/g, M_w} (Goh and Goh 2007),

R_f is the friction ratio in percent, and defined as:

$$R_f = (f_s/q_c) \times 100 \tag{4.19}$$

c_i is a constant, f is the function defined by the user and n is the number of terms of target expression and c_0= bias. Here, also the MGGP as per Searson et al. (2010)is used and the present model is developed and implemented using Matlab (Math Works Inc. 2005).

4.3.1 Database and Reprocessing

The database (Juang et al. 2003) used in this study consists of total 226 cases, 133 out of them are liquefied cases and other 93 are non-liquefied cases. It contains information about soil and seismic parameters (q_c, R_f, σ_v, σ'_v, a_{max}, M_w),which are derived from the CPT measurements at over 52 sites along with field performance observations (LI) of six different earthquakes. The soil in these cases ranges from sand to silty sand to silt mixtures (sandy and clayey silt). The depths at which CPT measurements are reported in the database range from 1.4m to 14.1m. The q_c values range from 0.5 to 25.0 MPa and the R_f values range from 0.05 to 5.24%. The σ_v and σ'_v values are in the range of 26.6-274.0 kPa and 22.5-215.2 kPa respectively. The $a_{\max}$ and M_w values are in the range of [0.08, 0.8g] and [6, 7.6] respectively. It is pertinent to mention here that the pore pressure parameter was not available in the present database and thus, σ'_v is derived using hydrostatic pressure. The present database consists of the above parameters incorporating all necessary corrections to the raw CPT data. Out of the mentioned 226 data, 151 data are selected for training and remaining 75 data are used for testing the developed model as per Juang et al. (2003). Goh and Goh (2007) also used this database with same number of training and testing data for developing the SVM- based liquefaction classification model. Here in the MGGP approach

normalization or scaling of the data is not required, which is an advantage over ANN and SVM approach.

4.3.2 Results and discussion

In this section, the result of deterministic model based on post liquefaction CPT database is presented. A limit state function that separates liquefied cases from the non-liquefied cases and also represents cyclic resistance ratio (*CRR*) of soil is also developed by using MGGP. The developed *CRR* model in conjunction with widely used $CSR_{7.5}$ (Juang et al. 2000) is used to evaluate liquefaction potential in terms of F_s and the results are presented in following sequence.

4.3.2.1 MGGP Model for Liquefaction Index (LI)

In the present MGGP procedure a number of potential models are evolved at random and each model is trained and tested using the training and testing cases respectively as described above. The fitness of each model is determined by minimizing the error function (E_f), as given by Eq. (4.5) of section 4.2.2.1. If the errors calculated by using Eq. (4.5) for all the models (individuals) in the existing population do not satisfy the termination criteria, the generation of new population continues till the best model is developed as per the earlier discussion. Here in the MGGP model development controlling parameters are obtained following the procedure as described in the section 4.2.2.1 and following parameters ranges as per Table 4.1. The optimum values of obtained controlling parameters are presented in Table 4.5.

Using the above optimum controlling parameters several models for LI_p are obtained. The "best" model for Model-I and Model-II are selected out of various developed MGGP models after carefully analyzing and considering various alternatives with physical interpretation of *LI* and are described as Eqs. (4.20) and (4.21), respectively.

$$LI_p = 1.268\left[sin\left(I_c\right) + tanh\left(CSR_{7.5}\right)\right] - 0.005\left(\sigma_v^{'} + q_{c1N}\right) - \frac{0.016}{CSR_{7.5}} + \frac{8.406 I_c\, sin\left(I_c\right)}{q_{c1N}} - \frac{3.937}{I_c \sigma_v^{'} CSR_{7.5}} + 0.076 \quad (4.20)$$

Table 4.5 Optimum values of controlling parameters for MGGP-based LI_p models (Model-I and Model-II) using CPT data

Parameters	Model-I	Model-II
Population size	3000	3000
Number of generations	150	200
Maximum number of genes	4	5
Maximum tree depth	3	3
Selection Type	Tournament	Tournament
Tournament size	7	6
Reproduction probability	0.05	0.05
Crossover probability	0.85	0.85
Mutation probability	0.1	0.1
High level cross over probability	0.2	0.2
Low level cross over probability	0.8	0.8
Sub-tree mutation	0.9	0.9
Substituting input terminal with another random terminal	0.05	0.05
Gaussian perturbation of randomly selected constant	0.05	0.05
Ephemeral random constants	[-10 10]	[-10 10]

$$LI_p = 0.314\left[\cos\left(R_f\right) - \tanh\left(R_f\right)\right] - 0.0073\left(\sigma_v^{'} + q_c + M_w^{\,2}\right) - 0.438\cos\left(R_f + M_w\right) - 1.695\exp\left[-5.72\left(a_{\max}/g\right)\right] - \frac{11.36\left(q_c + R_f\right)}{\sigma_v^{'} + \sigma_v} + 2.522 \quad (4.21)$$

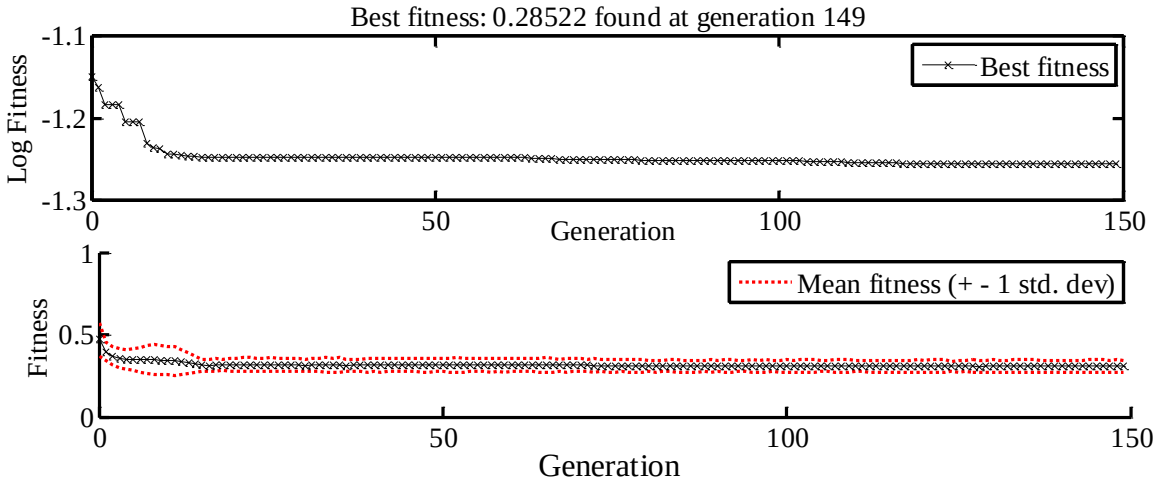

Fig. 4.8 Variation of the best and mean fitness with the number of generation.

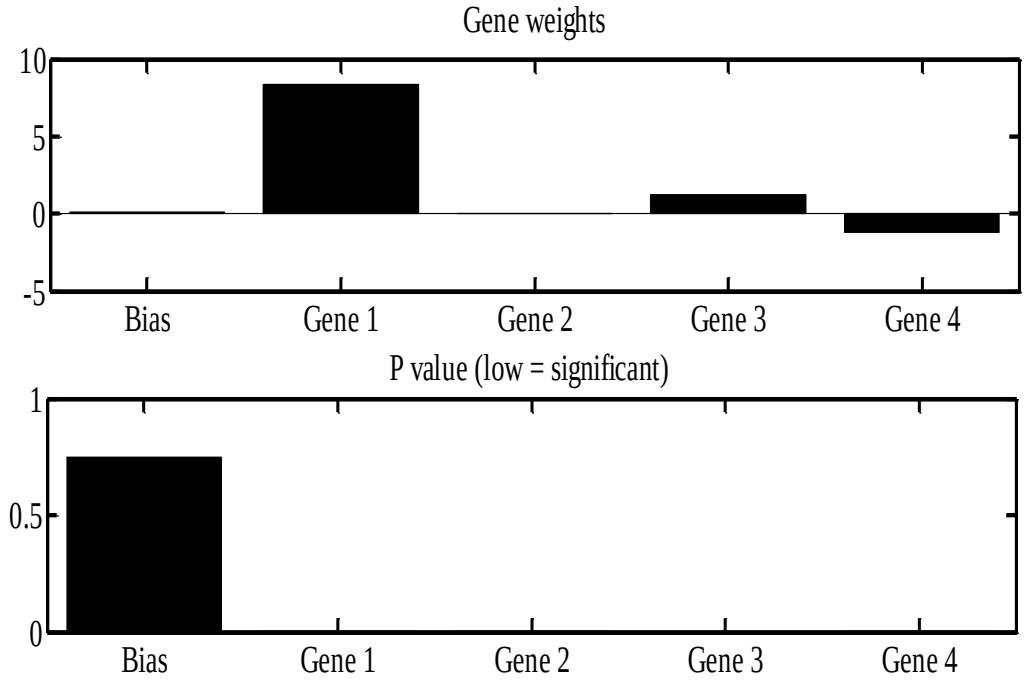

Fig.4.9 Statistical properties of the evolved 'best' MGGP model (on training data)

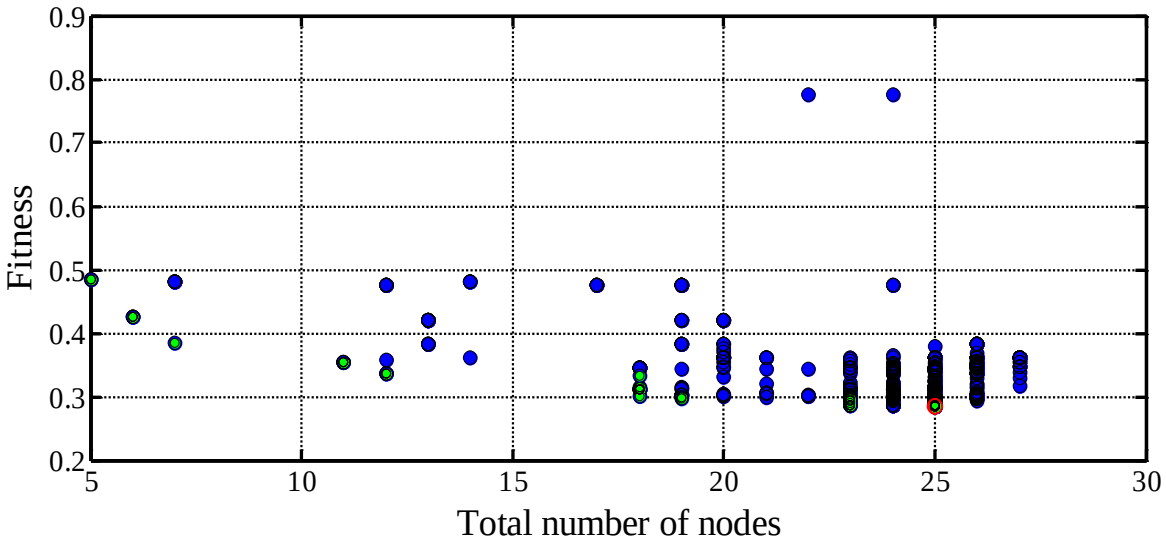

Fig 4.10 Population of evolved models in terms of their complexity and fitness.

The "best" model for Model-I has been characterized by the Figs. 4.8, 4.9, 4.10. Fig. 4.8 shows the variation of the best fitness (log values) and mean fitness with number of generations. It can be seen from this figure, the fitness values decrease with increasing the number of generations. The best fitness was found at the 149^{th} generation (fitness =0.2852).The statistical significance of each of four genes of the developed model is shown in Fig. 4.9. As shown in the Fig. 4.9a the weight of the the gene-1 is higher than the other genes and bias. The degree of significance of each gene using *p* values is also shown in Fig. 4.9b. It can be noted that the contribution of all the genes towards prediction of *LI*(i.e., LI_p) is very high, as their corresponding *p* values are very low, whereas the bias contribution is very less. Fig. 4.10 presents the population of evolved models in terms of their complexity and fitness value.The developed models that perform relatively well with respect to the "best" model and are much less complex (having less number of nodes) than the "best" model in the population can be identified in this figure as green circles. The "best" model in the population is highlighted with a red circle.

Similarly, the "best" model for Model-II has been characterized by the Figs. 4.11, 4.12, 413. Fig. 4.11 shows the variation of the best (log values) and mean fitness with with number of generations. It can be seen from this figure, the fitness values decrease with increasing the

number of generations. The best fitness was found at the 146th generation (fitness =0.28047).The statistical significance of each of five genes of the developed model is shown in Fig. 4.12. As shown in the Fig. 4.12(a) the weight of the the Gene-4 is higher than the other genes and bias. The degree of significance of each gene using *p* values is also shown in Fig. 4.12(b). It can be noted that the contribution of all the genes as well as the bias towards prediction of *LI*(i.e., LI_p) is very high, as their corresponding *p* values are very low except Gene-2. Fig. 4.13 presents the population of evolved models in terms of their complexity (number of nodes) and fitness value.

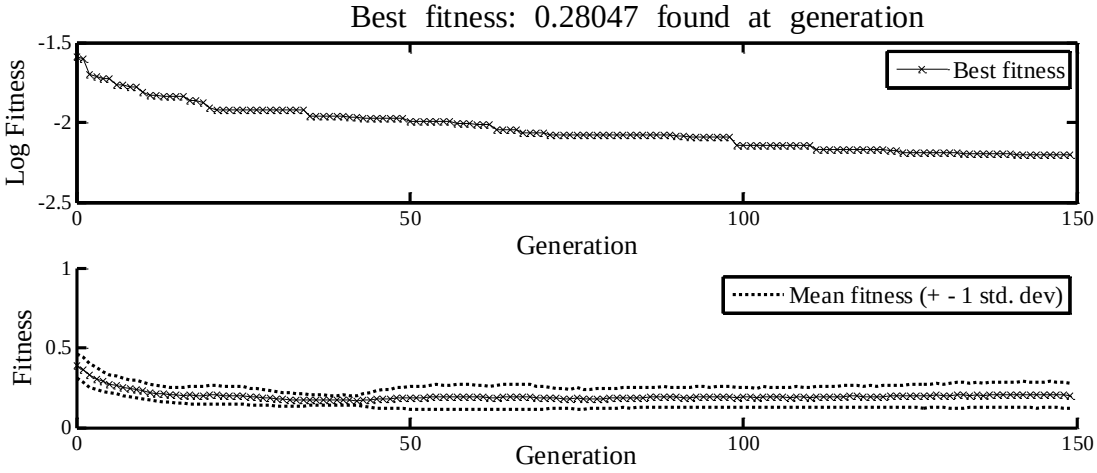

Fig. 4. 11 Variation of the best and mean fitness with the number of generation.

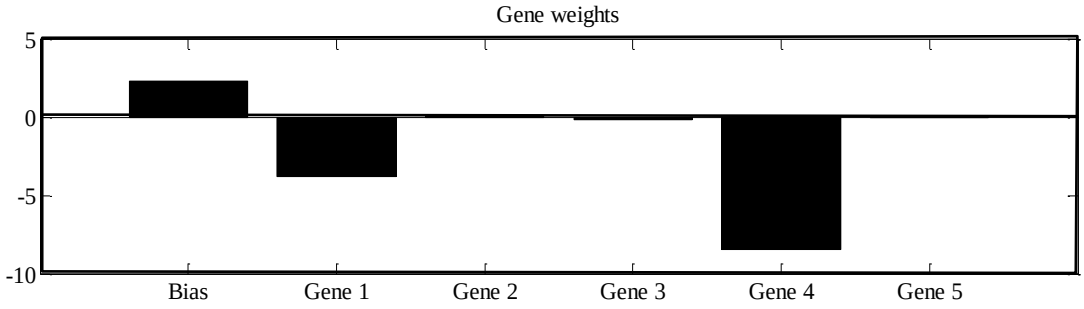

(a)

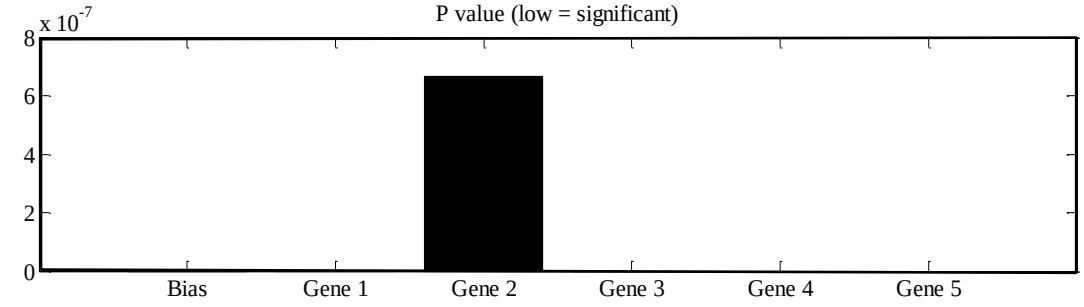

(b)

Fig.4.12 Shows statistical properties of the evolved 'best' MGGP model (on training data)

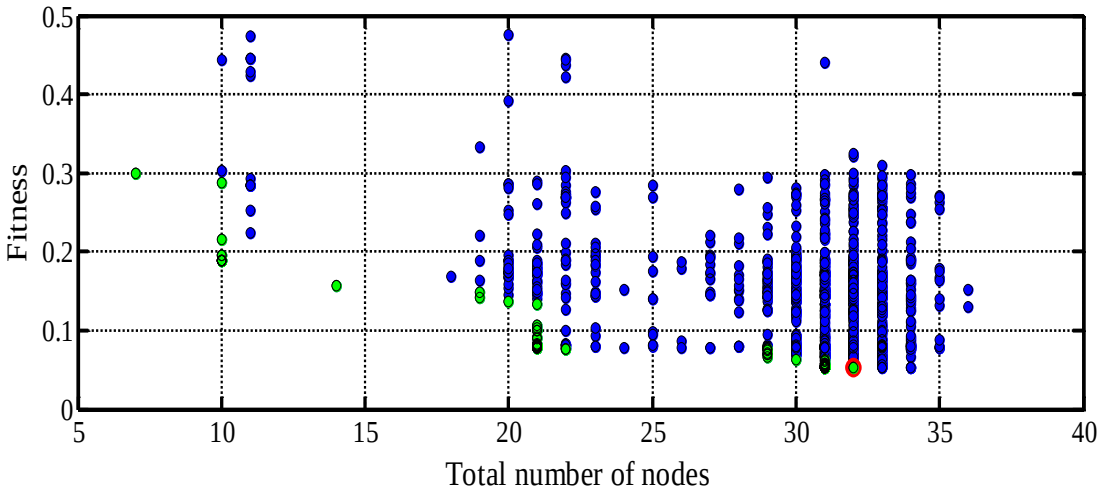

Fig 4.13 Population of evolved models in terms of their complexity and fitness.

Table 4.6 Comparison of results of developed MGGP models with available ANN (Juang et al. 2003) and SVM (Goh and Goh 207) models.

Model No.	Input variables	Performance in terms of successful prediction (%)							
		MGGP	ANN	MGGP	ANN	MGGP	SVM	MGGP	SVM
		Training data		*Testing data*		*Training data*		*Testing data*	
I	q_{c1N}, I_c, σ'_v,$CSR_{7.5}$	97	98	95	91	-	-	-	-
II	q_c, R_f, σ'_v, σ_v, a_{max}, M_w	-	-	-	-	98	98	97	97

As per the results presented in Table 4.6 the performances of Model-I for training and testing data are comparable. The successful prediction values are 97% for training and 95% for testing data whereas the overall success rate in predicting liquefaction in all cases is 96%. The classification accuracy of the available ANN model (Juang et al. 2003) is 98%, 91% and 96% for training, testing and overall data respectively. As described earlier, the comparison of efficacy of different models are also made on the basis of the testing data only. It is found that the performance of MGGP based prediction model (Model-I) is better than that of the ANN model (Juang et al. 2003) in terms of rate of successful prediction of liquefaction and non- liquefaction cases. Similarly from Table 2, it can also be noted that the liquefaction classification accuracies for training, testing and total dataset of the Model-II are 98%, 97% and 97% respectively. The classification accuracy of the available SVM model (Goh and Goh 2007) is 98%, 97% and 97% for training, testing and overall data, respectively. Hence, the prediction performance of the developed Model-II is found to be at par with the SVM model. The number of training data (170) and testing data (56) used by Gandomi and Alavi (2012) for development of their MGGP based model is different from that of the proposed MGGP model (Model-II) and the SVM model of Goh and Goh (2007). Thus, the comparison of efficacy of the above models could not be done, even though the model parameters and database is same. Table 4.7 shows the statistical performances of both

training and testing data for the developed Model-I and Model-II in terms of *R*, *E*, *AAE*, *MAE and RMSE*.

Table 4.7 Statistical performances of developed MGGP models

Model No.	Input variables	Data	*R*	R^2	*E*	*AAE*	*MAE*	*RMSE*
I	q_{c1N}, I_c, σ'_v, $CSR_{7.5}$	Training	0.81	0.86	0.66	0.24	0.64	0.29
		Testing	0.81	0.84	0.65	0.24	0.73	0.30
II	q_c, R_f, σ'_v, σ_v,a_{max}, M_w	Training	0.83	0.86	0.68	0.23	0.62	0.28
		Testing	0.85	0.89	0.70	0.21	0.79	0.27

The performances of both Model- I and Model- II for training and testing data are found to be comparable showing good generalization of the developed models. As $R > 0.8$, for both Model-I and Model-II, there is a strong correlation between predicted and actual vales (Smith 1986).It is evident from the results presented in Table 4.6 and Table 4.7 that the proposed MGGP based models (Model-I and Model-II) are able to learn the complex relationship between the liquefaction index and its main contributing factors with a very high accuracy. The Eq. (4.20) and (4.21) can be used by geotechnical engineering professionals with the help of a spreadsheet to evaluate the liquefaction potential of soil for a future seismic event without going into complexities of model development whereas the available ANN and SVM models do not provide any such explicit equations for professionals. Even if the performance of both the developed models is equally good in separating liquefied cases from the non-liquefied cases, model equation of Model-I is more compact having less number of input parameters.

An independent CPT-based post liquefaction database of 96 cases (58 liquefied and 38 non-liquefied) as given in Juang et al. (2006) is also used to verify the efficacy of the proposed models. From the results presented in Table 4.8 it can be observed that overall prediction rates are 87% and 86% for Model-I and Model-II, respectively. Samui and Sitharam (2012) similarly used an independent SPT dataset to evaluate the performance of their developed

ANN and SVM-based models for predicting soil liquefaction susceptibility and the overall classification accuracies were 71% and 78% for ANN and SVM models, respectively. It is pertinent to mention here that both the models (Model-I and Model-II) are able to predict liquefied cases with a very high rate of accuracy of 97% and 95%, respectively whereas the successful prediction rates for non-liquefied cases are 70% for Model-I and 71% for Model-II. Thus, the performance of both the present MGGP models based on the independent dataset is very efficient in predicting liquefied cases but, not that efficient for non-liquefied cases. It may be mentioned here that as a professional engineer, the prediction of liquefied case is more important than that of non-liquefied case.

Table 4.8 Comparison of performance of the developed MGGP models with respect to an independent dataset (Juang et al. 2006).

Model No.	Input variables	Performance in terms of successful prediction (%)		
		Liquefied cases (58)	Non-liquefied cases (38)	Over all Cases (96)
I	q_{c1N}, I_c, σ'_v, $CSR_{7.5}$	97	70	87
II	q_c, R_f, σ'_v, σ_v,a_{max}, M_w	95	71	86

4.3.2.2 *Parametric study and Sensitivity analysis*

Parametric study was made for each of the developed models (Model-I and Model-II) and presented in the addendum.

The sensitivity analysis is an important aspect of a developed model to identify important input parameters. In the present study, sensitivity analyses were made following Liong et al. (2000). As per Liong et al. (2000) the sensitivity (S_i) of each parameter, is expressed as Eq. (4.22).

$$S_i = \frac{1}{N}\sum_{i}^{N}\left(\frac{\%\,\text{Change in output}}{\%\,\text{Change in input}}\right)_i \times 100 \qquad (4.22)$$

where N is the number of data points. In the present study N=151. The analysis has been carried out on the trained model by varying each of the input parameters, one at a time, at a constant rate of 30%. Table 4.9 presents the results of above analysis for both the proposed MGGP models. As per Model-I soil type index (I_c) is the most important parameter. The

other important inputs are $CSR_{7.5}$, and σ'_v with q_{c1N} is the least important parameter. For Model-II the most important parameter is measured cone tip resistance (q_c). The other input parameters in decreasing order of their contribution in governing the prediction of *LI* are (a_{max}/g), σ_v, M_w and R_f. It is well known that q_c is the most important soil parameter for liquefaction susceptibility analysis, which is *LI* for the present case. However, as defined earlier, Model –I is developed using derived parameters, q_{c1N} and I_c , where $q_{c1N}$is a function of q_c and σ'_v , and I_c is a function of q_{c1N}, q_c, f_s, σ'_v and σ_v. Thus, as per sensitivity analysis I_c, which is a function of other parameters along with q_{c1N} is found to be a better parameter to predict *LI* than q_{c1N} alone. But in Model- II, as basic soil and seismic parameters are considered, q_c is found to be most important parameter.

Table 4.9 Sensitivity analysis of inputs for the developed MGGP models

	Model -I				Model - II					
Parameters	q_{c1N}	I_c	σ'_v	$CSR_{7.5}$	q_c	R_f	σ'_v	σ_v	a_{max}/g	M_w
Sensitivity (%)	-4.4	-460.4	-10.4	50.2	-283.7	-79.6	-90.7	145.2	184.6	136.0
Rank	4	1	3	2	1	6	5	3	2	4

In the present study, sensitivity analyses were also made as per Gandomi et al. (2013) and the results are presented in Table 4.9(a) in the ADDENDUM.

4.3.2.3 *Generation of artificial points on the limit state curve*

To approximate a limit state function that will separate liquefied cases from the non-liquefied ones, artificial data points on the boundary curve are generated using the Eq. (4.20) and following a simple but robust search technique developed by Juang et al. (2003). The technique is explained conceptually with the help of Fig. 4.14. Let a liquefied case, '*L*' (target output *LI*=1) of the database as shown in the Fig.4.14, can be brought on to the boundary or limit state curve [i.e., when the case becomes just non-liquefied according to the evaluation by Eq. (4.20)] if $CSR_{7.5}$ is allowed to decrease (path *P*) or q_{c1N} is allowed to increase (path *Q*). Further, for a non-liquefied case, '*NL*' (target output *LI* = 0) of the database, the search for a point on the boundary curve involves an increase in $CSR_{7.5}$ (path *T*) or a decrease in q_{c1N} (path *S*) and the desired point is obtained when the case just becomes

liquefied as adjudged by Eq. (4.20). Fig.4.15 shows the detailed flow chart of this search technique for path '*P*' and '*T*'. A multi-dimensional (q_{c1N}, I_c, σ_v', $CSR_{7.5}$) data point on the unknown boundary curve is obtained from each successful search. A total of 406 multi-dimensional artificial data points (q_{c1N}, I_c, σ_v', $CSR_{7.5}$), which are located on the boundary curve are generated using the developed MGGP-based model Eq. (4.20) and the technique explained in the Figs. 4.14 and 4.15. These data points are used to approximate the limit state function in the form of $CRR = f(q_{c1N}, I_c, \sigma_v')$ using MGGP and is presented below.

4.3.2.4 MGGP Model for CRR

The MGGP is also adopted for development of *CRR* model using 406 artificially generated data points, out of which 285 data points are selected randomly for training and the remaining 121 for testing the developed model. The optimum values of the controlling parameters are obtained as explained above in section 4.2.2.1 and using the range of values given in Table 4.1. Several *CRR* models were obtained by running the MGGP using optimum values of controlling parameters as explained earlier for the development of the LI_p model.

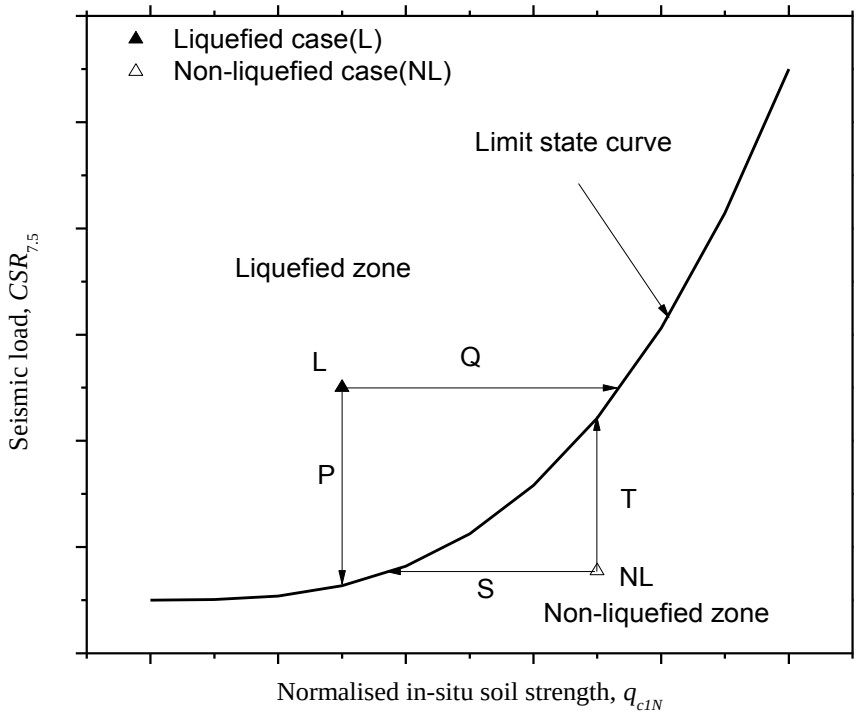

Fig. 4.14 Conceptual model of the search technique for artificial data points on limit state curve (modified from Juang et al. 2000)

Then, the developed models were analyzed with respect to physical interpretation of *CRR* of soil and after careful consideration of various alternatives, the following expression (Eq. 4.23) was found to be most suitable.

$$CRR = 5.561\times10^{-6}\,\sigma_v^{'}\left(q_{c1N}+\sigma_v^{'}\right) - 0.187\sin\left(I_c\right) + \frac{2.02}{\sigma_v^{'}} + \frac{0.0022\left(q_{c1N}+7.399\right)}{\sin\left(I_c\right)} + 0.018 \qquad (4.23)$$

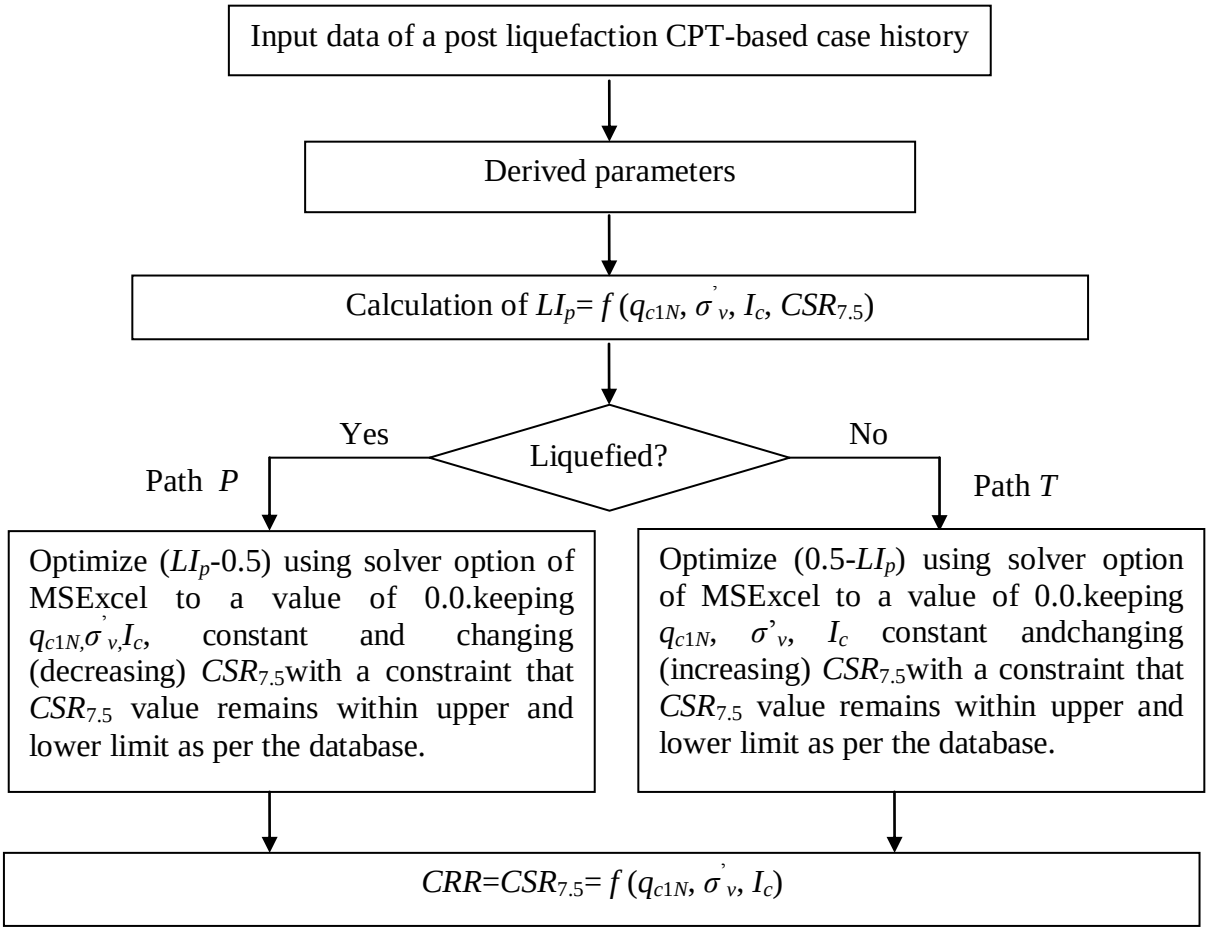

Fig.4.15 Search algorithm for data points on limit state curve

Table 4.10 Statistical performances of developed MGGP-based *CRR* model.

Data (Numbers)	*R*	R^2	*E*	*AAE*	*MAE*	*RMSE*
Training (285)	0.961	0.983	0.923	0.021	0.124	0.028
Testing (121)	0.958	0.983	0.918	0.018	0.112	0.025

The statistical performances in terms of *R*, R^2, *E*, *RMSE*, *AAE* and *MAE* as presented in Table 4.10 for training and testing data are comparable showing good generalization of the developed *CRR* model, which also ensures that there is no over-fitting. The performance of MGGP-based *CRR* model as shown in Fig.4.16 clearly indicates that Eq. (4.23) is a very good approximation of the limit state function.

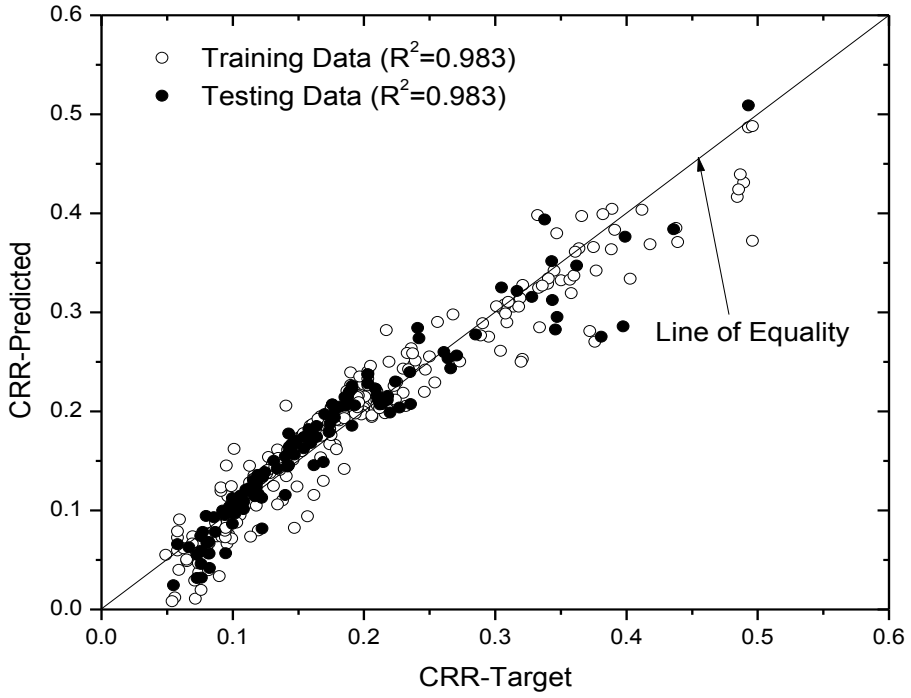

Fig. 4.16 Performance of proposed MGGP based *CRR* model

The performance of the proposed *CRR* model is also evaluated by calculating the F_s for each case of the present database as discussed earlier. In deterministic approach $F_s \leq 1$ predicts occurrence of liquefaction and $F_s > 1$ refers to non-liquefaction. A prediction (liquefaction or non-liquefaction) is considered to be successful if it agrees with the field manifestation. The

deterministic approach is preferred by the geotechnical professionals and various design decisions for further works to be taken up at the site under consideration, are taken on the basis of F_s. In the present study, Eq. (4.23) in conjunction with the model for $CSR_{7.5}$ (Eq. 4.2) forms the proposed CPT-based deterministic method for evaluation of liquefaction potential. The performance of the proposed MGGP-based deterministic model is compared with that of the ANN-based model (Juang et al. 2003) and the results are presented in Table 4.11. It can be noted from the Table 4.11 that the success rate in prediction of liquefied cases is 98% and that for non-liquefied cases is 91% and the overall success rate is found to be 95% by the present MGGP model, whereas the accuracies in prediction of liquefied cases, non-liquefied cases and for overall cases are 93%, 88% and 91%, respectively by the available ANN-based deterministic model (Juang et al. 2003). This clearly indicates the robustness of the proposed deterministic method.

Table 4.11 Comparison of performance of the developed MGGP-based deterministic model with ANN-based deterministic model of Juang et al. (2003) based on present database.

Performance in terms of successful prediction (%)					
Liquefied cases(133)		Non-liquefied cases(93)		Overall (226)	
MGGP	ANN	MGGP	ANN	MGGP	ANN
98	93	91	88	95	91

4.3.2.5 Comparison with existing methods using independent database

It is always required to compare the efficacy of a newly developed method with that of the existing methods. In the present study, the efficiency of the developed MGGP-based method is compared with that of widely used statistical methods as per Olsen (1997), and Robertson and Wride (1998) and ANN-based method of Juang et al. (2003) in terms of rate of successful prediction of liquefied and non-liquefied cases. Henceforth, these three methods are referred to as Olsen method, Robertson method and Juang method for convenience.

Table 4.12 Comparison of results of proposed MGGP-based deterministic model with the existing models based on independent database (Moss 2003 and Juang et al. 2006)

Criterion (F_s)	Olsen method		Robertson method		Juang method		MGGP-based method (Present study)	
	No. of successful prediction	Rate (%)	No. of successful prediction	Rate (%)	No. of successful prediction	Rate (%)	No. of successful prediction	Rate (%)
Liquefiedcases (139)	110	80	116	84	123	89	131	95
Non-liquefied cases (61)	33	54	46	76	45	74	36	60
Total cases (200)	143	72	162	81	168	84	167	84

To study the efficacy of the proposed MGGP-based deterministic method to a new database, an independent post liquefaction CPT database [obtained from Moss (2003) and Juang et al. (2006)], consisting of total 200 cases, out of which 139 cases having surface evidence of liquefaction and the remaining 61 cases of non-liquefaction, is considered. As mentioned earlier, the F_s for the total 200 cases of the database are evaluated using Olsen, Robertson, Juang and the proposed MGGP-based methods. According to the comparison presented in Table 4.12, the accuracy in prediction of liquefied cases (95%)by the proposed MGGP-based deterministic method is better than that obtained by Juang method (89%), Robertson method (84%), and Olsen method (80%), whereas for non-liquefied cases the rate of successful prediction by Robertson method (76%) is better than that of Juang method (74%),MGGP method (60%) and Olsen method (54%). Similarly, overall rate of successful prediction by the proposed MGGP method (84%) is at par with that of Juang method (84%) and better than that of Robertson method (81%) and Olsen method (72%).

4.4 CONCLUSIONS

The conclusions drawn from deterministic method for both SPT and CPT-based models are presented separately as follows.

4.4.1 Conclusions based on SPT- based liquefaction potential evaluation

The following conclusions are drawn based on the results and discussion of the SPT- based liquefaction potential evaluation by the proposed deterministic method:

i. A compact LI_p model equation is presented based on MGGP to predict the soil liquefaction in a future seismic event using SPT data. The liquefaction classification accuracy (94.19%) of present model is found to be better than that of available ANN (88.37%) model and at par with the available SVM (94.19%) model on the basis of the testing data.

ii. A MGGP-based model equation is also presented for *CRR* of soil using SPT data which in conjunction with $CSR_{7.5}$ can be used to predict the factor of safety against liquefaction occurrence. The overall success rate of prediction of liquefaction and non-liquefaction cases by the proposed method for all 288 cases in the present database is found to be 93.40% on the basis of calculated F_s.

iii. Using an independent database (Idriss and Boulanger 2010) the proposed MGGP-based deterministic method (87%) is found to more accurate in predicting liquefied and non-liquefied cases than the existing ANN based method (86%) and statistical method (84%) on the basis of calculated F_s. The proposed method is also found to be efficient in isolating non-liquefied cases without considering the effect of fines content.

4.4.2 Conclusions based on CPT- based liquefaction potential evaluation

Similarly, the following conclusions are drawn from the results and discussion of the CPT-based liquefaction potential evaluation studies by the proposed deterministic methods:

i. CPT-based post liquefaction database (Juang et al. 2003) is analyzed using multi-gene genetic programming approach to predict the liquefaction potential of soil in terms of liquefaction field performance indicator, *LI*.

ii. The efficacy of the developed MGGP-based models: Mode-I and Model-II are compared with that of the available ANN and SVM models, respectively. It is found that the performance of Model-I is better than the ANN model in terms of rate of successful prediction of liquefaction and non-liquefaction cases, whereas Model-II is as good as the SVM model.

iii. The statistical performance parameters (*R, R^2, E, AAE, MAE, RMSE*) for training and testing data are comparable in both the proposed models, which show good generalization capabilities of multi-gene GP approach. Using an independent global database the performance of Model -I and Model-II in terms of overall classification accuracy is found to be 87% and 86% respectively. Unlike available ANN and SVM models, the proposed model equations can be used by geotechnical engineering professionals with the help of a spreadsheet to predict the liquefaction potential of soil for future seismic event without going into the complexities of model development using MGGP.

iv. Based on sensitivity analysis the soil type index and the measured cone tip resistance are found to be "most" important parameters contributing to the prediction of liquefaction index for Model-I and Model-II, respectively.

v. For the proposed deterministic method based on developed *CRR* model and widely used $CSR_{7.5}$ model, the rates of successful prediction of liquefaction and non-liquefaction cases are 98%, and 91% respectively. The overall success rate of the proposed method for all 226 cases in the present database is found to be 95%. The performance of the present deterministic method is better than that of the ANN-based Juang method.

vi. Based on an independent database the overall rate of successful prediction by the proposed MGGP method (84%) is at par with that of Juang method (84%) and better than that of widely used Robertson method (81%) and Olsen method (72%) in terms of calculated F_s.

Based on the comparisons as presented above the deterministic methods, which are predicting well the liquefied cases than non-liquefied cases, indicate the conservativeness of the developed boundary surfaces (limit state functions) separating liquefied and non-liquefied cases being biased towards non-liquefied cases. Though, correct prediction of liquefied cases is more important in the perspective of geotechnical professionals, the degree of conservativeness associated with the boundary surfaces needs to be quantified in terms of probability of occurrence of liquefaction, which is required for better design decision to be taken for precautionary measures to be considered for construction works to be done on the liquefied site. This is a disadvantage of deterministic method as it is unable to quantify the degree of conservativeness, which is addressed in the next chapter in terms of probabilistic approach.

Chapter 5

PROBABILISTIC EVALUATION OF LIQUEFACTION POTENTIAL

5.1 INTRODUCTION

The discussed methods in the previous chapter are deterministic methods, in which liquefaction potential of soil is evaluated in terms of factor of safety against liquefaction (F_s).However, due to parameter and model uncertainties, F_s>1 does not always indicate non-liquefaction and similarly $F_s \leq 1$ does not always correspond to liquefaction, which is already mentioned in the first chapter. The boundary curve (surface) that separates liquefaction and non-liquefaction cases in the deterministic approach is found to be biased towards conservative side by encompassing most of the liquefied cases as discussed in the previous chapter. But, the degree of conservatism is not quantified. In order to overcome the mentioned difficulties in deterministic approach, probabilistic evaluation of liquefaction potential has been performed where liquefaction potential is expressed in terms of probability of liquefaction(P_L) and the degree of conservatism can be quantified in terms of P_L.

Thus, attempts have been made by several researchers to quantify the unknown degree of conservatism associated with the limit state function and to assess liquefaction potential in terms of probability of liquefaction (P_L) using statistical or probabilistic approaches and the same has been discussed elaborately in the Chapter-II.

In the present study an attempt has been made to develop a probability design chart using a mapping function based on post liquefaction SPT database (Hwang and Yang 2001). The mapping function is developed on the basis of Bayesian theory of conditional probability to relate F_s with P_L. Herein, the limit state function for assessing cyclic resistance ratio (*CRR*) of soil and thus, the factor of safety (F_s) against liquefaction occurrence is assessed using the

developed MGGP-based deterministic model as present in the previous chapter. Using an independent post liquefaction SPT dataset, a comparative study among the present MGGP model, available ANN and statistical models is made in terms of rate of successful prediction of liquefaction and non-liquefaction cases based on P_L.

Similarly in this chapter, an attempt has also been made to develop a P_L-based design chart using a mapping function based on available post liquefaction CPT database (Juang et al. 2003). The mapping function is developed on the basis of Bayesian theory to relate F_s with P_L as explained above using the developed CPT-based deterministic model as presented in the Chapter-IV. And also using an independent CPT database, a comparative study among the present MGGP method, available ANN and statistical methods is made in terms of rate of successful prediction of liquefaction and non-liquefaction cases on the basis of P_L.

5.2 SPT-BASED PROBABILISTIC MODEL DEVELOPMENT

The SPT-based deterministic method as proposed in the previous chapter is calibrated with the liquefaction field performance observations using Bayesian theory of conditional probability and case histories of post liquefaction SPT database to develop a probabilistic model, referred herein as Bayesian mapping function, which is used to correlate F_s with P_L.

5.2.1 Development of Bayesian mapping function

According to Juang et al.(1999b) the probability of liquefaction occurrence of a case in the database, for which the F_s has been calculated, can be found out using Bayes' theorem of conditional probability as given below.

$$P\left(L/F_s\right)=\frac{P\left(F_s/L\right)P\left(L\right)}{P\left(F_s/L\right)P\left(L\right)+P\left(F_s/NL\right)P\left(NL\right)} \tag{5.1}$$

where $P(L/\ F_s)$ = probability of liquefaction for a given F_s ; $P(F_s/L)$ = probability of F_s, assumed that liquefaction did occur; F_s, assumed that liquefaction did occur; $P(F_s/\text{NL})$ = probability of F_s, assumed that liquefaction did not occur; $P(L)$ = prior probability of

liquefaction; and $P(NL)$ = prior probability of non-liquefaction. $P(F_s/L)$ and $P(F_s/NL)$ can be obtained by using Eq. (5.2a), (5.2b), respectively.

$$P(F_s/L) = \int_{F_s}^{F_s+\Delta F_s} f_L(x)dx \tag{5.2a}$$

$$P(F_s/NL) = \int_{F_s}^{F_s+\Delta F_s} f_{NL}(x)dx \tag{5.2b}$$

where $f_L(x)$ and $f_{NL}(x)$ are the probability density functions of F_s for liquefied cases and non-liquefied cases of the database respectively. As $\Delta F_s \rightarrow 0$ Equation (5.1) can be expressed as Equation (5.3).

$$P(L/F_s) = \frac{f_L(F_s)P(L)}{f_L(F_s)P(L) + f_{NL}(F_s)P(NL)} \tag{5.3}$$

If the information of prior probabilities $P(L)$ and $P(NL)$ is available Eq.(5.3) can be used to determine the probability of liquefaction for a given F_s. In absence of $P(L)$ and $P(NL)$ values it can be assumed that $P(L) = P(NL)$ on the basis of the maximum entropy principle (Juang et al. 1999b). Thus, under the assumption that $P(L) = P(NL)$, Eq. (5.3) can be presented as Eq.(5.4).

$$P_L = \frac{f_L(F_s)}{f_L(F_s) + f_{NL}(F_s)} \tag{5.4}$$

where, $f_L(F_s)$ and $f_{NL}(F_s)$ are the probability density functions (PDFs) of F_s for liquefied cases and non-liquefied cases respectively.

In the present investigation, the calculated F_s values, using the SPT-based deterministic method as presented in the previous chapter, for different cases of the database (Hwang and Yang 2001) are grouped according to the field performance observation of liquefaction (L)

and non-liquefaction (*NL*). Several different probability density functions are considered and out of them the three best fitting curves (Lognormal, Weibull and Rayleigh) to the histogram for both *L* and *NL* groups are shown in Figs 5.1a to F. It is found from the above figures that the factor of safety of *L* group is best fitted by Weibull distribution with scale parameter (λ) and shape parameter (k) of 0.580 and 2.437, respectively and the PDF of the above Weibull distributions shown in Figure 5.1 (b), can be presented as Eq. (5.5) :

$$f(x;\lambda,k)=\frac{k}{\lambda}\left(\frac{x}{\lambda}\right)^{k-1}e^{-\left(\frac{x}{\lambda}\right)^{k}}, \qquad x\geq 0 \tag{5.5}$$

And the *NL* group is best fitted by Rayleigh distribution (λ= 1.476)as shown in Figure 5.1 (f) and the corresponding PDF can be presented as Eq. (5.6).

$$f(x;\lambda)=\left(\frac{x}{\lambda^{2}}\right)e^{-\left(\frac{x^{2}}{2\lambda^{2}}\right)}, \qquad x\geq 0 \tag{5.6}$$

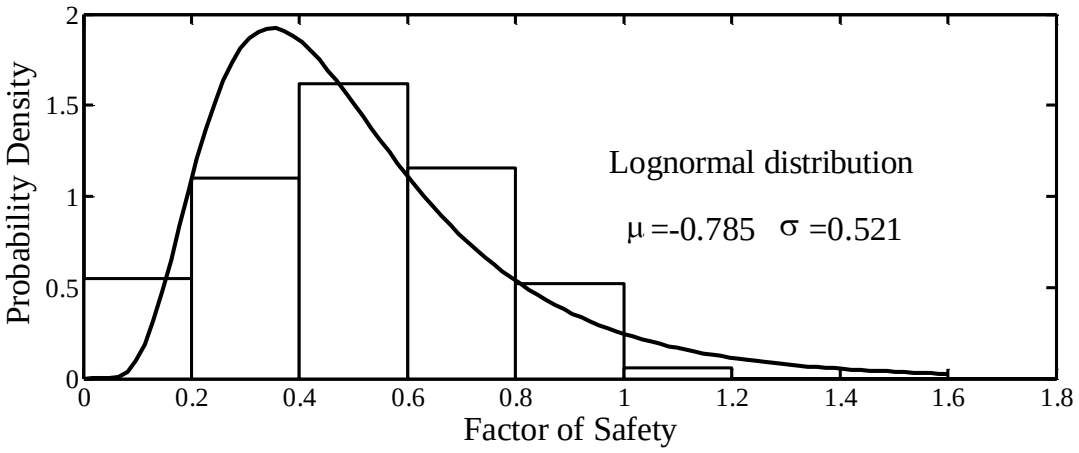

(a)

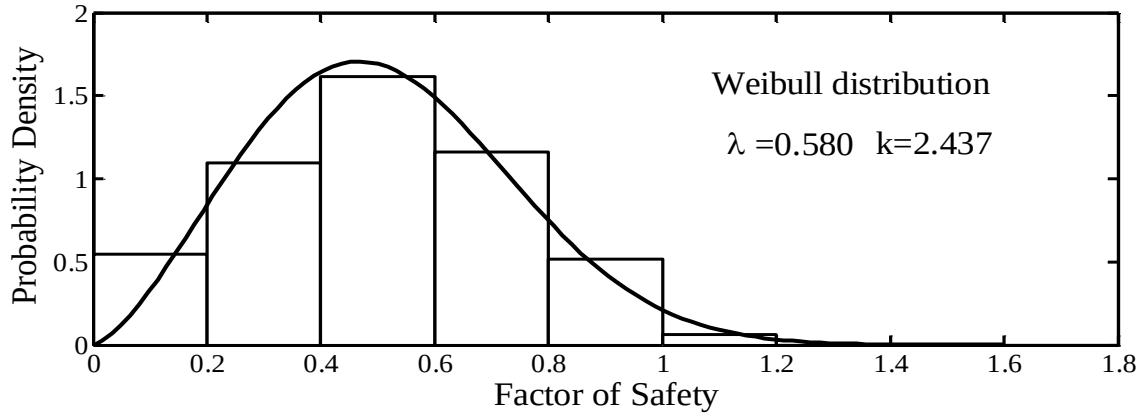
Probability Density
Weibull distribution
λ =0.580 k=2.437
Factor of Safety

(b)

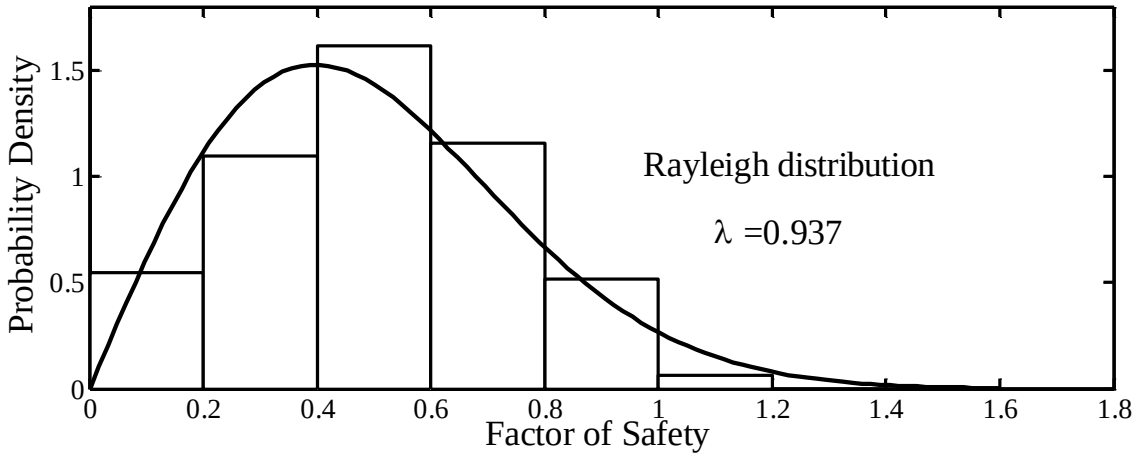
Probability Density
Rayleigh distribution
λ =0.937
Factor of Safety

(c)

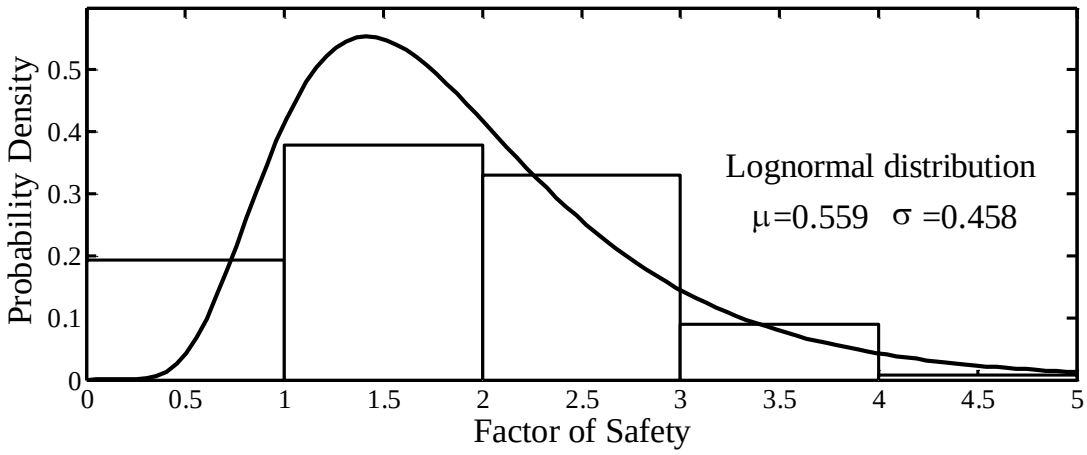
Probability Density
Lognormal distribution
μ=0.559 σ =0.458
Factor of Safety

(d)

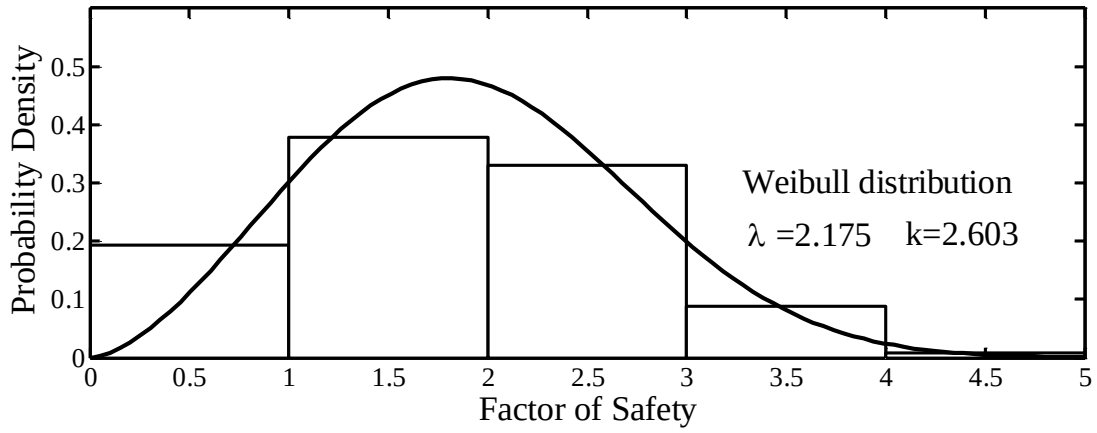

(e)

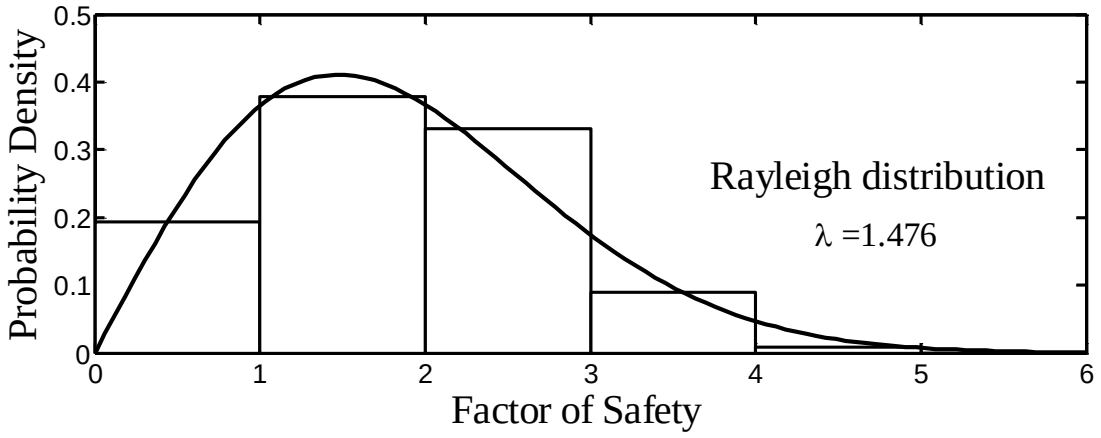

(f)

Fig. 5.1 Histogram showing the distributions (PDFs) of calculated factor of safeties: (a),(b), (c) Liquefied (*L*) cases; (d),(e),(f) Non-liquefied (*NL*) cases.

Based on the obtained probability density functions, P_L is calculated using Eq. (5.4) for each case in the database. The F_s and the corresponding P_L of the total 288 cases of database are plotted and the mapping function is obtained through curve fitting as shown in Fig.5.2. The mapping function is presented as Eq. (5.7), which is having R^2value of 0.99.

$$P_L = \frac{1}{1+\left(\frac{F_s}{E}\right)^F} \tag{5.7}$$

where E and F are the parameters (E=0.95 and F=7.7) of the fitted logistic curve. The factor of safety against the occurrence of liquefaction is calculated using the proposed MGGP-based deterministic method and corresponding probability of liquefaction can be found out using the developed mapping function.

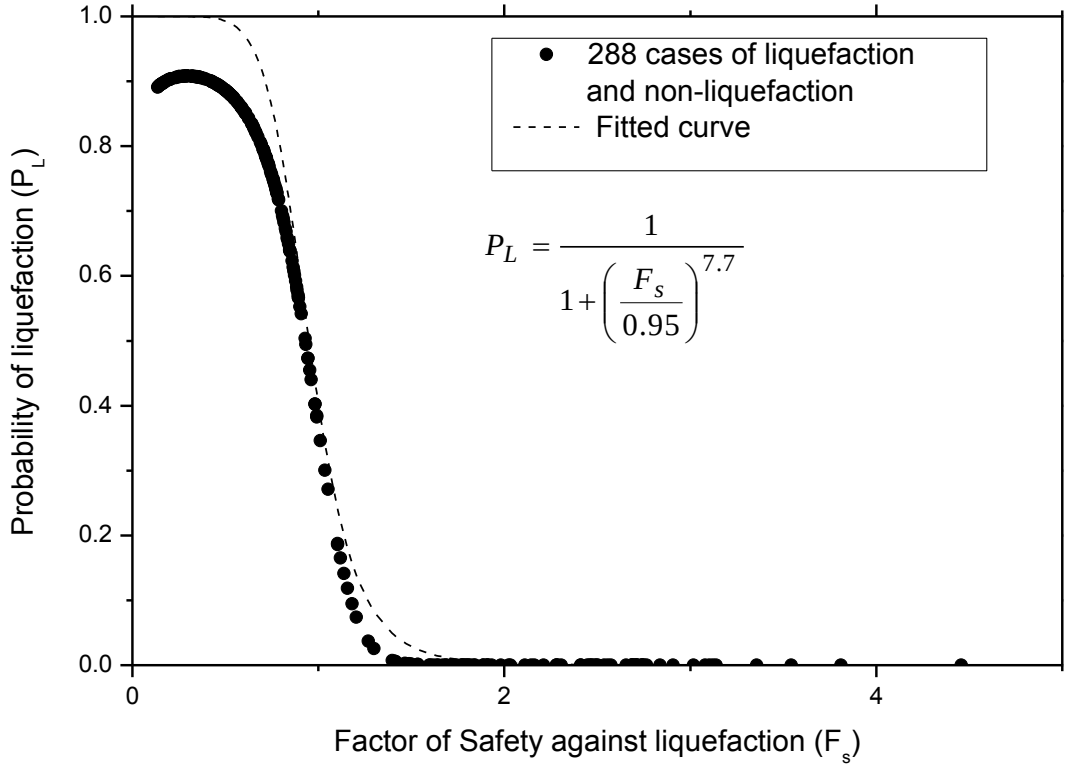

Fig.5.2 Plot of P_L-F_s showing the mapping function obtained through curve fitting.

Probability curves generated using the mapping function (Eq. 5.7) and the deterministic limit state curve represented by Eq. (4.7) are shown in Fig.5.3, wherein, the data points representing field performance cases of the database (Hwang and Yang 2001) is also presented. The relative position of the proposed deterministic limit state curve corresponds to a probability of 40% with respect to the probability curves. As the deterministic limit state curve (i.e., boundary curve) corresponds to a F_s = 1, Eq. (5.5) yields a P_L = 0.40, which is also confirmed from the relative position of the deterministic curve in the probability chart as mentioned above. This is close to the 50% probability that is associated with a

completely unbiased limit state curve corresponding to factor of safety of 1.0 and mapping function parameter (E) value of 1.0. The mapping function can be utilized as a tool for selecting proper factor of safety based on the risk (i.e., the probability of liquefaction) that is acceptable for a particular project under consideration.. For example while applying the present deterministic method with a factor of safety of 0.95 would result in a probability of liquefaction 50% whereas an increased F_s of 1.14 corresponds to a P_L of 20%. If a probability of liquefaction less than 20% is required for a particular project in a site then, this can be achieved by selecting a larger factor of safety on the basis of the developed mapping function.

5.2.2 Probability-based chart for evaluation of liquefaction potential

The mapping function as presented by Eq. (5.7) is used to develop a probability chart as shown in Fig. 5.4. This chart can be used by the geotechnical professionals to find out the probability of occurrence of liquefaction for a given soil under a given seismic load ($CSR_{7.5}$) and soil resistance (CRR). It can also be used to assess the soil strength in terms of CRR or $N_{1,60}$ at a design level of seismic loading with an assured level of risk (i.e., probability of liquefaction). The use of the design chart (Fig.5.4) is explained by considering the same example as presented by Juang et al. (2000b) for their ANN-based probabilistic model. Let a sandy soil layer is having following properties: depth, z = 5.8m, vertical effective stress of soil at the depth studied, σ'_v=84kPa, vertical total stress of soil at that depth, σ_v= 111kPa, fines content, FC=2%, and $N_{1,60}$ = 6. The structure to be built at the site is to be designed for an earthquake of moment magnitude, M_w =7 and peak horizontal ground surface acceleration, a_{max}= 0.2g. In this case the $CSR_{7.5}$ is found out to be 0.14 as per Eq. (4.2) and corresponding CRR is found out to be 0.10 as per the present MGGP model (Eq.4.7), which is close to the CRR value (0.09) as obtained by the AAN-based method of Juang et al. (2000b).

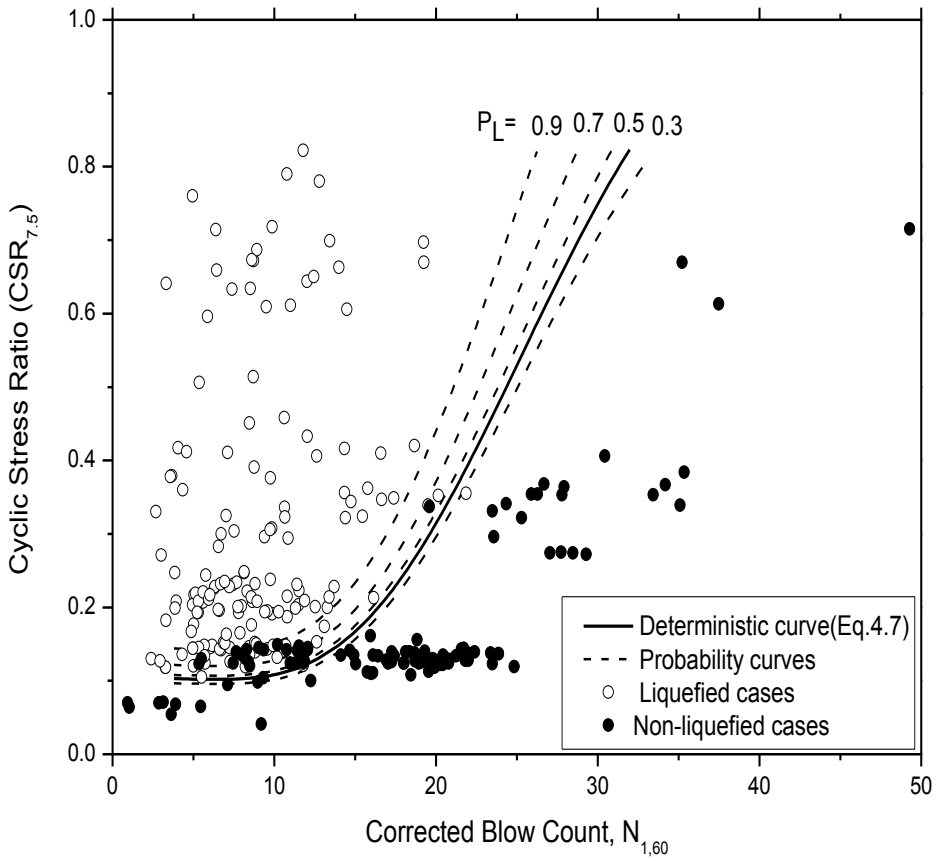

Fig.5.3 SPT-based deterministic and probability curves with liquefied and non-liquefied cases of the database (Data from Hwang et al. 2001)

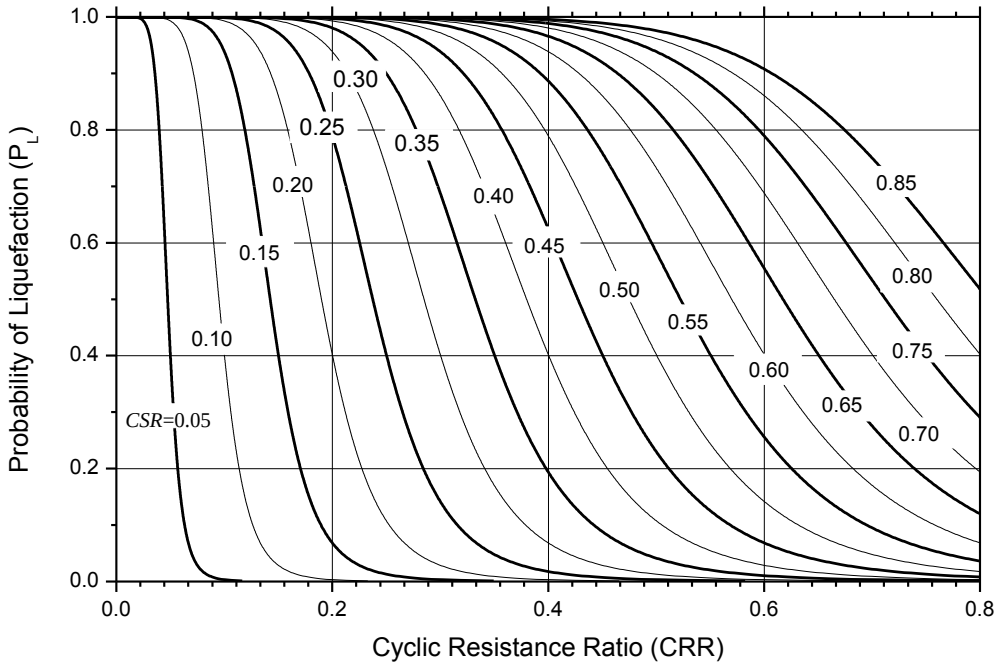

Fig.5.4 Probability-based design chart for evaluation of liquefaction potential of soil

If the accepted level of risk is 20% (i.e. P_L=0.2) for the said project, then minimum required *CRR* value as per the proposed design chart (Fig.5.4) is 0.16 whereas, the *CRR* value obtained by Juang et al. (2000b) is 0.2. For a ground improvement project, the required $N_{1,60}$ values corresponding to the obtained *CRR* value of 0.16 is found out to be 14.63 as per the Eq.(4.7). Thus, after ground improvement the $N_{1,60}$ value should reach a value greater than 14.63. The corresponding $N_{1,60}$value obtained by the ANN based design chart and associated equations proposed by Juang et al. (2000b) is 16.0, which is slightly more than that obtained by the present MGGP-based model and probability chart. It may be mentioned here that the efficacy of the ANN model, based on which probability design chart was prepared by Juang et al., (2000b) were 91% and 82% for training and testing data respectively. In the present study, the design chart is prepared based on MGGP model (Eq.4.6), which has successful prediction rate of 94.55% for training and 94.19% for testing data.

The proposed probability-based design chart and the associated model equations can be utilized by the geotechnical engineering professionals to take a risk-based design decision

regarding liquefaction potential depending on the importance of the structure to be built and the necessary $N_{1,60}$value for the possible ground improvement work.

5.2.3 Comparison with existing methods using independent database

It is always required to compare the efficacy of a newly developed method with that of the existing methods. In the present study the developed MGGP-based method is compared with the statistical and ANN-based method proposed by Juang et al. (2000b) in terms of rate of successful prediction of liquefied and non-liquefied cases. An independent post liquefaction SPT-based database (Idriss and Boulanger 2010) consisting of total 230 cases, out of which 115 cases having surface evidence of liquefaction, 112 cases of non-liquefaction and 3 marginal cases provides a good basis for comparison of efficacy of the above methods.

The probability of liquefaction of the total 227 cases of the database (neglecting 3 marginal cases) are calculated using ANN-based method (Juang et al. 2000b), statistical method (Juang et al. 2000) and the proposed MGGP-based method. The assessed probability of liquefaction, P_L is used to judge the correctness of the prediction on the basis of field manifestations. In the present study the success rate of prediction for liquefaction is measured based on three criteria from stringent to liberal (A to C); P_L (0.85 to 1.0) is the stringent criterion (A), P_L (0.65 to 1) is the intermediate criterion (B) and P_L (0.5 to 1.0)is the liberal criterion (C). Similarly for non- liquefied cases stringent (A) if P_L is in the range [0, 0.15]; if P_L is within the range 0 to 0.5 then considered to be liberal (C) criterion and for the intermediate criterion (B), P_L>=0 and P_L<0.35 (Juang et al., 2002b). As per the comparison presented in Table 5.1 the rate of successful prediction by the proposed MGGP-based probabilistic model on the basis of the stringent criteria: A (73%) and B (80%) is better than that of the statistical method: A(34%), B(61%); and ANN-based method: A(36%), B(62%) for liquefied cases. Similar observations can be drawn for non-liquefied cases and overall cases of the database. The prediction results as obtained by the three mentioned methods are comparable on basis of the liberal criterion, C.

It is pertinent to mention here that the proposed MGGP based *CRR* model is a function of $N_{1,60}$ whereas the *CRR* models of Juang et al. (2000b) are function of clean sand equivalence

of the overburden stress corrected SPT blow count, $N_{1,60,cs.}$, the parameter which takes care of the effect of fines content on the resistance of soil. The ANN and statistical methods (Juang et al., 2000b) are applicable for $N_{1,60,cs}$<35 and $N_{1,60,cs}$<30 respectively, otherwise the soil is considered to be too clay rich to liquefy. It is found that in the mentioned database 27 cases are having $N_{1,60,cs}$ value more than or equal to 35 and for 31 cases $N_{1,60,cs}$ >= 30. For these cases P_L is considered to be zero for the comparative study presented in Table 5.1. Even though, the proposed MGGP-based *CRR* model does not incorporate fines content (*FC*) parameter, it predicts well all the 31 cases of database having $N_{1,60,cs}$ >= 30 as non liquefied cases based on the calculated P_L. This shows the compactness as well as the effectiveness of the developed *CRR* model, which is a function of only parameter $N_{1,60}$ compared to the available ANN and statistical methods.

Table 5.1 Comparison of results of probabilistic models of proposed MGGP method with Statistical and ANN-based methods on independent database (Idriss and Boulanger 2010)

Criterion For P_L	Statistical method (Juang et al., 2000b)		ANN-based method (Juang et al., 2000b)		MGGP-based method (Present study)	
	No. of successful prediction	Rate (%)	No. of successful prediction	Rate (%)	No. of successful prediction	Rate (%)
Based on 115 Liquefied cases						
A(P_L>0.85)	38	34	41	36	83	73
B(P_L>0.65)	70	61	71	62	91	80
C(P_L>0.5)	87	76	95	83	96	84
Based on 112 Non liquefied cases						
A(P_L<0.15)	69	62	60	54	89	80
B(P_L<0.35)	95	85	84	75	95	85
C(P_L<0.5)	106	95	103	92	101	91
Based on all 227cases						
A	107	48	101	45	172	76
B	165	73	155	69	186	82
C	193	86	198	88	197	87

5.3 CPT-BASED PROBABILISTIC MODEL DEVELOPMENT

The CPT-based deterministic method as proposed in the previous chapter is calibrated with the liquefaction field manifestations using Bayesian theory of conditional probability and the case histories of post liquefaction CPT database to develop a mapping function that correlates F_s with P_L.

5.3.1. Development of Bayesian mapping function

The probability of liquefaction occurrence of a case in the database, for which the F_s has been calculated, can be found out using Bayesian theory of conditional probability as explained above in the section 5.2.1 and the relation between the F_s and P_L is presented by Eq. (5.4). The calculated F_s values, for different cases of the present database (Juang et al. 2003) using the MGGP-based deterministic method as presented in Chapter-IV, are grouped according to the field performance observation of liquefaction (*L*) and non-liquefaction (*NL*). Several probability density functions are considered and fitted with *L* and *NL* groups and few of fitted distribution curves (lognormal, Weibull, Rayleigh and Normal distributions) are shown in Figs. 5.5a to 5.5h. It is found that the liquefied and non-liquefied groups are best fitted by Weibull distribution (parameters: λ=0.588, k=2.362) and lognormal distribution (parameters: μ=0.476, σ=0.422), respectively as shown in Figs. 5.5 (b) and (e).The PDF of the above Weibull distribution is already presented by Eq. 5.5. Similarly the PDF of lognormal distribution can be presented by Eq. (5.8).

$$f(x) = \frac{1}{x\sigma_1\sqrt{2\pi}} \exp\left[-\frac{(\ln x - \mu_1)^2}{2\sigma_1^2} \right] \tag{5.8}$$

where $\mu_1 = ln\left(\frac{\mu^2}{\sigma^2 + \mu^2} \right)$ and $\sigma_1 = \sqrt{ln\left(\frac{\sigma^2 + \mu^2}{\mu^2} \right)}$

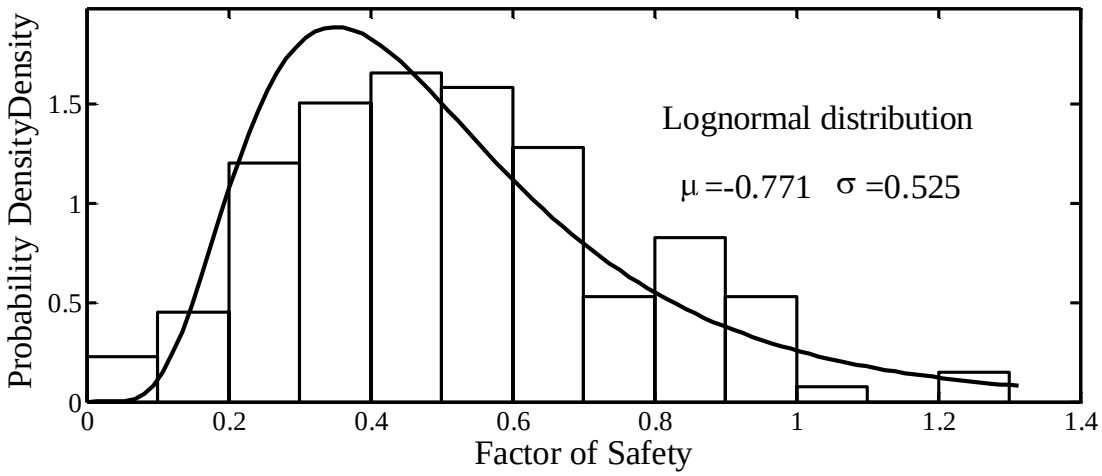
Probability DensityDensity
Lognormal distribution
μ =-0.771 σ =0.525
Factor of Safety

(a)

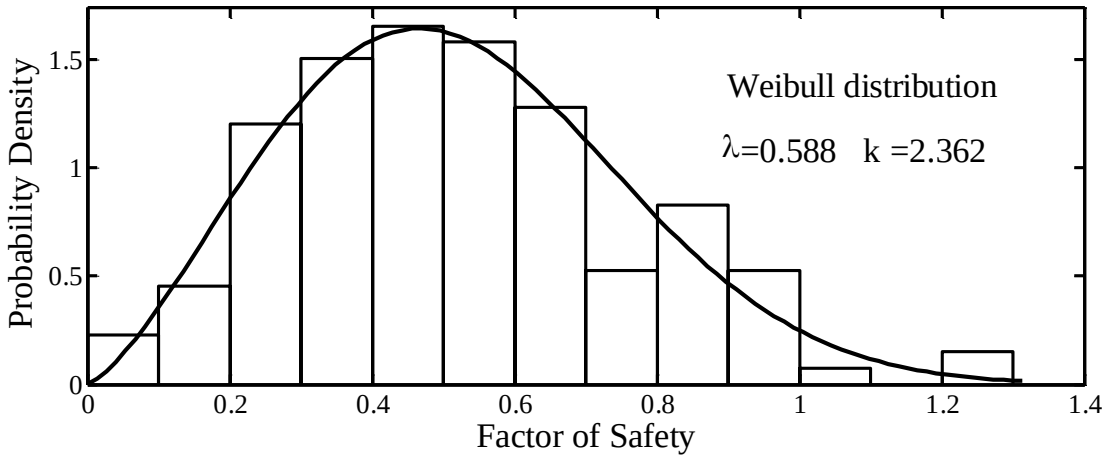
Probability Density
Weibull distribution
λ=0.588 k =2.362
Factor of Safety

(b)

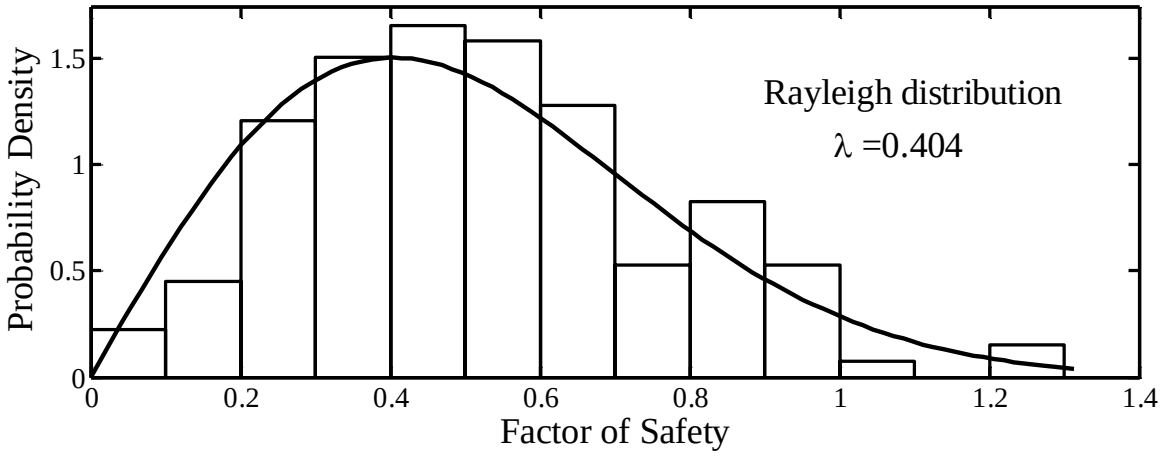
Probability Density
Rayleigh distribution
λ =0.404
Factor of Safety

(c)

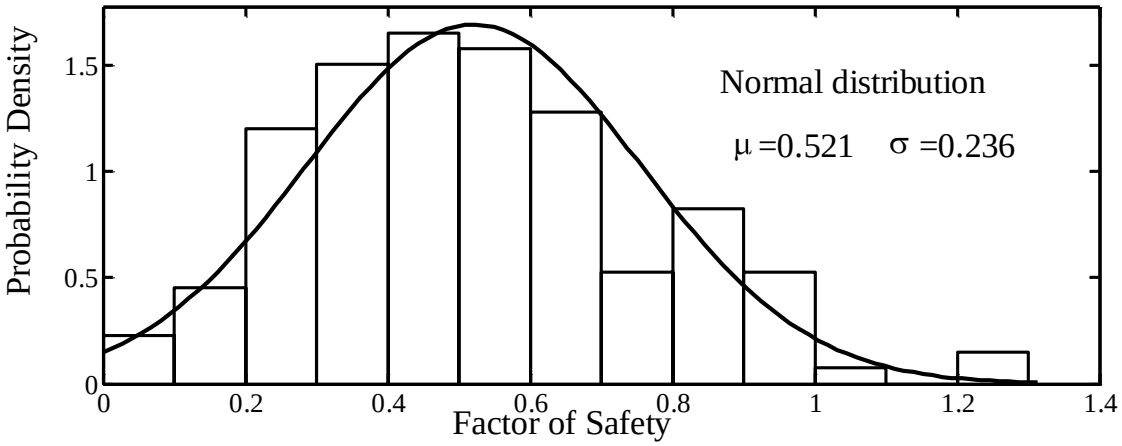
Probability Density
Normal distribution
μ =0.521 σ =0.236
Factor of Safety

(d)

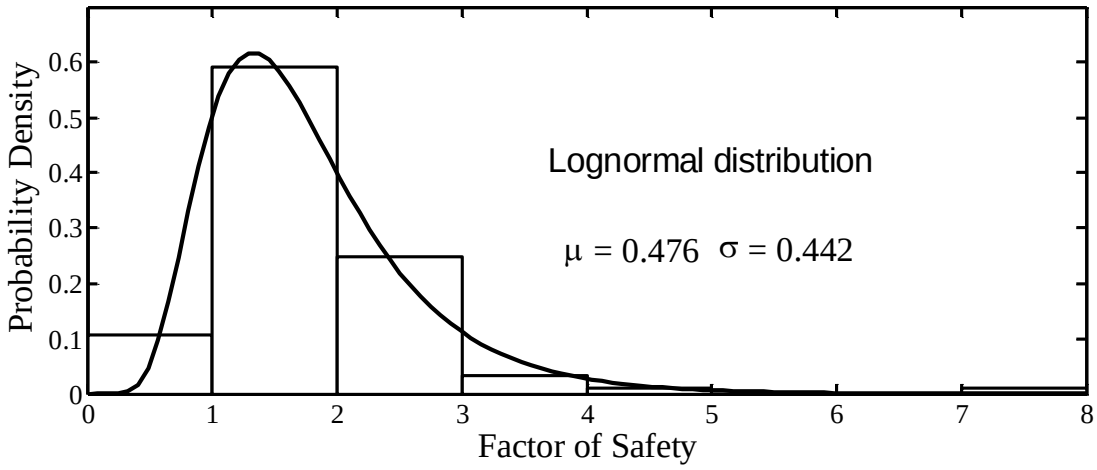
Probability Density
Lognormal distribution
μ = 0.476 σ = 0.442
Factor of Safety

(e)

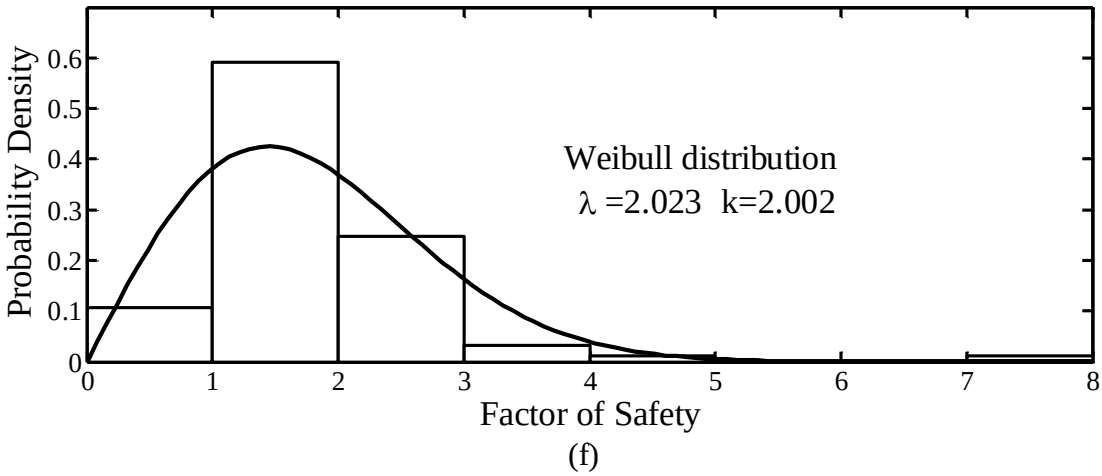
Probability Density
Weibull distribution
λ =2.023 k=2.002
Factor of Safety

(f)

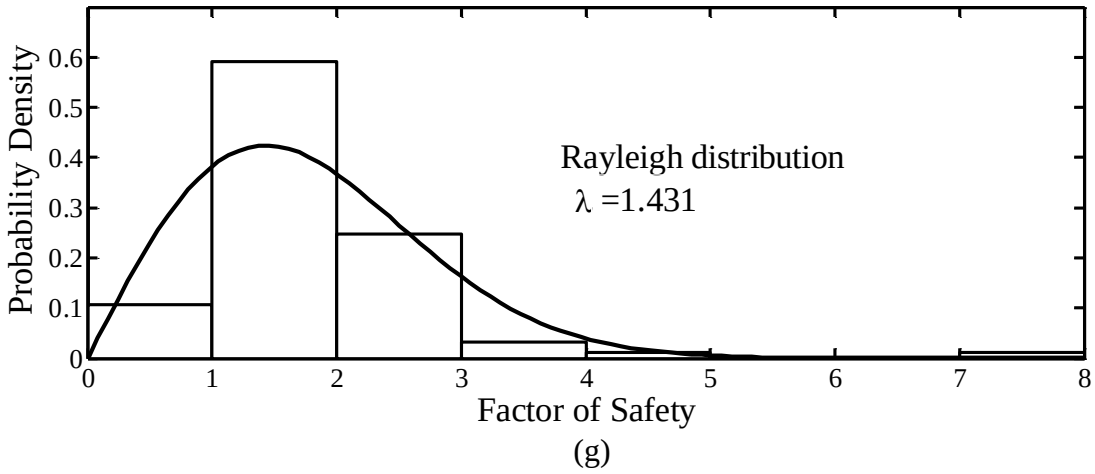

(g)

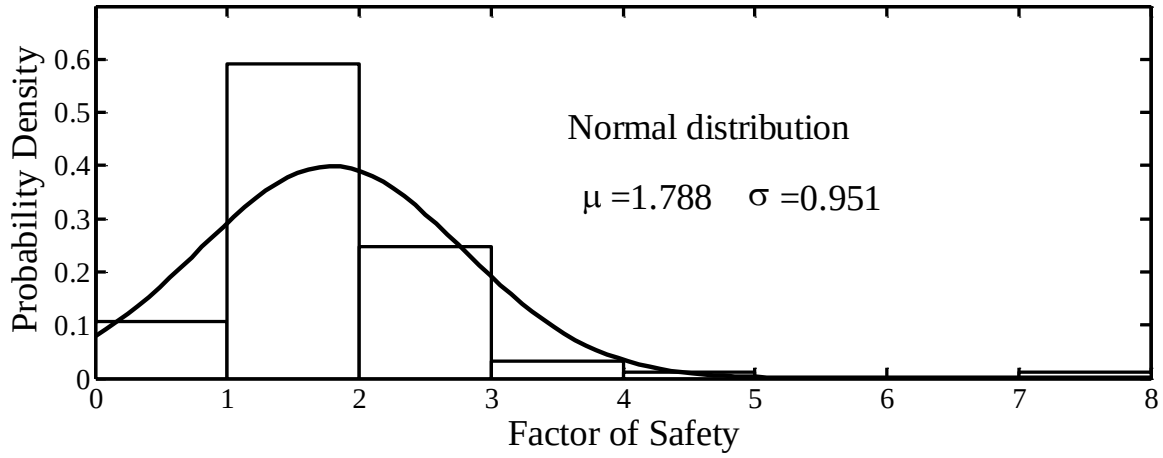

(h)

Fig. 5.5 Histogram showing the distributions of calculated factor of safeties: (a), (b), (c), (d) Liquefied (*L*) cases; (e), (f), (g), (h) Non-liquefied (*NL*) cases.

For the present CPT database, $f_L(F_s)$ and $f_{NL}(F_s)$ are the Weibull and lognormal probability density functions of F_s for liquefied cases and non-liquefied cases, respectively. Based on the obtained probability density functions, P_L is calculated using Eq. (5.4) for each case in the database. The F_s and the corresponding P_L of the total 226 cases of database are plotted and the mapping function is approximated through curve fitting as shown in Fig.5.6. The mapping function is presented as Eq. (5.9) with a high value of R^2 (0.993).

$$P_L = \frac{1}{1+\left(\frac{F_s}{a}\right)^b} \tag{5.9}$$

where *a* (0.96) and *b* (7.3) are the parameters of the fitted logistic curve. The F_s is calculated using the proposed MGGP-based deterministic method and the corresponding P_L can be found out using the developed mapping function.

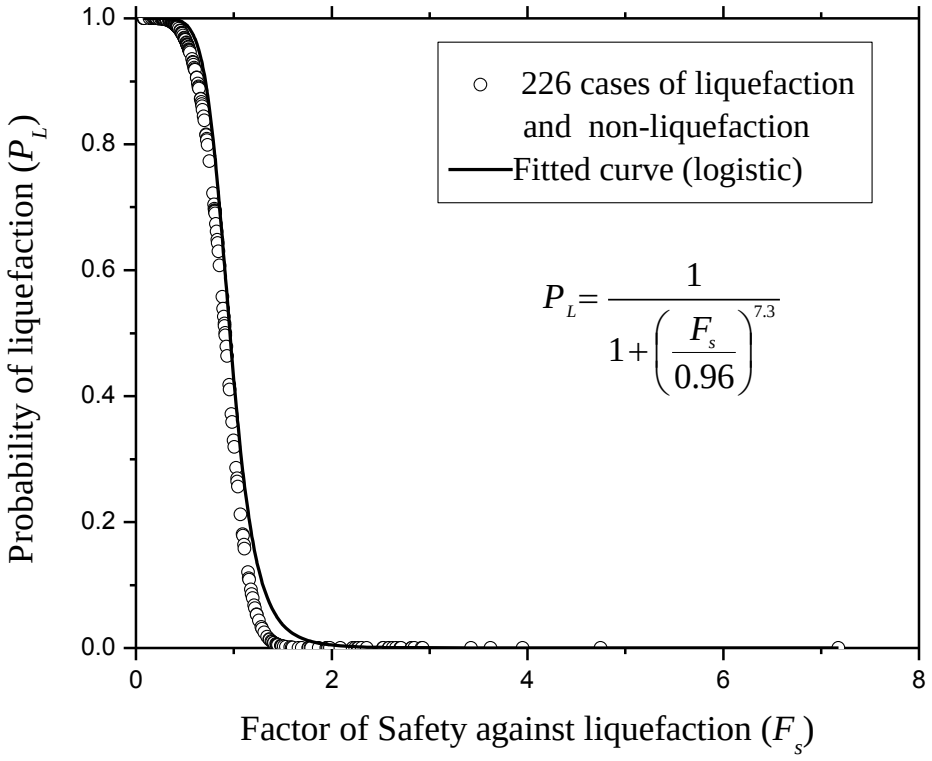

Fig.5.6 Plot of P_L-F_s showing the mapping function approximated through curve fitting.

The proposed deterministic limit state surface (F_s=1.0) corresponds to a probability of 42.6% according to the Eq. (5.9). This is close to the 50% probability that is associated with a completely unbiased limit state curve corresponding to a factor of safety of 1.0 and mapping function parameter (*a*) value of 1. The mapping function can be utilized as a tool for selecting proper factor of safety based on the probability of liquefaction that is acceptable for a particular project under consideration. For example, applying the present deterministic method with a factor of safety of 0.96 would result in a probability of liquefaction (P_L) of 50%, whereas an increased F_s of 1.15 corresponds to a reduced P_L of 21%. If a probability of liquefaction less than 21% is required for a particular project in a

site, this can be achieved by selecting a larger factor of safety on the basis of the developed mapping function.

5.3.2 P_L-based design chart

The mapping function as presented by Eq. (5.9) is used to develop a P_L-based design chart as shown in Fig.5.7. This chart can be used by the geotechnical professionals to find out the probability of occurrence of liquefaction for a given soil under a given seismic load ($CSR_{7.5}$) and soil resistance (*CRR*). It can also be used to assess the soil strength in terms of *CRR* or q_{c1N}at a design level of seismic loading with a given probability of liquefaction. The use of the design chart (Fig. 5.7) is explained by considering an example as presented below. Let a soil layer have the following properties: depth, z = 4.35m, σ'_v=32.44 kPa, σ_v= 47.94 kPa, sleeve friction resistance (f_s) = 42.86 kPa and q_c = 3360 kPa. The structure to be built at the site is to be designed for an earthquake of moment magnitude, M_w = 7.5 and peak horizontal ground surface acceleration (a_{max}) of 0.16g. In this case the $CSR_{7.5}$ (Eq. 4.2) is found out to be 0.15 and the corresponding *CRR* (Eq.4.23) is 0.122 according to the proposed CPT-based deterministic method as presented in the previous chapter.

If the accepted probability of liquefaction is 20% (i.e. P_L=0.2) for the said project, then minimum required *CRR* value as per the proposed design chart (Fig. 5.7) is 0.175. For a ground improvement project, the required q_{c1N} value corresponding to the obtained *CRR* is found to be 85.65 using the Eq. (4.23). With the above q_{c1N} value, the $q_c$value is found to be 4880 kPa using Eq. (4.16). Thus, after desired ground improvement work the q_c should have a value greater than 4880 kPa.

The proposed probability-based design chart and the associated model equations can be utilized by the geotechnical engineering professionals to take a probability-based design decision on selecting desired F_s value depending on the importance of the structure to be built. The necessary q_c value for the possible ground improvement work can be worked out.

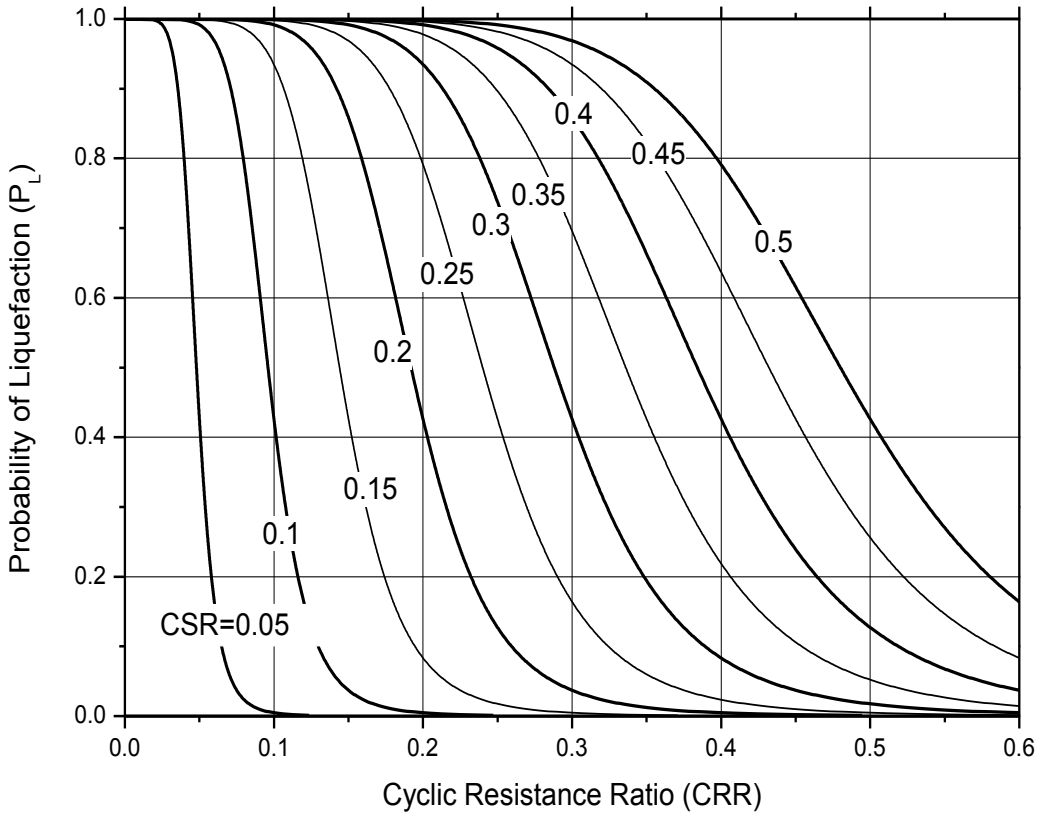

Fig. 5.7 P_L-based design chart for evaluation of liquefaction potential of soil using CPT data.

5.3.3 Comparison with existing methods

It is always required to compare the efficacy of a newly developed method with that of the existing methods. In the present study, the developed MGGP-based method is compared with widely used Robertson method and Olsen method and Juang method in terms of rate of successful prediction of liquefied and non-liquefied cases. The comparison of performance of these methods are made using the present database (Juang et al. 2003), based on which the proposed MGGP method and the Juang method are developed. The statistical methods: Olsen method and Robertson method were developed using another database. It may be mentioned here that performances of statistical methods do not depend upon the database used. The probabilities of liquefaction for the total 226 cases of the database are calculated using Olsen, Robertson, Juang and the proposed MGGP methods. The assessed probability of liquefaction is used to judge the correctness of the prediction on the basis of field manifestation. If the P_L value is found out to be 1.0 for a particular case then, there is

maximum probability that liquefaction will occur and similarly, P_L = 0 corresponds to maximum probability of non-liquefaction. But, it is not always possible to get the P_L values as 1.0 or 0. Hence, in the present study, the success rate of prediction of liquefied cases is measured on the basis of three different limits of P_L values and are as follows: [0.85 - 1.0], [0.65 - 1] and [0.5 - 1.0]. Similarly, for non- liquefied cases the three P_L limits considered for comparison of prediction efficacy of the above methods are in the range [0, 0.15], [0, 0.35] and [0, 0.5] (Juang et al. 2002b). In order to compare the efficacy of the proposed MGGP-based probabilistic model with the available ANN-based and other two statistical regression-based probabilistic models, the above criteria are considered here.

As per the comparison presented in Table 5.2, the rate of successful prediction by the proposed MGGP-based probabilistic model for liquefied cases on the basis of above three different P_L limits are (83%), (91%) and (97%) respectively, which is better than that obtained by Juang method: (58%), (79%), (91%); Olsen method: (22%), (49%), (71%) and Robertson method: (45%), (76%), (85%). Similar observations can be drawn for non-liquefied cases and overall cases of the database. Thus, the proposed MGGP-based probabilistic method out performs all other methods for the database considered in the present study. It is pertinent to mention here that 24 cases of the database are representing soils with $I_c \geq 2.6$, which are considered to be too clay rich to liquefy as per Robertson and Wride (1998). However, out of these 24 cases 8 cases are identified as liquefied cases based on field manifestations. The proposed MGGP method as well as Juang method predicts all the above 8 liquefied cases correctly. This can be considered as one improvement in the present method over the Olsen method and Robertson method.

Table 5.2 Comparison of results of proposed MGGP-based probabilistic model with available statistical and ANN-based probabilistic models using the database of Juang et al. (2003).

Criterion (P_L range)	Juang Method		Olsen Method		Robertson Method		Present MGGP Method	
	No. of successful prediction	Rate (%)	No. of successful prediction	Rate (%)	No. of successful prediction	Rate (%)	No. of successful prediction	Rate (%)
Based on133 Liquefied case								
0.85-1.00	77	58	28	22	59	45	110	83
0.65-1.00	105	79	64	49	100	76	121	91
0.5-1.00	120	91	94	71	112	85	129	97
Based on 93 Non liquefied cases								
0-0.15	63	68	43	47	48	52	67	73
0-0.35	75	81	74	80	56	61	79	85
0-0.5	85	92	83	90	64	69	84	91
Based on all 226 cases								
0.85-1.00 and 0-0.15	140	62	71	32	107	48	177	79
0.65-1.00 and 0-0.35	180	80	138	62	156	70	200	89
0.5-1.00 and 0-0.5	205	91	177	79	176	78	213	95

To study the efficiency of the proposed MGGP method to a new database, an independent post liquefaction CPT database (Moss 2003 and Juang et al.2006), consisting of 200 cases, out of which 139 cases having surface evidence of liquefaction and the remaining 61 cases of non-liquefaction, is also considered. As mentioned earlier, the P_L for the total 200 cases of the database are evaluated using Olsen, Robertson, Juang and the proposed MGGP-based probabilistic methods. According to the comparison presented in Table 5.3, the accuracy in prediction of liquefied cases [(83%), (91%) and (93%)] by the proposed MGGP-based probabilistic model within the three different limits of P_L as mentioned earlier is better than that obtained by Juang method [(67%), (80%) and (87%)], Olsen method [(36%), (68%) and

(80%) and Robertson method [(53%), (76%) and (83%)] for liquefied cases. Similarly, for non-liquefied cases the successful prediction rates are as follows: MGGP method [(50%), (55%), (60%)], Juang method [(50%), (66%), (78%)], Olsen method [(23%), (43%), (55%)] and Robertson method [(40%), (51%), (63%)]. The overall accuracies are as follows: MGGP method [(73%), (80%), (83%)], Juang method [(61%), (75%), (84%)], Olsen method [(32%), (60%), (72%)] and Robertson method [(49%), (68%), (77%)].

Table 5.3 Comparison of results of proposed MGGP-based probabilistic model with available statistical and ANN-based probabilistic models using independent database.

Criterion (P_L range)	Juang Method		Olsen Method		Robertson Method		Present MGGP Method	
	No. of successful prediction	Rate (%)	No. of successful prediction	Rate (%)	No. of successful prediction	Rate (%)	No. of successful prediction	Rate (%)
Based on139 Liquefied case								
0.85-1.00	92	67	50	36	73	53	115	83
0.65-1.00	110	80	94	68	105	76	126	91
0.5-1.00	120	87	110	80	115	83	129	93
Based on 61 Non-liquefied cases								
0-0.15	30	50	14	23	24	40	30	50
0-0.35	40	66	26	43	31	51	33	55
0-0.5	47	78	33	55	38	63	36	60
Based on all 200 cases								
0.85-1.00 and 0-0.15	112	61	64	32	97	49	145	73
0.65-1.00 and 0-0.35	150	75	120	60	136	68	159	80
0.5-1.00 and 0-0.5	167	84	143	72	153	77	165	83

Based on the comparison as presented above the developed MGGP-based probabilistic method is found to be more efficient than the other methods considered in this study and is applicable to a wider range of soils like the Juang method.

5.4 CONCLUSIONS

The conclusions drawn from probabilistic method for both SPT and CPT-based models are presented separately as follows.

5.4.1 Conclusions based on SPT- based liquefaction potential evaluation

The following conclusions are reached from the results and discussion of SPT-based probabilistic evaluation of liquefaction potential.

i. The SPT-based deterministic method, as proposed in the Chapter-IV, is characterized with a probability of 40% by means of the developed Bayesian mapping function relating F_s to P_L. The developed mapping function can be utilized as a tool for selecting proper factor of safety in deterministic approach based on the probability of liquefaction that is acceptable for a particular project under consideration. For example while applying the present deterministic method with a factor of safety of 0.95 would result in a probability of liquefaction 50% whereas an increased F_s of 1.14 corresponds to a reduced P_L of 20%. If a probability of liquefaction of less than 20% is required, it can be achieved by selecting a larger F_s based on the mapping function.

ii. A probability-based design chart is prepared for evaluation of liquefaction potential of soil in terms of P_L. It can be used along with the developed SPT-based *CRR* model of Chapter-IV as a practical tool by the geotechnical professionals to take P_L-based design decisions.

iii. Using an independent database the proposed MGGP-based method is found to be more accurate than the existing ANN and statistical methods in predicting occurrence of liquefaction and non- liquefaction on the basis of calculated P_L.

5.4.2 Conclusions based on CPT- based liquefaction potential evaluation

The following conclusions are drawn based on the results and discussion as presented above for CPT-based probabilistic evaluation of liquefaction potential.

i. The CPT-based deterministic method, as proposed in the Chapter-IV, is characterized with a probability of 42.6% by means of the developed Bayesian mapping function relating F_s to P_L. The developed Bayesian mapping function can be utilized as a tool for selecting proper factor of safety in deterministic approach based on the probability of liquefaction that is acceptable for a particular project under consideration. For example, applying the present deterministic method with a factor of safety of 0.96 would result in a probability of liquefaction (P_L) of 50%, whereas an increased F_s of 1.15 corresponds to a reduced P_L of 21%. If a probability of liquefaction of less than 21% is required, it can be achieved by selecting a larger F_s based on the proposed mapping function.

ii. A P_L-based design chart is prepared for evaluation of liquefaction potential of soil using CPT data. It can be used along with the developed CPT-based *CRR* model of Chapter-IV as a practical tool by the geotechnical professionals to take probability-based design decisions.

iii. Using the present database as well as an independent database the proposed MGGP method is found to be more accurate than the existing ANN and statistical methods in predicting occurrence of liquefaction on the basis of calculated P_L.

The calculation of P_L using the developed semi-empirical models requires only the mean values of the input variables, whereas the uncertainty in the parameters and the model are excluded from the analysis. Thus, resulting P_L might be subjected to error if the effect of parameter and model uncertainties are significant. This is a draw back of mean value based probabilistic model. These difficulties can be overcome by adopting reliability based probabilistic analysis of liquefaction, which considers both model and parameter uncertainties. To conduct a thorough reliability analysis, knowledge of the uncertainties that are associated with both the input parameters and the limit state model is required. However, most of the existing simplified methods have not been fully examined for its model uncertainty, though the simplified methods developed within deterministic framework of analysis tend to be conservative to some extent. Thus, reliability-based probabilistic methods have been developed using post liquefaction SPT and CPT database in the following chapter.

Chapter 6

RELIABILITY-BASED LIQUEFACTION POTENTIAL EVALUATION

6.1 INTRODUCTION

Several probabilistic models (Lioet al. 1988; Youd and Nobble 1997;Toprak et al.1999; Juang et al. 2002a; Cetin et al. 2004), including the present SPT and CPT-based probabilistic models as presented in the previous chapter, have been developed for evaluation of liquefaction potential in terms of P_L. These models are all data-driven as they are based on statistical analyses of the databases of post liquefaction case histories. Calculation of P_L using these semi-empirical models requires only the mean values of the input variables, whereas the uncertainties in both the parameters and the model are excluded from the analysis. Thus, resulting P_L might be subjected to error if the effect of parameter and model uncertainties are significant. These difficulties can be overcome by adopting reliability based probabilistic analysis of liquefaction, which considers both model and parameter uncertainties. In the framework of reliability analysis, the boundary surface separating liquefaction and non-liquefaction cases is a limit state function. But, the reliability method needs knowledge of uncertainties associated with the input parameters and the limit state function.

As very few reliability-based models are available and those have already been discussed in Chapter-II, in the present study, an attempt has been made to evaluate reliability-based liquefaction potential of soil in terms of probability of liquefaction using first order reliability method (FORM) based on the post liquefaction SPT database (Cetin 2000). The MGGP is used to develop *CRR* model of soil. The developed *CRR* model along with the *CSR* model (Idriss and Boulanger 2006) forms the limit state function of liquefaction for reliability analysis. The uncertainties of input parameters are obtained from the database.

But, a rigorous reliability analysis associated with the Bayesian mapping function approach is carried out to estimate model uncertainty of the limit state function, which is represented by a lognormal random variable, and is characterized in terms of its two statistics, namely, the mean and the coefficient of variation. A mapping function is also developed on the basis of Bayesian theory to relate F_s with P_L, which can be used in absence of parameter uncertainties. Similarly, following the same procedure as mentioned above another reliability-based liquefaction potential evaluation model using FORM on the basis of the post liquefaction CPT database (Moss, 2003) has been developed and the model uncertainty of the developed CPT-based limit state function has been characterized through rigorous reliability analysis.

6.2 DEVELOPMENT OF SPT-BASED RELIABILITY MODEL

6.2.1 Methodology

In the present study, first, the MGGP is used to develop a liquefaction field performance observation function termed as liquefaction index (*LI*), which has already been defined in Chapter-IV. In the second step, artificial data points are generated for the unknown boundary curve separating liquefied cases from non-liquefied cases using a search technique (Juang et al. 2000). The boundary curve referred as a "limit state function" representing the *CRR* of the soil is approximated with the generated data points using MGGP. The developed *CRR* model along with the *CSR* model (Idriss and Boulanger 2006) forms the performance functions or limit state model of liquefaction for reliability analysis. Here, FORM (Hasofer and Lind 1974) is used to evaluate the liquefaction potential of soil in terms of P_L, which requires the knowledge of both parameter and model uncertainties. The uncertainty associated with proposed limit state model is determined following the extensive sensitive analysis as adopted by Juang et al. (2006) through a rigorous reliability analysis associated with the Bayesian mapping function approach. Bayesian theory of conditional probability is used to create a mapping function to relate F_s with P_L.

The GP and its variant, the MGGP have already been described in Chapter -III hence, only the general form of the model equation for the present problem is presented in the following section. A brief description about FORM for determination of reliability index and its

corresponding P_L using genetic algorithm (GA) as optimization tool is presented in the sub sections.

6.2.2 MGGP-based LI_p model

The general form of MGGP model for the development of the SPT-based LI_p model for the present problem is presented as Eq. (6.1)

$$LI_p = \sum_{i=1}^{n} F\left[X, f(X), c_i\right] + c_0 \tag{6.1}$$

where LI_p = predicted value of LI, F = the function created by the MGGP referred herein as liquefaction index function, X = vector of input variables = { $N_{1,60}$, FC, σ_v', $CSR_{7.5}$}, $N_{1,60}$is normalized standard penetration resistance as per Idriss and Boulanger (2006):

$$N_{1,60} = C_N N_{60} \tag{6.2}$$

$$C_N = \left(\frac{P_a}{\sigma_v'}\right)^{\alpha} \leq 1.7 \tag{6.3}$$

$$\alpha = 0.784 - 0.0768\sqrt{N_{1,60}} \tag{6.4}$$

where N_{60} value corresponds to measured standard penetration resistance N_m after correction to an equivalent 60% hammer efficiency as per Cetin (2000), which is a modified version of Seed et al. (1985):

$$N_{60} = N_m C_R C_S C_B C_E \tag{6.5}$$

C_R= correction for "short" rod length, C_S=correction for non-standardized sampler configuration, C_B= correction for borehole diameter, C_E= correction for hammer energy efficiency, FC= fines content in percentage (Idriss and Boulanger 2006), σ'_v = vertical effective stress of soil at the depth under consideration, P_a= 1 atm of pressure in the same units used for σ'_v, $CSR_{7.5}$ is the cyclic stress ratio adjusted to a benchmark earthquake of

moment magnitude (M_w) of 7.5 and to an equivalent σ'_v of 101kPa (Idriss and Boulanger 2006):

$$CSR_{7.5} = 0.65\left(\frac{\sigma_v}{\sigma_v'}\right)\left(\frac{a_{\max}}{g}\right)(r_d)\Big/MSF\Big/K_\sigma \tag{6.6}$$

where σ_v = total vertical stress of soil at the depth under consideration, a_{max}= peak horizontal ground surface acceleration, g = acceleration due to gravity, r_d = shear stress reduction coefficient, which is a function of depth and earthquake magnitude , is presented as follows:

$$Ln(r_d) = \alpha(z) + \beta(z)M_w \tag{6.7}$$

$$\alpha(z) = -1.012 - 1.126\sin\left(\frac{z}{11.73} + 5.133\right) \tag{6.8}$$

$$\beta(z) = 0.106 + 0.118\sin\left(\frac{z}{11.28} + 5.142\right) \tag{6.9}$$

in which z is depth in meters and M_w is moment magnitude. These equations are applicable to a depth, $z \leq 34$m and for $z \geq 34$m the following equation is applicable:

$$r_d = 0.12\exp(0.22M_w) \tag{6.10}$$

MSF is the magnitude scaling factor, which is expressed by following expression:

$$MSF = 6.9\exp\left(\frac{-M_w}{4}\right) - 0.058 \tag{6.11}$$

$$MSF \leq 1.8 \tag{6.12}$$

$K_\sigma$is the overburden correction factor as given below:

$$K_{\sigma} = 1 - C_{\sigma} \ln \left(\frac{\sigma_v'}{P_a} \right) \leq 1.0 \tag{6.13}$$

$$C_{\sigma} = \frac{1}{18.9 - 2.55\sqrt{(N_{1,60})}} \leq 0.3 \tag{6.14}$$

and c_i is a constant, f are the functions defined by the user, n is the number of terms of target expression and c_0= bias. The MGGP as per Searson et al. (2010) is used and the present model is developed and implemented using Matlab (Math Works Inc. 2005).

6.2.3 Reliability Analysis

In order to overcome the limitations of the conventional factor of safety approach and mean value-based probabilistic approach in liquefaction potential evaluation as discussed in the earlier sections, reliability analyses have been performed in the present study using first-order reliability method, FORM (Hasofer and Lind 1974). The Hasofer- Lind approach is one of the most widely used reliability methods (Haldar and Mahadevan 2000; Baecher and Christian 2003). It is an improvement over the first order second moment reliability method (FOSM) developed by Cornell (1969) and avoids its lack of invariance problem. A brief description of the formulation of the present problem as per FORM is discussed below.

In the liquefaction potential evaluation the *CSR* (loading) and the *CRR* (resistance) are denoted by *Q* and *R* respectively. The margin of safety, Z (Baecher and Christian 2003) is defined as the difference between the resistance and the load, which is also the performance function for liquefaction potential assessment and is presented by Eq. (6.15).

$$Z = R - Q \tag{6.15}$$

If Z < 0, it indicates the occurrence of liquefaction. If Z> 0, it suggests that there will be no liquefaction. If Z = 0 the performance state is designated as a limit state, which is the boundary between liquefaction and non-liquefaction. It is to be noted that both *R* and *Q* are

uncertain and thus, can be treated as random variables and reliability index (β) can be presented by Eq. (6.16) following Baecher and Christian (2003).

$$\beta = \frac{\mu_Z}{\sigma_Z} = \frac{\mu_R - \mu_Q}{\sqrt{\left(\sigma_R^2 + \sigma_Q^2 - 2\rho_{RQ}\sigma_R\sigma_Q\right)}} \tag{6.16}$$

If the load and resistance are uncorrelated (i.e. correlation coefficient is zero), Eq. (6.16) reduces to

$$\beta = \frac{\mu_Z}{\sigma_Z} = \frac{\mu_R - \mu_Q}{\sqrt{\left(\sigma_R^2 + \sigma_Q^2\right)}} \tag{6.17}$$

In Eqs. (6.16) and (6.17), μ_R, μ_Q are the mean values of *R* and *Q*, respectively; σ_R, σ_Q are the standard deviations of *R* and *Q*, respectively; σ^2_R, σ^2_Q are the variances of *R* and *Q*, respectively, and ρ_{RQ} is the correlation coefficient between *R* and *Q*. Reliability index βdefined by Eq. (6.17) is same as the first order second moment (FOSM) reliability method developed by Cornell (1969) using first-order Taylor series expansion approximation.

If *R* and *Q* are the random variables with normal distribution, then the performance function, *Z* = *R* - *Q*, is also normally distributed. Fig. 6.1 shows the resulting probability density function (PDF) of *Z*. The probability of liquefaction is defined as the probability that $Z \leq 0$. The dark area of the PDF of *Z* as shown in Fig. 6.1 indicates the probability of liquefaction. Greater the dark region the greater is the probability of liquefaction. Then, the probability of liquefaction, p_f (P_L) can be calculated from Eq. (6.18) as presented below.

$$p_f = P_L = P[Z \leq 0] == \Phi\left(-\frac{\mu_Z}{\sigma_Z}\right) = \Phi(-\beta) = 1 - \Phi(\beta) \tag{6.18}$$

where $\mathbf{\Phi}(\cdot)$ is the cumulative distribution function (CDF) for a standard normal variable.

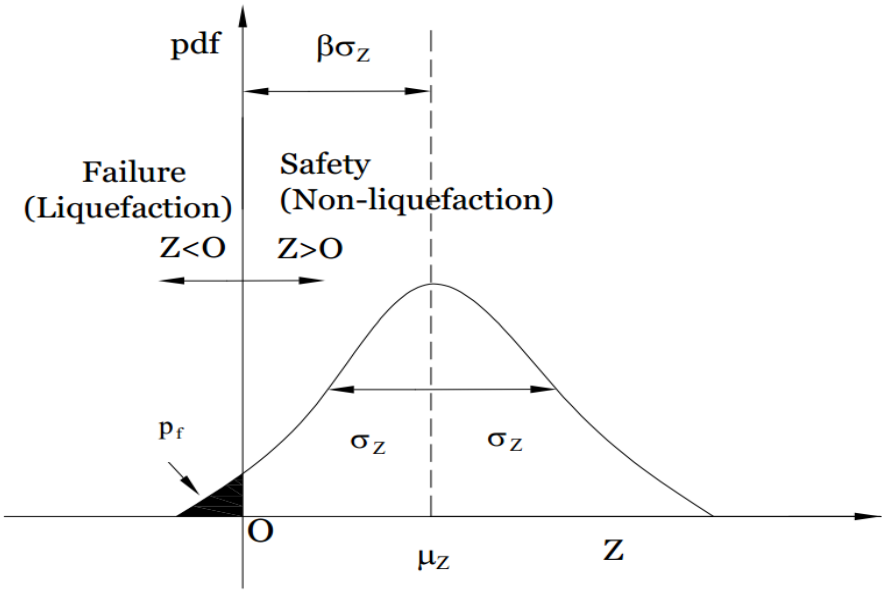

Fig. 6.1 Probability density function of liquefaction performance function, *Z* (modified from Baecher and Christian 2003).

In most of the practical problems, the performance function does depend on multiple basic variables as in case of liquefaction potential evaluation: z = *g* (z_1, z_2….z_n). In these cases the computation of probability of liquefaction is dependent on the joint probability density function of load and resistance random variables and can be presented as given below:

$$p_f = \int \ldots \int_{g(z)\leq 0} f_z(z_1, z_2, \ldots, z_n) dz_1 dz_2 \ldots dz_n \tag{6.19}$$

where f_z (z_1, z_2,…, z_n) is the joint PDF for basic random variables z_1, z_2, ….,z_n and the integration is performed over the failure region, i.e., g(z)≤0. In general, obtaining joint probability density function and the evaluation of multiple integral for large numbers of random variables is extremely difficult. Hence, to quantify the probability of liquefaction (failure), weighted average methods like point estimate method, analytical approximation methods such as first-order reliability method (FORM), which includes both first order second moment method (FOSM) and advanced first order second moment method (Hasofer-Lind method), second-order reliability methods (SORM), and simulation based methods like Monte Carlo Simulation (MCS) approach are available in the literature (e.g

Haldar and Madhadevan 2000; Baecher and Christian 2003). Since, in the present study, Hasofer-Lind reliability method, which is well known as FORM is used for the analysis of liquefaction potential of soil, the following sub-section, presents a discussion on the formulation of FORM for the present problem.

6.2.3.1 FORM (Hasofer -Lind approach)

As per Hasofer-Lind approach all the normal random variables are transformed to their reduced form in standard normal space with zero mean and unit standard deviation. Thus, *R* and *Q* in liquefaction analysis can be expressed as standard normal variables as given below.

$$R' = \frac{R - \mu_R}{\sigma_R} \qquad Q' = \frac{Q - \mu_Q}{\sigma_Q} \tag{6.20}$$

If *R* and *Q* are uncorrelated, Eq. (6.15) for the performance function becomes:

$$Z = R - Q = R'\sigma_R - Q'\sigma_Q + \mu_R - \mu_Q \tag{6.21}$$

Fig. 6.2 shows a plot of the liquefaction limit state criterion using the standard normal variables as the axes. The origin is the point at which both *R* and *Q* are equal to their mean values. The distance, *d* between the origin and the limit state line, Z= 0 is

$$d = \frac{\mu_R - \mu_Q}{\sqrt{\sigma_R^2 + \sigma_Q^2}} \tag{6.22}$$

which is identical to the definition of the reliability index β given by Eq. (6.17). This result suggests that the reliability index can be interpreted geometrically as the shortest distance from the point defined by the mean values of the variables to performance function surface defining the limit state.

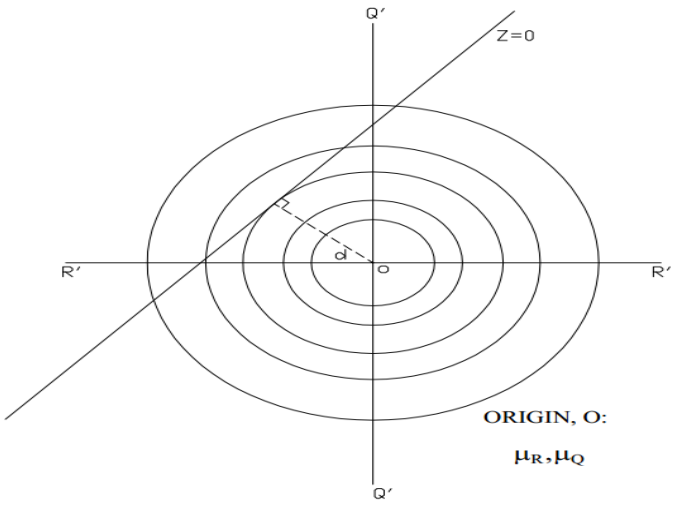

Fig. 6.2. Plot of *R'* (*CRR*) and $Q^{'}$ (*CSR*) showing definition of reliability index (modified from Baecher and Christian 2003).

But, the liquefaction performance function, Z depends on *R* and *Q*, which are also the functions of multiple basic variables such as measured standard penetration resistance (N_m), *FC*, σ_v, σ'_v, a_{max} and M_w. Thus, the performance function can be presented as $Z = R - Q = g(z)$, where *z* is a vector of uncorrelated random variables i.e.

z = {N_m, *FC*, σ_v, σ'_v, a_{max}, M_w}. Each variable, z_i is defined in terms of its mean μ_{zi} and its standard deviation σ_{zi}. The above interpretation of reliability index (Eq.6.22) can be generalized for *n* (6) number of random variables, which are first converted to standard normal variables (z_i') as per Eq. (6.20). In the multi-dimensional standard normal space, the distance from the origin to a point on the liquefaction limit state is

$$d = \sqrt{z_1^{'2} + z_2^{'2} + \ldots + z_n^{'2}} = \sqrt{z^{'T} z^{'}} \tag{6.23}$$

where the superscript T denotes the transpose of the vector $z^{'}$.

Thus, determination of β using Hasofer-Lind first order reliability formulation for liquefaction potential assessment can be stated as follows:

Minimize:

$$\beta = \min\left(z'^{T} z'\right)^{1/2} \tag{6.24a}$$

Subjected to:

$$g(z) = 0 \tag{6.24b}$$

This is a constrained optimization problem that can be solved using the various approaches such as the method of Lagrange multipliers and method of the Taylor series. Hasofer-Lind reliability approach as described above for reliability based liquefaction triggering analysis can be extended to the non-linear limit state function and to the correlated and/or non-normal random variables by suitable transformation algorithms.

In the present study, Cholesky approach (Baecher and Christian 2003) is used to convert uncorrelated standard normal variables to correlated standard normal variable using the correlation matrix (*K*) of variables as given below.

$$K = \begin{bmatrix} 1 & \rho_{12} \ldots \rho_{1n} \\ \rho_{12} & 1 \ldots \ldots \rho_{2n} \\ . & . & . \\ . & . & . \\ . & . & . \\ \rho_{1n} & \rho_{2n} \ldots . 1 \end{bmatrix} \tag{6.25}$$

where ρ_{ij} is the correlation coefficient between the variables z_i and z_j . *K* must be symmetric and positive definite, it can be factored into two matrices that are the transposes of each other:

$$K = SS^{T} \tag{6.26}$$

$$w = Sz' \tag{6.27}$$

where *w* is a vector of *n* (6) variables, each of which has a standard normal distribution, with correlation matrix *K*. *S* is a lower triangular matrix, and its transpose S^T is an upper triangular matrix. z' is vector of standard normal variables of *z*.

As in the present study, the random variables, $z = \{N_m, FC, \sigma_v, \sigma'_v, a_{max}, M_w\}$, are assumed to follow lognormal distribution, then, the mean and standard deviation of equivalent normal variables can be calculated as given below following Der Kiureghian et al.(1987):

$$\xi_i = \sqrt{\ln\left(1+\delta_{zi}^2\right)} \tag{6.28}$$

$$\lambda_i = \ln \mu_{zi} - 0.5\xi_i^2 \tag{6.29}$$

where ξ_i = the standard deviation of the equivalent normal variable; λ_i = the mean of the equivalent normal variable; μ_{zi}= the mean of the random variable z_i and δ_{zi}= the coefficient of variation of z_i.

Though, Rackwitz and Fiessler (1978) iterative algorithm is widely used for reliability problem for finding out the minimum value of β out of various algorithms available in literature (Lin and Der Kiureghian 1991) but, for the complex and non-linear limit state functions there is a tendency to attain local minima by most of the algorithms resulting in failure to locate true β value. This difficulty can be overcome by using full population based iterative procedures such as the Monte Carlo or heuristic optimization algorithm, GA (Xue and Gavin 2007; Gavin and Xue 2008; Gavin and Xue 2009). In the present study, GA has been used as the optimization tool for the reliability analysis.

The GA is a random search algorithm based on the concept of natural selection inherent in natural genetics, which presents a robust method to search for the optimum solution to the complex problems. In the present study, the GA is implemented using pseudo code (toolbox) available in Matlab (Math Works Inc. 2005).

6.2.4. Database and Pre-processing

In the present study, the models are developed based on the post liquefaction SPT database compiled and reassessed by Cetin (2000). The total database consists of 198 cases from different earthquakes around the world. But, in the present study 163 cases are considered and the remaining 35 cases of proprietary data of 1995 Hyogoken-Nambu ("Kobe") earthquake could not be considered as the details are not available in Cetin (2000). The database contains information about soil and seismic parameters such as: N_m, correction for "short" rod length (C_R), correction for non-standardized sampler configuration (C_S), correction for borehole diameter (C_B), correction for hammer energy efficiency (C_E), *FC*, σ_v, σ'_v, a_{max}, $M_w$and liquefaction field performance observation, *LI*. The soil in these cases ranges from sand to silt mixtures (sandy and clayey silt). As per Cetin (2000) the case histories in the database have been classified in three groups as Class A, Class B and Class C in decreasing order according to the quality of informational content. In the present study, 43cases out of 44 Class A data, 111 cases from 113 Class B data and all the 6 Class C data have been considered as the left out cases are marginally liquefied cases. Out of total 160 cases of data considered for model development 92 cases are liquefied and 68 cases are non-liquefied. The summarized extract of the database used for model development is provided in the Table 6.1 in terms of maximum and minimum values of the mean and coefficient of variation (COV) of the various variables considered in the present investigation as inputs and output.

6.2.5 Results and Discussion

In the MGGP procedure a number of potential models are evolved at random and each model is trained and tested using the training and testing cases respectively. The fitness of each model is determined by minimizing *RMSE* between the predicted and actual value of the output variable (*LI*) as the objective function or error function (E_f),

$$RMSE = E_f = \sqrt{\frac{\sum_{i=1}^{N}\left(LI - LI_p\right)^2}{n}} \tag{6.30}$$

where, *LI*= 1 (liquefied case), 0 (non-liquefied case), *n* = number of cases in the fitness group. If the errors calculated by using Eq. (6.30) for all the models in the existing population do not satisfy the termination criteria, the generation of new population continues until the best model is developed as per the earlier discussion.

Table 6.1 Summary of the database used for development of different models in the present study.

Model Variables	Type	Maximum mean Value	Minimum mean Value	Maximum COV Value	Minimum COV Value
d (m)	Input	20.400	1.100	-	-
N_m		37.000	1.500	0.815	0.007
FC(%)		92.000	0	2.000	0
σ_v (kPa)		383.930	15.470	0.280	0.031
σ'_v (kPa)		198.660	8.140	0.378	0.044
a_{max}(g)		0.693	0.090	0.300	0.011
M_w		8.000	5.900	0.025	0
LI	Output	1.000	0	-	-

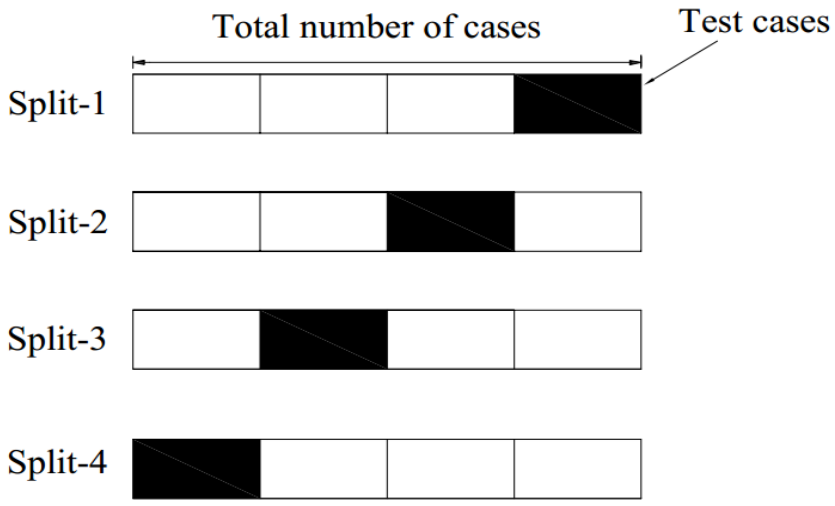

Fig. 6.3 An example of *K*-fold cross validation approach where the data are split into *K* (4) equal folds (modified from Oommen and Baise, 2010).

It is pertinent to mention here that to make a substantive claim that the developed MGGP-based LI_p model is the "best", some sort of repeated validation scheme such as *K*-fold cross-validation or repeated random sub-sampling needs to be followed. Thus, in the present study, *K*-fold cross validation (Oommen and Baise 2010), which is a more reliable and robust approach has been used to obtain the most "efficient" LI_p-based predictive model by the MGGP. Here, the original data (160 cases) of the present database is split into approximately *K* (4) equal folds. For each *K* split, (*K*-1)-folds are used for training and the remaining one fold is used for testing the developed model as shown in Fig. 6.3. Therein, the filled rectangles represent testing data, whereas the open rectangles represent the training data for each split. Hence, in each split out of the mentioned 160data, 120 data are selected for training and remaining 40 data are used for testing the developed model. The advantage of *K*-fold cross validation is that all the cases in the database are ultimately used for both training and testing. For each split, several LI_p models were obtained by using optimized values of the controlling parameters of MGGP as explained in the Chapter-IV. Then, the developed models were analyzed with respect to physical interpretation of *LI* of soil, and after careful consideration of various alternatives, four models, "best" one of each split, are selected.

Table 6.2 Performance in terms of the rate of successful prediction of MGGP-based LI_p models on the basis of *K*-fold cross validation

Model	Rate of successful prediction (%)				
	Split -1	Split -2	Split -3	Split -4	Summary
MGGP based LI_p model	85	83	80	88	84

It is important to note that the efficiency of different models should be compared in terms of testing data rather than as per training data (Das and Basudhar, 2008). Hence, the efficiency of each of the 4 developed LI_p models are evaluated by calculating the rate of successful prediction in percentage on test data of each of the *K* (4) splits. From Table 6.2 it can be observed that the efficiency of developed MGGP-based "best" LI_p model, out of the four models, in terms of rate of successful prediction of liquefied and non-liquefied cases is 88%. The "best" MGGP-based LI_p model was obtained with population size of 4000 individuals at

150 generations with reproduction probability of 0.05, crossover probability of 0.85, mutation probability of 0.1., G_{max} as 4 and d_{max} as 3. The developed "best" LI_p model can be described as Eq. (6.31).

$$LI_p = 1.823\tanh\left(6.024CSR_{7.5}\right) - 0.0368\left(N_{1,60} + CSR_{7.5} - \cos N_{1,60}\right) + \frac{26.16CSR_{7.5}\sin\left(FC\right)}{\sigma_v'} - 0.3728 \quad (6.31)$$

The statistical performances of both training and testing data for the developed LI_P model (Eq. 6.31) in terms of R (0.74,0.73), R^2(0.8, 0.79), E (0.55,0.54), *AAE* (0.27,0.29), *MAE* (0.76,0.70) and *RMSE* (0.33,0.35) are found to be comparable showing good generalization of the developed model, which also ensures that the model is not over-fitting to training data. A prediction in terms of LI_p is said to be successful if it agrees with field manifestation of the database. As per Eq. (6.31) the rate of successful prediction of liquefied and non-liquefied cases are 85% for training and 88% for testing data.

The Eq. (6.31) can be used by geotechnical engineering professionals with the help of a spreadsheet to predict the occurrence of liquefaction based on soil properties in a future seismic event without going into complexities of model development. In the present study, the developed LI_p model is further used for the development of a proposed *CRR* model.

6.2.5.1 Generation of artificial points on the limit state curve

To approximate a limit state function that will separate liquefied cases from the non-liquefied ones, artificial data points on the boundary curve are generated using the Eq. (6.31) and following a simple but robust search technique developed by Juang et. al (2000b). The technique is explained conceptually with the help of Fig. 4.4 of Chapter-IV and same is followed for the present problem. Fig. 6.4 shows the detailed flow chart of this search technique for path '*P*' and '*T*'. A multi-dimensional data point ($N_{1,60}$, *FC*, σ'_v, $CSR_{7.5}$) on the unknown boundary curve is obtained from each successful search. A total of 240 multi-dimensional artificial data points ($N_{1,60}$, *FC*, σ'_v, $CSR_{7.5}$), which are located on the boundary curve are generated using the developed MGGP-based LI_p model (Eq. 6.31) and following

the Figs.4. 4 and 6.4. The data points are used to approximate the limit state function in the form of $CRR = f(N_{1,60}, FC, \sigma'_v)$ using MGGP and is presented below.

6.2.5.2 MGGP Model for CRR

The MGGP is adopted to develop the *CRR* model using the above 240 artificially generated data points. The *K*-fold (4) cross validation procedure is also adopted to find the "best" MGGP-based *CRR* model. Here, out of 240 generated data points in each of *K* (4) split 180 data points are selected for training and the remaining 60 for testing the developed model. For each split, several *CRR* models were obtained by using the obtained optimum values of controlling parameters of the MGGP as explained earlier in Chapter-IV for the development of the LI_p model. Similarly, four models, "best" one of each split are selected and their statistical performances in terms of *R*, R^2, *E, AAE, MAE and RMSE* on the basis of testing data are evaluated and presented in Table 6.3. The model obtained from split-1 is found to be the "best" among these four models on the basis of above statistical performances and is described below as Eq. (6.32).

$$CRR = 1.235\times10^{-5}\left(N_{1,60}\right)^2\left(N_{1,60}+8.706\right)-0.0001253\left(N_{1,60}\right)^2\sin\left(FC\right) - \frac{6.371\sin\left(FC\right)}{\sigma'_v-3.302}+\frac{8.398\sin\left(FC\right)}{N_{1,60}+\sigma'_v}+0.1129 \tag{6.32}$$

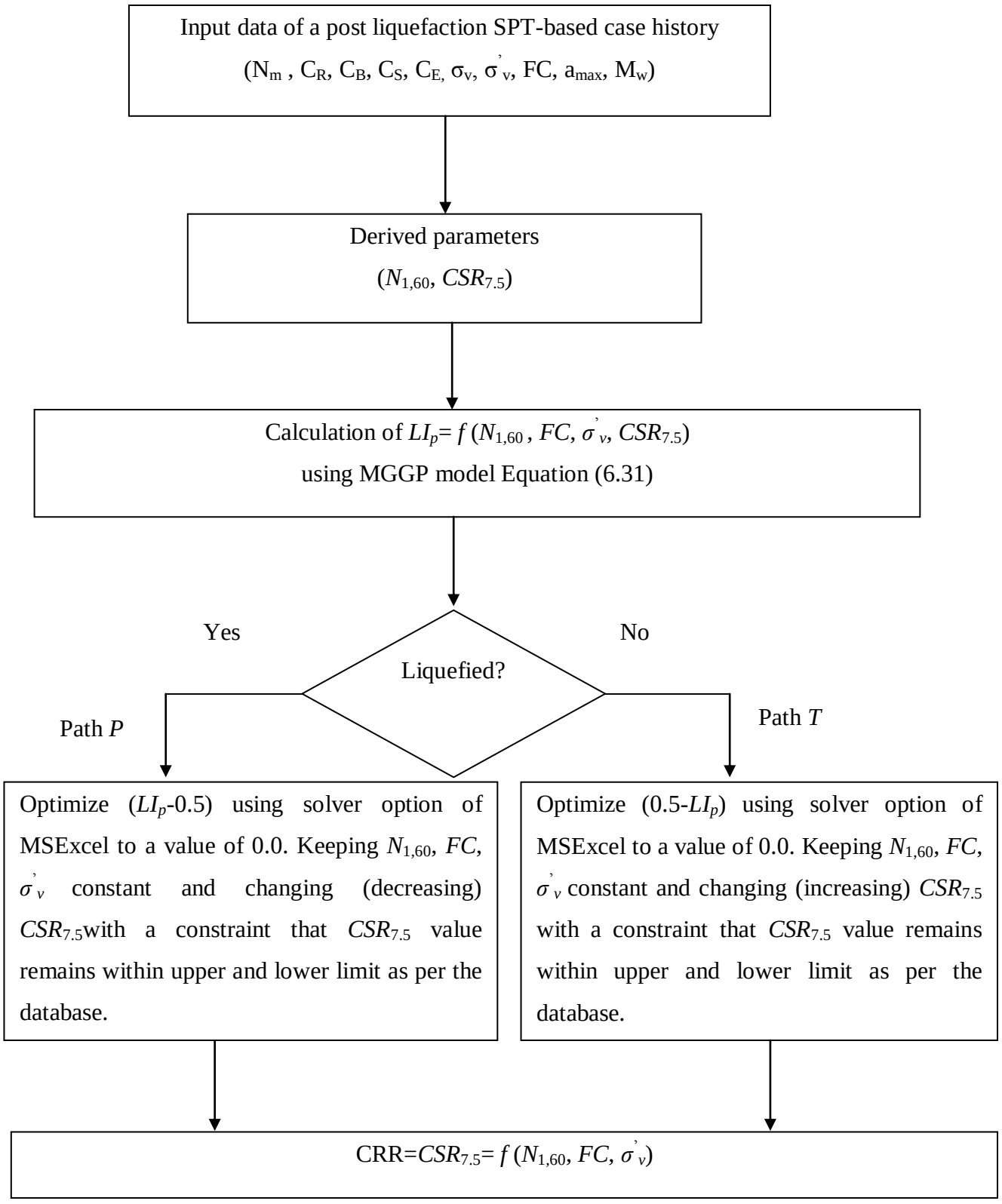

Fig. 6.4 Search algorithm for data points on limit state curve.

Table 6.3 Performance in terms statistical parameters of MGGP-based *CRR* models on the basis of *K*-fold cross validation.

	R	R^2	*E*	*AAE*	*MAE*	*RMSE*
Split -1	0.98	0.99	0.95	0.01	0.05	0.02
Split -2	0.89	0.97	0.79	0.02	0.18	0.04
Split -3	0.93	0.98	0.86	0.02	0.16	0.03
Split -4	0.97	0.99	0.94	0.01	0.08	0.02
Summary	0.95	0.98	0.89	0.02	0.12	0.03

The statistical performances of the "best" MGGP-based *CRR* model in terms of *R*, R^2E, *RMSE*, *AAE* and *MAE* as presented in Table 6.4 for both training and testing data are comparable showing good generalization of the developed model (Eq. 6.32), which ensures that there is no over-fitting. Thus, in the present study a single, comprehensive and compact model (Eq. 6.32) for *CRR* is obtained using MGGP unlike the most widely used regression-based lengthy model equation as recommended by Youd et al. (2001).Unlike, the *CRR* model of Youd et al. (2001) the present *CRR* model can be used without converting $N_{1,60}$ to the equivalent clean-sand overburden stress corrected SPT blow count ($N_{1,60,cs}$).

Table 6.4 Statistical performances of the developed "best" MGGP-based *CRR* model.

Data (Numbers)	*R*	R^2	*E*	*AAE*	*MAE*	*RMSE*
Training (180)	0.96	0.99	0.92	0.01	0.13	0.02
Testing (60)	0.98	0.99	0.95	0.01	0.05	0.02

The performance of the proposed *CRR* model is also evaluated by calculating the F_s for each case of field performance of the present database as discussed earlier. In deterministic approach $F_s \leq 1$ predicts occurrence of liquefaction and $F_s > 1$ refers to non-liquefaction. A prediction (liquefaction or non-liquefaction) is considered to be successful if it agrees with the field manifestation. The deterministic approach is preferred by the geotechnical professionals and the design decisions are taken on the basis of F_s. In the present study, Eq. (6.32) in conjunction with the model for $CSR_{7.5}$ (Eq. 6.6) is proposed for evaluation of liquefaction potential in deterministic approach. It can be noted that the success rate in prediction of liquefied cases is 89% and that for non-liquefied cases is 81% and the overall

success rate is found to be 85% by the present MGGP model. The prediction performances for liquefied and non-liquefied cases are nearly equal, which indicates the un-biasedness of the developed boundary surface. Ideally, a boundary surface (i.e., *CRR* model) is said to be unbiased if the probability of occurrence of liquefaction, P_L is 50% corresponding to $F_s = 1$. Further, the model is calibrated with respect to the liquefaction field manifestations of the present database to develop a relationship between F_s and P_L using Bayesian theory, and also to quantify the degree of conservatism associated with the developed *CRR* model (relative to *CSR* model).

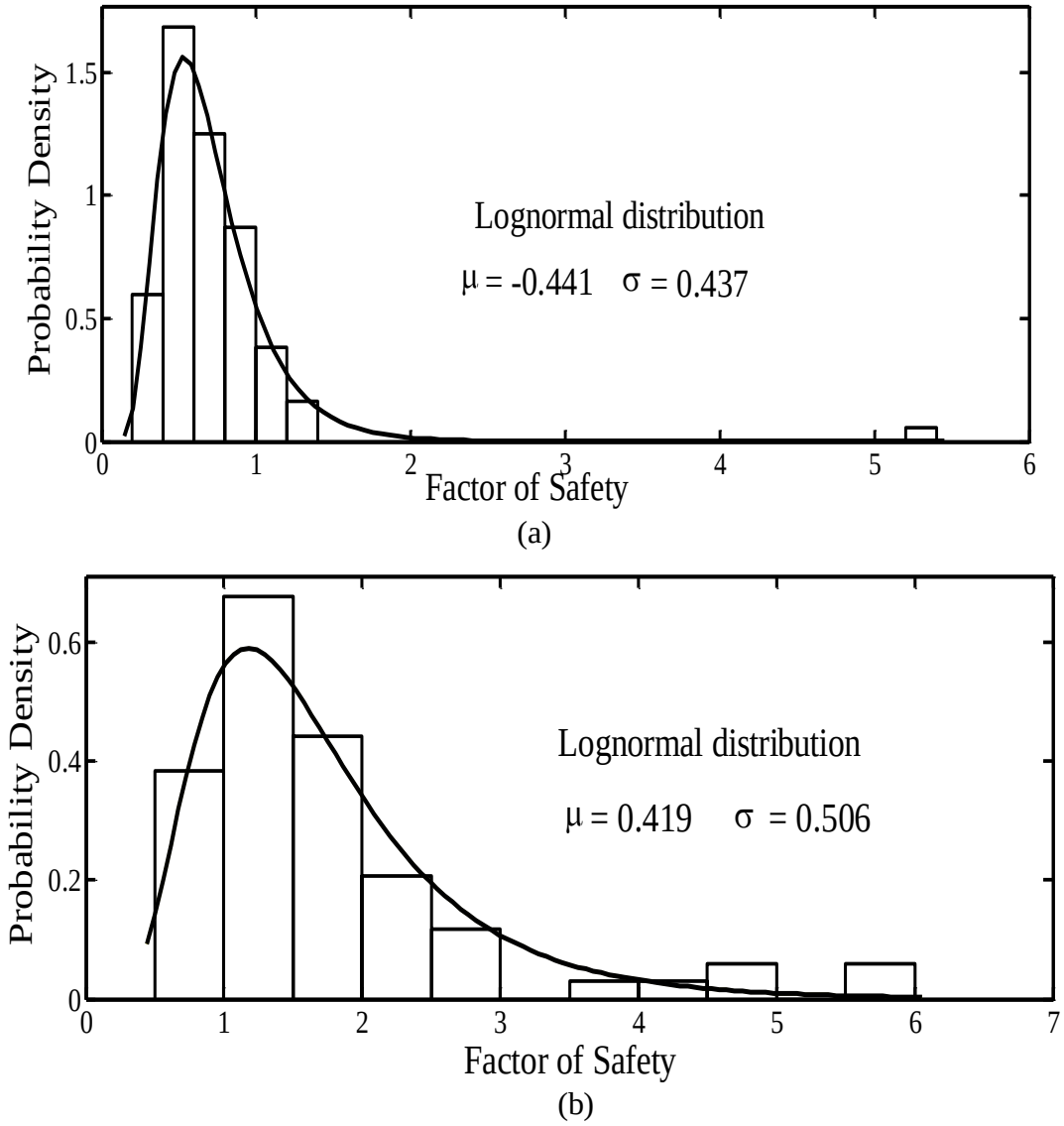

Fig. 6.5 Histogram showing the distributions of calculated factor of safeties: (a) Liquefied (*L*) cases; (b) Non-liquefied (*NL*) cases.

6.2.5.3 P_L-F_s mapping function

The calculated F_s values for different cases of the present database are grouped according to the field performance observation of liquefaction (*L*) and non-liquefaction (*NL*).After considering several different probability density functions, it is found that both the liquefied and non-liquefied groups are best fitted by lognormal distribution with parameters (μ , σ) are (-0.441, 0.437) and (0.419, 0.506) respectively as shown in Fig. 6.5 (a) and (b)**.** According to Juang et al.(1999b) the probability of liquefaction occurrence of a case in the database, for which the F_s has been calculated, can be found out by using Bayesian theorem of conditional probability and following Eq. (5.4) of the Chapter-V. For the present SPT-based database f_L (F_s) and f_{NL} (F_s) of Eq. (5.4) are the lognormal probability density functions (PDFs) of F_s for liquefied cases and non-liquefied cases, respectively. Based on the obtained probability density functions, P_L is calculated using Eq. (5.4) for each case in the database. The F_s and the corresponding P_L of the total 160 cases of database are plotted and the mapping function is approximated through curve fitting as shown in Fig. 6.6. The mapping function is presented as Eq. (6.33) with a high coefficient of determination value (R^2) of 0.99.

$$P_L = \frac{1}{1+\left(\frac{F_s}{a}\right)^b} \tag{6.33}$$

where *a* (1.003) and *b* (4) are the parameters of the fitted logistic curve. The F_s is calculated using the proposed MGGP-based deterministic method (Eq.6.6 and Eq.6.32) and then, corresponding P_L can be found out using the developed mapping function.

The proposed *CRR* model is also characterized with a probability of 50.3% as P_L=0.503according to the Eq. (6.33) when F_s=1.0, which indicates that *CRR* model is unbiased relative to $CSR_{7.5}$model (Juag et al. 2000b). Ideally, a boundary surface (i.e. *CRR* model) is said to be unbiased if its probability of occurrence of liquefaction, P_L is 50% corresponding to F_s = 1.

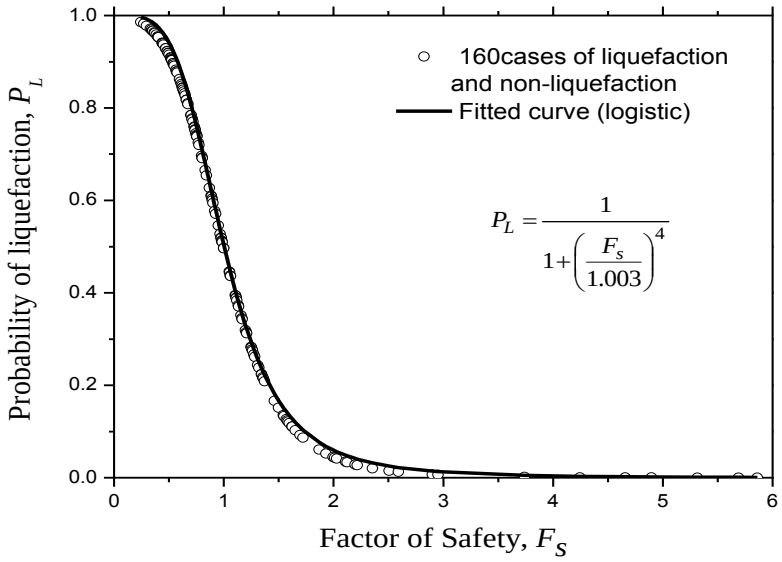

Fig. 6.6 Plot of P_L-F_s showing the mapping function approximated through curve fitting.

Thus, the degree of conservatism of the developed limit state boundary surface can be quantified in terms of P_L as 50.3%. Juang et al. (2008) developed a SPT-based P_L-F_s mapping function, which characterizes their adopted *CRR* model (Youd et al., 2001) by a P_L of 55% corresponding to F_s=1.

6.2.5.4 Estimation of model uncertainty from reliability analysis

The most unbiased evaluation of liquefaction potential of soil is possible with a boundary surface, separating liquefied and non-liquefied cases, having 50% of the P_L. Such a limit state model is considered to have no model uncertainty. Alternately, unbiased evaluation of liquefaction potential is possible by quantifying the model uncertainty of the limit state and incorporating correct model uncertainty in the reliability analysis for liquefaction potential evaluation. The model uncertainty of the liquefaction limit state model (Eq. 6.15) may be represented with a random variable 'c_{mf}' and referred herein as model factor (Juang et al. 2006). Thus, the liquefaction limit state model can be presented as given below:

$$g(z) = c_{mf}\ R - Q = c_{mf}\ CRR - CSR \tag{6.34}$$

where $g(z)$ = limit state function considering model uncertainty and z= vector of input parameters. The uncertainty in the *CRR* model (Eq.6.44) is only considered, and the effect of the unrealized uncertainty associated with the *CSR* model is realized in the *CRR* model as the *CRR* model is developed using *CSR* model (Eq.6.6).

In the present study, the model factor 'c_{mf}' is treated as a random variable and then, combining it with the basic input parameters from the *CRR* (Eq.6. 32)and *CSR* (Eq.6.6) models, the limit state function (Eq. 6.34) for the reliability analysis can be presented as Eq. (6.35):

$$g(z) = c_{mf}\, CRR - CSR = g(c_{mf}, N_m, FC, \sigma_v, \sigma_v^{'}, a_{\max}, M_w) \tag{6.35}$$

Each of the six basic input parameters in Eq.(6.35); N_m, FC, σ_v, σ'_v, a_{max} and M_w is considered as a random variable and is assumed to follow a lognormal distribution, which has been shown to provide a good fit to the measured geotechnical parameters (Jeffries et al. 1988). The mean and coefficient of variation (COV) of each of the input parameters for the 94 cases considered in the present study for reliability analysis are obtained from Cetin (2000) and Moss (2003). Here, only 94 cases (59 liquefied and 35 non-liquefied cases) out of total 160 cases of the above database are considered for reliability analysis as the site specific COV of the parameter M_w is not available in Cetin (2000) but, the same is obtained for the mentioned 94 cases from Moss (2003). Juang et al. (2008) assumed a single value of COV of M_w as 0.1 for each case of database instead of site specific COV for their SPT-based reliability method. The model factor (c_{mf}) is also assumed to follow lognormal distribution, which is very well accepted in reliability analysis (Juang et al. 2006).The model factor (c_{mf}) is also characterized with a mean (μ_{cmf}) and a COV. Thus, estimation of model uncertainty includes determination of these two statistical parameters of 'c_{mf}'.

In the present study, the correlations among the input variables are incorporated in the reliability analysis. The correlation coefficients between each pair of parameters used in the proposed limit state are provided in Table 6.5 as estimated by Juang et al. (2008) from the original database of Cetin (2000). As per Phoon and Kulhawy (2005), the model factor, c_{mf}

is very weakly correlated to input variables. Thus, in the present study no correlation is assumed between c_{mf} and the other six input parameters considered herein.

Table 6. 5 Coefficients of correlation among six input variables as per Juang et al.(2008).

Input Parameters	Input Parameters					
	$N_{1,60}$	FC	σ'_v	σ_v	a_{max}	M_w
$N_{1,60}$	1	0	0.3	0.3	0	0
FC	0	1	0	0	0	0
σ'_v	0.3	0	1	0.9	0	0
σ_v	0.3	0	0.9	1	0	0
a_{max}	0	0	0	0	1	0.9
M_w	0	0	0	0	0.9	1

In the present FORM analysis, the GA is used as optimization tool to obtain reliability index, β. Thus, the limit state function, $g(z) = 0$ (Eq. 6.35) is used as constrained function and the Eq. (6.24a) is the objective function. Some of the GA parameters such as initial population size (*Npop*), probability of crossover (P_c), probability of mutation (P_m) and maximum number of generation (*MaxGen*) affect the convergence rate. Thus, through a sensitivity analysis the following appropriate values are found and are applied for GA analysis: *Npop* = 200, P_c= 0.75, P_m =0.05 and *MaxGen* = 100. Following the flow chart as shown in Fig. 6.7, a code is developed in MATLAB (Math Works Inc. 2005) to estimate β. Then, notional probability of liquefaction, P_L is obtained using Eq. (6.18).

In the present study, as the model uncertainty is not known initially, the reliability index calculated without considering model uncertainty or considering any assumed value will result in incorrect calculation of β and the corresponding notional probability P_L. Hereafter, reliability index calculated without taking into account the model uncertainty is designated as β_1, whereas the reliability index calculated considering any value of model uncertainty is denoted as β_2.

In the first step of model uncertainty determination procedure, the reliability index,β_1 is calculated for each of the 94 cases of the database considered for the present study. Following Bayesian mapping function approach and calibrating with field manifestations of

the database as explained in the section, 6.2.5.3, P_L-β relationship is obtained as given below.

$$P_L = \frac{f_L(\beta)}{f_L(\beta) + f_{NL}(\beta)} \tag{6.36}$$

where $f_L(\beta)$ and $f_{NL}(\beta)$ are the PDFs of the calculated β of group *L* and *NL* cases, respectively. P_L for each case of the database is calculated using Eq. (6.36). Fig.6.8 shows a plot of P_L- β_1 relationship obtained from the reliability analyses of 94 cases of database without considering the model uncertainty. The notional probability of each case of the database using Eq. (6.18) is calculated and plotted the same inFig.6.8. A difference is observed between the national concept-based P_L-curve and Bayesian mapping function-based P_L-curve. The later curve is calibrated empirically with the field manifestations of case history database considered herein the present study and thus, it is assumed to be most probable evaluation of the "true" probability of liquefaction.

It can also be observed from the Bayesian mapping function-based P_L-curve of the Fig. 6.8 that P_L =0.52 when β_1 =0. This result is consistent with the 50.3% probability of the developed *CRR* model as suggested by P_L-F_s mapping function (Eq. 6.33), which has been discussed in the earlier section. This indicates the robustness of the proposed methodology. The accuracy of calculated probability on the basis of notional concept depends on the accuracy with which β is calculated. As in the above study, β is calculated without considering limit state model uncertainty in reliability analysis, it is subjected to some error and thus, the resulting notional probability may not be completely accurate. But, notional probability concept always yields: P_L=0.5 at β=0. If "true" model uncertainty can be incorporated with the limit state model then, the resulting reliability index (β_2) at 0 will produce a P_L value of 0.5 from the calibrated Bayesian mapping function approach.

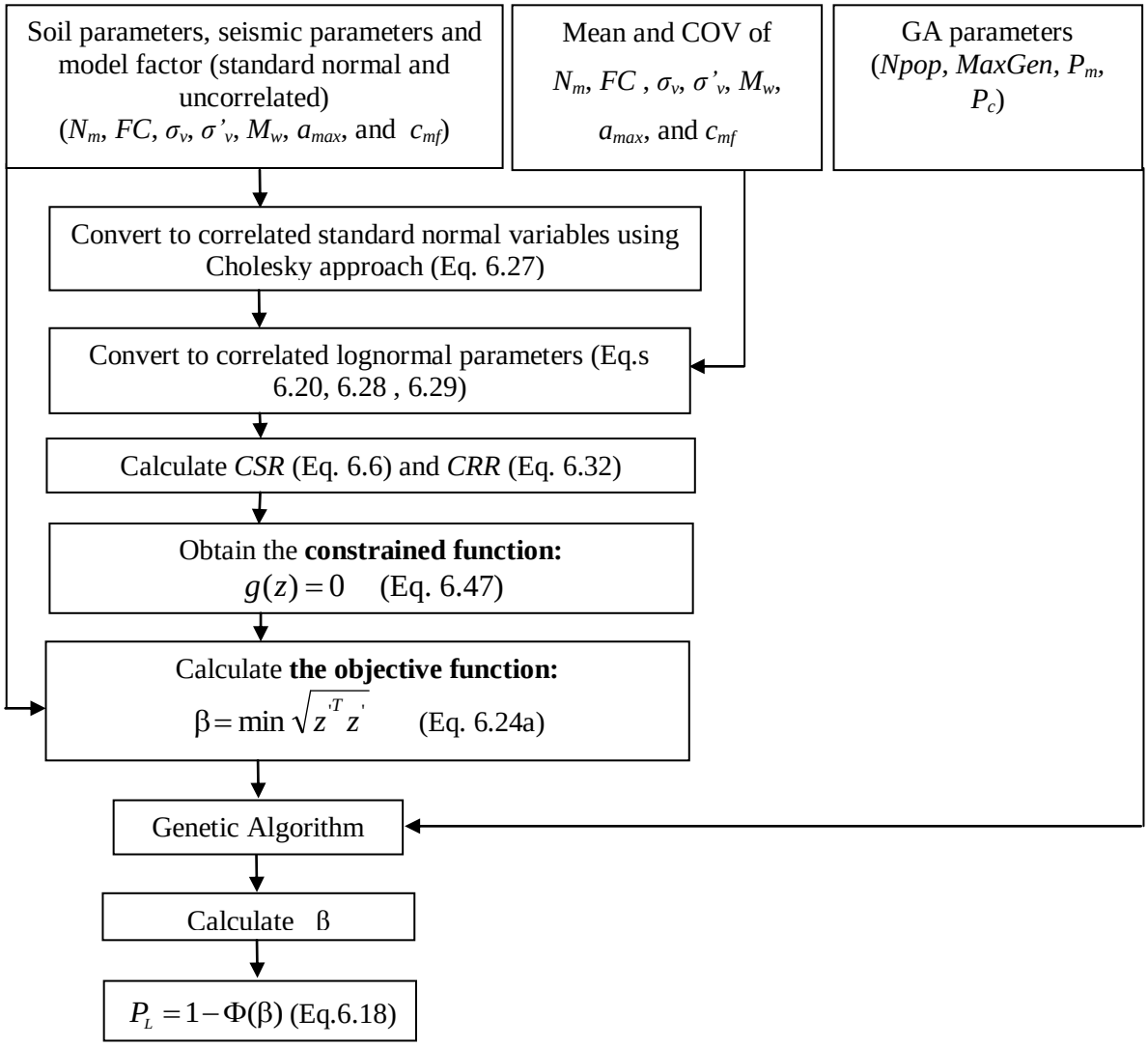

Fig. 6.7 Flow chart of the proposed FORM analysis with GA as optimisation tool.

The methodology for estimating the uncertainty of the adopted limit state model (Eq. 6.35) is based on the proposition that a calibrated Bayesian mapping function produces a most accurate estimate of the "true probability of liquefaction" for any given case. With the above idea, a simple but, trial-and-error procedure is adopted to estimate model uncertainty. The "true" model uncertainty is the one that yields the reliability indices and the corresponding notional probabilities matching best with those probabilities calculated from the calibrated Bayesian mapping function (Juang et al., 2006). And also the plot of $\beta_2$versus P_L as obtained from the calibrated Bayesian mapping function will produce a P_L value of 0.5 at β_2=0.

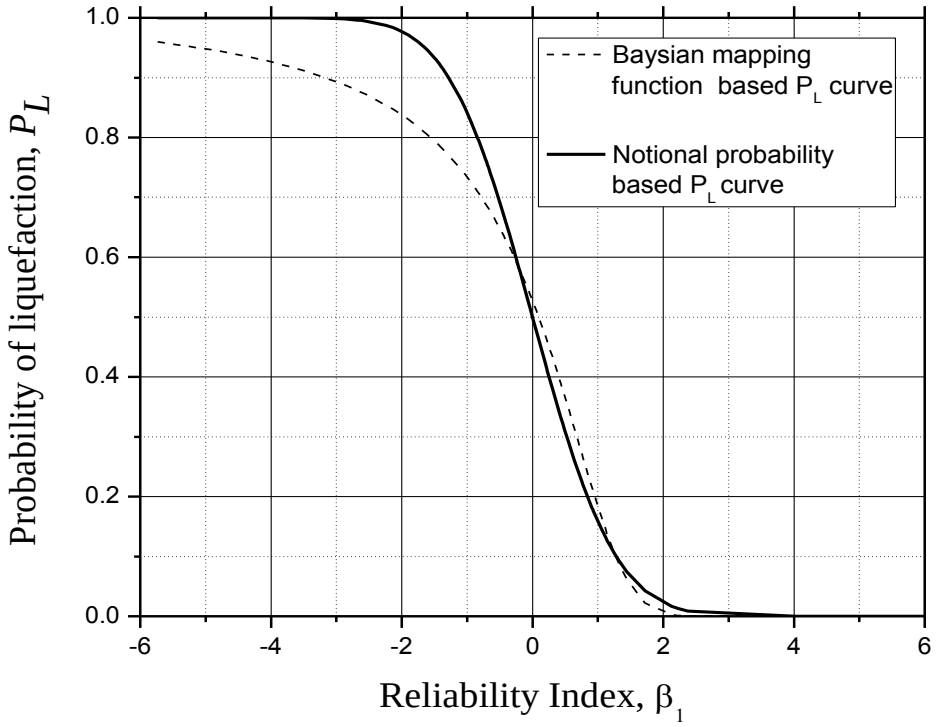

Fig. 6.8. P_L- β_1 mapping function obtained from the reliability analysis of 94 cases of liquefaction and non-liquefaction without considering model uncertainty.

In the first phase of model uncertainty estimation procedure, a series of reliability analysis of 94 cases of the database are performed to study the effect of COV component of the model factor, c_{mf}. Four cases of model uncertainty, each with the mean of the model factor being kept equal to1.0 (μ_{cmf}= 1.0) and a different COV of 0.0, 0.1, 0.2, 0.3 are studied. For each case of model uncertainty, β_2 values are calculated for the 94 cases of the database. A Bayesian mapping function is obtained for each model uncertainty scenario, as discussed above and presented a P_L-β relationship using Eq. (6.36). From the developed mapping function for each of the above mentioned model uncertainty scenario liquefaction probabilities are obtained from the corresponding β_2 values. Fig. 6.9 shows the plot between β_2 versus P_L for each of the above mentioned model uncertainty. It is clearly indicated that within the considered range of COV value: [0–0.3], COV component of the model uncertainty has got significant effect on the calculated probability.

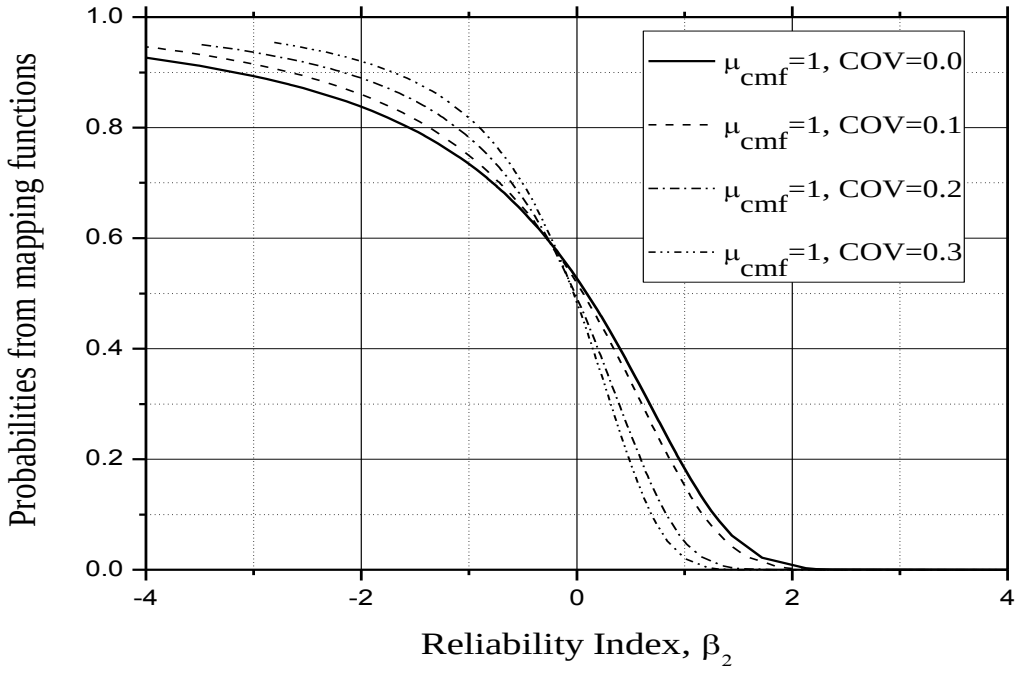

Fig. 6.9 P_L- β mapping functions showing effect of COV of model factor on probability of liquefaction.

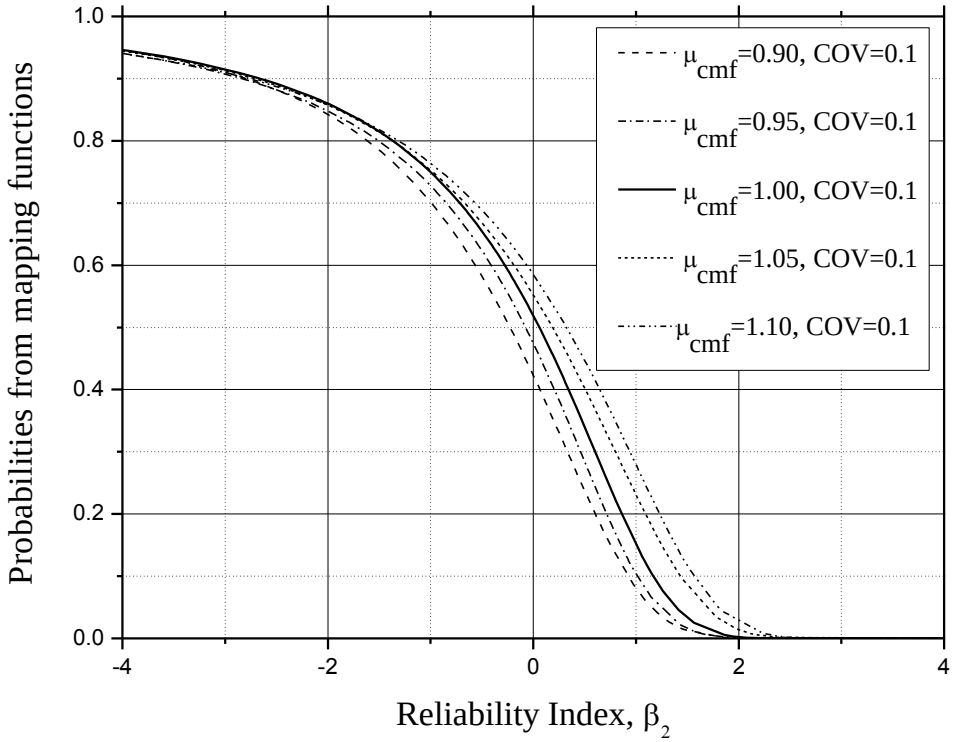

Fig. 6.10. P_L- β mapping functions showing effect of mean of model factor (μ_{cmf}) on probability of liquefaction

In second phase of investigation COV component of model uncertainty is kept constant at 0.1, whereas the mean value of c_{mf} is varied from 0.9 to 1.1 at an interval of 0.05 (i.e. μ_{cmf}= 0.9, 0.95, 1.0, 1.05 and 1.1). For each of the above scenario of model uncertainty, Bayesian mapping function is developed using all the 94 cases of liquefaction and non-liquefaction for reliability analysis as mentioned previously. Then, P_L values calculated from the mapping functions are plotted against the corresponding reliability index (β_2) for different cases of model uncertainty as mentioned above and presented in Fig.6.10. It can also be observed from the above figures that the mapping function is shifted from left to right as μ_{cmf} increases, and also the probability corresponding to β_2= 0 increases. As per Fig. 6.10, at μ_{cmf}= 1 and COV = 0.1, the P_L= 0.52 at β= 0, whereas μ_{cmf} =0.95 produces a lower value of P_L(0.48) at β= 0. Thus, an intermediate value of μ_{cmf} = 0.98is considered for further reliability analysis. As already it has been observed that COV has got significant effect on calculated P_L, keeping μ_{cmf}= 0.98 and changing COV component from 0 to 0.30 a series of reliability analysis of all the 94 cases are performed and similarly, the Bayesian mapping functions are obtained. The P_L versus β_2 plot for the above cases is shown in Fig.6.11 and it is clearly observed that from the mapping function curves for the two uncertainty scenarios: μ_{cmf} = 0.98; COV=0, and for μ_{cmf} = 0.98; COV=0.1, the $P_L$is found out to be 0.5 at β= 0. The latter scenario of model uncertainty is considered as "true" model factor considering the explanation given below.

Fig.6.12 shows a comparison of the probability of liquefaction for each of 94 case- histories obtained from two mapping functions, one with considering the "true" model uncertainty (i.e. μ_{cmf}= 0.98 and COV = 0.1) and the other without considering the model uncertainty (i.e. μ_{cmf} = 1.00 and COV = 0). In the earlier case, the reliability index, β_2 for each case is calculated and then, the corresponding mapping function is established using Eq. (6.36).In the latter case, reliability index $\beta_1$for each case is determined and then, the corresponding mapping function is developed in the similar manner using Eq. (6.36). The two sets of probabilities obtained for all the 94 cases based on the two sets of mapping functions agree well with each other, which is evident from the statistical parameters (R =0.99, E = 0.99 and $RMSE$ = 0.02) as mentioned in the Fig. 6.12.

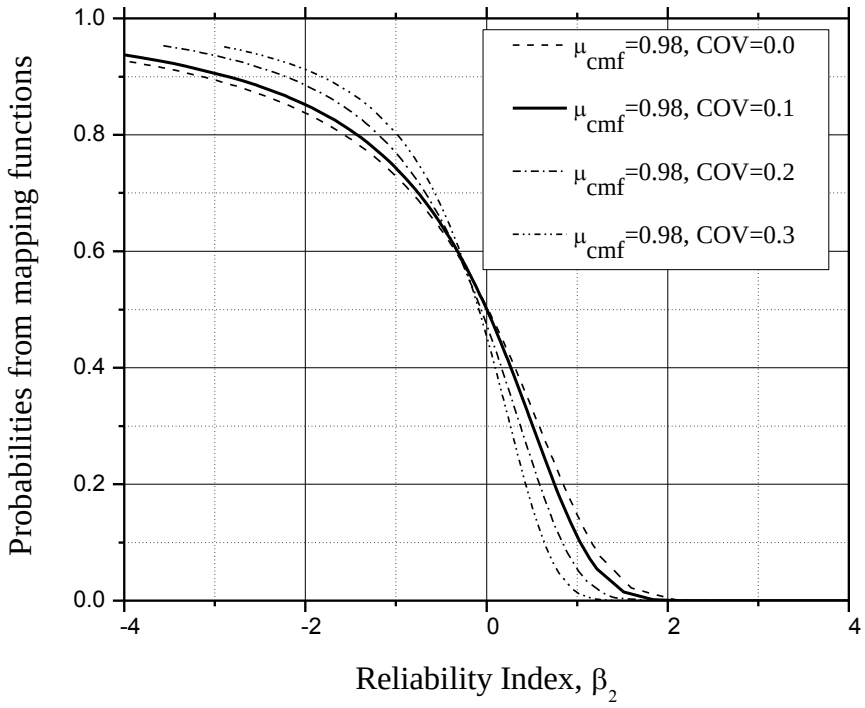

Fig. 6.11 P_L- β mapping functions showing effect of mean (μ_{cmf}) and COV of "true" model factor on probability of liquefaction i.e. at β=0, P_L = 0.5.

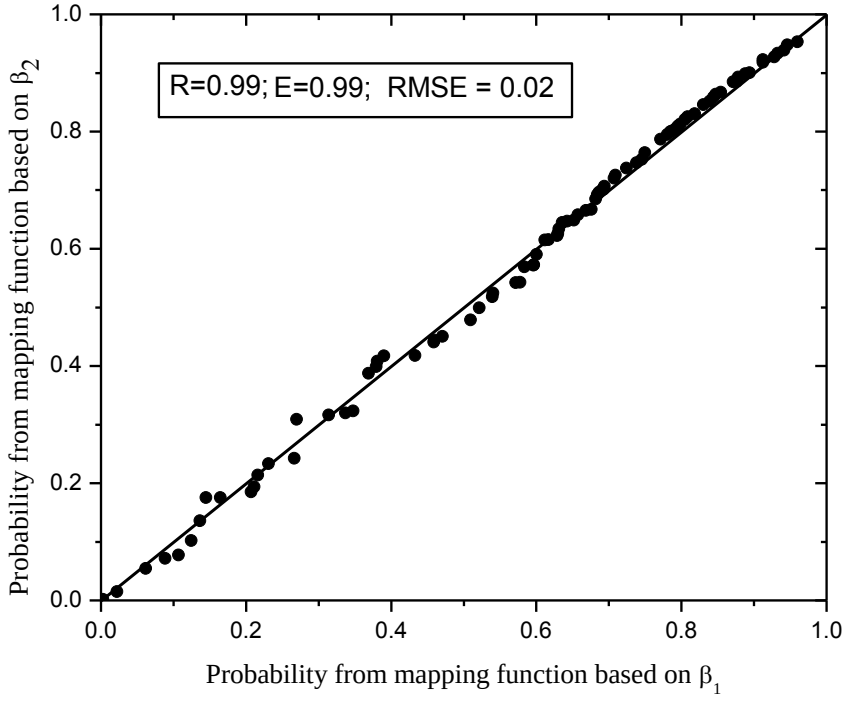

Fig. 6.12 Comparison of probability of liquefaction obtained for the 94 cases of the database from the mapping functions, one based on β_2 (using μ_{cmf} =0.98 and COV=0.1) and other based on β_1.

Fig. 6.13 shows the comparison of the notional probabilities obtained for all the 94 cases of present database using the reliability index β_2 calculated by taking into account the "true" model factor(μ_{cmf} = 0.98 and COV = 0.1) with the probabilities obtained from the P_L-β_1 mapping function, which has not considered model uncertainty in the reliability analyses. The Fig. 6.13 also shows very good agreement (R=0.99, E=0.94 and $RMSE$ = 0.10) between the probabilities obtained from two different concepts, which indicates that the probability of liquefaction can be correctly calculated from the notional concept if the right model uncertainty is incorporated in the reliability analysis. Similar analysis is made with the model uncertainty scenario of μ_{cmf} = 0.98; COV = 0, and it is found that earlier case (μ_{cmf} = 0.98; COV = 0.1) is yielding better result as per the above considered statistical parameters. Thus, in the present study, the "true" model uncertainty of the developed limit state, considering the present database, is characterized by μ_{cmf}= 0.98 and COV = 0.1. Juang et al. (2008) using the same SPT database characterized the limit state model formed by *CSR* and *CRR* model as presented in Youd et al. (2001) with a model uncertainty of μ_{cmf} = 0.96 and COV=0.04 using FORM analysis.

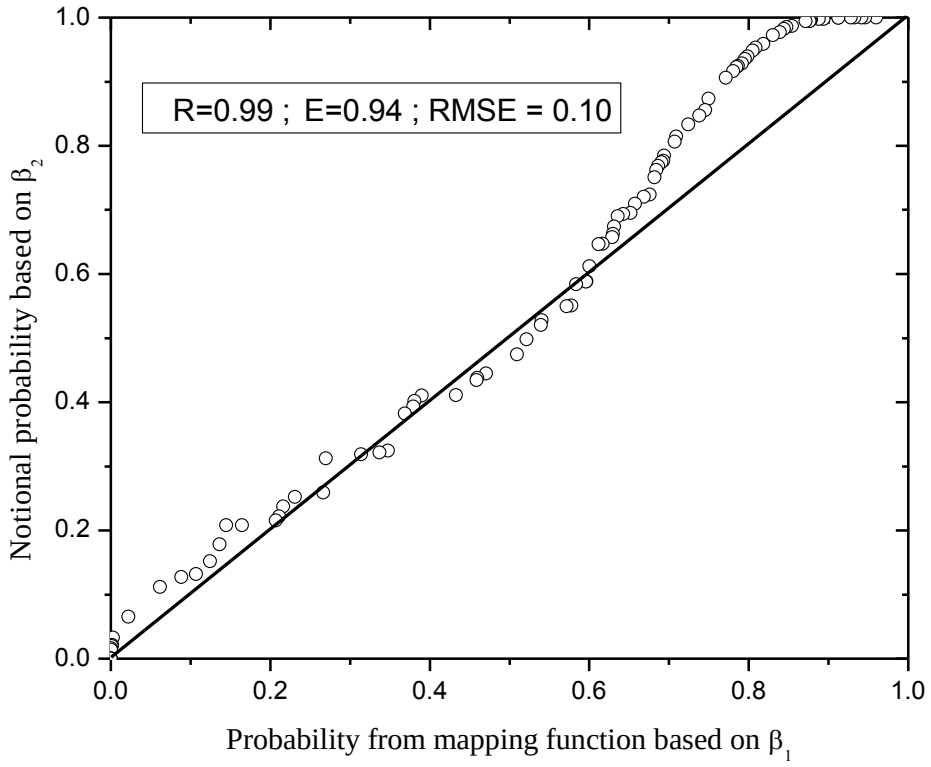

Fig. 6.13. Comparision of notional probability of liquefaction obtained for the 94 cases based on β_2 (using μ_{cmf} =0.98 and COV=0.1) with P_L obtained from mapping functions based on β_1.

Finally, the P_L can be estimated from the developed P_L-β_1 mapping function using a reliability index, β_1 that is calculated by FORM considering only parameter uncertainties. Alternatively, the reliability index β_2 can be determined by FORM considering both model and parameter uncertainties, and then, the P_L can be obtained with the notional concept using Eq. (6.18). The notional concept to estimate the P_L of a future case is preferred as the model uncertainty of the adopted limit state has been determined and also it is a well-accepted approach in the reliability theory (Juang et al. 2006).

To explain the above findings one example of liquefied case from 1978, Miyagiken-Oki earthquake atIshinomakai-2 site as presented in the database of Cetin (2000) has been analyzed to find the P_L. The soil and seismic parameters at critical depth (d =3.7m) are given as follows: N_m = 3.7; C_B=1; C_S =1; C_R=0.77; C_E=1.09; FC= 10%; σ_v =58.83kPa; σ'_v =36.28 kPa; a_{max} = 0.2 g and M_w = 7.4. The COV of the parameters: N_m, FC, σ_v, σ'_v, a_{max} are 0.189,

0.2, 0.217, 0.164, 0.2 respectively, whereas the COV of M_w is taken as 0.1 as per Juang et al. (2008) as it is not available in Cetin (2000).The Eq.(6.6) and Eq.(6.32) are used to form the limit state model of liquefaction and considering the model uncertainty (μ_{cmf}= 0.98 and COV = 0.1), FORM analysis is made using the developed code in MATLAB. The reliability index, β_2 and corresponding notional probability of liquefaction, P_L using Eq. (6.18) are found out to be -1.3437 and 0.91 respectively. The above example was also solved by Juang et al. (2008) and the reliability index-based notional P_L value was obtained as 0.91. The results of both the methods confirm the case as liquefied, and the P_L calculated by the proposed MGGP-based reliability method is also found to be equal to that obtained by statistical regression-based reliability method of Juang et al. (2008).Similarly, probability of liquefaction can be evaluated using P_L-F_s mapping function using only the mean values of the input variables. For the above example of liquefied case, using Eq. (6.6) and Eq. (6.32) F_s is found out to be 0.575, and thus, P_L = 0.90 according to Eq. (6.33). Thus, the consistent results are obtained considering two different approaches.

Another example of a non-liquefied case from 1977, Argentina earthquake at San Juan B-5 as presented in Cetin (2000) has been analyzed to find P_L. The mean values of seismic and soil parameters at the critical depth (d =2.9 m) are given as follows: N_m = 15.2; C_B=1; C_S =1; C_R=0.72; C_E=0.75; FC= 3%; σ_v = 45.61 kPa; σ'_v = 38.14 kPa; a_{max} = 0.2 g and M_w = 7.4 and the corresponding COV of these parameters are 0.026, 0.333, 0.107, 0.085,and 0.075, respectively, whereas the COV of M_w is taken as 0.1as per Juang et al. (2008) as it is not reported in Cetin (2000).Similarly as explained above, *CSR* and the *CRR* model equations are used to form the limit state of liquefaction and considering the model uncertainty (μ_{cmf} = 0.98 and COV = 0.1), FORM analysis was made using the developed code in MATLAB. The reliability index, β_2 and corresponding notional probability of liquefaction P_L using Eq. (6) are found out to be 0.0213 and 0.491 respectively, and the result confirms the case as non-liquefied one. The above example is also presented in Juang et al. (2008) and the corresponding reliability index and notional P_L are obtained as 0.533 and 0. 297. But, in this example the COV of $N_{1,60}$ is wrongly taken to be 0.23 in stead of 0.023 as presented in Cetin (2000).Thus, there is a discrepancy in the results of the above example as obtained by proposed method and the method of Juang et al. (2008).For the above example of non-

liquefied case, using the mean values of parameters and the Eq. (6.6) and Eq. (6.32), $F_s$is found out to be 1.044, and thus, as per Eq. (6.33) P_L = 0.460, which is nearly equal to the P_L of 0.491 as obtained from the reliability analysis.

The consistent results are obtained in the above two examples, which suggests the robustness of the present methodology. These two examples also illustrate the procedure for evaluation of P_L of a site in a future seismic event using the proposed reliability based analysis if the uncertainties of soil and seismic parameters of the site are known. The Eq. (6.33) can be used for preliminary estimation of P_L of cases where there is lack of knowledge of parameter uncertainties.

6.3 DEVELOPMENT OF CPT-BASED RELIABILITY MODEL

6.3.1 Methodology

Similarly as explained above, first, the MGGP is used to develop a liquefaction field performance observation function termed as liquefaction index (*LI*) using post liquefaction CPT database. In the second step, artificial data points are generated for the unknown boundary curve separating liquefied cases from non-liquefied cases using a search technique as explained in Chapter-IV. The boundary curve referred as a "limit state function" representing the *CRR* of the soil is approximated with the generated data points using MGGP. The developed *CRR* model along with the *CSR* model (Idriss and Boulanger 2006) forms the performances function or limit state model of liquefaction for reliability analysis. Here, FORM is used to evaluate the liquefaction potential of soil in terms of P_L, which requires the knowledge of both parameter and model uncertainties. The uncertainty associated with proposed limit state model is determined following the extensive sensitive analysis as adopted by Juang et al. (2006) through a rigorous reliability analysis associated with Bayesian mapping function approach. Bayesian theory of probability is used to create a mapping function to relate F_s with P_L.

6.3.2 MGGP-based LI_p model

The general form of MGGP-based LI_p model for the present CPT database can be presented as:

$$LI_p = \sum_{i=1}^{n} F\left[X, f(X), c_i\right] + c_0 \tag{6.37}$$

where LI_p = predicted value of LI, F = the function created by the MGGP referred herein as liquefaction index function, X = vector of input variables = { q_{c1N}, I_c, σ_v', $CSR_{7.5}$}, $q_{c1N}$is normalized cone tip resistance (Idriss and Boulanger 2006):

$$q_{c1N} = q_{c1}/P_a \tag{6.38}$$

$$q_{c1} = C_N q_c \tag{6.39}$$

$$C_N = \left(\frac{P_a}{\sigma_v'}\right)^{\beta} \leq 1.7 \tag{6.40}$$

$$\beta = 1.338 - 0.249\left(q_{c1N}\right)^{0.264} \tag{6.41}$$

I_c = soil type index (Juang et al. 2003) as per Eq. (4.17),$CSR_{7.5}$ is the cyclic stress ratio as presented by Eq. (6.6), f are the functions defined by the user, n is the number of terms of target expression and c_0= bias. The MGGP as per Searson et al. (2010) is used and the present model is developed and implemented using Matlab (Math Works Inc. 2005).

6.3.3 Reliability Analysis

Reliability analysis using the present CPT database can be done following the methodology as described in the section 6.2.3 with little modification to the liquefaction performance function, Z. The Z for the CPT analysis depends on R and Q, which are the functions of multiple basic variables such as measured cone tip resistance (q_c), sleeve friction (f_s), σ_v, σ'_v, a_{max} and M_w.

6.3.4 Database and Pre-processing

In the present study, the models developed based on the post liquefaction CPT database compiled and reassessed by Moss (2003).The database consists of 182 cases from 18 different earthquakes around the world, 139 of them are liquefied cases and the other 43 are non-liquefied cases. It contains information about soil and seismic parameters such q_c, f_s, σ_v, σ'_v, a_{max}, M_w and liquefaction field performance observation, *LI*. The soil in these cases ranges from sand to silt mixtures (sandy and clayey silt). As per Moss (2003) the case histories in the database have been classified in four groups as Class A, Class B, Class C and Class D in decreasing order according to the quality of informational content. In the present study, all the 27 cases of Class A and 117 cases out of 125 Class B data have been considered. 8 cases of Class B data are not considered due to some ambiguity in statistical information of data, whereas none of the class C and D data is considered for the present model development. Thus, out of total 144 cases of data considered for model development 110 cases are liquefied and 34 cases are non-liquefied. The summarized extract of the database used for model development is provided in the Table 6.6 in terms of maximum and minimum of mean values and COV of various parameters considered in the present investigation as inputs and output.

Table 6.6 Summary of the database (Moss 2003) used for development of different models in the present study

Model Variables	Type	Maximum mean Value	Minimum mean Value	Maximum COV Value	Minimum COV Value
d (m)	Input	10.750	1.380	-	-
q_c (kPa)		18830.000	730.000	0.954	0.032
f_s(kPa)		216.230	1.160	1.126	0.027
σ_v (kPa)		193.690	26.000	0.206	0.031
σ'_v (kPa)		144.990	14.100	0.196	0.036
a_{max}(g)		0.770	0.090	0.351	0.036
M_w		7.700	5.900	0.025	0.013
LI	Output	1	0	-	-

6.3.5 Results and Discussion

In the MGGP procedure a number of potential models are evolved at random and each model is trained and tested using the training and testing cases respectively. The fitness of each model is determined by minimizing the *RMSE* between the predicted and actual value of the output variable (*LI*) as the objective function or error function (E_f),

$$RMSE = E_f = \sqrt{\frac{\sum_{i=1}^{N}\left(LI - LI_p\right)^2}{n}} \tag{6.42}$$

where, *LI*= 1 (liquefied case), 0 (non-liquefied case), *n* = number of cases in the fitness group. If the errors calculated by using Eq. (6.42) for all the models in the existing population do not satisfy the termination criteria, the generation of new population continues until the best model is developed as per the earlier discussion.

As described in previous section for SPT data analysis, *K*-fold cross validation (Oommen and Baise 2010), which is a more reliable and robust approach has been used to obtain the most "efficient" LI_p-based predictive model by the MGGP. Here, the original data (144 cases) of the present database is split into approximately *K* (3) equal folds. For each *K* split, (*K*-1)-folds are used for training and the remaining one fold is used for testing the developed model as shown in Fig. 6.14. Therein, the filled rectangles represent testing data, whereas the open rectangles represent the training data for each split. Hence, in each split out of the mentioned 144 data, 96 data are selected for training and remaining 48 data are used for testing the developed model. The advantage of *K*-fold cross validation is that all the cases in the database are ultimately used for both training and testing.

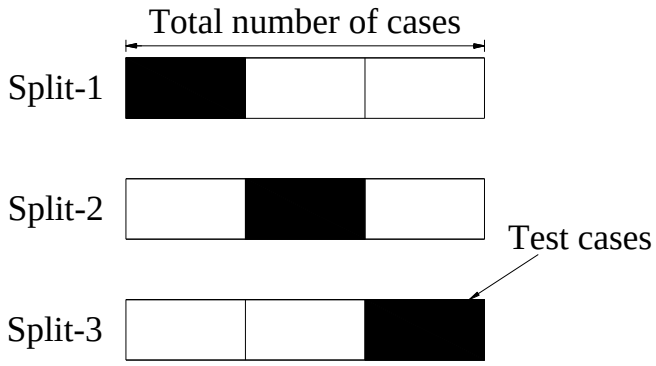

Fig. 6.14 An example of *K*-fold cross validation approach where the data are split into *K* (3) equal folds (modified from Oommen and Baise 2010).

For each split, several LI_p models were obtained by using the optimum values of controlling parameters of the MGGP as obtained following the explanation given in Chapter-IV. Then, the developed models were analysed with respect to physical interpretation of *LI* of soil, and after careful consideration of various alternatives, three models, "best" one of each split, are selected. Hence, the efficiency of each of the 3 developed LI_p models are evaluated by calculating the rate of successful prediction in percentage on test data of each of the *K* (3) splits. From Table 6.7 it can be observed that the efficiency of developed MGGP-based "best" LI_p model, out of the three models, in terms of rate of successful prediction of liquefied and non-liquefied cases is 96%. The "best" MGGP-based LI_p model was obtained from split-3 with population size of 3000 individuals at 250 generations with reproduction probability of 0.05, crossover probability of 0.85, and mutation probability of 0.1, G_{max} as 4 and d_{max} as 3.

Table 6.7 Performance in terms of the rate of successful prediction of MGGP-based LI_p models on the basis of *K*-fold cross validation.

Model	Rate of successful prediction (%)			
	Split-1	Split-2	Split-3	Summary
MGGP based LI_p model	94	89	96	93

The developed "best" LI_p model can be presented as Eq. (6.43).

$$LI_P = 0.00052\sigma_v^{'} - 0.7753\tanh\left(\frac{14.47}{q_{c1N}}\right) + \frac{0.0034q_{c1N}}{CSR_{7.5}} - \frac{0.00243I_c\left(q_{c1N}-5.287\right)}{CSR_{7.5}} - \frac{0.01698q_{c1N}}{I_c\left(I_c - CSR_{7.5}\right)} + 1.604 \quad (6.43)$$

Table 6.8 shows the statistical performances of both training and testing data for the developed LI_P model (Eq. 6.43) in terms of R,R^2, E, *AAE*, *MAE* and *RMSE* and are found to be comparable showing good generalization of the developed model, which also ensures that the model is not over-fitting to training data. A prediction in terms of LI_p is said to be successful if it agrees with field manifestation of the database. As per Eq. (6.43) the rate of successful prediction of liquefied and non-liquefied cases are 93% for training and 96% for testing data. The developed LI_p model is further used for the development of a proposed *CRR* model.

Table 6.8. Statistical performances of the developed "best" MGGP- based LI_p model

Input variables	Data	R	R^2	E	*AAE*	*MAE*	*RMSE*
q_{c1N}, I_c, $\sigma_v^{'}$, $CSR_{7.5}$	Training (96)	0.78	0.90	0.61	0.19	0.79	0.27
	Testing (48)	0.77	0.92	0.59	0.19	0.81	0.26

6.3.5.1 Generation of artificial points on the limit state curve

To approximate a limit state function that will separate liquefied cases from the non-liquefied ones, artificial data points on the boundary curve are generated using the Eq. (6.43) and following a simple but robust search technique as explained in Chapter-IV. The technique is already explained conceptually in section 4.3.2.4 with the help of Fig. 4.14 and Fig. 4.15 of Chapter-IV. A total of 213 multi-dimensional artificial data points (q_{c1N}, I_c, $\sigma_v^{'}$, $CSR_{7.5}$), which are located on the boundary curve are generated using the developed MGGP-based model Eq. (6.43). These data points are used to approximate the limit state function in the form of $CRR = f(q_{c1N}, I_c, \sigma_v^{'})$ using MGGP and presented below.

6.3.5.2 MGGP Model for CRR

The MGGP is adopted to develop the *CRR* model using the above 213 artificially generated data points. *K*-fold (3) cross validation procedure is also adopted to find the "best" MGGP-based *CRR* model. Here, out of 213 generated data points in each of *K* (3)-split 142 data points are selected for training and the remaining 71 for testing the developed model. For each split, several *CRR* models were obtained by using optimized controlling parameters of the MGGP as mentioned earlier in Chapter-IV. Similarly, three models, "best" one of each split are selected and their statistical performances in terms of *R*, R^2, *E*, *AAE*, *MAE and RMSE* on the basis of testing data are evaluated and presented in Table 6.9. The model obtained from split-2 was found to be the "best" among these three models on the basis of above statistical performances and described below as Eq. (6.44).

$$CRR = 1.224 \times 10^{-9} q_{c1N}^{\ 4} - 0.00216 \cos\left(I_C \right) [q_{c1N} + 15.72] + 3.544 \times 10^{-5} \tag{6.44}$$

The statistical performances in terms of *R*, R^2, *E*, *RMSE*, *AAE* and *MAE* as presented in Table 6.10 for both training and testing data are comparable showing good generalization of the developed *CRR* model (Eq. 6.44), which ensures that there is no over-fitting.

Table 6.9 Performance in terms statistical parameters of MGGP-based *CRR* models on the basis of *K*-fold cross validation.

	R	R^2	*E*	*AAE*	*MAE*	*RMSE*
Split1	0.94	0.96	0.88	0.02	0.16	0.03
Split2	0.98	0.99	0.97	0.01	0.09	0.02
Split3	0.92	0.94	0.85	0.02	0.28	0.03
Summary	0.95	0.96	0.90	0.02	0.18	0.03

Table 6.10. Statistical performances of developed "best" MGGP-based *CRR* model.

Data (Numbers)	*R*	R^2	*E*	*AAE*	*MAE*	*RMSE*
Training (142)	0.99	0.99	0.97	0.01	0.11	0.02
Testing (71)	0.98	0.99	0.97	0.01	0.09	0.02

The performance of the proposed *CRR* model is also evaluated by calculating the F_s for each case of field performance of the present database as discussed earlier. In deterministic approach $F_s \leq 1$ predicts occurrence of liquefaction and $F_s > 1$ refers to non-liquefaction. A prediction (liquefaction or non-liquefaction) is considered to be successful if it agrees with the field manifestation. The deterministic approach is preferred by the geotechnical professionals and the design decisions are taken on the basis of F_s. In the present study, Eq. (6.44) in conjunction with the model for $CSR_{7.5}$ (Eq.6.6) is proposed for evaluation of liquefaction potential in deterministic approach. It can be noted that the success rate in prediction of liquefied cases is 99% and that for non-liquefied cases is 65% and the overall success rate is found to be 91% by the present MGGP-based deterministic model. The poor prediction performance for non-liquefied cases may be attributed to the conservativeness of the developed boundary surface, which encompasses almost all the liquefied cases. The boundary surface (i.e. *CRR* model) is said to be unbiased if its P_L is 50% corresponding to F_s = 1. Further, the model is calibrated with respect to the liquefaction field manifestations of the present database to develop a relationship between F_s and P_L using Bayesian theory, and also to quantify the degree of conservatism associated with the developed *CRR* model (relative to *CSR* model) as presented below.

6.3.5.3 P_L-F_s mapping function

The calculated F_s values for different cases of the present database are grouped according to the field performance observation of liquefaction (*L*) and non-liquefaction (*NL*). After considering several different probability density functions as explained in section 5.2.1, it is found that the liquefied and non-liquefied groups are best fitted by Rayleigh distribution ($\lambda = 0.303$) and log normal distribution ($\mu=0.415$, $\sigma=0.861$), respectively as shown in

Fig.6.15 (a) and (b). The probability of liquefaction occurrence of a case in the database, for which the F_s has been calculated, can be found out by using Bayesian theorem of conditional probability as given by the Eq. (5.4).The F_s and the corresponding P_L of the total 144 cases of database are plotted and the mapping function is approximated through curve fitting as shown in Fig. 6.16. The mapping function is presented as Eq. (6.45) with a high R^2 value of 0.99.

$$P_L = \frac{1}{1+\left(\frac{F_s}{a}\right)^b} \tag{6.45}$$

where a (0.74) and b (4.65) are the parameters of the fitted logistic curve. The F_s is calculated using the proposed MGGP-based deterministic method (Eq.6.6 and Eq.6.44) and then, corresponding P_L can be found out using the developed mapping function. The proposed *CRR* model is also characterized with a probability of 20% as P_L=0.20 according to the Eq.(6.45) when F_s=1.0.

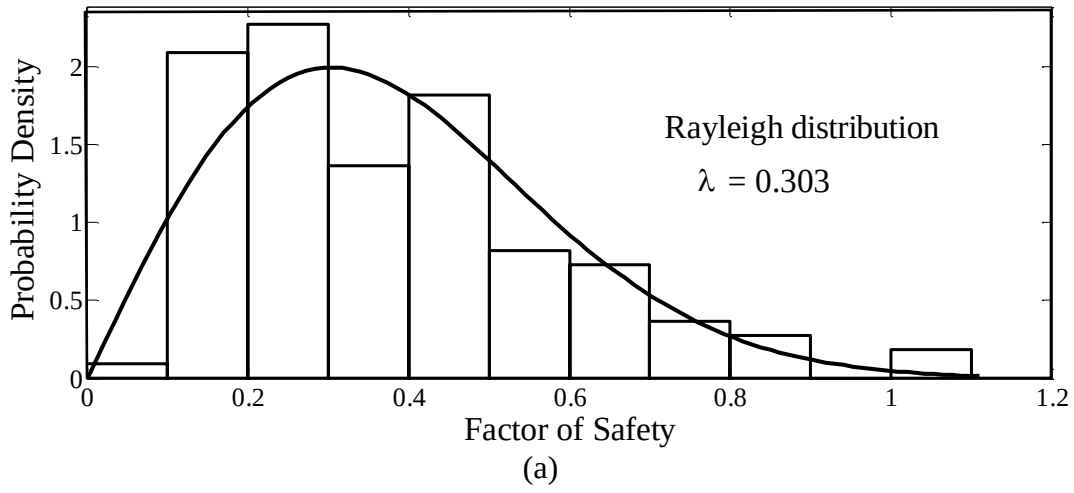

(a)

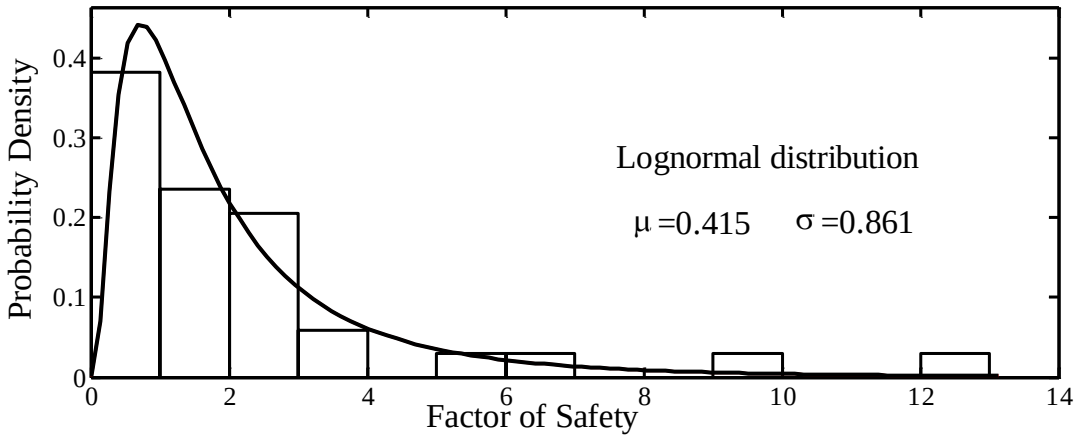

(b)

Fig. 6.15 Histogram showing the distributions of calculated factor of safeties: (a) Liquefied (*L*) cases; (b) Non-liquefied (*NL*) cases.

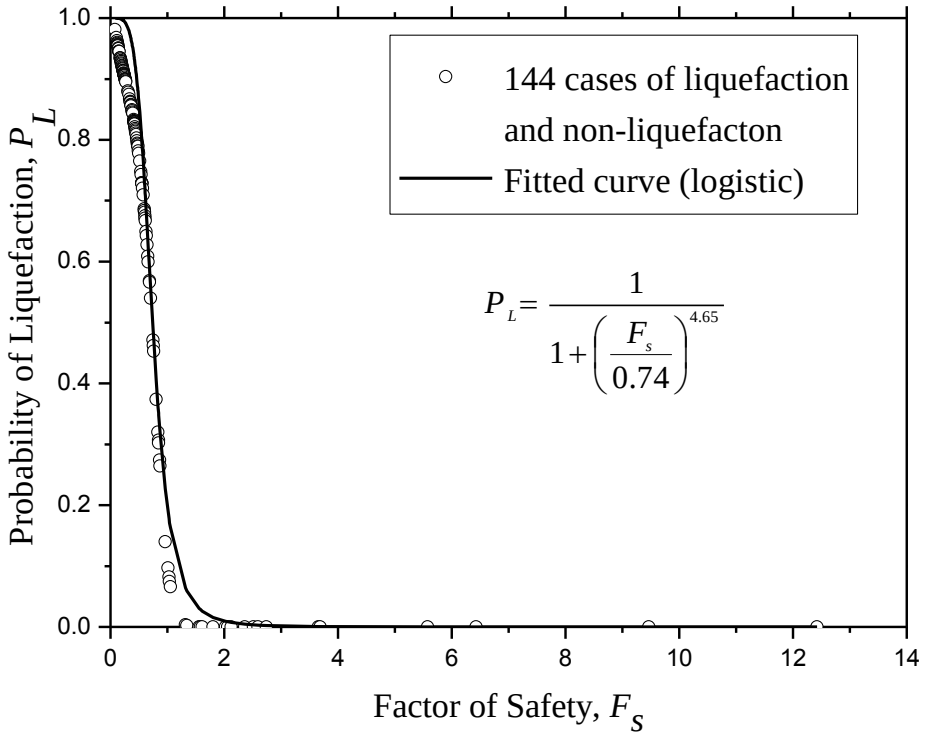

Fig. 6.16 Plot of P_L-F_s showing the mapping function approximated through curve fitting

6.3.5.4 Estimation of model uncertainty from reliability analysis

The most unbiased evaluation of liquefaction potential of soil is possible with a boundary surface, separating liquefied and non-liquefied cases, having 50% of the P_L. Such a limit state model is considered to have no model uncertainty. Alternately, unbiased evaluation of liquefaction potential is possible by quantifying the model uncertainty of the limit state and incorporating correct model uncertainty in the reliability analysis for liquefaction potential analysis. The model uncertainty of the liquefaction limit state model (Eq. 6.15) may be represented with a random variable 'c_{mf}' and referred herein as model factor (Juang et al. 2006). Thus, the liquefaction limit state model can be presented as given below:

$$g(z) = c_{mf}\ R - Q = c_{mf}\ CRR - CSR \tag{6.46}$$

where $g(z)$ = limit state function considering model uncertainty and z= vector of input parameters. The uncertainty in the *CRR* model (Eq.6.44) is only considered, and the effect of the unrealized uncertainty associated with the *CSR* model is realized in the *CRR* model as the *CRR* model is developed using *CSR* model (Eq.6.6).

In the present study, the model factor 'c_{mf}' is treated as a random variable and then, combining it with the basic input parameters from the *CRR* (Eq.6.44)and *CSR* (Eq.6.6) models, the limit state function for the reliability analysis can be presented as:

$$g(z) = c_{mf}\ CRR - CSR = g(c_{mf}, q_c, f_s, \sigma_v, \sigma_v^{'}, a_{\max}, M_w) \tag{6.47}$$

Each of the six basic input parameters in Eq.(6.47); q_c, f_s, σ_v, σ'_v, a_{max} and M_w is considered as a random variable and is assumed to follow a lognormal distribution, which has been shown to provide a good fit to the measured geotechnical parameters (Jeffries et al. 1988). The mean and coefficient of variation (COV) of each parameter for all the 144 cases considered in the present study for reliability analysis are obtained from Moss (2003). The model factor (c_{mf}) is also assumed to follow lognormal distribution, which is very well accepted in reliability analysis (Juang et al. 2006).The model factor (c_{mf}) is also characterized with a mean (μ_{cmf}) and a COV. Thus, estimation of model uncertainty includes

determination of these two statistical parameters of 'c_{mf}'. In the present study, the correlations among the input variables are incorporated in the reliability analysis.

Table 6.11 Coefficients of correlation among six input parameters (Juang et al. 2006)

Input Parameters	Input Parameters					
	q_c	f_s	σ'_v	σ_v	a_{max}	M_w
q_c	1	0.6	0.3	0.2	0	0
f_s	0.6	1	0.4	0.3	0	0
σ'_v	0.3	0.4	1	0.9	0	0
σ_v	0.2	0.3	0.9	1	0	0
a_{max}	0	0	0	0	1	0.9
M_w	0	0	0	0	0.9	1

The correlation coefficients between each pair of parameters used in the proposed limit state are provided in Table6.11 as estimated by Juang et al. (2006) from the original database of Moss (2003). As per Phoon and Kulhawy (2005), the model factor, c_{mf} is very weakly correlated to input variables. Thus, in the present study no correlation is assumed between c_{mf} and the other six input parameters considered herein.

In the present FORM analysis, GA is used as optimization tool to obtain reliability index, β. Thus, the limit state function, $g(z)=0$ (Eq. 6.47) is used as constrained function and the Eq. (6.24a) is the objective function. Following the flow chart as shown in Fig. 6.17, a code is developed in MATLAB (Math Works Inc. 2005) to estimate β. Then, notional probability of liquefaction, P_L is obtained using Eq. (6.18).

In the present study, as the model uncertainty is not known initially, the reliability index calculated without considering model uncertainty or considering any assumed value will result in incorrect calculation of β and the corresponding notional probability P_L. Hereafter, reliability index calculated without taking into account the model uncertainty is designated as β_1, whereas the reliability index calculated considering any value of model uncertainty is denoted as β_2.

In the first step of model uncertainty determination procedure, the reliability index,β_1 is calculated for each of the 144 cases of the database considered for the present study.

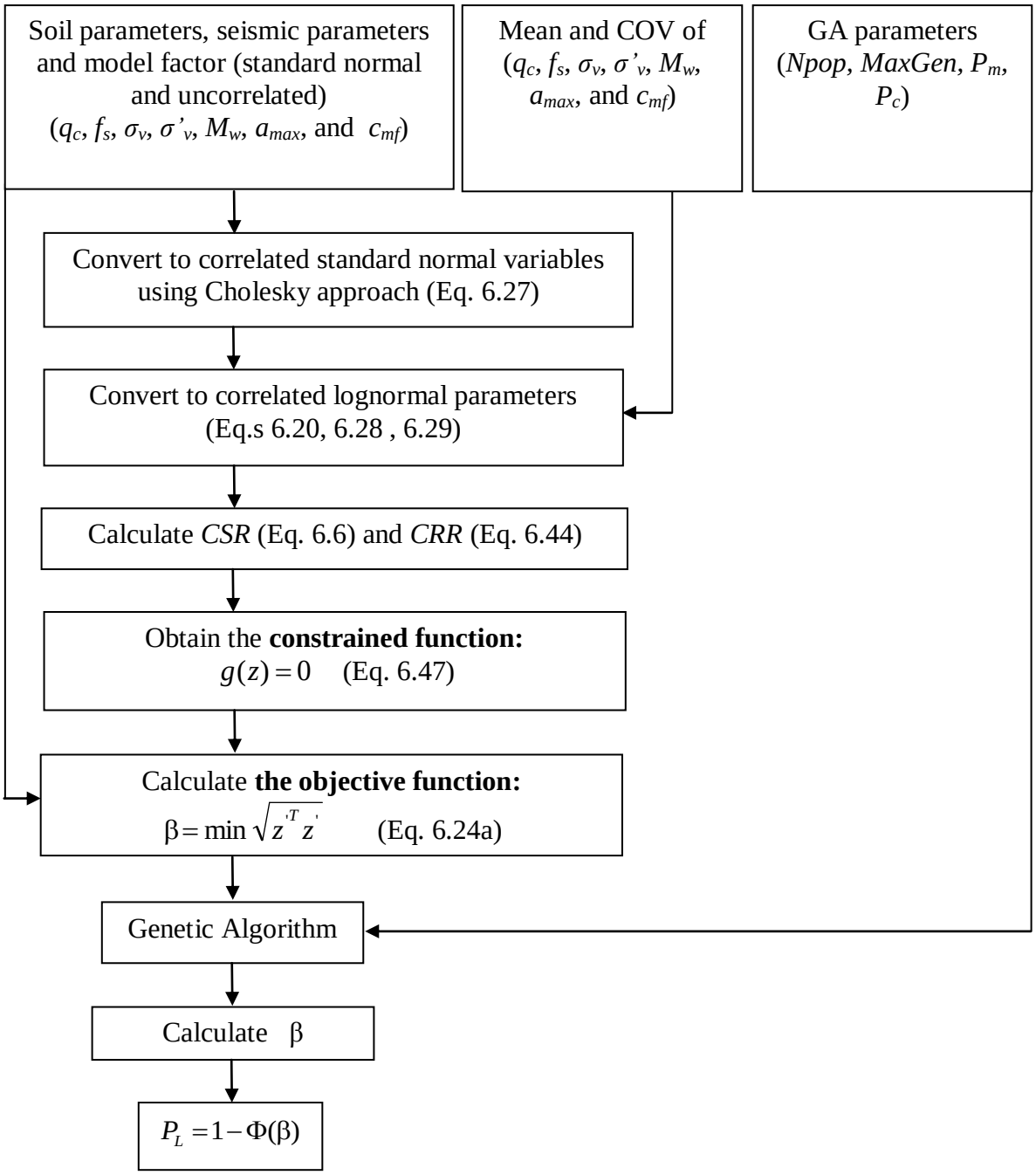

Fig. 6.17. Flow chart of the proposed FORM analysis with GA as optimisation tool.

Following Bayesian mapping function approach and calibrating with field manifestations of the database as explained in 6.2.5.4, P_L-β relationship can be obtained using Eq.(6.36). $P_L$for each case of the database is calculated using Eq. (6.36). Fig.6.18 shows a plot of P_L- β relationship obtained from the reliability analyses of 144 cases of database considered for limit state model development without considering the model uncertainty. The notional probability of each case of the database using Eq. (6.18) is calculated and plotted in the same Fig.6.18.A difference is observed between the national concept-based P_L-curve and Bayesian mapping function-based P_L-curve. The later curve is calibrated empirically with the field manifestations of case history database considered herein the present study and thus, it is assumed to be most probable evaluation of the "true" probability of liquefaction. It can also be observed from the Bayesian mapping function-based P_L-curve of the Fig. 6.18 that P_L=0.195, when β =0. This result is consistent with the 20% probability of the developed *CRR* model as obtained by P_L-F_s mapping function (Eq. 6.45), which has been discussed in the earlier section. This indicates the robustness of the proposed methodology.

The accuracy of calculated probability on the basis of notional concept depends on the accuracy with which β is calculated. As in the above study, β is calculated without considering limit state model uncertainty in reliability analysis, it is subjected to some error and thus, the resulting notional probability may not be completely accurate. But, notional probability concept always yields: P_L=0.5 at β=0. If "true" model uncertainty can be incorporated with the limit state model then, the resulting reliability index (β_2) at 0 will produce a P_L value of 0.5 from the calibrated Bayesian mapping function approach.

The methodology for estimating the uncertainty of the adopted limit state model (Eqs. 6.6 and 6.44) is based on the proposition that a calibrated Bayesian mapping function produces a most accurate estimate of the "true probability of liquefaction" for any given case. With the above idea, a simple but, trial-and-error procedure is adopted to estimate model uncertainty. The "true" model uncertainty is the one that yields the reliability indices and the corresponding notional probabilities matching best with those probabilities calculated from the calibrated P_L-mapping function (Juang et al.2006). And also the plot of $\beta_2$versus P_L as

obtained from the calibrated Bayesian mapping function will produce a P_L value of 0.5 at β_2=0.

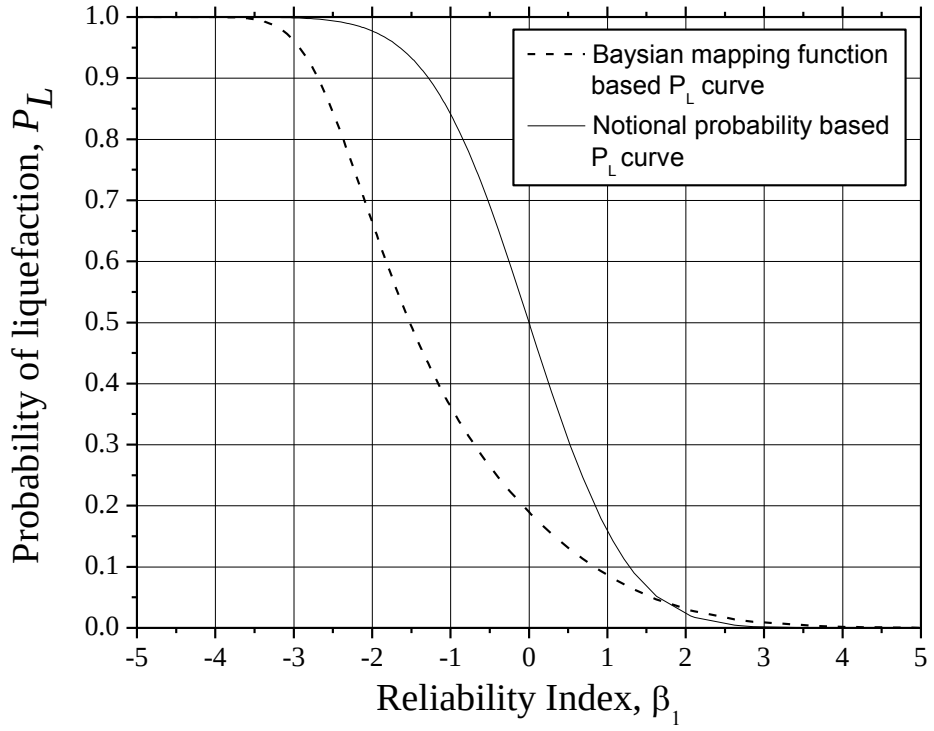

Fig. 6.18.P_L- β mapping function obtained from the reliability analysis of 144 cases of liquefaction and non-liquefaction without considering model uncertainty

In the first phase of model uncertainty estimation procedure, a series of reliability analysis of all the 144 cases of the database are performed to study the effect of COV component of the model factor, c_{mf}. Six cases of model uncertainty, each with the mean of the model factor being kept equal to1.0 (μ_{cmf}= 1.0) and a different COV of 0.0, 0.1, 0.2, 0.3, 0.4 and 0.5, are studied. For each case of model uncertainty, β_2 values are calculated for all 144 cases of the database. A Bayesian mapping function is obtained for each model uncertainty scenario, as discussed above. From the developed mapping function for each of the above mentioned model uncertainty scenario liquefaction probabilities are obtained from the corresponding β_2 values. Fig. 6.19 shows the plot between β_2 versus P_L for each of the above mentioned model uncertainty. It is clearly indicated that within the range of COV value [0–0.5] the model uncertainty has got significant effect on the calculated probability. But, Juang et al. (2006)

observed the effect of COV component of model uncertainty on P_L as insignificant in their reliability analysis.

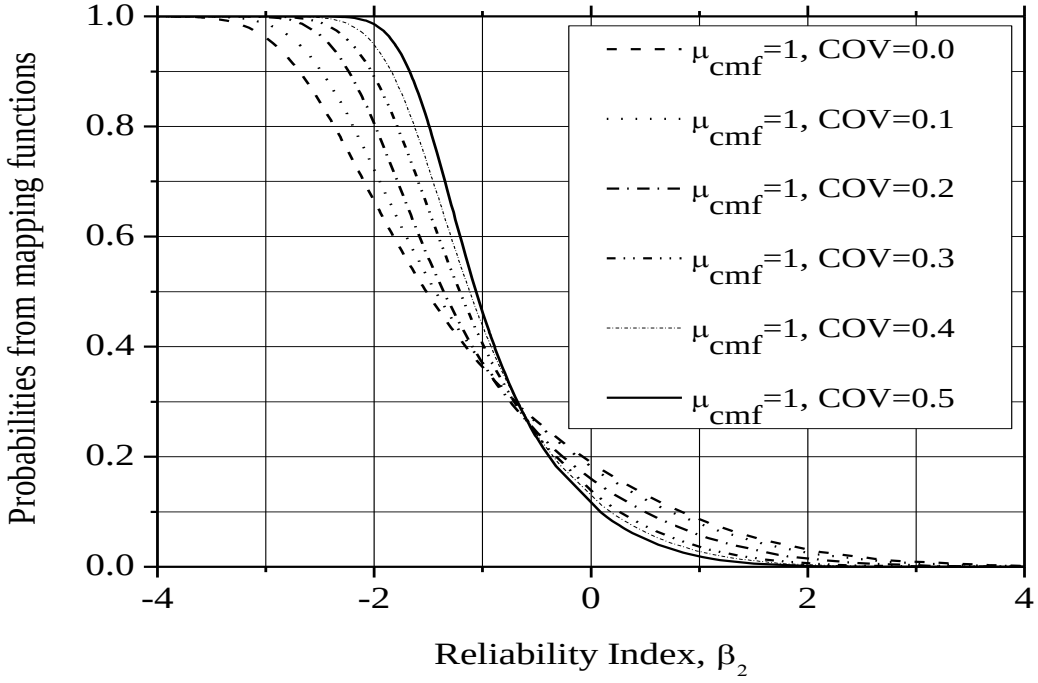

Fig. 6.19. P_L- β mapping functions showing effect of COV of model factor on probability of liquefaction

In second phase of investigation COV component of model uncertainty is kept constant at 0.1, whereas the mean value of c_{mf} is varied from 1.0 to 2.1 at an interval of 0.1(i.e. μ_{cmf}= 1.0,1.1,1.2,1.3,….2.1). For each of the above scenario of model uncertainty, Bayesian mapping function is developed using all the 144 cases of liquefaction and non-liquefaction for reliability analysis as mentioned previously. Then, P_L values calculated from the mapping functions are plotted against the corresponding reliability index (β_2) for different cases of model uncertainty as mentioned above and presented in two figures, Fig.6.20a and b, as it becomes illegible while presenting all the plots in one figure. It can also be observed from the above figures that the mapping function is shifted from left to right as μ_{cmf} increases, and also the probability corresponding to β_2= 0 increases.

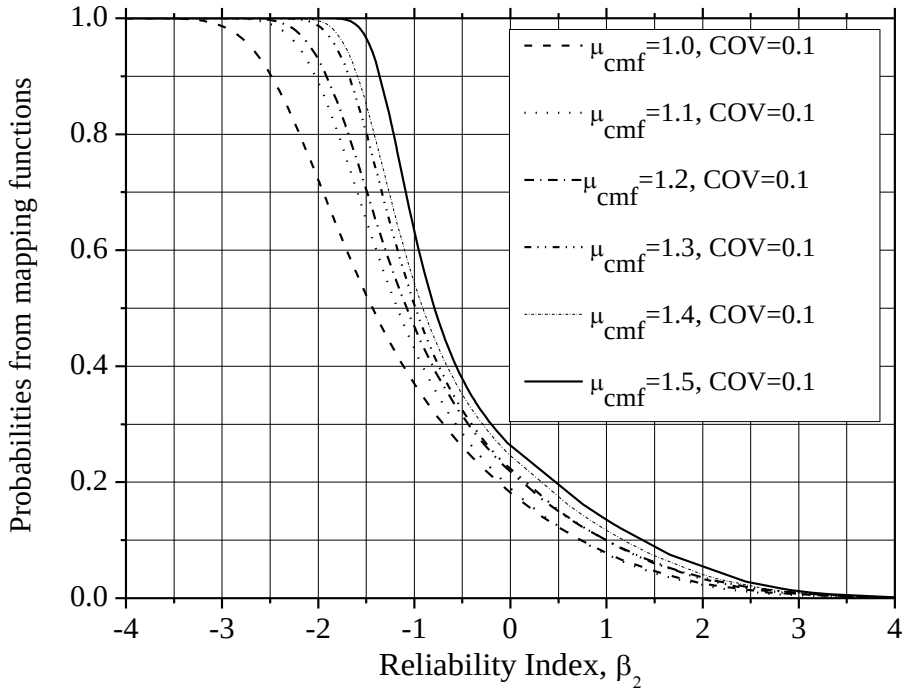

(a)

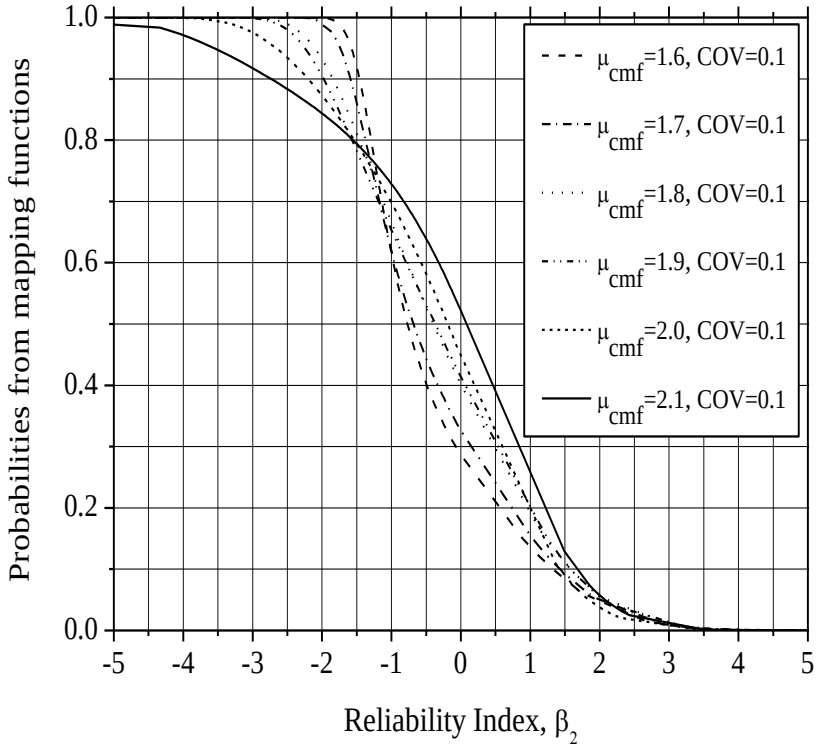

(b)

Fig. 6.20 (a) and (b) P_L- β mapping functions showing effect of mean of model factor (μ_{cmf}) on probability of liquefaction

As per Fig. 13b, at μ_{cmf} = 2.1 and COV = 0.1, the P_L= 0.52 at β= 0, whereas μ_{cmf} = 2.0 produces a lower value of P_L (0.46) at β= 0. Thereafter, at an intermediate value of μ_{cmf} = 2.08 and COV=0.1, the P_L is found out to be 0.48 at β= 0. As already it has been observed that COV has got significant effect on calculated P_L, keeping μ_{cmf} = 2.08 and changing COV component from 0 to 0.20 a series of reliability analysis of all the144 cases are performed and similarly, the Bayesian mapping functions are obtained. The P_L versus β plot for the above cases are shown in Fig.6.21 and it is clearly observed that at μ_{cmf} = 2.08 and COV=0.2 the $P_L$is found out to be 0.5 at β= 0.

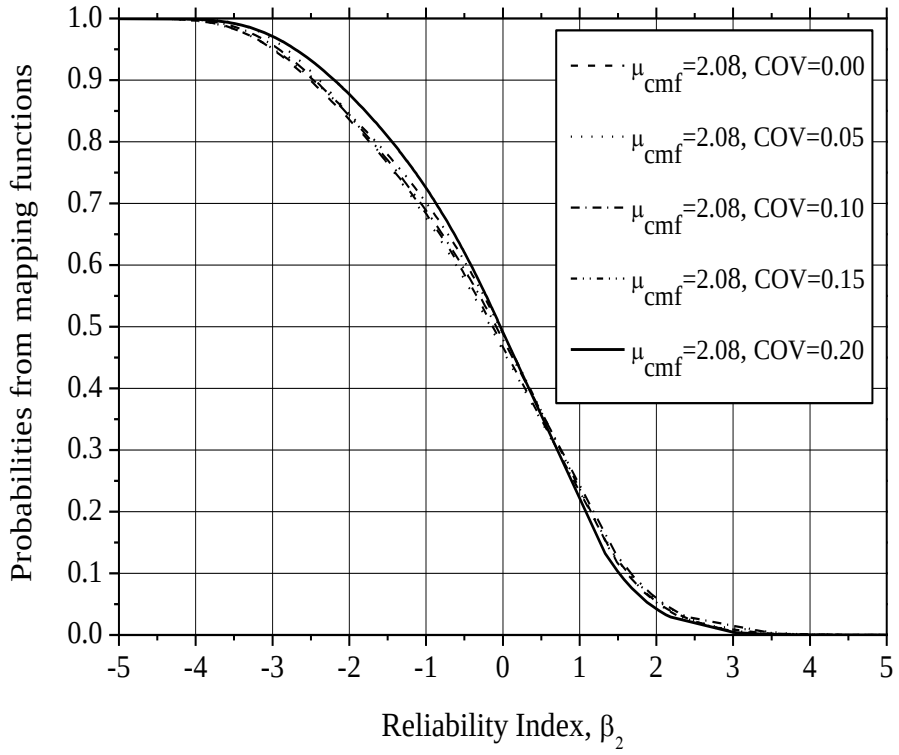

Fig. 6.21 P_L- β mapping functions showing effect of mean (μ_{cmf}) and COV of "true" model factor on probability of liquefaction i.e. at β=0, P_L = 0.5.

Fig.6.22 shows a comparison of the probability of liquefaction for each of 144 case-histories obtained from two mapping functions, one with considering the "true" model uncertainty (i.e. μ_{cmf} = 2.08 and COV = 0.2) and the other without considering the model uncertainty (i.e. μ_{cmf} = 1.00 and COV = 0). In the earlier case, the reliability index, β_2 for each case is calculated and then the corresponding mapping function is established using Eq.

(6.36).In the latter case, reliability index $\beta_1$for each case is determined and then, the corresponding mapping function is developed in the similar manner using Eq. (6.36). The two sets of probabilities obtained for all the 144 cases based on the two sets of mapping functions agree well with each other, which is evident from the statistical parameters (R =0.94, E = 0.87 and $RMSE$ = 0.18) as mentioned in the Fig. 6.22. Fig. 6.23 shows the comparison of the notional probabilities obtained for all the 144 cases of present database using the reliability index β_2 calculated by taking into account the "true" model factor(μ_{cmf}= 2.08 and COV = 0.2) with the probabilities obtained from the P_L-β_1 mapping function, which has not considered model uncertainty in the reliability analyses.

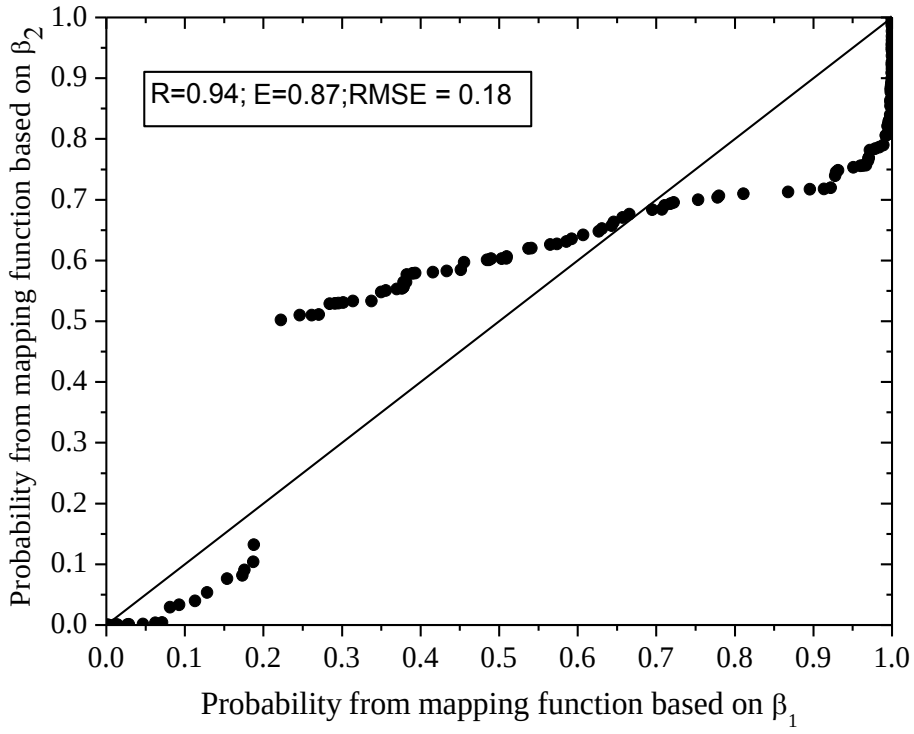

Fig. 6.22 Comparision of probabilities of liquefaction obtained from 144 cases of the database obtained from two mapping functions one based on β_2 (using μ_{cmf}=2.08 and COV=0.2) and other based on β_1

The Fig. 6.23 also shows good agreement (R=0.95, E=0.89 and $RMSE$ = 0.17) between the probabilities obtained from two different concepts, which indicates that the probability of liquefaction can be correctly calculated from the notional concept if the right model uncertainty is incorporated in the reliability analysis. Thus, in the present study, the "true"

model uncertainty of the developed limit state, considering the present database, is characterized by μ_{cmf} = 2.08 and COV = 0.2. However, Juang et al (2006) developed a limit state model of liquefaction using ANN and the model was characterized with an uncertainty of mean value 1.24 and COV of 0.1. There the model uncertainty was determined on the basis of reliability analyses of only 64 cases of the database (Moss 2003; Ku et al. 2004) with maximum COV value of the input parameters was 0.3. But, the present study was based on 144 cases of the database (Moss 2003) with maximum COV value of the input parameters was 1.126.

Finally it can be noted that the P_L can be estimated from the developed P_L-β_1 mapping function using a reliability index, β_1 that is calculated by FORM considering only parameter uncertainties. Alternatively, the reliability index β_2 can be determined by FORM considering both model and parameter uncertainties, and then, the P_L can be obtained with the notional concept using Eq. (6.18). The notional concept to estimate the P_L of a future case is preferred as the model uncertainty of the adopted limit state has been determined and also it is a well-accepted approach in the reliability theory (Juang et al. 2006).

To explain the above findings one example from 1989, Loma Prieta earthquake at Tanimura105 site as presented in Juang et al. (2006) has been analyzed to find P_L. There was no occurrence of liquefaction with critical depth, d =5.5m; q_c = 3.84 MPa; f_s = 15.8 kPa; σ_v=92.3 kPa; σ'_v =79.5 kPa; a_{max} = 0.15 g and M_w = 7. The COV of the parameters: q_c, f_s, σ_v, σ'_v, a_{max} and M_w are 8.9, 9.8, 9.6, 5.5, 26.7 and 1.7% respectively. The Eq.(6.6) and Eq.(6.44) are used to form the limit state of liquefaction and considering the model uncertainty (μ_{cmf} = 2.08 and COV = 0.2) FORM analysis is made using the developed code in MATLAB. The reliability index, β_2 and corresponding notional probability of liquefaction P_L using Eq. (6.18) are found out to be 0.961 and 0.17 respectively, whereas Juang et al. (2006) found the reliability index as 0.626 and corresponding P_L as 0.27. The results of both the methods confirm the case as non-liquefied, and as the P_L calculated by the present method is less than that of the ANN-based reliability method of Juang et al. 2006, the present method can be considered as more accurate method based on this example.

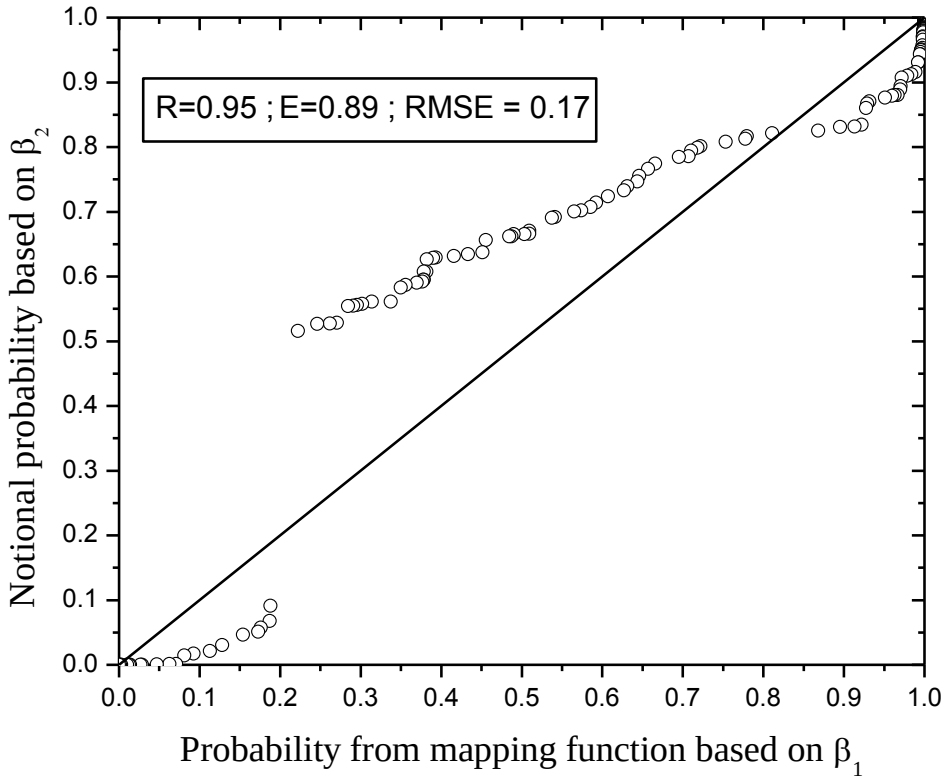

Fig. 6.23 Comparision of notional probabilities of liquefaction obtained for 144 cases based on β_2 (using μ_{cmf}=2.08 and COV=0.2) with P_L obtained from mapping function based on β_1

Another example of a liquefied case from 1979, Imperial Valley, California earthquake at Mckim Ranch A as presented in Moss (2003) has been analyzed to find P_L. There was occurrence of liquefaction at critical depth, d =2.75m; q_c = 2.69 MPa; f_s = 30.56 kPa; σ_v = 47.75 kPa; σ'_v = 35.49 kPa; a_{max} = 0.51 g and M_w = 6.5. The COV of the parameters: q_c, f_s, σ_v, σ'_v, a_{max} and M_w are 32.3, 14.2, 17, 12.3, 9.8 and 2%, respectively. The *CSR* model (Eq.6.6) and the *CRR* (Eq.6.44) are used to form the limit state of liquefaction and considering the model uncertainty (μ_{cmf} = 2.08 and COV = 0.2), FORM analysis was made using the developed code in MATLAB. The reliability index, β_2 and corresponding notional probability of liquefaction P_L using Eq. (6.18) are found out to be -2.271 and 0.99 respectively, and the result confirms the case as liquefied one. These two examples illustrate the procedure for evaluation of P_L of a site in a future seismic event using the proposed reliability based analysis if the uncertainties of soil and seismic parameters of the site are known.

6.4 CONCLUSIONS

The conclusions drawn from probabilistic method for both SPT and CPT-based models are presented separately as follows.

6.4.1 Conclusions based on SPT- based reliability analysis

The following conclusions are drawn based on the results and discussion of SPT-based reliability analysis as presented above.

i. The developed MGGP-based *CRR* model has been characterized with an uncertainty of mean value 0.98 and COV of 0.1 on the basis rigorous FORM analysis of 94 cases of the database. As the mean value of model uncertainty is very close to 1 the *CRR* model, which represents the boundary surface separating the liquefied cases from non-liquefied cases, can be considered as un-biased one. This is also evident from the proposed P_L-F_s mapping function that yields P_L=0.503, when F_s=1. Thus, the degree of conservatism of the limit state boundary surface is quantified in terms of P_L as 50.3%.

ii. The probability of liquefaction, P_L can be estimated from the developed P_L-β_1 mapping function using a reliability index, β_1 that is calculated by FORM considering only parameter uncertainties. Alternatively, the reliability index β_2 can be determined by FORM considering both model and parameter uncertainties, and then, the P_L can be obtained with the notional probability concept (using Eq. 6.18).The notional concept to estimate the P_L of a future case is preferred as the model uncertainty of the adopted limit state has been determined and also it is a well-accepted approach in the reliability theory.

iii. In absence of parameter uncertainties the proposed P_L-F_s mapping function as defined by Eq.(6.33) can be used to estimate probability of liquefaction, where the F_s is calculated based on the *CSR* and *CRR* models as presented by Eq. (6.6) and Eq. (6.32), respectively.

iv. Using the developed code for FORM two examples, one liquefied case and the other non-liquefied case, are analyzed and corresponding probability of liquefaction on the

basis of notional probability concept, using the obtained "true" uncertainty of the limit state model were found out to be 0.91 and 0.49, respectively. The P_L of the above liquefied case was also found out to be 0.91 as per the available regression-based reliability method. This indicates accuracy of the proposed MGGP-based reliability method for evaluation liquefaction potential on the basis of the above example.It is pertinent to mention here that the proposed MGGP-based reliability method is developed on basis of the most recent *CSR* formulation whereas the available reliability method is based on an older *CSR* model.

6.4.2 Conclusions based on CPT- based reliability analysis

The following conclusions are drawn based on the results and discussion of CPT-based reliability analysis as presented above.

i. The developed MGGP-based *CRR* model has been characterized with an uncertainty of mean value 2.08 and COV of 0.2 on the basis rigorous FORM analysis of 144 cases of the post liquefaction CPT database.

ii. As discussed for the SPT database, the probability of liquefaction, P_L can be estimated from the developed P_L-β_1 mapping function using a reliability index, β_1 that is calculated by FORM considering only parameter uncertainties. Alternatively, the reliability index β_2 can be determined by FORM considering both model and parameter uncertainties, and then, the P_L can be obtained with the notional probability concept (using Eq. 6.18).The notional concept to estimate the P_L of a future case is preferred as the model uncertainty of the adopted limit state has been determined and also it is a well-accepted approach in the reliability theory.

iii. The characterization of the developed MGGP-based limit state model uncertainty using the proposed reliability analysis was based on all the 144 cases of the database with maximum COV of input parameters is 1.26, whereas the estimation of uncertainty of available ANN-based limit state model was made using only 64 cases of the same database with maximum COV of the input parameters is 0.30. Thus, the proposed MGGP-based reliability method can be used for wider range of COV of

soil parameters compared to the available ANN-based reliability method of Juang et al. (2006).

iv. In absence of parameter uncertainties the proposed P_L-F_s mapping function as defined by Eq.(6.45) can be used to estimate probability of liquefaction, where the F_s is calculated based on the *CSR* and *CRR* model as presented by Eq. (6.6) and Eq. (6.44), respectively.

v. Using the developed code for FORM two examples, one non-liquefied case and the other liquefied case, are analyzed and the corresponding probability of liquefaction on the basis of notional probability concept, using the obtained "true" uncertainty of the limit state model, are found out to be 0.17 and 0.99, respectively. But, the P_L of the non-liquefied case was found out to be 0.27 as per the available ANN-based reliability method, which is slightly more than the present finding. This indicates accuracy of the proposed MGGP-based reliability method for evaluation liquefaction potential is more than that of the available ANN-based reliability method on the basis of the above example.

Chapter 7

SUMMARY AND CONCLUSIONS

7.1 SUMMARY

Natural hazards like earthquake, tsunami, flood, cyclone and landslide pose severe threat to human life and its environment. But, now days natural hazards are no longer considered as a rare act of God, but as a recurrent natural phenomenon whose disastrous effects can and should be mitigated. Out of the various seismic hazards, soil liquefaction is a major cause of both loss of life and damage to infrastructures and lifeline systems. Soil liquefaction phenomena have been noticed in many historical earthquakes after first large scale observations of damage caused by liquefaction in the 1964 Niigata, Japan and 1964 Alaska, USA, earthquakes. Accurate evaluation of liquefaction potential of soil is one of the most important steps towards mitigating liquefaction hazard. Though, different approaches like cyclic strain-based, energy-based and cyclic stress-based approach are in use, the stress-based approach is the most widely used method for evaluation of liquefaction potential of soil. Seed and Idriss (1971) first developed a stress-based simplified semi-empirical model, using laboratory tests and post liquefaction SPT-based field manifestations in earthquakes, which presents a limit state function that separates liquefied cases from the non-liquefied cases. Due to difficulty in obtaining high quality undisturbed samples and cost involved therein, further development of this simplified method was made using SPT- based field test data (Seed et al. 1983 and Seed et al. 1985). Though, SPT is most widely used soil exploration method now a days cone penetration test (CPT) is also preferred by geotechnical engineers for liquefaction potential evaluation as it is consistent, repeatable and also able to identify continuous soil profile.

Although, different approaches and methodologies have been used to develop predictive models for evaluation of liquefaction potential over the years by various researchers any attempt to improve the existing methods for assessing liquefaction potential is considered as a contribution to the field of geotechnical engineering in mitigating the liquefaction hazards. In recent years, soft computing techniques such as ANN, SVM and RVM have been successfully implemented for evaluation liquefaction potential. However, the ANN has poor generalization, attributed to attainment of local minima during training and needs iterative learning steps to obtain better learning performances. The SVM has better generalization compared to ANN, but the parameters 'C' and insensitive loss function (ε) needs to be fine-tuned by the user. Moreover, these techniques will not produce a comprehensive relationship between the inputs and output, and are called as 'black box' systems.

In the recent past, evolutionary soft computing technique, genetic programming (GP) based on Darwinian theory of natural selection is being used as an alternate soft computing technique. The GP is defined as the next generation soft computing technique and also called as a 'grey box' model (Giustolisi et al. 2007) in which the mathematical structure of the model can be derived, allowing further information of the system behaviour. The GP models have been applied to some difficult geotechnical engineering problems (Yang et al. 2004; Javadi et al. 2006; Rezania and Javadi 2007; Alavi et al. 2011; Gandomi and Alavi 2012b; Muduli et al. 2013) with success. However, its use in liquefaction susceptibility assessment is very limited (Gandomi and Alavi 2012b). The main advantage of GP and its variant, MGGP over traditional statistical methods and other artificial soft computing techniques is its ability to develop a compact and explicit prediction equation in terms of different model variables.

Out of different analysis frameworks, which are in use deterministic method is preferred by the geotechnical engineering professional because of its simple mathematical approach with minimum requirement of data, time and effort though, probabilistic methods are also in use for taking risk-based (i.e., P_L-based) design decisions. Thus, in the present study first, MGGP has been used as an analysis tool to develop deterministic models using available high quality post liquefaction SPT and CPT-based case history databases. Here, the

liquefaction potential is evaluated and expressed in terms of liquefaction field performance indicator, referred as liquefaction index (*LI*) and factor of safety against occurrence of liquefaction (F_s). The predicted value of *LI* in a future seismic event can be obtained by using developed SPT and CPT-based LI_p model equations with the help of a spread sheet, which will indicate the occurrence or non-occurrence of liquefaction. The efficacy of the developed LI_p models in terms of rate of successful prediction of liquefaction and non-liquefaction cases have been compared with available soft computing technique (ANN, SVM)-based models using independent data and are found to be comparable. Further, the developed LI_p models have been used to develop both SPT and CPT-based *CRR* models. These developed *CRR* models in conjunction with the widely used $CSR_{7.5}$ model, form the proposed MGGP-based deterministic methods. These developed SPT and CPT-based deterministic models can be used to evaluate liquefaction potential in terms of F_s. The efficiency of both the developed SPT and CPT-based deterministic models have been compared with that of available statistical and ANN-based models on the basis of independent database and it has been found that the results are quite good. Using the obtained F_s, further design decision can be taken by the geotechnical professionals regarding extent of ground improvement techniques to be followed for a liquefaction susceptible site. Two examples have been solved to show the use of developed deterministic methods to find out the extent of ground improvement works needs to be done in terms of $N_{1,60}$ and q_{c1N} using the adopted factor of safety.

However, because of uncertainties associated with the parameters and developed deterministic models, F_s greater than 1.0does not necessarily guarantee zero chance of being liquefied and similarly, F_s less or equal to 1 does not always correspond to liquefaction. In order to overcome the mentioned difficulties in the proposed SPT and CPT-based deterministic methods, probabilistic evaluation of liquefaction potential has been performed where liquefaction potential is expressed in terms of probability of liquefaction(P_L) and the degree of conservatism associated with developed deterministic models are quantified in terms of P_L. By calibrating the calculated F_s of each of the case of the database with field manifestations (liquefaction or non-liquefaction) as recorded in the database and using Bayesian theory of conditional probability the F_s is related with the P_L through the

developed mapping functions. The developed SPT and CPT-based probabilistic models have been compared in terms of rate of successful prediction within different limits of P_L**,** with that of the available statistical and ANN-based probabilistic models. The results are found to be better than that of the available methods. Two examples, one from SPT-based and the other from CPT-based post liquefaction data, have been illustrated to show the use of developed probabilistic methods to take risk-based (i.e., on the basis of P_L) design decision for carrying out ground improvement work for a site susceptible to liquefaction.

Several probabilistic models including the present SPT and CPT-based probabilistic models as presented in the Chapter-V, have been developed for evaluation of liquefaction potential in terms of P_L. These models are all data-driven as they are based on statistical analyses of the databases of post liquefaction case histories. Calculation of P_L using these semi-empirical models requires only the mean values of the input variables, whereas the uncertainties in both the parameters and the model are excluded from the analysis. Thus, resulting P_L might be subjected to error if the effect of parameter and model uncertainties are significant. To overcome these disadvantages reliability analysis following FORM has been carried out using high quality SPT and CPT database, which considers both model and parameter uncertainties. In the framework of reliability analysis, the boundary curve separating liquefaction and non-liquefaction is a limit state. The multi-gene GP (MGGP) has been used to develop *CRR* model of soil using new SPT and CPT database as per Cetin (2000) and Moss (2003), respectively. Each of the developed *CRR* model along with most recent *CSR* model (Idriss and Boulanger 2006) forms the limit state model of liquefaction for reliability analysis. The uncertainties of input parameters were obtained from the database. But, a rigorous reliability analysis associated with the Bayesian mapping function approach was followed to estimate model uncertainty of the limit state, which is represented by a lognormal random variable, and is characterized in terms of its two statistics, namely, the mean and the coefficient of variation. Four examples, two from SPT data (one liquefied and the other non-liquefied case) and the other two from CPT data (one liquefied and the other non-liquefied case), have been illustrated to show the procedure of reliability-based liquefaction potential evaluation in terms of notional probability of liquefaction (P_L) considering the corresponding "true" model uncertainty as obtained for SPT and CPT-based

limit state models in the analysis. The P_L of a site in a future seismic event using the proposed reliability-based analysis can be evaluated if the uncertainties of soil and seismic parameters of the site are known and without any more back analysis of post liquefaction SPT/CPT database.

7.2 CONCLUSIONS

The major conclusions of the present study are given as below:

7.2.1 *Based on Deterministic method*

i. A compact MGGP-based LI_p model equation is presented to predict the soil liquefaction in a future seismic event using SPT data. The liquefaction classification accuracy (94.19%) of the above developed model is found to be better than that of available ANN-based model (88.37%) and at par with the available SVM-based model (94.19%) on the basis of the testing data.

ii. A MGGP-based model equation is also presented for *CRR* of soil using SPT data which in conjunction with $CSR_{7.5}$ (Youd et al. 2001) can be used to predict the factor of safety against occurrence of liquefaction. The overall success rate of prediction of liquefaction and non-liquefaction cases by the proposed method for all 288 cases in the present database is found to be 93.40%.

iii. Using an independent database (Idriss and Boulanger 2010) the proposed MGGP-based deterministic method (87%) is found to more accurate in predicting liquefied and non-liquefied cases than the existing ANN based method (86%) and statistical method (84%) on the basis of calculated F_s. The proposed method is also found to be efficient in isolating non-liquefied cases without considering the effect of fines content.

iv. CPT-based post liquefaction database (Juang et al. 2003) is analyzed using multi-gene genetic programming approach to predict the liquefaction potential of soil in terms of liquefaction field performance indicator, *LI*.

v. The efficacy of the developed MGGP based models (Mode-I and Model-II) are compared with that of the available ANN and SVM-based models, respectively. It is

found that the performance of Model-I is better than that of the ANN model in terms of rate of successful prediction of liquefaction and non-liquefaction cases, whereas Model-II is as good as the SVM-based model in predicting both liquefaction and non-liquefaction cases.

vi. The statistical performance parameters (*R*, R^2, *E*, *AAE*, *MAE*, *RMSE*) for training and testing data are comparable in both the proposed models, which show good generalization capabilities of multi-gene GP approach. Using an independent global database the performance of Model -I and Model-II in terms of overall classification accuracy is found to be 87% and 86% respectively. Unlike available ANN and SVM-based models, the proposed model equations can be used by geotechnical engineering professionals with the help of a spreadsheet to predict the liquefaction potential of soil in terms of *LI* for future seismic event without going into the complexities of model development using MGGP.

vii. Based on sensitivity analysis, the soil type index and the measured cone tip resistance are found to be "most" important parameters contributing to the prediction of *LI* for Model-I and Model-II, respectively.

viii. For the proposed CPT-based deterministic method based on developed *CRR* model and widely used $CSR_{7.5}$ model (Youd et al. 2001), the rates of successful prediction of liquefaction and non-liquefaction cases are 98%, and 91% respectively. The overall success rate of the proposed method for all the 226 cases in the present database is found to be 95%. The performance of the present deterministic method is better than that of the ANN-based Juang method.

ix. Based on an independent database the overall rate of successful prediction in terms of calculated F_s by the proposed MGGP method (84%) is at par with that of Juang method (84%) and better than that of widely used Robertson method (81%) and Olsen method (72%).

7.2.2 *Based on Probabilistic method*

i. The proposed SPT-based deterministic method is characterized with a probability of 40% by means of the developed Bayesian mapping function relating F_s to P_L. The developed mapping function can be utilized as a tool for selecting proper factor of safety in deterministic approach based on the probability of liquefaction that is acceptable for a particular project under consideration. For example while applying the present deterministic method with a factor of safety of 0.95 would result in a probability of liquefaction 50% whereas an increased F_s of 1.14 corresponds to a P_L of 20%. If a probability of liquefaction of less than 20% is required, it can be achieved by selecting a larger F_s based on the developed mapping function.

ii. A probability design chart is prepared for evaluation of liquefaction potential of soil in terms of P_L. It can be used along with the developed SPT-based *CRR* model as a practical tool by the geotechnical professionals to take risk-based (i.e., P_L-based) design decisions.

iii. Using an independent database the proposed MGGP-based method is found to be more accurate than the existing ANN and statistical methods in predicting occurrence of liquefaction and non-liquefaction on the basis of calculated P_L.

iv. The proposed CPT-based deterministic method is characterized with a probability of 42.6% by means of the developed Bayesian mapping function relating F_s to P_L. The developed Bayesian mapping function can be utilized as a tool for selecting proper factor of safety in deterministic approach based on the probability of liquefaction that is acceptable for a particular project under consideration. For example, applying the present deterministic method with a factor of safety of 0.96 would result in a probability of liquefaction (P_L) of 50%, whereas an increased F_s of 1.15 corresponds to a P_L of 21%. If a probability of liquefaction of less than 21% is required for any site susceptible to liquefaction, it can be achieved by selecting a larger F_s based on the proposed mapping function.

v. A P_L-based design chart is prepared for evaluation of liquefaction potential of soil using CPT data. It can be used along with the developed CPT-based *CRR* model of

as a practical tool by the geotechnical professionals to take probability-based design decisions.

vi. Using the present database as well as an independent database the proposed MGGP method is found to be more accurate than the existing ANN and statistical methods in predicting occurrence of liquefaction on the basis of calculated P_L.

7.2.3 *Based on reliability method*

i. On the basis rigorous FORM analysis of 94 cases of the database of Cetin (2000),the developed MGGP-based *CRR* model has been characterized with an uncertainty of mean value 0.98 and COV of 0.1. As the mean value of model uncertainty is very close to 1 the *CRR* model, which represents the boundary surface separating the liquefied cases from non-liquefied cases, can be considered as un-biased one. This is also evident from the proposed P_L-F_s mapping function that yields P_L=0.503 when F_s=1. Thus, the degree of conservatism of the limit state boundary surface is quantified in terms of P_L as 50.3%.

ii. The probability of liquefaction, P_L can be estimated from the developed P_L-β_1 mapping function using a reliability index, β_1 that is calculated by FORM considering only parameter uncertainties. Alternatively, the reliability index β_2 can be determined by FORM considering the "true" model and parameter uncertainties, and then, the P_L can be obtained with the notional probability concept. The notional concept to estimate the P_L of a future case is preferred as the model uncertainty of the adopted limit state has been determined and also it is a well-accepted approach in the reliability theory.

iii. In absence of parameter uncertainties the proposed P_L-F_s mapping function as defined by Eq.(6.33) can be used to estimate probability of liquefaction, where the F_s is calculated based on the *CSR* and *CRR* models as presented by Eq. (6.6) and Eq. (6.32) respectively.

iv. Using the developed code for FORM two examples, one liquefied case and the other non-liquefied case, are analyzed and corresponding probability of liquefaction on the basis of notional probability concept, using the obtained "true" limit state model uncertainty were found out to be 0.91 and 0.49, respectively. The P_L of the above

liquefied case was also found out to be 0.91 as per the available regression-based reliability method. This indicates accuracy of the proposed MGGP-based reliability method for evaluation liquefaction potential on the basis of the above example. It is pertinent to mention here that the proposed MGGP-based reliability method is developed on basis of the most recent *CSR* formulation whereas the available reliability method is based on an older *CSR* model.

v. On the basis rigorous FORM analysis of 144 cases of the database of Moss(2003) the developed MGGP-based *CRR* model has been characterized with an uncertainty of mean value 2.08 and COV of 0.2

vi. The characterization of the developed MGGP-based limit state model uncertainty using the proposed reliability analysis is based on all the 144 cases of the database with maximum COV of input parameters is 1.26, whereas the estimation of uncertainty of available ANN-based limit state model was made using only 64 cases of the database with maximum COV of the input parameters is 0.30. Thus, the proposed MGGP-based reliability method can be used for wider range of COV of soil parameters than the available ANN-based reliability method.

vii. In absence of parameter uncertainties the proposed P_L-F_s mapping function as defined by Eq.(6.45) can be used to estimate probability of liquefaction, where the F_s is calculated based on the *CSR* and *CRR* model as presented by Eq. (6.6) and Eq. (6.44) respectively.

viii. Using the developed code for FORM two examples, one non-liquefied case and the other liquefied case, are analyzed and corresponding probability of liquefaction on the basis of notional probability concept, using the obtained "true" uncertainty of limit state model, are found out to be 0.17 and 0.99, respectively. But, the P_L of the non-liquefied case was found out to be 0.27 as per the available ANN-based reliability method, which is slightly more than the present finding. This indicates accuracy of the proposed MGGP-based reliability method for evaluation liquefaction potential is more than that of the available ANN-based reliability method on the basis of the above example.

7.3 RECOMMENDATIONS FOR FURTHER RESEARCH

The use of evolutionary soft computing technique, the multi-gene genetic programming (MGGP) for evaluation of liquefaction potential of soil within deterministic, probabilistic and reliability-based probabilistic framework, has given some promising results. The following are the recommendation for further research.

i. Effort should be made to include pore pressure into the limit state function to study its effect on liquefaction triggering.
ii. The second order reliability method (SORM) and Monte Carlo simulations can be used for reliability analysis for highly non-linear limit state function for achieving more accuracy in finding reliability index and thus, the notional probability of liquefaction.
iii. These studies can be extended using shear wave velocity (V_s) measurement-based in-situ testing method for liquefaction potential evaluation and efficacy of the MGGP can be tested.
iv. The liquefaction hazard analysis efforts can be extended to develop probabilistic model for estimation of liquefaction induced ground deformation.

REFERENCES

Alavi, A. H., Aminian, P., Gandomi, A. H., and Esmaeili, M. A. (2011). "Genetic-based modeling of uplift capacity of suction caissons." *Expert Systems with Applications*, 38, 12608- 12618.

Alavi, A. H., and Gandomi, A. H. (2012). "Energy-based numerical models for assessment of soil liquefaction." *Geoscience Frontiers*, 3(4), 541-555.

Ambraseys, N. N. (1988). "Engineering Seismology." *Earthquake Engineering and Structural Dynamics*, 17, 1-105.

Andrus, R. D., and Stokoe, K. H. (1997a). ''Liquefaction resistance based on shear wave velocity.'' *Proc., NCEER Workshop on Evaluation of Liquefaction Resistance of Soils, Tech. Rep. NCEER-97-0022*, T. L. Youd and I. M. Idriss, eds., Nat. Ctr. for Earthquake Engrg. Res., State University of New York at Buffalo, Buffalo, 89–128.

Andrus, R. D., and Stokoe, K. H. (1997b). ''Liquefaction resistance based on shear wave velocity.'' *Proceedings NCEER Workshop on Evaluation of Liquefaction Resistance of Soils, Tech. Rep. NCEER-97-0022*, T. L. Youd and I. M. Idriss, eds., Nat. Ctr. for Earthquake Engineering Res., State University of New York at Buffalo, Buffalo, 89–128.

Arango, I. (1996), ''Magnitude scaling factors for soil liquefaction evaluations.'' *Journal of Geotechnical Engineering*, ASCE, 122(11), 929–936.

Baecher, G. B., and Christian, J. T. (2003). *Reliability and Statistics in Geotechnical Engineering*. Wiley, London, UK.

Baziar, M. H., and Jafarian, Y. (2007). "Assessment of liquefaction triggering using strain energy concept and ANN model: Capacity Energy." *Soil Dynamics and Earthquake Engineering*, 27, 1056–1072.

Becker, D.E. (1996). "Eighteenth Canadian Geotechnical Colloquium: Limit states Design for foundations, Part I. An overview of the foundation design process." *Canadian Geotechnical Journal*, 33, 956-983.

Berger, J. O. (1985). *Statistical decision theory and Bayesian analysis*. 2nd ed., Springer, New York.

Berrill, J. B., and Davis, R. O. (1985). "Energy Dissipation and seismic liquefaction of sands: Revised model." *Soils and foundations*, 25(2), 106-118.

Boser, B. E., Guyon, I. M., and Vapnik, V. N. (1992). "A training algorithm for optimal margin classifiers." *Proceedings 5th Annual ACM Workshop on COLT*, Pittsburgh, PA, 144–152.

Bray, J. D., and Sancio, R. B. (2006). "Assessment of liquefaction susceptibility of fine-grained soils." *Journal of Geotechnical and Geoenvironmental Engineering*, 132 (9), 1165-1177.

Cetin K. O., Seed, R. B., Kiureghian, Tokimatsu, K., Harder Jr, L. F., Kayen, R. E., and Moss, R. E. S. (2004). "SPT based probabilistic and deterministic assessment of seismic soil Liquefaction potential." *Journal of Geotechnical and Geoenvironmental Engineering,* 130 (12), 1314-1340.

Cetin, K. O. (2000). "Reliability based assessment of seismic soil liquefaction initiation hazard." Ph.D dissertation, University of California, Berkeley, California.

Chern, S. G., and Chang, T. S. (1995). "Simplified procedure for evaluating soil liquefaction characteristics." *Journal of Marine Science and Technology,* 3 (1), 35-42.

Cornell, C .A. (1969). "A probability-based structural code." *American Conc. Inst. (ACI) Journal*, 66(12), 974-985.

Cortes, C., and Vapnik, V. N. (1995). "Support vector networks." *Machine Learning*, 20, 273–297.

Cristianini, N., and J. Shawe-Taylor. (2000). *An Introduction to Support Vector Machine*. Cambridge University Press, London.

Das, S. K. (2013). "Artificial Neural Networks in Geotechnical Engineering: Modeling and Application Issues", *Metaheuristics in Water, Geotechnical and Transport Engineering*, Editors. X. Yang, A.H. Gandomi, S. Talatahari, A.H. Alavi, Elsevier**,** London.

Das, S. K. and Basudhar, P. K. (2008). "Prediction of residual friction angle of clays using artificial neural network." *Engineering Geology*, 100 (3-4), 142-145.

Das, S. K., and Muduli, P. K. (2011). "Evaluation of liquefaction potential of soil using genetic programming.." P*roceedings of the Golden Jubilee Indian Geotechnical Conference, Kochi, India,* 2, 827-830.

Das, S. K., and Muduli, P. K. (2013). "Probability-based method for assessing liquefaction potential of soil using genetic programming." S, Charaborty and G. Bhattacharya (eds.), *Proceedings of the International Symposium on Engineering under Uncertainty: Safety Assessment and Management* (ISEUSAM-2012), Springer India, 1153 - 1163.

Das, S. K., and Samuai, P. (2008). "Prediction of liquefaction potential based on CPT data: A relevance vector machine approach." *Proceedings of 12th International Conference of International Association for Computer Methods and Advances in Geomechanics (IACMAG), Goa, India.*

Davis, R. O., and Berrill, J. B. (1982). "Energy dissipation and seismic liquefaction in sands." *Earthquake Engineering and Structural Dynamics*, 10, 59–68.

Der Kiureghian, A., Lin, H. Z., and Hwang, S. J. (1987). "Second order reliability approximations." *Journal of Engineering Mechanics,* ASCE, 113(8), 1208-1225.

Dief, H. M. (2000). *Evaluating the liquefaction potential of soils by the energy method in the centrifuge.* Ph. D dissertation, Case Western Reserve University, Cleveland, OH.

Dobry, R., Ladd, R. S., Yokel, F. Y., Chung, R. M., and Powell, D. (1982). *Prediction of Pore Water Pressure Buildup and Liquefaction of Sands during Earthquakes by the Cyclic Strain Method.* National Bureau of Standards, Publication No. NBS-138, Gaithersburg, MD.

Dobry, R., Mohamad, R., Dakoulas, P., and Gazetas, G. (1984). "Liquefaction evaluation of earth dams - a new approach," *Proceedings, 8th World Conference on Earthquake Engineering*, 3, 333-340.

Douglas B. J., Olson, R. S., and Martin, G. R. (1981). "Evaluation of the cone penetrometer test for SPT liquefaction assessment." *Preprint 81 544, Session on In Situ Testing to Evaluate Liquefaction Susceptibility,* ASCE National Convention, St. Louis, MO.

Fardis, M. N., and Veneziano, D. (1981). "Statistical Analysis of Sand Liquefaction." *Journal of Geotechnical and Geoenvironmental Engineering*, ASCE, 107 (10), 1361-1377.

Fardis, M. N., and Veneziano, D. (1982). "Probabilistic analysis of deposit Liquefaction." *Journal Geotechnical And Geoenvironmental Engineering*, ASCE, 108(3), 395-417.

Figueroa, J. L., Saada, A. S., Liang, L., and Dahisaria, M. N. (1994). "Evaluation of soil liquefaction by energy principles." *Journal of Geotechnical Engineering*, ASCE, 120(9), 1554–69.

Gandomi, A. H., and Alavi, A. H., (2012a). "A new multi-gene genetic programming approach to nonlinear system modeling, Part I: materials and structural Engineering Problems*." Neural Computing and Application,* 21 (1), 171-187.

Gandomi, A. H., and Alavi, A. H. (2012b). "A new multi-gene genetic programming approach to nonlinear system modeling, Part II: Geotechnical and Earthquake Engineering Problems." *Neural Computing and Application*, 21 (1), 189-201.

Gandomi, A. H., and Alavi, A. H. (2013). "Hybridizing Genetic Programming with Orthogonal Least Squares for Modeling of Soil Liquefaction" *International Journal of Earthquake Engineering and Hazard Mitigation*, 1(1), 1-8.

Gandomi, A. H. Yun, G. J. and Alavi, A. H. (2013). "An evolutionary approach for modeling of shear strength of RC deep beams." *Materials and Structures*, 46(12), 2109-2119.

Gavin, K., and Xue, J. F. (2009). "Use of genetic algorithm to perform reliability analysis of unsaturated soil slopes." *Geotechnique*, *59* (6), 545-549.

Gavin, K., and Xue, J. F., (2008). "A simple approach to analyse infiltration into unsaturated slopes." *Computers and Geotechnics*, 35 (2), 223-230.

Giustolisi, O., Doglioni, A., Savic, D. A., and Webb, B.W. (2007). "A multi-model approach to analysis of environmental phenomena." *Environmental Modelling and Software*, 5, 674 – 682.

Goh, A. T. C. (1994). "Seismic liquefaction potential assessed by neural networks." *Journal of Geotechnical Engineering,* 120 (9), 1467-1480.

Goh, A. T. C. (1996.) "Neural-Network modeling of CPT seismic liquefaction data." *Journal of Geotechnical Engineering,* ASCE, 122 (1), 70-73.

Goh, A. T. C. (2002). "Probabilistic neural network for evaluating seismic liquefaction potential." *Canadian Geotechnical Journal,* 39, 219-232.

Goh, T. C., and Goh, S. H. (2007). "Support vector machines: Their use in geotechnical engineering as illustrated using seismic liquefaction data." *Journal of Computers and Geomechanics.,* 34, 410-421.

Haldar, A., and Tang, W. H. (1979). "Probabilistic evaluation of liquefaction potential." *Journal of Geotechnical Engineering Division,* ASCE, 105(GT2), 145-163.

Hanna, A. M., Ural, D., and Saygili, G. (2007). "Neural network model for liquefaction potential in soil deposits using Turkey and Taiwan earthquake data." *Soil Dynamics and Earthquake engineering,* 27, 521-540.

Harder, L. F. Jr., (1997). ''Application of the Becker Penetration test for evaluating the liquefaction potential of gravelly soils.'' *Proceedings, NCEER Workshop on Evaluation of Liquefaction Resistance of Soils,* National Center for Engineering Research, Buffalo, 129–148.

Harder, L. F. Jr., and Seed, H. B. (1986). ''Determination of penetration resistance for coarse grained soils using the Becker hammer drill.'' *Rep. UCB/EERC-86/06,* Earthquake Engineering. Res. Ctr., University of California at Berkeley.

Hasofer, A. M., and Lind, N. C. (1974). "Exact and invariant second moment code format*." Journal of Engineering Mechanics,* ASCE, 100(1), 111–121.

Hwang, H. H. M., and Lee, C. S. (1991). "Probabilistic Evaluation of Liquefaction potential." *Center for earthquake research and information. Technical report NCEER-91-0025.* Memphis State University. Memphis, TN.

Hwang, J. H., and Yang, C. W. (2001). "Verification of critical cyclic strength curve by Taiwan Chi-Chi earthquake data." *Soil Dynamics and Earthquake Engineering*, 21, 237-257.

Idriss, I. M., and Boulanger, R. W. (2004). "Semi-empirical procedures for evaluating liquefaction potential during earthquakes*." Proceedings of 11th International Conference on Soil Dynamics and Earthquake Engineering,* January 7-9, 2004, Berkeley, California, USA.

Idriss, I. M., and Boulanger, R. W. (2006). "Semi-empirical procedures for evaluating liquefaction potential during earthquakes." *Soil Dynamics and Earthquake Engineering,* 26, 115-130.

Idriss, I. M., and Boulanger, R. W. (2010). "*SPT-based liquefaction triggering procedures* (*Report No. UCD/CGM-10/02*)." Department of Civil and Environmental Engineering, College of Engineering, University of California, Davis.

Ishihara, K. (1993). "Liquefaction and flow failure during earthquakes." *Geotechnique,* 43 (3), 351-415.

Ishihara, K., and Koseki, J. (1989). "Discussion of Cyclic shear strength of fines containing sands." *12th International Conference on Soil Mechanics and Foundation Engineering,* Rio de Janerio, 19-39.

Javadi, A. A., Rezania, M., and Nezhad, M. M. (2006). ''Evaluation of liquefaction induced lateral displacements using genetic programming." *Journal of Computers and Geotechnics,* 33, 222-233.

Jefferies, M. G., Rogers, B. T., Griffin, K. M., and Been, K. (1988). "Characterization of sand fills with cone penetration test." *Penetration testing in the UK*, Thomas Telford, London, 199-202.

Johari, A., Habibagahi, G., and Ghahramani, A. (2006). "Prediction of soil-water characteristic curve using genetic programming." *Journal of Geotechnical and Geoenvironmental Engineering,* ASCE, 132(5), 661-665.

Juang, C. H., Chen, C. J., and Tien, Y. M. (1999a). "Apprising cone penetration test based liquefaction resistance evaluation methods: artificial neural network approach." *Canadian Geotechnical Journal*, 36, 443-454.

Juang, C. H., Rosowsky D. V., and Tang, W. H. (1999b). "Reliability based method for assessing liquefaction potential of soils." *Journal of Geotechnical and Geoenvironmental Engineering,* ASCE, 125 (8), 684-689.

Juang, C. H., and Chen, C. J., (2000a) "A Rational Method for development of limit state for liquefaction evaluation based on shear wave velocity measurements." *International Journal for Numerical and Analytical methods in Geomechanics,* 24, 1-27.

Juang, C. H., Chen, C. J., Jiang, T., and Andrus, R. D. (2000b). "Risk-based liquefaction potential evaluation using standard penetration tests." *Canadian Geotechnical Journal,* 37, 1195-1208.

Juang, C. H., Chen, C. J., Rosowsky, D. V., and Tang, W. H. (2000c). "CPT based liquefaction analysis, Part 1: Detemination of limit state function." *Geotechnique,* 50 (5), 583-592

Juang, C. H., Chen, C. J., Rosowsky, D. V., and Tang, W. H. (2000d). ''CPT-based liquefaction analysis. Part 2: Reliability for design.'' *Geotechnique,* 50 (5), 593–599.

Juang, C. H., Chen, C. J., and Jiang, T. (2001). "Probabilistic framework for liquefaction potential by shear wave velocity." *Journal of Geotechechnical and Geoenvironmental Engineering,* ASCE, 127 (8), 670–678.

Juang, C. H., Jiang, T., and Andrus, R. D. (2002a). "Assessing probability based methods for liquefaction potential evaluation." *Journal of Geotechechnical and Geoenvironmental Engineering,* ASCE, 128(7), 580–589.

Juang, C. H., Yuan, H., Lee, D. H., and Ku, C. S. (2002b). "Assessing CPT-based methods for liquefaction evaluation with emphasis on the cases from the Chi-Chi, Taiwan, Earthquake." *Journal of Soil Dynamics and Earthquake Engineering,* 22, 241-258.

Juang, C. H., Yuan, H., Lee, D. H., and Lin, P. S. (2003). "Simplified Cone Penetration Test- based method for evaluating liquefaction resistance of soils." *Journal of Geotechnical and Geoenvironmental Engineering,* ASCE, 129 (1), 66-80.

Juang, C. H., Fang, S. Y., and Khor, E. H. (2006). "First order reliability method for probabilistic liquefaction triggering analysis using CPT." *Journal of Geotechechnical and Geoenvironmental Engineering* ASCE, 132 (3), 337-350.

Juang, C. H., Fang, S. Y., and Li, D. K. (2008). "Reliability analysis of liquefaction potential of soils using standard penetration test." *Reliability-based design in geotechnical engineering, Computers and Applications*, edited by K. K. Phoon, Taylor & Francis, London.

Koza, J. R. (1992). Genetic programming: on the programming of computers by natural selection, The MIT Press, Cambridge, Mass.

Kramer, S. L., and Elgamal, A. (2001). "Modeling Soil Liquefaction Hazards for Performance-Based Earthquake Engineering." *Report No. 2001/13*, Pacific Earthquake Engineering Research (PEER) Center, University of California, Berkeley, CA. 2110–23.

Krammer, S. L. (1996). *Geotechnical earthquake engineering,* Pearson Education (Singapore) Pte. Ltd., New Delhi, India.

Ku, C. S., Lee, D. H., and Wu, J. H. (2004). "Evaluation of soil liquefaction in the Chi-Chi, Twain earthquake using CPT." *Journal of Soil Dynamics and Earthquake Engineering*, 24, 659-673.

Law, K. T., Cao, Y. L., and He, G. N. (1990)." An energy approach for assessing seismic liquefaction potential." *Canadian Geotechnical Journal*, 27(3), 320-329.

Lee, C. J., and Hsiung, T. K. (2009). "Sensitivity analysis on a multilayer perceptron model for recognizing liquefaction cases." *Computers and Geotechnics*, 36(7), 1157-1163.

Liang, L., Figueroa, J. L., and Saada, A. S. (1995). "Liquefaction under random loading: unit energy approach." *Journal of Geotechnical and Geoenvironmental Engineering*, ASCE, 121 (11), 776–81.

Lin, P. L., and Der Kiureghian A. (1991). "Optimization algorithms for structural reliability." *Structural Safety*, 9(3), 161–177.

Lio, S. S. C., Veneziano, D., and Whitman, R. V. (1988). "Regression models for evaluating liquefaction probability." *Journal of Geotechnical Engineering Division,* ASCE, 114(4), 389-411.

Liong, S.Y., Lim, W.H., and Paudyal, G.N. (2000). "River stage forecasting in Bangladesh: neural network approach." *Journal of Computing in Civil Engineering,* ASCE, 14(1), 1–8.

Low, B. K., and Tang, W. H. (1997). "Efficient reliability evaluation using spreadsheet." *Journal of Engineering Mechanics,* ASCE, 123(7), 749–752.

MathWork Inc. (2005). "*Matlab User's Manual, Version 6.5*." The MathWorks, Inc, Natick.

Mitchell J. K., and Tseng, D. J. (1990). ''Assessment of liquefaction potential by cone penetration resistance.'' *Proceedings H. Bolton Seed Memorial Symp.,* J. M. Duncan, ed., BiTech Publishing, Vancouver, B.C., 2, 335–350.

Moss, R. E. S. (2003). "CPT-based probabilistic assessment of seismic soil liquefaction initiation." PhD dissertation, Univ. of California, Berkeley, Calif.

Moss, R. E. S., Seed, R. B., Kayen, R. E., Stewart, J. P., and Tokimatsu, K. (2005). "Probabilistic liquefaction triggering based on the cone penetration test." *Geotechnical Special Publication,* 133, E. M. Rathje, ed., (CD Rom) ASCE, Reston, Va.

Muduli, P. K., and Das, P. K. (2012). "Determination of limit state function in SPT-based liquefaction analysis using genetic programming for reliability analysis." *Proceedings of the Indian Geotechnical Conference, IGC-2012 on Advances in Geotechnical Engineering, December 13-15,* 2, 672-675, New Delhi, India.

Muduli, P. K., Das, M. R., Samui, P., and Das, S. K. (2013). "Uplift capacity of suction caisson in clay using artificial intelligence techniques". *Marine Georesources and Geotechnology*, 31, 375-390.

Najjar,Y. M., Ali, H. E. (1998). "CPT-based liquefaction potential assessment: A neuronet approach." *Geotechnical special publication, ASCE,* 1, 542-553.

Olsen, R. S. (1988). ''Using the CPT for dynamic site response characterization.*'' Proc., Earthquake Engineering and Soil Dynamics II Conference,* J. L. Von Thun, ed., *Geotechnical Special Publ. No. 2,* ASCE, New York, 374 –388.

Olsen, R. S. (1997). "Cyclic liquefaction based on the cone penetration test." *Proceedings of the NCEER Workshop of Evaluation of liquefaction resistance of soils. Technical report No.NCEER-97-0022,* T. L. Youd and I. M. Idriss, eds., Buffalo. NY: National center for Earthquake Engineering Research. State University of New York at Buffalo. 225-276.

Oommen, T., and Baise, L. G., (2010). "Model development and validation for intelligent data collection for lateral spread displacements." *Journal of Computing in Civil Engineering*, ASCE, 24(6), 467–477.

Ostadan, F., Deng, N., and Arango, I. (1996). "Energy-based Method for Liquefaction Potential Evaluation." *Phase 1: Feasibility Study. Report No. NIST GCR 96-701,* National Institute of Standards and Technology, Gaithersburg, MD.

Pal, M. (2006). "Support vector machines-based modeling of seismic liquefaction potential." *Journal of Numerical and Analytical Methods in Geomechachanics*, 30, 983-996.

Phoon, K. K., and Kulhawy, F. H. (2005). "Characterization of model uncertainties for lateral loaded rigid drilled shafts." *Geotechnique*, 55(1), 45-54.

Rackwitz, R., and Fiessler, B. (1978). "Structural reliability under combined random load sequences." *Computers and Structures*, 9(5), 489–494.

Rahman, M. S., and Wang, J. (2002). "Fuzzy neural models for liquefaction prediction." *Soil dynamics and earthquake engineering*, 22, 685-694.

Rezania, M., and Javadi, A. A. (2007). "A new genetic programming model for predicting settlement of shallow foundations." *Canadian Geotechnical Journal*, 44, 1462-1473

Robertson, P. K., and Campanella, R. G. (1985). "Liquefaction potential of sands using the CPT." *Journal of Geotechnical Engineering*, ASCE, 111(3), 384-403.

Robertson, P. K., and Wride, C. E. (1998). "Evaluating cyclic liquefaction potential using cone penetration test." *Canadian Geotechnical journal*, 35(3), 442-459

Robertson, P. K., Woeller, D. J., and Finn, W. D. L. (1992). ''Seismic cone penetration test for evaluating liquefaction potential under cyclic loading.'' *Canadian Geotechnical Journal*, 29, 686–695.

Samui, P. (2007). "Seismic liquefaction potential assessment by using Relevance Vector Machine." *Earthquake Engineering and Engineering Vibration*, 6 (4), 331-336.

Samui. P., and Sitharam, T. G. (2011). "Machine learning modelling for predicting soil liquefaction susceptibility." *Natural Hazards and Earth Sciences*, 11, 1-9.

Searson, D. P., Leahy, D. E., and Willis, M. J. (2010). "GPTIPS: an open source genetic programming toolbox from multi-gene symbolic regression." *In: Proceedings of the International multi conference of engineers and computer scientists*, Hong Kong.

Seed H. B., and Idriss, I. M. (1982). *Ground Motions and Soil Liquefaction During Earthquakes*, Earthquake Engineering Research Institute, Oakland, CA, 134.

Seed, H. B, and Idriss, I. M. (1967). "Analysis of soil liquefaction: Niigata Earthquake." *Journal of Soil Mechanics and Foundation Division.*, ASCE, 97(9), 1249-1273.

Seed, H. B., and de Alba, P. (1986). ''Use of SPT and CPT tests for evaluating liquefaction resistance of sands.'' *Proc., Specialty Conf. on Use of In Situ Testing in Geotechnical Engineering, Geotechnical Special Publ. No. 6*, ASCE, New York, 281–302.

Seed, H. B., and Idriss, I. M. (1971). "Simplified procedure for evaluating soil liquefaction potential." *Journal of the Soil Mechanics and Foundations Division*, ASCE, 97(SM9), 1249-1273.

Seed, H. B., and Idriss, I. M. (1981). "Evaluation of liquefaction potential of sand deposits based on observations of performance in previous earthquakes." *Preprint 81 544, Session on In Situ Testing to Evaluate Liquefaction Susceptibility*, ASCE National Convention, St. Louis, MO.

Seed, H. B., and Lee, K. L. (1966). "Liquefaction of saturated sands during cyclic loading." *Journal of the Soil Mechanics and Foundation Division,* ASCE, 92 (SM6), 105-134.

Seed, H. B., Idriss I. M., Makadisi, F., and Banerjee, N.(1975). "Representation of irregular stress time histories by equivalent uniform stress series in liquefaction analyses." *EERC 75-29,* Earthquake Engg. Reasearch Centre, University of California, Berkeley.

Seed, H. B., Idriss, I. M., and Arango, I. (1983). "Evaluation of liquefaction potential using field performance data." *Journal of Geotecchnical Engineering Division*, ASCE, 109 (3), 458-482.

Seed, H. B., Tokimatsu, K., Harder, L. F., and Chung, R. (1985). "Influence of SPT procedures in soil liquefaction resistance evaluations." *Journal of Geotechnical Engineering,* ASCE, 111(12), 1425-1445.

Shahin, M. A., Maier, H. R., and Jaksa, M. B. (2002). "Predicting settlement of shallow foundations using neural network." *Journal of Geotechnical and Geoenvironmental Engineering*, ASCE, 128(9), 785-793.

Shibata, T., Teparaksa, W. (1988). "Evaluation of liquefaction potential of soil using cone penetration tests. *Soils and Foundations*, 28(2), 49-60.

Sitharam, T. G., and Samui, P. (2007). "Support Vector Machine for evaluating seismic liquefaction potential using shear wave velocity." *Proceedings of workshop on microzonation,* Interline Publishing, Bangalore.

Skempton, A. K. (1986). "Standard penetration test procedures and the effects in sands of overburden pressure, relative density, particle size, aging, and over consolidation." *Geotechnique*, 36(3), 425–47.

Smith, G.N. (1986). Probability and Statistics in civil engineering. Collins, London.

Smola, A. J., and Scholkopf, B. (2004). "A tutorial on support vector regression." *Statistics and Computing*, 14, 199–222.

Stark, T. D., and Olson, S. M. (1995). *''*Liquefaction resistance using CPT and field case histories*.'' Journal of Geotechnical Engineering, ASCE, 121(12), 856 – 869.*

Stokoe II, K. H. Roesset, J. M., Bierschwale, J. G., and Aouad, M. (1988). ''Liquefaction potential of sands from shear wave velocity.'' *Proceedings 9th World Conf. on Earthquake Engineering* 3, 213–218.

Su, K. Y., and Tak. K. B. (2006). "Use of artificial neural network in the prediction of liquefaction resistance of sands." *Journal of Geotechnical and Geoenvironmental Engineering*, ASCE, 132(11), 1502-1504.

Suzuki, Y., Tokimatsu, K., Koyamada, K., Taya, Y., and Kubota, Y. (1995). ''Field correlation of soil liquefaction based on CPT data.''*Proc., Int. Symp. on Cone Penetration Testing*, 2, 583–588.

Terzaghi, K., and Peck, R.B. (1948). *Soil mechanics in engineering practice*, 1st Edition, John Wiley & Sons, New York.

Tipping, M. E. (2001). "Sparse Bayesian learning and the relevance vector machine." *Journal of Machine Learning Research*, 1, 211–244.

Tokimatsu, K., and Uchida, A. (1990). ''Correlation between liquefaction resistance and shear wave velocity.'' *Soils and Foundations*, Tokyo, 30(2), 33–42.

Toprak, S., Holzer, T. L., Bennett, M. J. and Tinsley, J. C. III, (1999). "CPT- and SPT-based probabilistic assessment of liquefaction." *Proceedings 7th U.S.–Japan Workshop on Earthquake Resistant Design of Lifeline Facilities and Counter measures against Liquefaction*, Seattle, Multidisciplinary Center for Earthquake Engineering Research, Buffalo, N.Y., 69–86.

Vapnik, V. (1998). *Statistical learning theory*. Wiley, New York.

Whitman, R. V. (1971). "Resistance of soil to liquefaction and settlement." *Soils and Foundations*, 11 (4), 59-68.

Xue, J. F., and Gavin, K. (2007). "Simultaneous determination of critical slip surface and reliability index for slopes." *Journal of Geotechnical and Geoenvironmental Engineering*, ASCE 133 (7), 878-886.

Yang, C. X., Tham, L. G., Feng, X. T., Wang, Y. J., and Lee, P. K. (2004). "Two stepped evolutionary algorithm and its application to stability analysis of slopes." *Journal of Computing in Civil Engineering*, ASCE, 18(2), 145-153.

Youd, T. L., and Noble, S. K. (1997a), ''Magnitude scaling factors,'' *Proceedings NCEER Workshop on Evaluation of Liquefaction Resistance of Soils*, Nat. Ctr. for Earthquake Engineering Res., State Univ. of New York at Buffalo, 149–165.

Youd, T. L., and Nobble, S. K. (1997b). "Liquefaction criteria based statistical and probabilistic analysis." *In: Proceedings of NCEER workshop on Evaluation of Liquefaction Resistance of Soils, technical Report No. NCEER-97-0022*, State University of New York at Buffalo, Buffalo, New York, 201-216.

Youd, T. L., Idriss I. M., Andrus R. D., Arango, I., Castro, G., Christian, J. T., Dobry, R., Liam Finn, W. D., Harder Jr, L. F., Hynes, M. E., Ishihara, K., Koester, J. P., Liao, S. S. C., Marcuson III W. F., Martin, G. R., Mitchell, J. K., Moriwaki, Y., Power, M. S., Robertson,

P. K., Seed, R. B., and Stokoe II, K. H. (2001). "Liquefaction resistance of soils: summary report from the 1996 NCEER and 1998 NCEER/NSF workshops on evaluation of liquefaction resistance of soils." *Journal of Geotechnical and Geoenvironmental Engineering,* ASCE,127 (10), 817-833.

Youd, T.L., and Idriss, I. M. (1997). *Proc., NCEER Workshop on Evaluation of Liquefaction Resistance of Soils, tech. Rep.No. NCEER-97-0022*, T. L. Youd and I. M. Idriss, eds., National Centre for Earthquake Engineering Research, State Univ. of New York at Buffalo, N.Y.

Zhou, S. (1980). "Evaluation of the liquefaction of sand by static cone penetration test." *Proceedings of 7th World Conference on Earthquake Engineering,* Istanbul, turkey, 3, 156-162.

web references:

www.en.wikipedia.org/wiki/Geohazard (2010) Geohazards

www.em-dat.net/ (2010) The International emergency disaster database

www.ngdc.noaa.gov/ (2010) National Geophysical data centre

www.nidm.net/ (2010) National Institute of disaster management

www.saarc-sdmc.nic.in/index.asp (2010) SAARC disaster management centre

APPENDIX-A

SPT-based Post liquefaction case histories of Chi Chi, Taiwan, earthquake, 1999

(Hwang and Yang 2001)

Table A-1. Training Data

Liquefied?	Depth (m)	N_m	*FC* (%)	*CC* (%)	D_{50} (mm)	a_{max} (g)	*CSR*	$N_{1,60}$
No	9	14	17	4	0.13	0.124	0.14	14.29
No	9	21	14	3	0.23	0.124	0.127	20.7
No	5	16	46	5	0.09	0.124	0.127	20.61
Yes	7.5	12	55	8	0.08	0.428	0.384	12.14
No	8.2	1	42	6	0.111	0.084	0.069	0.97
Yes	7.8	7	16	4	0.3	0.42	0.363	6.99
Yes	1.3	1.5	65	23	0.055	0.789	0.741	3.6
Yes	4.3	9	26	4	0.14	0.211	0.165	10.65
Yes	3.6	6	11	3	2	0.42	0.289	7.53
Yes	4.5	7	26	4	0.135	0.211	0.222	9.85
No	9	19	10	1	0.26	0.124	0.113	17.72
Yes	6.3	11	30	6	0.11	0.42	0.363	12.13
Yes	8.3	12	13	3	0.56	0.428	0.386	11.62
No	16.2	28	31	9	0.3	0.42	0.374	20.82
Yes	12.8	5	26	10	0.11	0.211	0.178	7.95
No	7	16	8	1	0.22	0.124	0.131	17.97
Yes	10.3	14	15	5	0.38	0.211	0.228	13.7
No	13.2	12	61	6.9	0.068	0.055	0.042	8.95
Yes	6	2	33	7	0.16	0.124	0.13	2.39
No	9	21	12	2	0.2	0.124	0.133	21.09
Yes	7.3	13	40	11	0.095	0.789	0.644	12.03
Yes	3.8	6	17	2	0.17	0.211	0.208	8.65
Yes	2.2	6	23	5	0.15	0.42	0.304	7.51
Yes	4	5	21	3	0.14	0.124	0.126	7.27
Yes	13.5	13	14	3	0.16	0.211	0.223	11.53
No	9	16	29	6	0.2	0.124	0.135	16.11
No	10	20	18	4	0.19	0.124	0.125	19.01
No	10	22	15	3	0.18	0.124	0.118	19.91
Yes	19.5	9	46	18	0.093	0.211	0.196	6.6
No	5	18	14	3	0.2	0.124	0.137	23.86
Yes	3	2	36	5	0.1	0.124	0.118	3.26
Yes	5.8	11	22	4	0.13	0.789	0.78	12.79
No	10	25	14	3	0.22	0.124	0.123	23.49

Liquefied?	Depth (m)	N_m	*FC* (%)	*CC* (%)	D_{50} (mm)	a_{max} (g)	*CSR*	$N_{1,60}$
Yes	5.8	6	10	3	0.28	0.211	0.231	7.46
Yes	7.3	5	16	2	0.21	0.211	0.244	5.76
Yes	4.2	7	27	5	0.19	0.428	0.634	8.52
No	10	18	7	1	0.29	0.124	0.126	17.27
Yes	13.5	7	47	5	0.091	0.211	0.226	6.29
No	15.7	46	29	5	0.1	0.42	0.384	35.34
Yes	10.9	26	31	8	0.12	0.42	0.355	21.87
Yes	2.8	3	38	11	0.097	0.789	0.76	4.94
No	9	22	16	3	0.15	0.124	0.139	22.39
Yes	3.7	9	11	3	0.19	0.165	0.128	11.57
Yes	8.8	13	40	14	0.1	0.789	0.611	11.01
No	4	8	15	3	0.18	0.124	0.124	11.41
Yes	13.3	16	11	4	0.34	0.211	0.2	13.29
Yes	12	8	41	6	0.104	0.211	0.234	7.69
Yes	5.5	15	17	3	0.7	0.42	0.42	18.66
No	10	20	15	3	0.17	0.124	0.134	19.33
Yes	8.8	5	31	±	0.125	0.165	0.193	5.31
No	17.3	13	23	3	0.148	0.181	0.095	7.11
No	18.8	9	45	10	0.11	0.181	0.123	5.34
Yes	3.8	3	24	±	0.138	0.165	0.217	5.04
Yes	3	7	5	0	0.2	0.124	0.121	11.8
Yes	8.8	5	24	2	0.4	0.211	0.219	5.13
No	8	20	13	2	0.22	0.124	0.129	20.82
Yes	7.4	13	25	4	0.18	0.42	0.416	14.34
Yes	5.3	10	21	4	0.23	0.42	0.294	10.86
Yes	6.8	8	59	9	0.07	1	0.633	7.39
Yes	4.2	3	62	17	0.1	0.211	0.417	4.05
Yes	5.8	7	25	7	0.15	0.428	0.283	6.55
No	9.5	27	17	4	1	0.42	0.296	23.58
Yes	6.3	16	15	5	0.27	0.428	0.41	16.59
Yes	8.8	7	37	11	0.11	0.211	0.228	7.22
No	8	20	13	2	0.17	0.124	0.113	19.55
No	5	15	17	4	0.17	0.124	0.13	19.8
Yes	3	2	9	1	0.2	0.124	0.118	3.28
Yes	9.2	12	49	3	0.078	0.211	0.203	11.49
No	16.8	40	39	8	0.1	0.42	0.275	27.73
Yes	9	7	42	9.4	0.1	0.789	0.714	6.38
Yes	11.8	10	24	5	0.2	0.211	0.165	7.88
No	9.1	44	32	5	0.15	1	0.613	37.49
No	6.5	26	17	4	0.28	0.42	0.353	27.8

Liquefied?	Depth (m)	N_m	*FC* (%)	*CC* (%)	D_{50} (mm)	a_{max} (g)	*CSR*	$N_{1,60}$
No	14.1	36	35	12	0.3	0.42	0.364	27.92
Yes	14.8	14	17	1	0.17	0.211	0.187	10.81
No	10	18	16	3	0.18	0.124	0.124	17.04
Yes	14.3	14	14	3	0.5	0.211	0.143	9.57
Yes	10.3	10	45	14	0.1	0.211	0.176	8.59
Yes	4.3	4	18	6	0.19	0.211	0.177	5.02
No	6	11	8	0	0.2	0.165	0.142	12.07
No	9	15	18	4	0.18	0.124	0.141	14.68
Yes	5.8	6	47	7	0.08	0.33	0.325	7.03
Yes	2.4	6	41	9	0.095	0.789	0.514	8.71
No	6	17	9	2	0.28	0.124	0.108	18.44
Yes	6.2	6	23	5	0.13	0.42	0.411	7.11
No	10	19	10	2	0.25	0.124	0.124	17.99
No	10.9	30	21	5	0.013	0.42	0.354	25.9
Yes	5.7	8	16	2	0.17	0.165	0.139	8.82
No	9.8	15	23	3	0.149	0.181	0.128	11.84
No	12.8	12	44	3	0.111	0.181	0.126	8.4
No	6.2	1	42	4.6	0.108	0.084	0.064	1.04
Yes	7.2	6	13	5	0.14	0.165	0.145	6.05
No	8	20	18	3	0.18	0.124	0.143	21.57
Yes	11.8	18	12	1	0.61	0.211	0.213	16.15
Yes	10.3	6	31	5	0.11	0.211	0.207	5.6
Yes	2.8	2	55	13	0.06	0.33	0.271	3.02
No	10	17	12	2	0.3	0.124	0.134	16.43
Yes	3.8	6	13	4	0.5	0.42	0.391	8.75
No	8	20	24	6	0.17	0.124	0.129	20.72
No	5	8	14	2	0.13	0.124	0.104	9.32
No	10	18	28	5	0.13	0.124	0.134	17.43
Yes	13.5	7	42	3	0.102	0.211	0.228	6.34
No	3	12	33	8	0.16	0.124	0.156	18.83
No	10	16	13	3	0.29	0.124	0.135	14.92
No	5	20	18	4	0.18	0.124	0.119	24.84
Yes	6	7	11	0	0.167	0.211	0.232	8.82
Yes	15.4	20	33	10	0.18	1	0.663	14
Yes	2.8	4	33	9	0.188	0.428	0.506	5.37
Yes	5.8	3	47	5	0.078	0.211	0.247	3.85
No	9	17	16	4	0.18	0.124	0.112	15.74
No	4	6	43	3	0.09	0.165	0.124	7.46
Yes	3	3	38	6	0.11	0.211	0.203	4.94
Yes	6.8	10	15	7	0.037	0.789	0.79	10.78

Liquefied?	Depth (m)	N_m	*FC* (%)	*CC* (%)	D_{50} (mm)	a_{max} (g)	*CSR*	$N_{1,60}$
No	10	21	21	9	0.15	0.124	0.123	19.62
Yes	8.8	17	39	9	0.1	1	0.606	14.48
Yes	11.7	10	13	2	1.2	0.165	0.146	8.44
Yes	7.2	5	30	13	0.024	0.165	0.144	4.99
No	9	17	31	5	0.1	0.124	0.139	17.26
No	10	20	12	3	0.2	0.124	0.124	18.95
Yes	12	9	39	5	0.108	0.211	0.222	8.33
No	10.8	44	32	5	0.16	1	0.67	35.22
Yes	4	11	11	0	0.12	0.428	0.356	14.34
Yes	13.2	26	31	8	0.1	0.42	0.352	20.15
Yes	8.1	17	18	6	0.2	0.42	0.347	16.64
Yes	9	12	4	3	0.22	0.124	0.127	11.86
No	6	18	19	4	0.19	0.124	0.138	21.97
No	18.8	13	15	1	0.164	0.181	0.142	8.29
No	10.6	40	14	1	0.3	0.42	0.353	33.43
Yes	2.8	6	22	5	0.18	0.428	0.458	10.62
Yes	4.8	9	29	±	0.129	0.165	0.214	13.4
Yes	3	5	24	6	0.13	0.428	0.3	6.71
Yes	16	11	20	0	0.3	0.165	0.152	8.79
No	15.4	28	18	6	0.1	0.42	0.337	19.59
Yes	5	9	20	6	0.15	0.428	0.296	9.4
No	17.3	22	39	3	0.12	0.181	0.1	12.26
Yes	7.3	12	18	5	0.21	0.211	0.201	12.54
Yes	8.8	4	30	4	0.1	0.211	0.208	3.94
Yes	6	7	61	13.5	0.075	0.428	0.451	8.47
Yes	7.5	7	47	9	0.091	0.211	0.247	8.14
Yes	3.7	7	28	1	0.1	0.165	0.148	9.93
No	10	20	14	4	0.18	0.124	0.125	19.04
Yes	5.3	17	21	3	0.3	0.42	0.339	19.51
Yes	2.8	4	18	2	0.18	0.211	0.197	6.53
Yes	12	7	48	10	0.089	0.211	0.232	6.67
Yes	5.7	5	40	10	0.08	0.165	0.14	5.58
No	9	22	10	1	0.22	0.124	0.128	21.8
Yes	5.8	12	49	12	0.075	0.428	0.65	12.45
No	8	22	15	4	0.19	0.124	0.138	23.37
Yes	7.7	7	18	3	0.17	0.165	0.142	6.72
Yes	2.1	2	18	4	0.13	0.42	0.33	2.69
No	7	17	20	3	0.115	0.124	0.14	19.31
Yes	5.7	13	34	7	0.15	0.42	0.322	14.4
Yes	2.3	8	29	6	0.1	0.42	0.336	10.63

Liquefied?	Depth (m)	N_m	*FC* (%)	*CC* (%)	D_{50} (mm)	a_{max} (g)	*CSR*	$N_{1,60}$
Yes	4.2	5	43	7	0.143	0.428	0.596	5.87
Yes	5.8	10	30	7	0.97	0.428	0.433	12.04
Yes	7.2	6	22	15	0.18	0.165	0.148	6.16
Yes	7.7	11	16	3	0.22	0.165	0.132	10.19
Yes	12	12	13	3	0.162	0.211	0.231	11.4
No	7.5	26	17	4	0.3	0.42	0.354	26.28
No	9	19	14	3	0.2	0.124	0.127	18.71
Yes	10.3	11	28	5	0.11	0.211	0.191	9.87
No	18	13	22	0	0.104	0.165	0.142	9.34
Yes	13.3	10	30	3	0.11	0.211	0.214	8.58
Yes	8.1	11	19	2	0.17	0.165	0.148	10.71
No	10	21	17	4	0.18	0.124	0.124	19.89
No	9	18	14	3	0.2	0.124	0.139	18.35
No	10	23	15	4	0.22	0.124	0.128	21.98
Yes	3	6	30	3	0.127	0.211	0.195	9.58
No	5	14	14	3	0.2	0.124	0.138	18.68
No	11.3	15	47	4	0.106	0.181	0.124	10.98
No	16.2	15	43	16	0.113	0.128	0.124	11.81
Yes	5.8	10	48	12	0.08	0.789	0.822	11.78
Yes	8.7	6	44	12	0.08	0.165	0.148	5.68
Yes	12	10	28	3	0.131	0.211	0.238	9.76
Yes	10.2	6	13	4	0.14	0.165	0.145	5.32
Yes	7.3	5	23	1	0.31	0.211	0.208	5.31
No	13	31	20	5	0.4	0.42	0.331	23.49
No	8	20	13	2	0.2	0.124	0.144	21.72
No	10	21	12	2	0.3	0.124	0.135	20.43
No	7.1	25	15	1	0.8	0.42	0.341	24.34
No	9	21	14	3	0.2	0.124	0.122	20.23
No	14.3	43	39	8	0.08	0.42	0.272	29.28
Yes	4.5	4	32	6	0.123	0.211	0.221	5.61
No	7.2	10	36	17	0.126	0.128	0.141	11.43
Yes	4	4	30	4	0.1	0.124	0.124	5.73
No	9	20	9	2	0.2	0.124	0.128	19.86
Yes	5.7	6	15	4	0.18	0.165	0.143	6.62
Yes	12.8	15	25	±	0.138	0.165	0.174	13.11
No	6.9	46	44	12	0.1	1	0.715	49.29
No	7.8	7	31	18	0.135	0.128	0.139	7.65
Yes	5.8	5	19	4	0.5	0.211	0.211	5.94
No	14.3	13	46	8	0.108	0.181	0.12	8.49
Yes	10	8	45	4	0.08	0.165	0.145	7.25

Liquefied?	Depth (m)	N_m	*FC* (%)	*CC* (%)	D_{50} (mm)	a_{max} (g)	*CSR*	$N_{1,60}$
No	12.6	33	29	6	0.3	0.42	0.368	26.67
Yes	3	5	12	2	0.19	0.124	0.119	8.22
Yes	5	14	25	3	0.8	0.42	0.324	15.45
Yes	2.7	4	22	15	0.18	0.165	0.105	5.52
No	5	18	14	3	0.2	0.124	0.137	23.86
No	2.8	11	33	18	0.155	0.211	0.161	15.95
No	10	18	23	5	0.13	0.124	0.111	16.09
No	14.7	13	25	6.91	0.16	0.055	0.041	9.2
No	9.2	1	39	4.8	0.128	0.084	0.07	0.93

Table A-2. Testing Data

Liquefied?	Depth (m)	*N*	*FC* (%)	*CC* (%)	D_{50} (mm)	a_{max} (g)	*CSR*	$N_{1,60}$
Yes	3.7	9	17	1	0.16	0.165	0.153	12.63
Yes	7.3	11	9	0	0.49	0.211	0.199	11.32
Yes	4.2	7	40	10	0.13	0.428	0.672	8.72
Yes	4.7	12	29	6	0.25	0.42	0.344	14.74
Yes	7.8	10	46	±	0.094	0.165	0.209	11.88
Yes	6	7	14	1	0.16	0.211	0.193	7.79
Yes	5.8	9	40	7	0.16	0.428	0.718	9.88
No	10	22	16	3	0.17	0.124	0.122	20.42
Yes	4.2	8	34	7	0.2	0.428	0.609	9.5
Yes	7.7	6	13	0	0.18	0.165	0.134	5.7
Yes	8.8	11	38	12	0.4	0.42	0.308	9.86
Yes	5.8	4	35	7	0.125	0.428	0.36	4.35
No	10	19	11	2	0.18	0.124	0.124	18.03
Yes	4.3	4	10	3	0.25	0.211	0.167	4.87
Yes	4.3	4	9	2	0.31	0.211	0.193	5.24
No	4.2	3	6	0	0.331	0.084	0.054	3.64
No	15.8	17	39	5	0.12	0.181	0.141	11.55
No	9	22	9	2	0.2	0.124	0.128	21.87
No	10	16	14	2	0.18	0.124	0.123	15.03
Yes	8.2	8	10	2	0.45	0.211	0.202	7.98
No	8	17	16	3	0.14	0.124	0.139	18.12
No	18	15	32	3	0.1	0.165	0.142	10.77
No	9.8	8	36	14	0.126	0.128	0.136	7.95

Liquefied?	Depth (m)	N	FC (%)	CC (%)	D_{50} (mm)	a_{max} (g)	CSR	$N_{1,60}$
Yes	11.8	11	31	9	0.13	0.211	0.194	9.41
Yes	8.7	7	42	1	0.08	0.165	0.152	6.86
No	17.1	50	20	5	0.1	0.42	0.339	35.09
Yes	16.9	28	49	7	0.08	1	0.67	19.25
Yes	7.2	9	29	5	0.185	0.428	0.687	8.93
Yes	11.8	12	17	3	0.22	0.211	0.194	10.27
No	9	20	12	2	0.22	0.124	0.128	19.92
No	12	12	8	0	0.201	0.165	0.149	10.2
Yes	14.8	11	12	3	0.21	0.211	0.208	8.94
No	18.1	48	18	5	0.85	0.42	0.367	34.18
Yes	5.8	3	34	6	0.1	0.211	0.182	3.31
No	9	17	15	4	0.19	0.124	0.128	16.94
Yes	6.4	11	16	5	0.4	0.42	0.406	12.63
No	14.7	4	39	5.7	0.126	0.084	0.071	3.13
Yes	8.8	8	25	8	0.12	0.211	0.201	7.76
Yes	5	3	22	3	0.065	0.428	0.379	3.67
No	10	18	13	3	0.18	0.124	0.11	15.99
No	10.4	33	30	12	0.04	0.42	0.406	30.44
Yes	8.8	4	46	19	0.11	0.211	0.199	3.86
Yes	7.7	9	48	5	0.08	0.165	0.15	8.89
Yes	4.9	9	29	6	0.2	0.42	0.323	10.66
Yes	7.5	7	13	1	0.162	0.211	0.248	8.14
Yes	5.8	5	10	4	0.36	0.211	0.217	6.03
Yes	11.8	12	13	1	0.3	0.211	0.215	10.81
Yes	6.5	4	17	4	0.3	0.42	0.412	4.58
Yes	4	2	36	5	0.1	0.124	0.127	2.93
No	9	22	6	1	0.22	0.124	0.128	21.93
Yes	8.1	9	16	3	0.19	0.165	0.136	8.48
Yes	3	3	6	3	0.08	0.124	0.12	5
Yes	17.6	19	26	5	0.2	1	0.699	13.43
Yes	7.7	7	19	1	0.17	0.165	0.151	6.96
No	14.5	28	18	6	0.1	0.42	0.322	25.3
Yes	3	4	26	2	0.135	0.211	0.235	6.94
No	9	22	7	1	0.28	0.124	0.128	21.93
Yes	2.3	2	22	6	0.15	0.789	0.641	3.33
No	8.7	3	23	3.5	0.227	0.084	0.07	2.87
No	16	16	18	0	0.14	0.165	0.145	12.08
No	11.8	9	36	14	0.126	0.128	0.131	8.19
No	16	12	18	4	0.14	0.165	0.145	9.06
No	18.1	42	39	8	0.08	0.42	0.274	27.04

Liquefied?	Depth (m)	*N*	*FC* (%)	*CC* (%)	D_{50} (mm)	a_{max} (g)	*CSR*	$N_{1,60}$
No	7.7	4	24	4.7	0.22	0.084	0.068	3.91
No	14.3	16	33	2	0.132	0.181	0.147	11.53
No	15.6	40	39	8	0.1	0.42	0.274	28.47
No	10	12	40	7	0.08	0.124	0.13	11.54
No	18.8	9	45	4	0.11	0.181	0.13	5.5
Yes	7.3	11	21	7	0.15	0.428	0.306	9.75
No	10	22	11	2	0.19	0.124	0.124	20.78
Yes	4	12	26	0	0.11	0.428	0.362	15.78
Yes	7.2	17	18	6	0.2	0.42	0.349	17.39
Yes	3.3	6	34	8	0.11	1	0.673	8.61
Yes	3	13	45	14	0.09	0.789	0.697	19.24
No	5	16	31	7	0.13	0.124	0.127	20.52
Yes	5.7	4	30	10	0.024	0.165	0.136	4.31
Yes	5.8	6	27	5	0.195	0.428	0.659	6.44
No	6.2	5	18	7.9	0.254	0.084	0.065	5.45
Yes	4.2	3	24	5	0.2	0.789	0.378	3.58
Yes	11.7	6	48	14	0.075	0.165	0.144	4.96
No	10	22	20	4	0.19	0.124	0.134	21.24
Yes	8.2	7	17	2	0.18	0.165	0.163	7.04
No	9	14	13	3	0.18	0.124	0.135	14.12
Yes	10.8	11	20	5	0.13	0.42	0.376	9.77
No	20.3	17	30	2	0.137	0.181	0.098	8.98
No	10	23	15	4	0.22	0.124	0.128	21.98

APPENDIX-B

CPT-based post liquefaction database (Juang et al. 2003)

Table B-1. Training Data

Depth (m)	q_c (MPa)	f_s (kPa)	R_f (%)	σ_v (kPa)	σ_v' (kPa)	a_{max} (g)	M_w	Liquefied?
5.8	9.4	84.6	0.9	109.3	67.6	0.27	7.1	YES
14	1.2	31.2	2.6	271.6	151.1	0.19	7.6	No
4.1	4.3	43	1	77.9	55.9	0.25	7.1	YES
8	2.3	92	4	158.4	102.5	0.19	7.6	No
4.8	3.8	83.6	2.2	90.3	51.8	0.15	6.6	No
10.8	6.2	124	2	204.3	161.6	0.16	7.1	No
5.8	6.8	34	0.5	109.3	79.3	0.21	7.1	YES
3.2	3.3	26.4	0.8	59.9	43.4	0.55	6.6	YES
9.5	25	75	0.3	180.5	103.5	0.25	7.1	No
4.8	4.5	31.5	0.7	90.3	59.8	0.15	6.6	No
4.3	5.3	37.1	0.7	80.8	73.4	0.57	7.1	YES
5	9	27	0.3	95	63	0.25	7.1	YES
2.1	1.3	1.3	0.1	32.7	27.1	0.21	7.1	YES
4.4	8.2	24.6	0.3	83.6	54.6	0.25	7.1	YES
4.8	3.9	81.9	2.1	90.3	51.8	0.15	6.6	No
2.5	3.4	27.2	0.8	47.5	42.6	0.27	7.1	YES
3.3	6.2	24.8	0.4	62.7	50	0.27	7.1	YES
3.2	4.3	47.3	1.1	59.9	40.7	0.23	7.1	YES
11	15.5	356.5	2.3	209	119	0.37	6	No
4.2	4.9	24.5	0.5	79.8	64.8	0.25	7.1	YES
11.6	1.9	38	2	220.4	112.6	0.19	7.6	YES
9.5	12.1	36.3	0.3	180.5	116.8	0.28	7.1	No
11	15.5	356.5	2.3	209	119	0.08	6.6	No
4	4.9	122.5	2.5	76	56	0.8	6.6	YES
2.8	2.4	2.4	0.1	52.3	43.9	0.21	7.1	YES
5.7	2.2	19.8	0.9	82.4	73.4	0.53	7.1	YES
6.6	7.7	69.3	0.9	128.7	85.7	0.24	7.1	No
4.1	6.2	55.8	0.9	77.9	55.9	0.25	7.1	YES
3	3	12	0.4	57	45	0.25	7.1	YES
2.8	1.4	16.8	1.2	52.3	42.9	0.21	7.1	YES
9.3	2	22	1.1	175.8	131.1	0.53	7.1	YES

Depth (m)	q_c (MPa)	f_s (kPa)	R_f (%)	σ_v (kPa)	σ_v' (kPa)	a_{max} (g)	M_w	Liquefied?
4.1	6.4	147.2	2.3	77.9	63.3	0.37	6	YES
2	3.1	12.4	0.4	38	28	0.25	7.1	YES
4.1	6.4	147.2	2.3	77.9	63.3	0.13	6.6	No
10.3	5.5	71.5	1.3	195.7	157.5	0.53	7.1	YES
4.2	5.5	66	1.2	79.8	70	0.49	7.1	YES
8	1.7	57.8	3.4	153.6	86	0.19	7.6	No
5.8	8.1	48.6	0.6	109.3	96	0.49	7.1	YES
1.8	1.4	16.8	1.2	33.3	23.9	0.21	7.1	YES
6	2.1	16.8	0.8	114	79.7	0.16	7.1	YES
4.8	3.9	81.9	2.1	90.3	51.8	0.33	6	YES
6	2.6	85.8	3.3	116	103.5	0.5	6.4	YES
5.9	14.5	87	0.6	115.1	83.1	0.24	7.1	No
8.6	4.3	55.9	1.3	163.4	90.4	0.25	7.1	YES
4.5	3.5	31.5	0.9	84.6	55.1	0.1	6	No
10.4	2.4	96	4	198.7	116.9	0.19	7.6	No
5.8	7.5	52.5	0.7	109.3	100.9	0.53	7.1	YES
4.8	5.1	91.8	1.8	90.3	59.8	0.15	6.6	No
7.3	6.7	46.9	0.7	137.8	121.6	0.59	7.1	YES
4.8	2.9	66.7	2.3	90.3	51.8	0.33	6	YES
8.3	10.3	61.8	0.6	156.8	88.6	0.21	7.1	No
11.8	8.1	40.5	0.5	218.3	115.3	0.19	7.6	YES
4.3	5.4	37.8	0.7	80.8	55.7	0.21	7.1	YES
10.8	9.5	57	0.6	204.3	116.5	0.21	7.1	No
5.1	3.9	15.6	0.4	96	87.6	0.19	7.1	YES
2.5	10.4	20.8	0.2	47.5	40.5	0.25	7.1	No
6	3.9	66.3	1.7	111.8	56.8	0.13	7.3	YES
4.5	1.8	21.6	1.2	83.3	53.3	0.19	7.6	YES
5.8	4.6	27.6	0.6	109.3	100.9	0.57	7.1	YES
6.8	3.9	31.2	0.8	128.3	103.2	0.54	7.1	YES
4.8	4.3	43	1	90.3	59.8	0.15	6.6	No
8.3	5.4	108	2	156.8	105.3	0.53	7.1	YES
2.4	2.2	8.8	0.4	45.6	39.7	0.21	7.1	YES
5.4	5	35	0.7	101.7	89.4	0.56	7.1	YES
6.5	5.8	121.8	2.1	123.5	73.5	0.55	6.6	YES
2.8	2.6	20.8	0.8	53.2	46.3	0.38	7.1	YES
2.9	5.1	10.2	0.2	55.1	39.1	0.25	7.1	YES
2.6	2.2	17.6	0.8	48.5	40.1	0.23	7.1	YES
13	6.6	330	5	253.5	181.5	0.5	6.4	No
3.7	1.8	14.4	0.8	70.8	55.1	0.21	7.1	YES
5	1.1	40.7	3.7	97	62.7	0.19	7.6	No

Depth (m)	q_c (MPa)	f_s (kPa)	R_f (%)	σ_v (kPa)	σ_v' (kPa)	a_{max} (g)	M_w	Liquefied?
2.8	12.8	51.2	0.4	52.3	35.1	0.32	7.1	No
2.7	1	1	0.1	42.1	33.1	0.21	7.1	YES
4	2	56	2.8	76	56	0.8	6.6	YES
3	1.4	14	1	57	47	0.29	6	YES
11	6.4	76.8	1.2	209	119	0.37	6	No
13.7	12.9	451.5	3.5	267.2	215.2	0.5	6.4	No
11	9.1	218.4	2.4	209	119	0.08	6.6	No
6.8	20.8	62.4	0.3	129.2	79.2	0.25	7.1	No
13.1	7.5	337.5	4.5	254.5	171	0.5	6.4	No
2.6	10	20	0.2	49.4	40.4	0.25	7.1	No
3.3	1	5	0.5	57.5	32.5	0.21	7.1	YES
2.5	1.6	16	1	46.3	36.3	0.19	7.6	YES
5.3	15.2	60.8	0.4	103.4	77.4	0.24	7.1	No
11	6.4	134.4	2.1	209	119	0.08	6.6	No
2.2	12.6	50.4	0.4	40.9	29.6	0.32	7.1	No
10.2	1.8	54	3	196.9	116.5	0.19	7.6	No
8.3	4.3	77.4	1.8	157.7	88.7	0.25	7.1	YES
10.3	8.5	42.5	0.5	194.8	144.2	0.55	7.1	YES
2.5	7.5	30	0.4	46.6	39.2	0.21	7.1	No
5.8	10.5	42	0.4	109.3	99.9	0.54	7.1	YES
6.8	11.8	59	0.5	128.3	95.4	0.32	7.1	No
6	6.4	25.6	0.4	114	84.6	0.28	7.1	YES
8.8	4.2	67.2	1.6	166.3	139.3	0.55	7.1	YES
7.3	5.7	39.9	0.7	137.8	115.7	0.5	7.1	YES
5.5	1.9	3.8	0.2	104.5	77.5	0.25	7.1	YES
4.6	3.5	24.5	0.7	86.5	62.4	0.21	7.1	YES
3.3	8.6	43	0.5	64.4	58.4	0.24	7.1	No
14	13.7	27.4	0.2	259	134	0.19	7.6	No
6.5	5.1	20.4	0.4	121.2	66.2	0.13	7.3	YES
6.2	4.5	40.5	0.9	117.8	109	0.49	7.1	YES
3.9	11.7	35.1	0.3	74.1	53.1	0.25	7.1	No
4.4	5.9	64.9	1.1	82.7	65.6	0.13	6.6	No
2.5	8.7	34.8	0.4	47.5	39.5	0.25	7.1	No
4	2.3	55.2	2.4	76	56	0.08	6.6	No
4.4	5.9	64.9	1.1	82.7	65.6	0.37	6	YES
4.8	4.8	33.6	0.7	90.3	51.8	0.15	6.6	No
4	16.4	49.2	0.3	76	70	0.25	7.1	No
4.7	9.2	27.6	0.3	89.3	79.3	0.25	7.1	No
2.8	1.9	22.8	1.2	54.6	50.6	0.24	7.1	YES
7.5	1.7	83.3	4.9	142.5	82.7	0.19	7.6	No

Depth (m)	q_c (MPa)	f_s (kPa)	R_f (%)	σ_v (kPa)	σ_v' (kPa)	a_{max} (g)	M_w	Liquefied?
5.3	3.6	32.4	0.9	100.7	78.1	0.56	7.1	YES
9.8	3.8	53.2	1.4	186.2	110.2	0.25	7.1	YES
5.8	6.8	27.2	0.4	111	87.4	0.21	7.1	YES
6	2.2	22	1	114	79.7	0.16	7.1	YES
2.5	5.5	82.5	1.5	47.5	42.5	0.29	6	No
3	3.8	19	0.5	57	45	0.25	7.1	YES
14.1	6.8	333.2	4.9	274	173.5	0.5	6.4	No
3.4	8.5	8.5	0.1	64.6	49.6	0.25	7.1	No
4.8	5.9	23.6	0.4	90.3	51.8	0.33	6	YES
7.3	4.5	18	0.4	114.7	86.4	0.53	7.1	YES
4.5	4.2	54.6	1.3	85.5	60.5	0.18	6.6	YES
11	6.4	134.4	2.1	209	119	0.37	6	No
9.8	1.1	12.1	1.1	185.3	134.7	0.53	7.1	YES
4.1	9.4	9.4	0.1	77.9	59.9	0.25	7.1	No
8	3.3	49.5	1.5	149	76.5	0.13	7.3	YES
3	4.3	17.2	0.4	56.1	47.7	0.21	7.1	YES
7	8.5	59.5	0.7	133	84	0.28	7.1	YES
7.3	5.5	115.5	2.1	137.8	129.4	0.16	7.1	No
3.5	1.5	28.5	1.9	64.8	49.8	0.43	7.6	YES
5	2.2	24.2	1.1	92.5	57.5	0.19	7.6	YES
8.2	6.9	117.3	1.7	158.8	101.9	0.17	7.1	No
4.8	5.1	45.9	0.9	90.3	59.8	0.15	6.6	No
5	15.5	46.5	0.3	95	57.7	0.23	7.1	No
2.3	2.8	14	0.5	42.8	35.4	0.23	7.1	YES
11	9.1	218.4	2.4	209	119	0.37	6	No
4.8	3.8	83.6	2.2	90.3	51.8	0.33	6	YES
3.8	4.3	30.1	0.7	71.3	58	0.38	7.1	YES
2	8.3	33.2	0.4	37.1	28.7	0.32	7.1	No
4.9	1.1	25.3	2.3	99.8	62.6	0.19	7.6	YES
5.8	4.8	24	0.5	111.3	83.8	0.21	7.1	YES
6.8	7.4	51.8	0.7	128.3	96.4	0.56	7.1	YES
4.5	4.2	54.6	1.3	85.5	60.5	0.29	6	YES
1.4	3	12	0.4	26.6	26.6	0.25	7.1	YES
12.7	6.2	37.2	0.6	235.5	118.5	0.13	7.3	No
3.2	1.2	22.8	1.9	62.4	43.8	0.19	7.6	YES
2.5	7.7	23.1	0.3	47.5	40.5	0.25	7.1	YES
4.1	13	26	0.2	77.9	62.9	0.25	7.1	No
3.5	15.5	31	0.2	66.5	49.5	0.25	7.1	No
2.1	1	8	0.8	28.4	22.5	0.21	7.1	YES
2.7	4.9	63.7	1.3	51.3	39.5	0.69	7.1	YES

Table B-2. Testing Data

Depth (m)	q_c (MPa)	f_s (kPa)	R_f (%)	σ_v (kPa)	σ_v' (kPa)	a_{max} (g)	M_w	Liquefied?
4.8	5.2	104	2	90.3	51.8	0.33	6	YES
4.8	4.5	31.5	0.7	90.3	59.8	0.33	6	YES
3.8	1.9	45.6	2.4	72.4	45.4	0.19	7.6	YES
12.2	1.6	43.2	2.7	234.2	132.3	0.19	7.6	No
4.8	5.2	104	2	90.3	51.8	0.15	6.6	No
3.5	1.4	37.8	2.7	69.7	53	0.19	7.6	No
8.5	1.2	37.2	3.1	158.1	88.5	0.19	7.6	No
2.5	5.5	82.5	1.5	47.5	42.5	0.18	6.6	No
9.8	8.6	129	1.5	187.7	145.5	0.17	7.1	No
3.4	3.1	12.4	0.4	63.7	55.3	0.21	7.1	YES
4.3	4.6	27.6	0.6	80.8	62.6	0.38	7.1	YES
4.8	3.2	38.4	1.2	91.2	58.2	0.55	6.6	YES
7.3	7.7	30.8	0.4	140.7	98.5	0.21	7.1	YES
4.3	4.3	25.8	0.6	80.8	57.7	0.21	7.1	YES
2.5	10.5	52.5	0.5	47.5	37.7	0.32	7.1	No
5.8	4.1	36.9	0.9	109.3	65.6	0.21	7.1	YES
3.2	3.3	26.4	0.8	59.9	43.4	0.1	6	No
6.5	1.1	28.6	2.6	125.3	68	0.19	7.6	YES
4.7	9	108	1.2	89.3	68.7	0.13	6.6	No
5.6	4.8	43.2	0.9	105.5	98.1	0.19	7.1	YES
2.9	6.6	19.8	0.3	55.1	38.1	0.25	7.1	YES
4.8	5.9	23.6	0.4	90.3	51.8	0.15	6.6	No
2.2	3.1	12.4	0.4	41.8	29.8	0.25	7.1	YES
3.9	7.2	72	1	73.2	61.1	0.37	6	YES
8	20	60	0.3	152	90	0.25	7.1	No
3.6	4.1	41	1	67.5	59.1	0.21	7.1	YES
3.9	7.2	72	1	73.2	61.1	0.13	6.6	No
6.5	5.8	121.8	2.1	123.5	73.5	0.1	6	No
4	2.3	55.2	2.4	76	56	0.37	6	YES
6.5	18.2	36.4	0.2	123.5	75.5	0.25	7.1	No
3.6	7.8	7.8	0.1	68.4	44.4	0.25	7.1	YES
4.8	5.1	45.9	0.9	90.3	59.8	0.33	6	YES
5	6.9	158.7	2.3	95	45	0.2	6.6	No
3	4.7	28.2	0.6	58.5	51.5	0.24	7.1	No
4.5	3.5	31.5	0.9	84.6	55.1	0.55	6.6	YES
6	3.9	19.5	0.5	99.8	79	0.53	7.1	YES
9.3	5	85	1.7	175.8	117.4	0.56	7.1	YES

Depth (m)	q_c (Mpa)	f_s (kPa)	R_f (%)	σ_v (kPa)	σ_v' (kPa)	a_{max} (g)	M_w	Liquefied?
3.7	7.9	31.6	0.4	70.4	59.7	0.22	7.1	No
4.8	5.1	91.8	1.8	90.3	59.8	0.33	6	YES
6.6	8	40	0.5	124.5	107.3	0.54	7.1	YES
2.1	2.5	5	0.2	39.9	33.9	0.25	7.1	YES
5.6	2.3	48.3	2.1	112	86.5	0.43	7.6	YES
11	6.4	76.8	1.2	209	119	0.08	6.6	No
7.3	4	40	1	116.3	96.9	0.49	7.1	YES
4.4	5.4	21.6	0.4	83.6	65.6	0.25	7.1	YES
6.2	7.2	57.6	0.8	117.8	101.1	0.49	7.1	YES
4.4	7.7	46.2	0.6	82.7	69.4	0.56	7.1	YES
4.8	2.9	66.7	2.3	90.3	51.8	0.15	6.6	No
4	1.9	70.3	3.7	76	56	0.08	6.6	No
9.5	19.4	562.6	2.9	185.3	149.3	0.5	6.4	No
2.8	2.8	11.2	0.4	52.3	42.9	0.21	7.1	YES
13.5	16.3	130.4	0.8	249.8	134.8	0.43	7.6	No
7.3	6.1	115.9	1.9	137.8	129.4	0.16	7.1	No
6.8	3.7	22.2	0.6	128.3	118	0.53	7.1	YES
5.9	1.3	11.7	0.9	115.1	85.1	0.24	7.1	YES
6.9	7	35	0.5	131.1	109.5	0.53	7.1	YES
4.8	4.8	33.6	0.7	90.3	51.8	0.33	6	YES
3	1.4	14	1	57	47	0.18	6.6	YES
5.1	2.4	64.8	2.7	96.9	61.6	0.19	7.6	No
1.9	10.4	31.2	0.3	36.1	34.1	0.25	7.1	No
2.8	0.9	44.1	4.9	52.3	34.1	0.38	7.1	No
4.8	4.3	43	1	90.3	59.8	0.33	6	YES
4.2	10.1	121.2	1.2	78.9	63.8	0.37	6	No
3.1	7.2	28.8	0.4	60.5	56.5	0.24	7.1	No
1.9	8.4	16.8	0.2	36.1	32.1	0.25	7.1	No
3.3	2.3	39.1	1.7	61.8	53.4	0.38	7.1	YES
4.7	4.1	24.6	0.6	89.3	72.3	0.25	7.1	YES
6.3	4.1	20.5	0.5	119.7	77.5	0.28	7.1	YES
8.4	5.9	29.5	0.5	172.2	143.2	0.24	7.1	No
3	1.4	18.2	1.3	55.9	35.9	0.13	7.3	YES
2.4	1	52	5.2	45.4	37.5	0.19	7.6	No
11	4.6	46	1	209	123	0.25	7.1	YES
7.2	5.7	28.5	0.5	136.8	99.5	0.21	7.1	YES
4.8	3.2	38.4	1.2	91.2	58.2	0.1	6	No
4.2	10.1	121.2	1.2	78.9	63.8	0.13	6.6	No

APPENDIX-C

Post liquefaction SPT-based data (Cetin 2000) used for reliability analysis

Table C-1. Training Data

Mean Depth (m)	Mean σ_v (kPa)	COV σ_v	Mean σ_v' (kPa)	COV σ_v'	Mean a_{max} *(g)*	COV	Mean N_m	COV N_m	Mean M_w	COV M_w	Mean *FC* (%)	COV *FC*	C_R	C_S	C_B	C_E	Liquefied?
4.2	69.61	0.149	51.85	0.107	0.24	0.2	6	0.333	7.4	-	10	0.2	0.8	1	1	1.09	Yes
5.2	89.15	0.085	57.29	0.084	0.4	0.1	11.7	0.248	8	-	2	0.5	0.85	1	1	1.22	Yes
3	49.07	0.118	22.22	0.139	0.24	0.2	7	0.229	7.4	-	12	0.167	0.73	1	1	1	Yes
4.5	73.26	0.078	46.37	0.08	0.2	0.075	6	0.017	7.4	-	50	0.1	0.82	1	1	0.75	Yes
3.7	58.83	0.217	36.28	0.164	0.2	0.2	3.7	0.189	7.4	-	10	0.2	0.77	1	1	1.09	Yes
4.7	72.78	0.157	35.43	0.189	0.17	0.265	7.8	0.449	6.5	0.02	40	0.075	0.83	1	1	1.05	No
6	102.7	0.123	67.73	0.103	0.24	0.2	9.9	0.424	7.4	-	10	0.2	0.88	1	1	1.09	No
9.9	184.6	0.179	135.57	0.126	0.4	0.1	17.5	0.154	6.9	0.016	20	0.25	1	1	1	1.22	No
3.5	53.89	0.057	44.04	0.073	0.26	0.096	13	0.238	7	0.017	3	0.333	0.76	1	1	1	Yes
8.5	137.8	0.105	69.39	0.109	0.1	0.2	9.5	0.158	7.3	0.015	5	0.4	0.95	1	1	1	Yes
5.5	90	0.095	45.05	0.109	0.095	0.011	4.6	0.087	6.1	-	13	0.077	0.86	1	1	1.09	No
11.4	211	0.054	116.24	0.068	0.18	0.15	24.7	0.121	7.5	0.015	8	0.25	1	1	1	1.21	No
6.2	112.6	0.04	93.48	0.044	0.54	0.074	10.3	0.155	6.7	0.019	38	0.605	0.89	1	1	1.13	Yes
3.2	52.82	0.133	30.77	0.137	0.09	0.2	2.7	0.556	7.5	0.015	5	0.4	0.74	1	1	1.22	Yes
10.7	200.1	0.106	110.44	0.106	0.4	0.1	26	0.096	8	-	0	0	1	1	1	1.22	No
2.4	38.18	0.093	27.02	0.113	0.24	0.2	11.5	0.191	7.4	-	7	0.143	0.68	1	1	1.12	Yes
6.5	117.4	0.036	83.12	0.053	0.22	0.045	13	0.315	7	0.017	5	0.2	0.9	1.1	1	0.92	Yes
6	82.08	0.066	57.57	0.072	0.165	0.079	4	0.35	7	0.017	25	0.2	0.88	1.1	1	0.92	Yes

Mean Depth (m)	Mean σ_v (kPa)	COV σ_v	Mean σ_v' (kPa)	COV σ_v'	Mean a_{max} *(g)*	COV	Mean N_m	COV N_m	Mean M_w	COV M_w	Mean *FC* (%)	COV *FC*	C_R	C_S	C_B	C_E	Liquefied?
8.9	159.8	0.043	142.12	0.049	0.693	0.087	20	0.22	6.7	0.019	43	0.302	0.97	1	1	1.13	Yes
7.9	129.6	0.194	66.05	0.169	0.13	0.2	8.4	0.19	7.3	0.015	67	0.104	0.94	1	1	0.83	Yes
7.9	143.2	0.137	88.63	0.121	0.24	0.2	19.3	0.13	7.4	-	5	0.2	0.94	1	1	1.21	No
2.7	44.57	0.28	22.52	0.257	0.12	0.2	4.6	0.348	6.7	-	5	0.2	0.71	1	1	1	Yes
5	84.97	0.206	44.91	0.185	0.1	0.2	8.8	0.318	6.7	-	0	0	0.84	1	1	1.09	No
3.7	60.52	0.162	32.09	0.156	0.24	0.2	8.8	0.42	7.4	-	0	0	0.77	1	1	1	Yes
3.7	58.83	0.217	36.28	0.164	0.12	0.2	3.7	0.189	6.7	-	10	0.2	0.77	1	1	1.09	No
5.5	97.24	0.069	52.15	0.089	0.35	0.2	18.1	0.088	8	0.011	20	0.15	0.86	1	1	1	Yes
2.5	35.74	0.089	30.84	0.113	0.18	0.111	10.9	0.202	6.7	0.019	30	0.167	0.69	1	1	1.05	No
5.7	94.84	0.108	38.48	0.153	0.116	0.155	8.9	0.079	7.7	0.013	3	0.333	0.87	1	1	1.22	Yes
2.9	45.74	0.238	25.71	0.207	0.2	0.2	5.6	0.143	7.9	-	20	0.15	0.72	1	1	1.17	Yes
8.5	155.1	0.15	120.82	0.102	0.4	0.1	19.7	0.142	6.9	0.016	20	0.25	0.95	1	1	1.22	No
7.7	146.5	0.24	94.08	0.192	0.34	0.029	5.7	0.246	6.9	0.016	20	0.25	0.93	1	1	1.22	Yes
4.7	84.15	0.096	40.83	0.196	0.19	0.105	21	0.024	6.7	0.019	18	0.167	0.83	1	1	1.05	No
3.5	61.66	0.206	38.13	0.171	0.22	0.2	19.7	0.157	8	0.011	5	0.6	0.76	1	1	1	No
4.5	72.31	0.118	40.16	0.118	0.13	0.2	9.5	0.263	8	0.011	12	0.25	0.81	1	1	1	Yes
4.5	65.59	0.117	41.08	0.102	0.09	0.278	4.5	0.778	6.2	0.023	75	0.133	0.81	1	1	1.05	No
7.2	127.4	0.156	78.84	0.126	0.25	0.1	20	0.205	7.6	-	19	0.105	0.92	1	1	0.65	Yes
3.5	53.41	0.065	48.51	0.053	0.28	0.2	11	0.245	7.4	-	5	0.4	0.76	1	1	1	Yes
2	30.93	0.257	16.28	0.256	0.2	0.3	1.8	0.333	8	-	27	0.111	0.64	1	1	1.17	Yes
3	49.72	0.12	29.14	0.126	0.32	0.2	15.5	0.31	7.4	-	4	0.25	0.73	1	1	1.12	No
4.6	68.04	0.099	57.01	0.1	0.14	0.093	4.6	0.717	7	0.017	30	0.233	0.82	1.1	1	0.92	No
2.4	41.9	0.223	26.96	0.188	0.225	0.111	14.4	0.153	7.9	-	5	0.4	0.68	1	1	1.21	No
2.6	41.67	0.181	28.44	0.144	0.32	0.2	5.2	0.385	7.4	-	4	0.25	0.7	1	1	1	Yes
5.7	94.84	0.108	38.48	0.153	0.213	0.141	8.9	0.079	7.8	-	3	0.333	0.87	1	1	1.22	Yes

Mean Depth (m)	Mean σ_v (kPa)	COV σ_v	Mean σ_v' (kPa)	COV σ_v'	Mean a_{max} *(g)*	COV	Mean N_m	COV N_m	Mean M_w	COV M_w	Mean *FC* (%)	COV *FC*	C_R	C_S	C_B	C_E	Liquefied?
6	87.58	0.066	63.07	0.067	0.13	0.1	4	0.35	7	0.017	25	0.12	0.88	1.1	1	0.92	Yes
4.5	75.4	0.089	60.7	0.069	0.5	0.2	29.4	0.139	8	0.011	10	0.2	0.81	1	1	1	No
4.2	66.67	0.115	54.66	0.142	0.28	0.2	13.2	0.424	7.4	-	0	0	0.8	1	1	1.21	No
3.6	57.38	0.18	39.24	0.13	0.12	0.2	2	0.4	6.7	-	60	0.083	0.77	1	1	1	No
5.3	81.54	0.073	70.93	0.086	0.45	0.1	3.4	0.265	6.6	-	55	0.091	0.85	1	1	1.13	Yes
6.6	96.57	0.071	87.5	0.085	0.46	0.109	10.2	0.363	7	0.017	27	0.185	0.9	1	1	1.13	Yes
6	101.6	0.093	63.9	0.084	0.24	0.2	21	0.09	7.4	-		0	0.88	1	1	1.12	No
3.3	51.47	0.188	33.55	0.142	0.09	0.256	5.9	0.288	5.9	0.025	31	0.097	0.75	1	1	1.05	No
4.5	65.59	0.117	41.08	0.102	0.17	0.118	4.5	0.778	5.9	0.025	75	0.133	0.81	1	1	1.05	Yes
7.5	123.1	0.226	53.4	0.23	0.227	0.154	7.6	0.224	7.7	0.013	1	1	0.93	1	1	1.22	Yes
4.2	66.08	0.131	51.14	0.091	0.13	0.077	6.4	0.516	6.5	0.02	92	0.109	0.8	1	1	1.05	No
4.7	72.78	0.147	35.43	0.148	0.1	0.05	7.8	0.449	6.2	0.023	40	0.075	0.83	1	1	1.05	No
3.6	57.38	0.18	39.24	0.13	0.24	0.2	2	0.4	7.4	-	60	0.083	0.77	1	1	1	Yes
9.2	158.3	0.056	77.4	0.085	0.15	0.2	13.1	0.229	7.1	-	0	0	0.97	1	1	1.22	No
9.5	174.8	0.17	130.65	0.119	0.4	0.1	30.2	0.235	6.9	0.016	20	0.25	0.98	1	1	1.22	No
3	49.07	0.118	22.22	0.139	0.12	0.2	7	0.229	6.7	-	12	0.167	0.73	1	1	1	No
4.5	76.85	0.124	55.93	0.097	0.24	0.2	11.9	0.227	7.4	-	26	0.192	0.82	1	1	1.09	No
2.5	39.27	0.092	34.37	0.078	0.24	0.104	17.9	0.173	7	0.017	1	2	0.69	1	1	1	No
3.4	54.08	0.172	37.9	0.225	0.47	0.106	10.6	0.302	6.5	0.02	37	0.135	0.76	1	1	1.13	No
4.1	68.41	0.205	45.87	0.15	0.27	0.093	15	0.22	7	0.017	1	2	0.79	1	1	1	No
3.5	53.57	0.169	36.9	0.125	0.29	0.086	6.1	0.557	7	0.017	2	1	0.76	1	1	1	Yes
5.2	85.16	0.123	42.66	0.146	0.16	0.15	7.9	0.177	7.5	0.015	8	0.25	0.85	1	1	1.09	Yes
6	82.08	0.119	57.57	0.084	0.15	0.087	3.9	0.487	7	0.017	50	0.1	0.88	1.1	1	0.92	Yes
5.5	104.4	0.155	71.52	0.122	0.225	0.111	25.5	0.067	7.9	-	5	0.4	0.86	1	1	1.21	No
3.5	54.98	0.153	37.83	0.118	0.25	0.22	9.7	0.227	7.7	0.013	1	1	0.76	1	1	1.22	Yes

Mean Depth (m)	Mean σ_v (kPa)	COV σ_v	Mean σ_v' (kPa)	COV σ_v'	Mean a_{max} *(g)*	COV	Mean N_m	COV N_m	Mean M_w	COV M_w	Mean *FC* (%)	COV *FC*	C_R	C_S	C_B	C_E	Liquefied?
4.5	73.01	0.15	53.9	0.103	0.24	0.104	15.7	0.204	7	0.017	1	2	0.82	1	1	1	Yes
3.7	60.52	0.162	32.09	0.156	0.12	0.2	8.8	0.42	6.7	-	0	0	0.77	1	1	1	No
6.5	123.3	0.051	113.51	0.087	0.24	0.1	37	0.038	7	0.017	7	0.286	0.9	1.2	1	0.92	No
7.5	122.3	0.124	57.72	0.152	0.16	0.15	9.4	0.16	7.5	0.015	8	0.25	0.93	1	1	1.09	Yes
11.4	210.5	0.225	136.98	0.171	0.34	0.118	11.6	0.31	6.9	0.016	20	0.25	1	1	1	1.22	Yes
5.2	88.44	0.119	71.78	0.081	0.4	0.125	20.7	0.454	6.9	0.016	18	0.222	0.85	1	1	1.22	No
7	117.4	0.108	63.66	0.119	0.2	0.2	12.4	0.056	7.3	0.015	48	0.104	0.91	1	1	1	Yes
4.2	66.08	0.142	51.14	0.179	0.19	0.132	6.4	0.516	5.9	0.025	92	0.109	0.8	1	1	1.05	Yes
3.5	56	0.199	32.48	0.166	0.22	0.2	5.9	0.136	8	0.011	3	0.667	0.76	1	1	1	Yes
4.7	82.08	0.128	35.52	0.165	0.25	0.16	8.5	0.247	6.9	0.016	20	0.35	0.83	1	1	1.22	Yes
2.7	44.57	0.28	22.52	0.257	0.32	0.2	4.1	0.39	7.4	-	5	0.2	0.71	1	1	1	Yes
8.2	131.4	0.031	95.58	0.046	0.2	0.075	9	0.233	7.4	-	20	0.15	0.95	1	1	0.75	Yes
7.9	130.5	0.137	61.06	0.161	0.16	0.15	8.8	0.25	7.5	0.015	8	0.25	0.94	1	1	1.09	Yes
4.2	66.08	0.131	51.14	0.091	0.174	0.115	6.4	0.516	6.7	0.019	92	0.109	0.8	1	1	1.05	No
4.2	69.32	0.26	37.46	0.215	0.2	0.2	4.8	0.583	7.7	0.013	15	0.267	0.8	1	1	1.22	Yes
7.5	131.4	0.082	70.63	0.106	0.24	0.2	20.5	0.215	7.4	-	17	0.176	0.93	1	1	1.12	No
9.9	183.8	0.139	115.18	0.115	0.34	0.118	9.5	0.137	6.9	0.016	20	0.25	1	1	1	1.22	Yes
1.1	15.47	0.243	8.14	0.378	0.16	0.281	5.8	0.241	6.5	0.02	80	0.125	0.5	1	1	1.05	Yes
3.3	51.47	0.188	33.55	0.142	0.51	0.098	5.9	0.288	6.5	0.02	31	0.097	0.75	1	1	1.05	Yes
6	108.3	0.066	61.46	0.077	0.18	0.15	30	0.097	7.5	0.015	0	0	0.88	1	1	1.21	No
4.9	85.81	0.181	59.83	0.13	0.25	0.1	34.2	0.216	7.6	-	19	0.105	0.84	1	1	0.65	No
4.2	69.61	0.149	51.85	0.107	0.14	0.171	6	0.483	6.7	-	10	0.2	0.8	1	1	1.09	No
2.9	49.88	0.163	39.1	0.169	0.156	0.128	26.4	0.394	6.7	0.019	25	0.16	0.72	1	1	1.13	No
4.2	71.87	0.067	40.01	0.095	0.2	0.2	10.4	0.538	8	0.011	5	0.6	0.8	1	1	1	Yes
1.1	15.47	0.243	8.14	0.378	0.19	0.105	5.8	0.241	6.7	0.019	80	0.125	0.5	1	1	1.05	No

Mean Depth (m)	Mean σ_v (kPa)	COV σ_v	Mean σ_v' (kPa)	COV σ_v'	Mean a_{max} *(g)*	COV	Mean N_m	COV N_m	Mean M_w	COV M_w	Mean *FC* (%)	COV *FC*	C_R	C_S	C_B	C_E	Liquefied?
6.2	117.8	0.048	85.96	0.057	0.25	0.04	6	0.65	7	0.017	8	0.375	0.89	1.1	1	0.92	Yes
3.7	61.59	0.214	24.99	0.231	0.16	0.15	3.9	0.179	7.5	0.015	10	0.3	0.77	1	1	1.09	Yes
7.9	141.6	0.053	98	0.054	0.4	0.125	25.9	0.193	6.9	0.016	2	0.5	0.94	1	1	1.22	No
4.7	72.78	0.148	35.43	0.249	0.23	0.087	7.8	0.449	5.9	0.025	40	0.075	0.83	1	1	1.05	Yes
5.9	91.33	0.119	74.9	0.114	0.14	0.171	9	0.2	6.7	-	5	0.6	0.88	1	1	1	No
12.1	165.6	0.187	78.98	0.155	0.135	0.111	13	0.269	7.5	-	3	0.333	1	1	1	0.75	No
4.5	73.95	0.153	33.27	0.176	0.12	0.183	7.7	0.091	7.1	-	0	0	0.81	1	1	1.22	Yes
7	115.4	0.084	92.84	0.062	0.41	0.122	20	0.165	7	0.017	13	0.154	0.91	1	1	1.13	Yes
9.1	129	0.238	54.35	0.213	0.135	0.111	4.3	0.302	7.5	-	3	0.333	0.97	1	1	0.75	Yes
6.5	98.26	0.086	82.58	0.063	0.46	0.109	9	0.1	7	0.017	15	0.133	0.9	1	1	1.13	Yes
4.5	65.59	0.117	41.08	0.102	0.2	0.2	4.5	0.778	6.6	0.02	75	0.133	0.81	1	1	1.05	No
3.2	52.33	0.089	44.37	0.08	0.14	0.2	9	0.233	6.7	-	20	0.15	0.74	1	1	1.09	No
7.5	135.6	0.119	80.04	0.108	0.18	0.15	17.5	0.063	7.5	0.015	8	0.25	0.93	1	1	1.21	No
4.7	80.68	0.066	37.36	0.105	0.17	0.118	21	0.024	5.9	0.025	18	0.167	0.83	1	1	1.05	No
9.2	172.4	0.045	120	0.048	0.51	0.118	24.4	0.123	6.7	0.019	25	0.2	0.97	1	1	1.13	Yes
4.2	133.4	0.122	105.94	0.072	0.2	0.2	23.3	0.094	7.4	-	10	0.2	0.8	1	1	1.21	No
4.2	69.32	0.26	37.46	0.215	0.15	0.2	4.8	0.583	7.1	-	15	0.267	0.8	1	1	1.22	No
4	65.91	0.183	32.15	0.211	0.225	0.111	4.5	0.156	7.9	-	5	0.4	0.79	1	1	1.09	Yes
3	47.6	0.144	34.39	0.115	0.24	0.2	4.3	0.581	7.4	-	10	0.2	0.73	1	1	1	Yes
4.5	65.59	0.118	41.08	0.104	0.18	0.106	4.5	0.778	6.5	0.02	75	0.133	0.81	1	1	1.05	Yes
3.3	53.17	0.224	32.21	0.175	0.4	0.3	3.6	0.278	7.3		0	0	0.75	1	1	1.17	Yes
4.7	72.78	0.147	35.43	0.148	0.18	0.028	7.8	0.449	6.6	0.02	40	0.075	0.83	1	1	1.05	Yes
3.5	53.06	0.157	38.2	0.123	0.2	0.3	6	0.333	8	-	13	0.077	0.76	1	1	1.17	Yes
1.7	26.7	0.15	19.35	0.166	0.25	0.1	6.5	0.062	7	0.017	35	0.143	0.61	1	1	1	Yes
6	86.4	0.12	66.79	0.078	0.42	0.119	8	0.45	7	0.017	22	0.136	0.88	1	1	1.13	Yes

Mean Depth (m)	Mean σ_v (kPa)	COV σ_v	Mean σ_v' (kPa)	COV σ_v'	Mean a_{max} *(g)*	COV	Mean N_m	COV N_m	Mean M_w	COV M_w	Mean *FC* (%)	COV *FC*	C_R	C_S	C_B	C_E	Liquefied?
4.2	65.12	0.154	47.19	0.114	0.2	0.3	1.5	0.4	8	-	25	0.12	0.8	1	1	1.17	Yes
3.9	61.38	0.144	46.19	0.183	0.24	0.104	10.2	0.039	7	0.017	3	0.333	0.79	1	1	1	Yes

Table C-2. Testing Data

Mean Depth (m)	Mean σ_v (kPa)	COV σ_v	Mean σ_v' (kPa)	COV σ_v'	Mean a_{max} *(g)*	COV	Mean N_m	COV N_m	Mean M_w	COV M_w	Mean *FC* (%)	COV *FC*	C_R	C_S	C_B	C_E	Liquefied?
6	86.01	0.091	71.3	0.145	0.37	0.135	9	0.244	7	0.017	8	0.25	0.88	1	1	1.13	Yes
5	81.53	0.076	38.4	0.114	0.16	0.15	4.4	0.364	7.5	0.015	0	0	0.84	1	1	1.09	Yes
20.4	383.9	0.04	198.66	0.065	0.4	0.1	8.5	0.259	8	-	10	0.3	1	1	1	1.22	Yes
7.5	140	0.071	95.86	0.068	0.25	0.04	12	0.425	7	0.017	10	0.1	0.93	1.1	1	0.92	Yes
7.5	137.9	0.168	103.54	0.117	0.4	0.125	14.5	0.407	6.9	0.016	25	0.2	0.93	1	1	1.22	Yes
3.4	54.08	0.179	37.9	0.235	0.13	0.154	10.6	0.302	6.7	0.019	37	0.135	0.76	1	1	1.13	No
14.4	238.5	0.044	105.28	0.074	0.095	0.011	3.6	0.167	6.1	-	27	0.037	1	1	1	1.09	No
4.5	73.95	0.153	33.27	0.176	0.278	0.144	7.7	0.091	7.7	0.013	0	0	0.81	1	1	1.22	Yes
8.7	152.6	0.056	101.11	0.058	0.4	0.125	11	0.236	6.9	0.016	2	0.5	0.96	1	1	1.22	Yes
2.5	35.74	0.075	30.84	0.099	0.16	0.125	10.9	0.183	5.9	0.025	30	0.167	0.69	1	1	1.05	No
6.5	106.4	0.142	67.22	0.119	0.18	0.15	12	0.25	7.5	0.015	0	0	0.9	1	1	1.09	No
4.2	71.34	0.158	53.42	0.112	0.24	0.2	9.6	0.448	7.4	-	3	0.333	0.8	1	1	1.09	Yes
3	47.6	0.144	34.39	0.115	0.12	0.2	4.3	0.581	6.7	-	10	0.2	0.73	1	1	1	No

Mean Depth (m)	Mean σ_v (kPa)	COV σ_v	Mean σ_v' (kPa)	COV σ_v'	Mean a_{max} *(g)*	COV	Mean N_m	COV N_m	Mean M_w	COV M_w	Mean *FC* (%)	COV *FC*	C_R	C_S	C_B	C_E	Liquefied?
2.5	35.74	0.079	30.84	0.102	0.16	0.119	10.9	0.202	6.5	0.02	30	0.167	0.69	1	1	1.05	No
2.4	39.26	0.182	27.31	0.144	0.2	0.075	13.9	0.007	7.4	-	4	0.375	0.68	1	1	0.75	No
3.2	47.09	0.157	32.88	0.266	0.47	0.106	2.7	0.815	6.5	0.02	29	0.155	0.74	1	1	1.13	Yes
4.2	71.34	0.158	53.42	0.112	0.14	0.2	9.6	0.448	6.7	-	3	0.333	0.8	1	1	1.09	No
6.2	94.92	0.072	84.47	0.077	0.45	0.1	7.2	0.333	6.6	-	50	0.1	0.89	1	1	1.13	Yes
5	84.97	0.206	44.91	0.185	0.2	0.2	8.8	0.318	7.4	-	0	0	0.84	1	1	1.09	Yes
3.2	47.09	0.166	32.88	0.276	0.15	0.133	2.7	0.815	6.7	0.019	29	0.155	0.74	1	1	1.13	No
11.6	181.8	0.052	133.22	0.05	0.2	0.075	11.4	0.14	7.4	-	20	0.15	1	1	1	0.75	Yes
7.9	132.2	0.197	90.83	0.143	0.35	0.3	16.1	0.155	7.3	-	4	0.25	0.94	1	1	1.3	Yes
8.5	124.5	0.068	70.58	0.077	0.41	0.122	18.5	0.151	7	0.017	20	0.15	0.95	1	1	1.13	Yes
8.3	104.3	0.186	63.97	0.121	0.135	0.111	14.9	0.154	7.5	-	3	0.333	0.95	1	1	0.75	No
4.7	83.3	0.095	47.19	0.101	0.2	0.2	9.8	0.204	8	0.011	12	0.25	0.83	1	1	1	Yes
3.5	53.41	0.065	48.51	0.053	0.14	0.2	11	0.209	6.7	-	5	0.4	0.76	1	1	1	No
2.9	45.61	0.107	38.14	0.085	0.2	0.075	15.2	0.026	7.4	-	3	0.333	0.72	1	1	0.75	No
4.2	68.93	0.221	41.97	0.202	0.18	0.056	6	0.55	7	0.017	20	0.2	0.8	1.1	1	1.13	Yes
5.9	91.33	0.119	74.9	0.114	0.24	0.2	9	0.444	7.4	-	5	0.6	0.88	1	1	1	Yes
2.4	38.18	0.093	27.02	0.113	0.12	0.2	11.5	0.191	6.7	-	7	0.143	0.68	1	1	1.12	No
1.1	15.47	0.243	8.14	0.378	0.17	0.118	5.8	0.241	5.9	0.025	80	0.125	0.5	1	1	1.05	No
3.2	52.33	0.089	44.37	0.08	0.24	0.2	9	0.256	7.4		20	0.15	0.74	1	1	1.09	Yes
13.5	240.2	0.045	141.19	0.058	0.4	0.125	5.8	0.483	6.9	0.016	18	0.222	1	1	1	1.22	Yes
6.5	119.9	0.037	88.49	0.045	0.4	0.1	9.5	0.074	6.7	0.019	37	0.135	0.9	1	1	1.13	Yes
6.1	111.1	0.043	80.23	0.085	0.22	0.045	12.6	0.246	7	0.017	3	0.333	0.88	1.1	1	0.92	Yes
7.5	121.3	0.14	62.7	0.13	0.2	0.2	10.3	0.32	7.3	0.015	5	0.4	0.93	1	1	1	Yes
3.4	54.08	0.17	37.9	0.124	0.26	0.096	10.5	0.067	7	0.017	2	1	0.76	1	1	1	Yes
2.9	49.88	0.163	39.1	0.169	0.47	0.106	26.4	0.394	6.5	0.02	25	0.16	0.72	1	1	1.13	No

Mean Depth (m)	Mean σ_v (kPa)	COV σ_v	Mean σ_v' (kPa)	COV σ_v'	Mean a_{max} *(g)*	COV	Mean N_m	COV N_m	Mean M_w	COV M_w	Mean *FC* (%)	COV *FC*	C_R	C_S	C_B	C_E	Liquefied?
2.6	41.67	0.181	28.44	0.144	0.12	0.2	5.2	0.385	6.7	-	4	0.25	0.7	1	1	1	No
3.3	51.47	0.188	33.55	0.142	0.16	0.125	5.9	0.288	6.7	0.019	31	0.097	0.75	1	1	1.05	No

APPENDIX-D

Post liquefaction CPT-based data (Moss 2003) used for reliability analysis

Table D-1. Training Data

Depth (mean) m	q_c (mean) kPa	q_c (COV)	fs (mean) kPa	fs (COV)	$\sigma'v$ (mean) kPa	$\sigma'v$ (COV)	σ_v (mean) kPa	σ_v (COV)	a_{max} (mean) (g)	a_{max} (COV)	M_w (mean)	M_w (COV)	Liquefied?
3.3	3120	0.247	38.04	0.427	44.46	0.111	68	0.189	0.16	0.188	7.5	0.015	Yes
1.95	5910	0.954	82.47	0.879	29.5	0.081	31.95	0.067	0.16	0.188	7.5	0.015	No
1.38	730	0.26	5.78	0.606	14.1	0.178	26.66	0.101	0.2	0.25	7.4	0.015	Yes
4.25	3140	0.503	30.28	0.333	52.75	0.086	74.72	0.11	0.18	0.111	6.5	0.02	Yes
2.75	2690	0.323	30.56	0.142	35.49	0.123	47.75	0.17	0.51	0.098	6.5	0.02	Yes
3.9	2800	0.679	68.56	0.356	54.5	0.084	65.88	0.129	0.13	0.308	6.5	0.02	No
5.2	5140	0.593	76.9	0.302	56.52	0.087	98.7	0.104	0.17	0.294	6.5	0.02	No
2.5	5750	0.637	80.79	0.485	36.66	0.101	41.47	0.088	0.16	0.125	6.5	0.02	No
2.7	3140	0.182	1.16	0.181	39.3	0.107	44.2	0.076	0.19	0.263	6.2	0.023	Yes
2.9	1720	0.174	13.45	0.176	39.37	0.113	48.2	0.116	0.19	0.263	6.2	0.023	Yes
3	1920	0.302	17.92	0.133	41.75	0.105	49.6	0.102	0.19	0.263	6.2	0.023	Yes
2.3	3000	0.087	24.15	0.08	34.46	0.118	37.4	0.061	0.19	0.263	6.2	0.023	Yes
4.72	5130	0.46	70.69	0.313	51.93	0.114	89.31	0.149	0.23	0.087	5.9	0.025	Yes
4.3	2570	0.588	71.54	0.259	58.18	0.084	73.48	0.133	0.19	0.158	5.9	0.025	Yes
4.25	3230	0.43	28.53	0.206	50.43	0.098	72.5	0.106	0.17	0.118	5.9	0.025	Yes
3.35	3310	0.254	37.22	0.119	39.15	0.142	57.3	0.194	0.09	0.222	5.9	0.025	No
5	2820	0.468	29.61	1.126	52.96	0.1	91.91	0.141	0.17	0.294	7.7	0.013	Yes
3	2720	0.239	48.22	0.457	43.91	0.075	49.8	0.132	0.17	0.294	7.7	0.013	No
2.75	4970	0.298	68.72	0.309	37.98	0.103	49.75	0.166	0.3	0.2	6.9	0.017	Yes

Depth (mean) m	q_c (mean) kPa	q_c (COV)	fs (mean) kPa	fs (COV)	$\sigma'v$ (mean) kPa	$\sigma'v$ (COV)	σ_v (mean) kPa	σ_v (COV)	a_{max} (mean) (g)	a_{max} (COV)	M_w (mean)	M_w (COV)	Liquefied?
2.4	5760	0.568	105.6	0.859	29.1	0.108	44.8	0.12	0.5	0.2	6.9	0.017	Yes
3.35	5290	0.459	206.28	0.651	50.01	0.071	59.33	0.109	0.5	0.2	6.9	0.017	Yes
7.3	8300	0.265	214.07	0.583	120.45	0.042	125.45	0.044	0.5	0.2	6.9	0.017	Yes
3.75	4920	0.415	18.07	0.296	28.03	0.153	57.37	0.161	0.44	0.205	6.6	0.02	Yes
2.7	3380	0.334	21.83	0.185	19.5	0.196	41.38	0.191	0.43	0.209	6.6	0.02	Yes
7.75	7610	0.112	28.38	0.114	58.46	0.085	118.5	0.047	0.42	0.19	6.6	0.02	Yes
2.8	6820	0.194	75.03	0.117	26.06	0.117	42.25	0.069	0.37	0.189	6.6	0.02	Yes
8	7290	0.144	22.47	0.129	67.9	0.077	121.46	0.071	0.31	0.194	6.6	0.02	Yes
5.1	5530	0.329	30.77	0.272	39.15	0.117	77.9	0.118	0.28	0.214	6.6	0.02	Yes
5.5	6070	0.196	19.51	0.098	41.43	0.098	84.1	0.055	0.27	0.185	6.6	0.02	Yes
4.1	4180	0.191	4.18	0.191	44.03	0.076	61.2	0.052	0.27	0.185	6.6	0.02	Yes
5	4030	0.313	11.94	0.624	39.81	0.149	76.21	0.206	0.26	0.192	6.6	0.02	Yes
5.45	6030	0.202	23.34	0.244	53.04	0.07	81.98	0.042	0.39	0.205	6.6	0.02	Yes
1.8	9200	0.177	40.6	0.553	18.17	0.152	27	0.037	0.37	0.189	6.6	0.02	No
4.2	7630	0.157	31.14	0.268	37.38	0.094	63.57	0.072	0.4	0.3	6.6	0.02	No
5.9	8010	0.17	25.02	0.341	52.07	0.077	89.35	0.051	0.41	0.293	6.6	0.02	No
4.7	13800	0.132	67.07	0.132	65.51	0.06	68.45	0.047	0.26	0.192	6.6	0.02	No
7.5	7390	0.273	31.37	0.277	55.36	0.088	114.81	0.041	0.27	0.296	6.6	0.02	No
5.2	5140	0.593	76.9	0.302	56.52	0.087	98.7	0.104	0.17	0.294	6.2	0.023	No
5.2	5140	0.593	76.9	0.302	56.52	0.087	98.7	0.104	0.21	0.238	6.6	0.02	Yes
6.75	5280	0.129	34.83	0.143	90.64	0.043	127.53	0.032	0.28	0.036	7	0.017	Yes
7.5	8660	0.221	47.96	0.349	96.79	0.049	141.03	0.055	0.28	0.036	7	0.017	Yes
6.15	5710	0.119	25.87	0.064	73.41	0.075	111.18	0.117	0.28	0.107	7	0.017	Yes
6.45	2140	0.285	13.36	0.139	74.42	0.056	114.15	0.07	0.16	0.188	7	0.017	Yes

Depth (mean) m	q_c (mean) kPa	q_c (COV)	fs (mean) kPa	fs (COV)	$\sigma'v$ (mean) kPa	$\sigma'v$ (COV)	σ_v (mean) kPa	σ_v (COV)	a_{max} (mean) (g)	a_{max} (COV)	M_w (mean)	M_w (COV)	Liquefied?
6	2030	0.433	9.66	0.206	71.48	0.056	106.8	0.065	0.16	0.188	7	0.017	Yes
6.5	2320	0.203	9.88	0.124	76.08	0.05	116.3	0.039	0.16	0.188	7	0.017	Yes
5.5	2120	0.198	10.91	0.232	66.32	0.048	95.75	0.035	0.25	0.12	7	0.017	Yes
8.3	4530	0.313	54.16	0.36	86.75	0.065	148.55	0.069	0.25	0.12	7	0.017	Yes
3.2	4680	0.145	25.76	0.118	44.55	0.087	52.4	0.107	0.25	0.12	7	0.017	Yes
2.85	5490	0.182	26.17	0.091	43.22	0.09	46.65	0.077	0.25	0.12	7	0.017	Yes
3.8	5940	0.582	34.21	0.227	47.86	0.089	66.5	0.092	0.25	0.32	7	0.017	Yes
5.25	3740	0.377	31.63	0.457	60.64	0.077	97.43	0.119	0.16	0.188	7	0.017	Yes
6.5	4050	0.119	28.58	0.08	87.13	0.044	106.75	0.042	0.31	0.258	7	0.017	Yes
7.4	4790	0.196	12.19	0.745	98.99	0.042	123.42	0.043	0.3	0.233	7	0.017	Yes
8.65	4790	0.503	92.4	0.099	99.92	0.054	155.35	0.061	0.3	0.233	7	0.017	Yes
7	7130	0.22	34.88	0.35	99.84	0.052	122.4	0.086	0.3	0.233	7	0.017	Yes
6.5	3170	0.442	22.66	0.42	95.7	0.047	103.55	0.065	0.3	0.233	7	0.017	Yes
4.1	5730	0.162	19.93	0.2	54.02	0.054	70.7	0.046	0.29	0.241	7	0.017	Yes
4.05	5280	0.303	15.88	0.207	53.56	0.057	69.75	0.066	0.29	0.241	7	0.017	Yes
7.7	8740	0.041	41.87	0.027	103.45	0.04	131.9	0.032	0.31	0.258	7	0.017	Yes
6.65	3890	0.136	31.53	0.062	86.39	0.045	110.43	0.047	0.31	0.258	7	0.017	Yes
7.5	4450	0.065	22.26	0.311	102.98	0.04	127.5	0.033	0.31	0.258	7	0.017	Yes
7.13	5670	0.159	25.38	0.074	90.33	0.046	126.88	0.041	0.18	0.278	7	0.017	Yes
3.8	1860	0.253	15.53	0.196	50.27	0.064	66.95	0.072	0.18	0.278	7	0.017	Yes
7.45	6890	0.251	26.06	0.129	94.12	0.045	137.78	0.033	0.18	0.222	7	0.017	Yes
2.7	2610	0.149	8.17	0.072	37.07	0.069	45.9	0.065	0.17	0.235	7	0.017	Yes
2.7	5070	0.108	60.88	0.234	36.38	0.07	48.15	0.063	0.32	0.25	7	0.017	Yes
3.5	3030	0.31	4.76	0.137	45.1	0.079	60.8	0.129	0.17	0.235	7	0.017	Yes

Depth (mean) m	q_c (mean) kPa	q_c (COV)	fs (mean) kPa	fs (COV)	$\sigma'v$ (mean) kPa	$\sigma'v$ (COV)	σ_v (mean) kPa	σ_v (COV)	a_{max} (mean) (g)	a_{max} (COV)	M_w (mean)	M_w (COV)	Liquefied?
3.4	1220	0.131	5.86	0.09	43.5	0.06	59.2	0.044	0.17	0.235	7	0.017	Yes
3.15	3560	0.124	10.12	0.375	44.82	0.061	55.13	0.062	0.17	0.235	7	0.017	Yes
8.6	7190	0.076	48.48	0.119	121.47	0.05	150.9	0.082	0.28	0.25	7	0.017	Yes
4.83	5210	0.146	38.3	0.14	72.26	0.049	79.38	0.056	0.28	0.25	7	0.017	Yes
3.25	1330	0.301	7.03	0.193	36.29	0.077	60.33	0.057	0.17	0.235	7	0.017	Yes
5.9	4820	0.062	33.17	0.031	79.83	0.054	103.37	0.08	0.28	0.25	7	0.017	Yes
6.75	3950	0.187	37.51	0.083	100.15	0.044	114.38	0.053	0.3	0.267	7	0.017	Yes
5.5	7100	0.38	152.37	0.166	74.32	0.048	103.75	0.041	0.24	0.083	7	0.017	No
3.75	13380	0.065	27.51	0.286	52.74	0.058	64.03	0.083	0.25	0.12	7	0.017	No
4.5	9330	0.066	27.61	0.18	66.95	0.048	74.8	0.056	0.25	0.12	7	0.017	No
3.75	16470	0.298	48.62	0.179	50.9	0.069	61.2	0.088	0.25	0.12	7	0.017	No
2.7	9360	0.154	29.57	0.083	39.09	0.096	48.9	0.078	0.25	0.12	7	0.017	No
2.9	9590	0.106	27.03	0.166	38.27	0.086	48.08	0.093	0.25	0.12	7	0.017	No
6.6	18830	0.032	56.94	0.146	85.64	0.05	123.9	0.031	0.25	0.12	7	0.017	No
2.9	10400	0.073	52.53	0.062	43.5	0.076	48.4	0.084	0.25	0.12	7	0.017	No
4.5	3900	0.231	13.48	0.1	58.38	0.075	78	0.133	0.17	0.235	7	0.017	No
4.15	2770	0.278	65.16	0.061	58.6	0.05	72.83	0.043	0.17	0.235	7	0.017	No
3.4	2860	0.189	13.46	0.087	43.5	0.099	60.18	0.185	0.15	0.267	7	0.017	No
2.75	3700	0.097	41.19	0.076	42.92	0.064	46.36	0.064	0.26	0.269	7	0.017	No
6.6	14930	0.072	103.79	0.032	109.48	0.042	113.4	0.043	0.28	0.25	7	0.017	No
6.93	7870	0.208	53.73	0.395	90.94	0.061	124.54	0.099	0.28	0.25	7	0.017	No
6.9	5530	0.148	90.75	0.185	109.97	0.043	113.97	0.046	0.12	0.25	7	0.017	No
5.5	3840	0.089	15.77	0.098	79.54	0.055	92.29	0.096	0.15	0.267	7	0.017	No
9	7260	0.566	187.3	0.278	144.99	0.039	162.74	0.042	0.69	0.087	6.7	0.019	Yes

Depth (mean) m	q_c (mean) kPa	q_c (COV)	fs (mean) kPa	fs (COV)	$\sigma'v$ (mean) kPa	$\sigma'v$ (COV)	σ_v (mean) kPa	σ_v (COV)	a_{max} (mean) (g)	a_{max} (COV)	M_w (mean)	M_w (COV)	Liquefied?
9.95	3110	0.479	73.46	0.254	110.45	0.049	169.8	0.038	0.51	0.118	6.7	0.019	Yes
6.5	6220	0.386	67.31	0.235	91.27	0.043	122.67	0.037	0.4	0.1	6.7	0.019	Yes
6.13	8770	0.643	98.79	0.418	94.85	0.036	112.76	0.031	0.54	0.074	6.7	0.019	Yes
4	3620	0.124	65.07	0.486	53.85	0.068	66.6	0.095	0.77	0.143	6.7	0.019	Yes
7	6250	0.323	30.8	0.248	70.45	0.07	119.5	0.056	0.37	0.297	7.2	0.015	Yes

Table D-2. Testing Data

Depth (mean) m	q_c (mean) kPa	q_c (COV)	fs (mean) kPa	fs (COV)	$\sigma'v$ (mean) kPa	$\sigma'v$ (COV)	σ_v (mean) kPa	σ_v (COV)	a_{max} (mean) (g)	a_{max} (COV)	M_w (mean)	M_w (COV)	Liquefied?
7	7830	0.068	97.46	0.698	95.07	0.042	124.5	0.037	0.45	0.311	7.2	0.015	Yes
6.5	2350	0.115	9.38	0.306	75.24	0.053	121.35	0.038	0.6	0.3	7.2	0.015	Yes
4.5	5090	0.104	44.37	0.161	55.86	0.056	82.35	0.048	0.6	0.3	7.2	0.015	Yes
4	3840	0.193	11.24	0.327	55.79	0.052	70.5	0.047	0.6	0.3	7.2	0.015	Yes
5.5	1900	0.242	33.32	0.401	71	0.048	99.45	0.042	0.45	0.311	7.2	0.015	Yes
4.75	4340	0.122	33.73	0.5	60.33	0.057	86.33	0.063	0.45	0.311	7.2	0.015	Yes
6.75	2840	0.489	61.63	0.486	94.01	0.042	119.03	0.039	0.45	0.311	7.2	0.015	Yes
5.5	2510	0.554	10.42	0.183	54.71	0.081	93.95	0.068	0.4	0.3	7.2	0.015	Yes
3.75	4650	0.217	30.19	0.254	49.96	0.077	67.13	0.124	0.5	0.3	7.2	0.015	Yes
3.7	2530	0.178	9.98	0.249	42.13	0.08	62.73	0.053	0.45	0.311	7.2	0.015	Yes
4.4	1490	0.342	5.91	0.342	50.98	0.068	74.52	0.041	0.5	0.3	7.2	0.015	Yes

Depth (mean) m	q_c (mean) kPa	q_c (COV)	fs (mean) kPa	fs (COV)	$\sigma'v$ (mean) kPa	$\sigma'v$ (COV)	σ_v (mean) kPa	σ_v (COV)	a_{max} (mean) (g)	a_{max} (COV)	M_w (mean)	M_w (COV)	Liquefied?
5.45	4070	0.246	24.66	0.549	69.15	0.051	99.08	0.05	0.6	0.3	7.2	0.015	Yes
5.5	4850	0.214	35.84	0.29	69.64	0.049	100.05	0.042	0.6	0.3	7.2	0.015	Yes
4	6290	0.169	27.13	0.185	55.79	0.064	70.5	0.097	0.6	0.3	7.2	0.015	Yes
4.25	3370	0.288	31.52	0.342	59.57	0.049	74.78	0.036	0.45	0.311	7.2	0.015	Yes
3.5	2330	0.227	21.81	0.646	51.62	0.054	60.45	0.046	0.45	0.311	7.2	0.015	Yes
5	14220	0.217	85.41	0.354	70.48	0.056	95	0.076	0.7	0.3	7.2	0.015	No
3.65	11380	0.394	216.23	0.563	57.62	0.05	64	0.037	0.5	0.3	7.2	0.015	No
4	7890	0.766	214.05	0.65	59.19	0.061	69	0.1	0.5	0.3	7.2	0.015	No
3.75	12930	0.041	94.75	0.591	46.11	0.073	63.28	0.053	0.65	0.308	7.2	0.015	No
2.8	10300	0.243	67.98	0.408	38.09	0.083	46.92	0.057	0.6	0.3	7.2	0.015	No
1.45	6040	0.356	63.38	0.479	21.59	0.107	26	0.1	0.65	0.308	7.2	0.015	No
1.6	950	0.432	4.27	0.466	17.31	0.154	28.1	0.18	0.37	0.243	7.4	0.015	Yes
1.8	1300	0.623	15.21	0.395	22.45	0.11	30.3	0.129	0.37	0.351	7.4	0.015	Yes
2.3	1150	0.2	21.62	0.209	26.8	0.093	39.55	0.085	0.4	0.25	7.4	0.015	Yes
3.8	3940	0.452	30.34	0.309	55.5	0.056	60.4	0.064	0.4	0.25	7.4	0.015	Yes
4.05	1740	0.58	17.96	0.455	38.19	0.089	73.61	0.071	0.4	0.25	7.4	0.015	Yes
2.15	1390	0.518	7.29	0.558	28.9	0.083	35.28	0.073	0.4	0.25	7.4	0.015	Yes
2.25	2030	0.463	8.24	0.483	22.96	0.12	40.13	0.121	0.4	0.25	7.4	0.015	Yes
2.4	3360	0.348	10	0.735	24.26	0.11	42.9	0.093	0.4	0.25	7.4	0.015	Yes
2.1	2520	0.254	7.95	0.481	21.31	0.121	37.5	0.106	0.4	0.25	7.4	0.015	Yes
2.5	2630	0.369	15.34	0.39	33.44	0.077	41.09	0.083	0.4	0.25	7.4	0.015	Yes
3.25	1740	0.27	9.75	0.497	33.08	0.081	58	0.042	0.4	0.25	7.4	0.015	Yes
2.5	1870	0.39	16.95	0.375	27.17	0.094	43.85	0.078	0.4	0.25	7.4	0.015	Yes
2.38	1300	0.477	7.41	0.409	32.35	0.076	38.78	0.071	0.4	0.25	7.4	0.015	Yes

Depth (mean) m	q_c (mean) kPa	q_c (COV)	fs (mean) kPa	fs (COV)	$\sigma'v$ (mean) kPa	$\sigma'v$ (COV)	σ_v (mean) kPa	σ_v (COV)	a_{max} (mean) (g)	a_{max} (COV)	M_w (mean)	M_w (COV)	Liquefied?
3.25	2540	0.465	23.39	0.488	36.68	0.1	58.75	0.138	0.38	0.211	7.6	0.013	Yes
4.25	2120	0.368	20.32	0.52	46.68	0.084	77.39	0.107	0.6	0.2	7.6	0.013	Yes
4	1880	0.234	34.61	0.68	44.93	0.093	72.4	0.135	0.6	0.2	7.6	0.013	Yes
7	750	0.387	15.42	0.459	69.78	0.078	130.6	0.079	0.6	0.2	7.6	0.013	Yes
4.75	1700	0.535	36.96	0.837	50.46	0.112	87.25	0.166	0.6	0.2	7.6	0.013	Yes
6.5	2060	0.194	22.23	0.191	63.62	0.074	121.79	0.057	0.25	0.2	7.6	0.013	Yes
3.25	2480	0.31	12.22	0.466	33.68	0.092	60.07	0.086	0.25	0.2	7.6	0.013	Yes
3.5	2720	0.136	12.59	0.345	39.86	0.076	63.11	0.077	0.25	0.2	7.6	0.013	Yes
6.2	3870	0.233	23.27	0.361	65.15	0.067	114.2	0.063	0.25	0.2	7.6	0.013	Yes
10.75	7740	0.141	61.67	0.198	122.76	0.05	193.69	0.049	0.25	0.2	7.6	0.013	Yes
6	3390	0.31	21.03	0.317	60.18	0.084	111.78	0.091	0.25	0.2	7.6	0.013	Yes
7	2750	0.105	57.1	0.163	71.14	0.085	130	0.102	0.38	0.211	7.6	0.013	Yes
3.5	1160	0.371	6.6	0.662	38.98	0.087	63.5	0.104	0.38	0.211	7.6	0.013	Yes

Research Publication

Published Journal Papers

I. Muduli, P.K., and Das, S.K. (2013). "First-order reliability method for probabilistic evaluation of liquefaction potential of soil using genetic programming". ***International Journal of Geomechanics***, **ASCE,** DOI:10.1061/(ASCE)GM.1943-5622.0000377

II. Muduli, P.K., and Das, S.K.(2013). "Evaluation of liquefaction potential of soil based on Standard Penetration Test using multi-gene genetic programming model." ***Acta Geophysica,*** DOI: 10.2478/s11600-013-0181-6.

III. Muduli, P.K., Das, M.R., Samui, P., and Das, S.K. (2013). "Uplift capacity of suction caisson in clay using artificial intelligence techniques". ***Marine Georesources & Geotechnology***, 31, 375-390.

IV. Muduli, P.K., Das, S.K., and Bhattacharya, S. (2013). "CPT-based probabilistic evaluation of seismic soil liquefaction potential using multi-gene genetic programming." ***Georisk: Assessment and Management of Risk for Engineered Systems and Geohazards***, DOI: 10.1080 / 17499518.2013.845720**.**

V. Muduli, P.K., and Das, S.K. (2013). "SPT-based probabilistic method for evaluation of liquefaction potential of soil using multi-gene genetic programming". ***International Journal of Geotechnical Earthquake Engineering***, 4(1), 42-60.

VI. Muduli, P.K., and Das, S.K. (2013). "CPT-based seismic liquefaction potential evaluation using multi-gene genetic programming approach". ***Indian Geotechnical Journal***, DOI 10.1007/s40098-013-0048-4.

National and International Conference Publications

I. Das, S.K., and Muduli, P.K. (2011). "Evaluation of liquefaction potential of soil using extreme learning machine." ***Proceedings of 13th International conference of the IACMAG 2011***, Melbourne, Austrailia.

II. Das, S.K., and Muduli, P.K. (2011). "Evaluation of liquefaction potential of soil using genetic programming." ***In: Proceedings of the Golden Jubilee Indian Geotechnical Conference, IGC-2011 on Geochallenges***, December 15-17, Vol. II, 827-830, Kochi, India.

III. Das, S.K., and Muduli, P.K. (2013). "Probability-based method for assessing liquefaction potential of soil using genetic programming." S. Chakraborty and G. Bhattacharya (eds.), ***In: Proceedings of the International Symposium on Engineering under Uncertainty: Safety Assessment and Management (ISEUSAM-2012)***, Springer India, 1153 - 1163, held in BESU, Shibpur, Jan. 1-4, 2012.

IV. Muduli, P.K., and Das, S.K. (2012). "Determination of limit state function in SPT-based liquefaction analysis using genetic programming for reliability analysis." ***In: Proceedings of the Indian Geotechnical Conference, IGC-2012 on Advances in Geotechnical Engineering***, December 13-15, Vol II, 672-675, New Delhi, India.

ADDENDUM

4.3.2.2 *Parametric study and Sensitivity analysis*

For verification of the developed MGGP-based LI_p models (Model-I and Model-II), a parametric analysis was performed in the present study. The parametric analysis investigates the response of the predicted liquefaction index from the above two models with respect to the corresponding input variables. The robustness of the developed model equations for LI_p [Eq. (4.20) and Eq. (4.21)] are evaluated by examining how well the predicted values agree with the underlying physical behavior of occurrence of liquefaction.

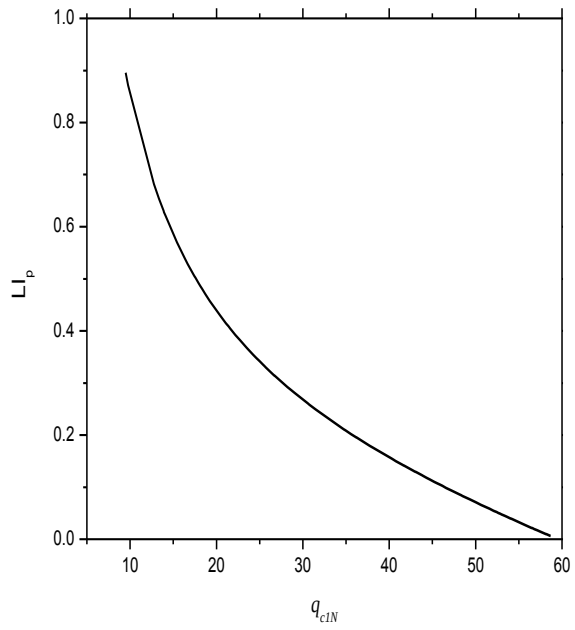

(a)

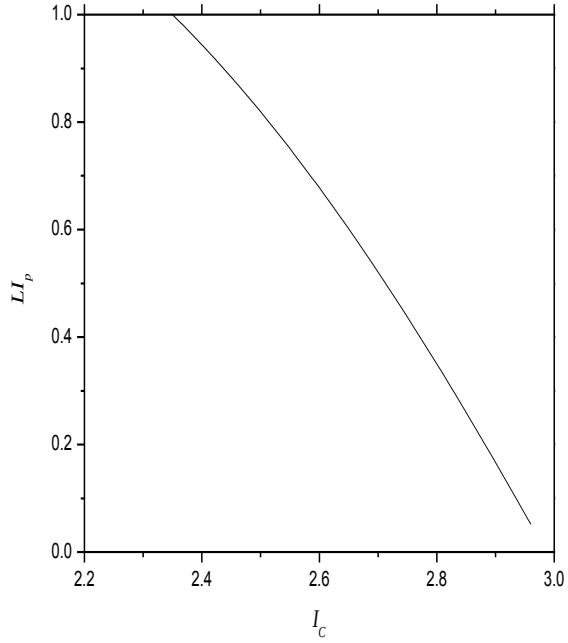

(b)

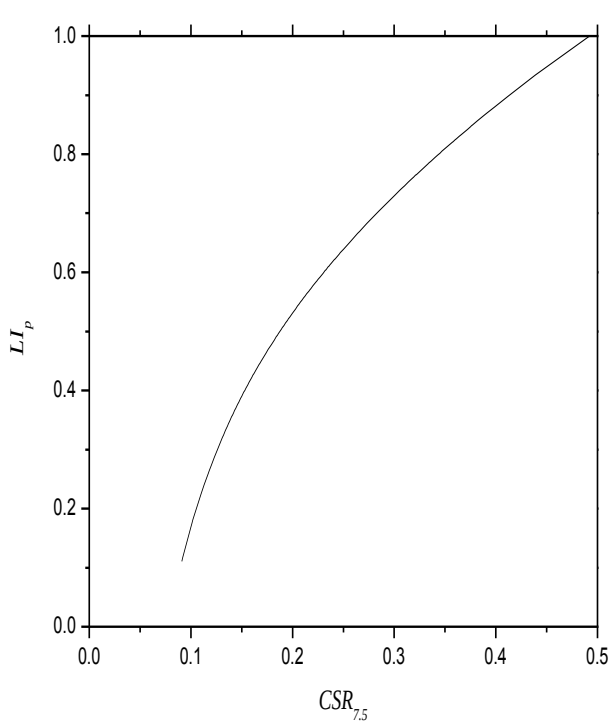

(c)

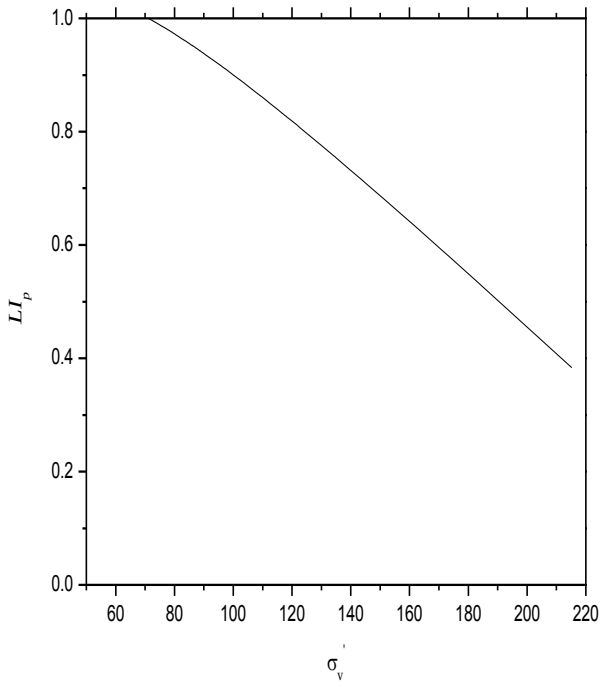

(d)

Fig. 4.13(A) Parametric analysis of LI_p for developed MGGP-based Model-I

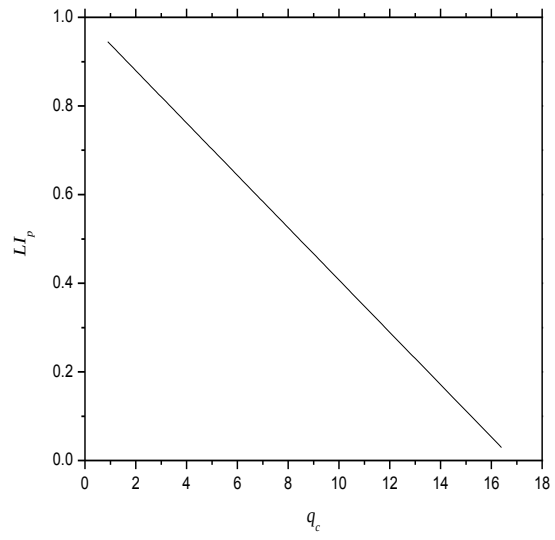

(a)

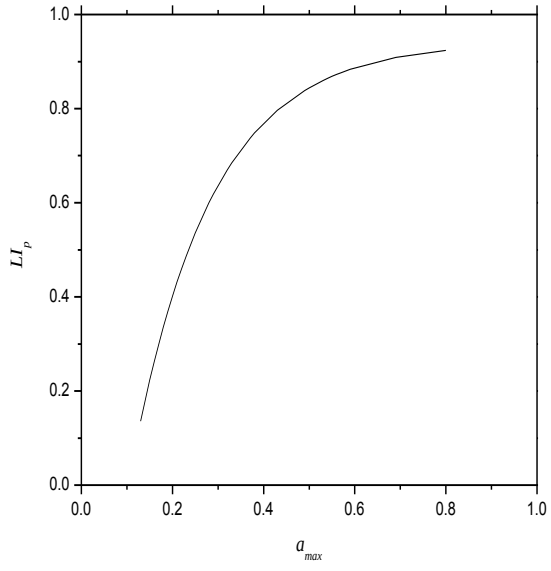

(b)

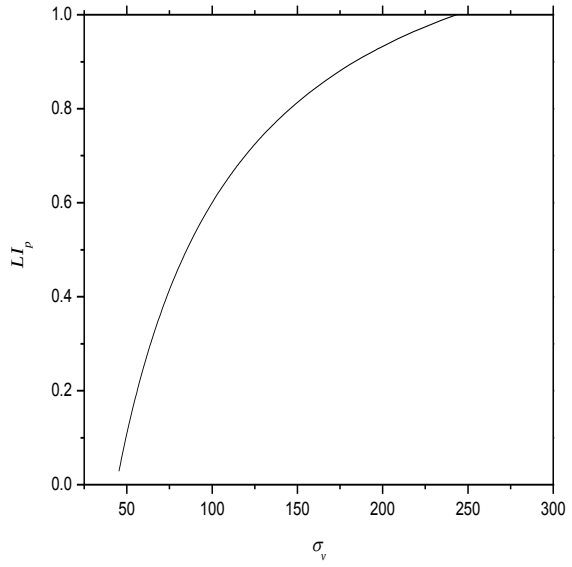

(c)

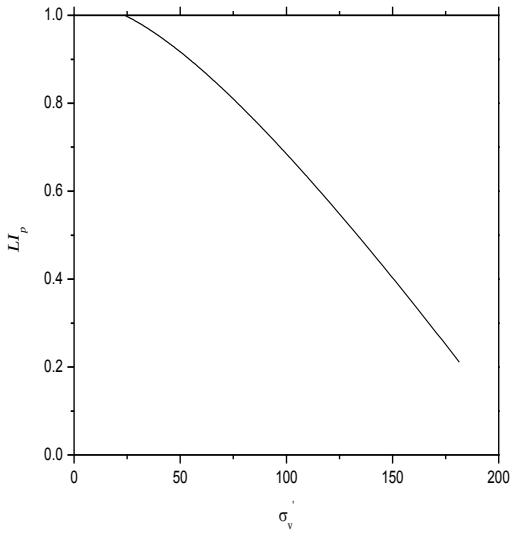

(d)

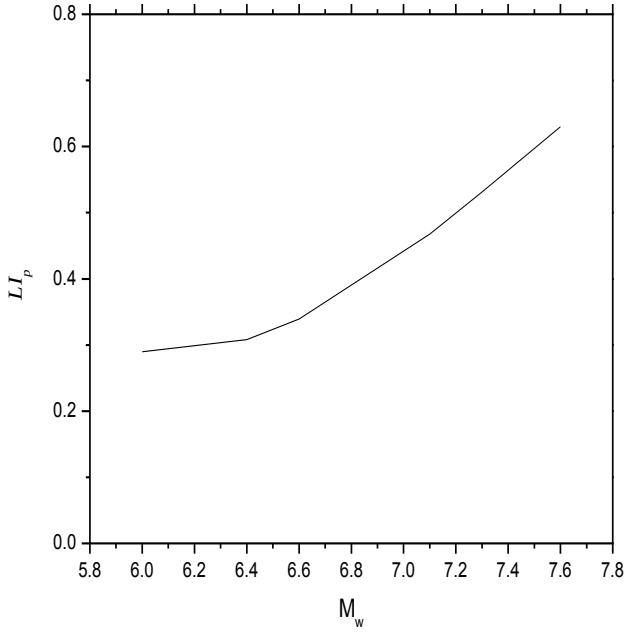

(e)

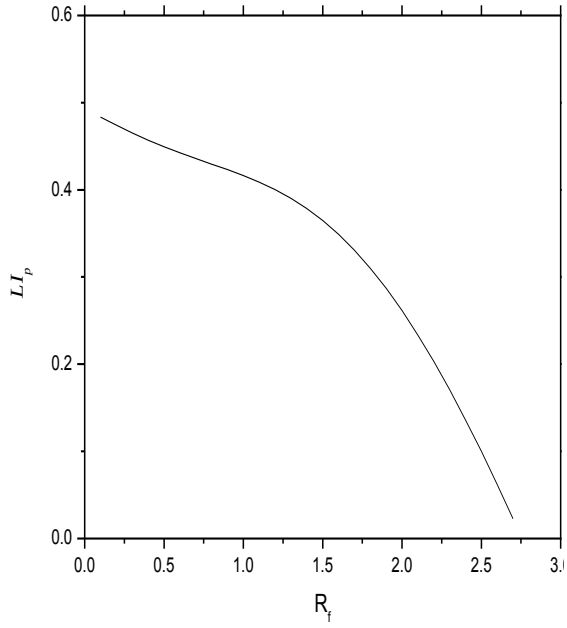

(f)

Fig. 4.13(B) Parametric analysis of LI_p for developed MGGP-based Model-II

It can be observed from Fig. 4.13 (A), that in case of the developed Model-I, LI_p decreased with increasing $q_{c1N,}$ I_c and σ'_v showing nonlinearity. But, it can be seen that LI_p increased with increasing $CSR_{7.5}$ nonlinearly. Similarly, Fig. 4.13 (B), which corresponds to the Model-

developed Model-II, shows that LI_p decreased with increasing q_c linearly whereas LI_p decreased with increasing R_f and σ'_v nonlinearly. It can also be noted that LI_p increased with increasing a_{max}, M_w and σ_v nonlinearly. The parametric analysis results are generally expected considering the physical behavior of liquefaction phenomenon. The above results confirm that the developed Model-I and Model-II are capable of showing the important characteristics of liquefaction index.

Table 4.9(a) Sensitivity analysis of inputs for the developed MGGP models as per Gandomi et al. (2013)

Model -I					Model - II					
Parameters	q_{c1N}	I_c	σ'_v	$CSR_{7.5}$	q_c	R_f	σ'_v	σ_v	a_{max}/g	M_w
Sensitivity (%)	46.2	20.6	11.7	21.4	29.8	15.1	18.4	9.9	18.7	8.2
Rank	1	3	4	2	1	4	3	5	2	6

Sensitivity analyses were made as per Gandomi et al. (2013) for the developed models (Model-I and Model-II) and presented in Table 4.9 (a). For Model-I, normalized cone tip resistance (q_{c1N}) is the most important parameter. The other important inputs are $CSR_{7.5}$, and I_c with σ'_v is the least important parameter. For Model-II the most important parameter is measured cone tip resistance (q_c). The other input parameters in decreasing order of their contribution in governing the prediction of LI are (a_{max}/g), σ'_v, R_f, σ_v, and M_w. It is well known that q_c is the most important soil parameter for liquefaction susceptibility analysis.